

Geological Field Trips and Maps

2022

Vol. 14 (2.2)



ISSN: 2038-4947



SOCIETÀ GEOLOGICA ITALIANA

FONDATA NEL 1881 - ENTE MORALE R. D. 17 OTTOBRE 1885



**The Tethyan and Tyrrhenian margin record of the Central Apennines:
a guide with insights from stratigraphy, tectonics, and hydrogeology**

“Field workshop: from the Tyrrhenian Sea to the Central Apennine front” organised by GeoSed - Italian Association for Sedimentary Geology, the section of the Italian Geological Society, 19th-23rd July 2021.

<https://doi.org/10.3301/GFT.2022.05>

GFT&M - *Geological Field Trips and Maps*

Periodico semestrale del Servizio Geologico d'Italia - ISPRA e della Società Geologica Italiana
Geol. F. Trips Maps, Vol. **14** No.2.2 (2022), 113 pp., 72 Figs. (<https://doi.org/10.3301/GFT.2022.05>)

The Tethyan and Tyrrhenian margin record of the Central Apennines: a guide with insights from stratigraphy, tectonics, and hydrogeology

"Field workshop: from the Tyrrhenian Sea to the Central Apennine front" organised by GeoSed - Italian Association for Sedimentary Geology, the section of the Italian Geological Society, 19th-23rd July 2021.

Giovanni Luca Cardello^{1*}, Laura Tomassetti², Irene Cornacchia³, Alessandro Mancini⁴, Marco Mancini⁵, Ilenia Mazzini⁵, Giovanni Rusciadelli⁶, Enrico Capezzuoli⁷, Valeria Lorenzi⁸, Marco Petitta⁸, Gian Paolo Cavinato⁵, Odoardo Girotti⁸, Marco Brandano^{5,8}

¹ Department of Chemistry, Physics, Mathematics and Natural Sciences, University of Sassari, Via Piandanna 4, 07100 Sassari, Italy. ² Department for the Geological Survey of Italy-ISPRA, Institute for Environmental Protection and Research, Via Vitaliano Brancati 48, 00100 Rome, Italy. ³ Institute of Geosciences and Georesources IGG-CNR, Via G. Moruzzi 1, 56124 Pisa, Italy. ⁴ Department of Earth Sciences "A. Desio", University of Milan, via Mangiagalli 34, 20133 Milan, Italy. ⁵ Institute of Environmental Geology and Geoengineering CNR IGAG, Rome 1 Research Area Montelibretti, Via Salaria km 29,300, 00015 Monterotondo Scalo, Rome, Italy. ⁶ Department of Engineering and Geology, "G. D'Annunzio" University of Chieti-Pescara, Via dei Vestini 31, 66100 Chieti, Italy. ⁷ Department of Earth Sciences, University of Florence, Via La Pira 4, 50121, Florence, Italy. ⁸ Department of Earth Sciences, Sapienza University of Rome, P.le Aldo Moro 5, 00185, Rome, Italy.

Corresponding author e-mail: glcardello@uniss.it

Responsible Director
Maria Siclari (ISPRA-Roma)

Editor in Chief
Andrea Zanchi (Università Milano-Bicocca)

Editorial Manager
Angelo Cipriani (ISPRA-Roma) - *Silvana Falchetti* (ISPRA-Roma)
Fabio Massimo Petti (Società Geologica Italiana - Roma) - *Diego Pieruccioni* (ISPRA - Roma) - *Alessandro Zuccari* (Società Geologica Italiana - Roma)

Associate Editors
M. Berti (Università di Bologna), *M. Della Seta* (Sapienza Università di Roma),
P. Gianolla (Università di Ferrara), *G. Giordano* (Università Roma Tre),
M. Massironi (Università di Padova), *M.L. Pampaloni* (ISPRA-Roma),
M. Pantaloni (ISPRA-Roma), *M. Scambelluri* (Università di Genova),
S. Tavani (Università di Napoli Federico II)

Editorial Advisory Board
D. Bernoulli, *F. Calamita*, *W. Cavazza*, *F.L. Chiocci*, *R. Compagnoni*,
D. Cosentino, *S. Critelli*, *G.V. Dal Piaz*, *P. Di Stefano*, *C. Doglioni*, *E. Erba*,
R. Fantoni, *M. Marino*, *M. Mellini*, *S. Milli*, *E. Chiarini*, *V. Pascucci*, *L. Passeri*,
A. Peccerillo, *L. Pomar*, *P. Ronchi*, *L. Simone*, *I. Spalla*, *L.H. Tanner*,
C. Venturini, *G. Zuffa*

Technical Advisory Board for Geological Maps
F. Capotorti (ISPRA-Roma), *F. Papasodaro* (ISPRA-Roma),
D. Tacchia (ISPRA-Roma), *S. Grossi* (ISPRA-Roma),
M. Zucali (University of Milano), *S. Zanchetta* (University of Milano-Bicocca),
M. Tropeano (University of Bari), *R. Bonomo* (ISPRA-Roma)

Cover page Figure: Panoramic view of the overturned Mesozoic to Palaeogene succession of Pizzo d'Intermesoli. (Gran Sasso Range; photo courtesy of L. Cardello).

ISSN: 2038-4947 [online]

<http://gftm.socgeol.it/>

The Geological Survey of Italy, the Società Geologica Italiana and the Editorial group are not responsible for the ideas, opinions and contents of the guides published; the Authors of each paper are responsible for the ideas, opinions and contents published.

Il Servizio Geologico d'Italia, la Società Geologica Italiana e il Gruppo editoriale non sono responsabili delle opinioni espresse e delle affermazioni pubblicate nella guida; l'Autore/i è/sono il/i solo/i responsabile/i.

Index

Information

Abstract	5
Program Summary	5
Safety	8
Overnight accommodation	8

Excursion notes

Itinerary

Day 1 – Quaternary evolution of the Tyrrhenian Apennine margin	12
Stop 1.1. The Middle Pleistocene Tiber deposits at Passo Corese (42°10'29"N; 12°38'26"E)	22
Stop 1.2. The Early Pleistocene transgression at Poggio Mirteto Scalo (42°14'23"N; 12°38'05"E)	25
Stop 1.3. The progradational shallow water delta of Torrita Tiberina (42°14'05"N; 12°36'42"E)	30
Stop 1.4. The Calabrian nearshore and the Middle Tiber Valley palaeogeographic evolution at Nazzano (42°14'07"N; 12°36'04"E)	32
Stop 1.5. The Acque Albule Basin and the <i>Lapis Tiburtinus</i> travertine (41°57'35.56"N; 12°44'24.42"E).....	34
Stop 1.6. The <i>Testina</i> travertine (41°58'29.83"N; 12°44'12.37"E)	36

Day 2 The Latium-Abruzzi carbonate platform: insights on the oceanographic events affecting the Tethyan margin

40

Stop 2.1. On the origin of the Palaeogene unconformity and Cretaceous platform facies at Santa Maria dei Bisognosi (42°02'29.0"N; 13°05'40.8"E).....

40

Stop 2.2. The Miocene carbon isotope events at Pietrasecca I (42°08'00.85"N; 13°07'21.16"E) and Pietrasecca II (42°08'08.41"N; 13°08'05.78"E)

42

Stop 2.3. The Palaeogene succession and the Early Miocene Carbon Maximum (42°18'16.64"N, 13°15'16.44"E)

44

Stop 2.4. The Tortonian phosphatic horizon of Tornimparte: hardground or conglomerate? (42°17'01.22"N, 13°17'02.00"E)

49

Day 3 – The Gran Sasso range: sedimentary succession, tectonics, and hydrogeology

53

Stop 3.1. A panoramic view on the Gran Sasso thrust front (42°30'49.26"N; 13°33'54.32"E)

56

Stop 3.2 Approaching the overturned succession (42°29'22.61"N; 13°32'53.72"E)

57

Stop 3.3. The Middle Miocene inner to outer ramp deposits (42°29'17.55"N; 13°32'44.41"E).....

57

Stop 3.4. The Early Miocene starving and siliceous production (42°29'12.70"N; 13°32'39.23"E) 58

Stop 3.5. The Oligocene distal ramp deposits (42°29'7.84"N; 13°32'32.78"E) 59

Stop 3.6. The Waterfall on the "Fonte Gelata fm" (42°29'6.47"N; 13°32'33.15"E) 59

Stop 3.7. The Rio Arno geology and hydrogeology (42°28'57.20"N; 13°32'34.22"E) 59

Stop 3.8. The Corniola syn-sedimentary features (42°28'37.77"N; 13°32'39.26"E) 62

Stop 3.9. The polyphase tectonics of the Tre Selle Fault (42°27'46.84"N; 13°32'16.08"E)..... 62

Stop 3.10. Pizzo Cefalone: a view on the Cretaceous base-of-slope architecture (42°27'28.34"N; 13°32'9.36"E) 63

Stop 3.11. Campo Pericoli: a glimpse on the Upper Jurassic carbonates (42°27'35.30"N; 13°32'54.92"E) 64

Stop 3.12. The Campo Pericoli reduced and discontinuous succession (42°27'26.78"N; 13°33'8.06"E)..... 66

Day 4 – The Maiella Mountain Pennapedimonte section 68

Stop 4.1. Pennapedimonte section, the Upper Cretaceous to Miocene slope to distal ramp successions, and the Eocene/Oligocene transition (42°09'08.80"N; 14°11'22.29"E)..... 77

Day 5 – The Maiella Mountain Mesozoic and Cenozoic evolution..... 82

Stop 5.1. The Monte D’Ugni and Cima delle Murelle panoramic view (42°09'31.49"N; 14°07'48.57"E) 82

Stop 5.2. The Monte Rotondo panoramic view (42°09'31.49"N; 14°07'48.57"E)..... 85

Stop 5.3. Monte Cavallo panoramic view of the platform-to-basin succession (42°07'45.78"N; 14°06'44.38"E)..... 87

Stop 5.4. Fonte Tettone section (42°10'14.47"N; 14°06'43.25"E)..... 96

Stop 5.5. The San Bartolomeo Valley Section (42°10'52.70"N; 14°02'05.61"E)..... 97

References 99

Abstract

This guide is a 5-day geotraverse across the Central Apennines, which expose the inherited Meso-Cenozoic sedimentary successions and tectonic architecture of the Apennine Tethyan passive margin. This structure was progressively involved into orogenic and post-orogenic tectonics, related to the Tyrrhenian back-arc dynamics. To show the different margin dynamics, we present: 1) sedimentologic and stratigraphic aspects, 2) relations with Neogene compressive and Quaternary extensional structures and 3) a hydrogeological case-study. The trip starts north of Rome, where Quaternary deposits at the transition from marine to continental deposition, including travertines, record the evolution of the Tyrrhenian passive margin. The excursion then moves to the Mesozoic platform margins of the Latium-Abruzzi and Apulia carbonate platforms, where perfectly preserved Cretaceous to Neogene successions occur. The Maiella mountain and Gran Sasso range testify for carbonate production changes, as recorded in facies associations and isotope geochemistry records, related to global climate shifts and regional tectonics. A focus on the hydrogeologic dynamics of the Gran Sasso aquifer is also offered in relation to the current climate change. This guide is the result of a workshop of GeoSed, the Italian Association for Sedimentary Geology, and it also aims at providing a scientific base for geo-touristic explorers.

Keywords

Carbonate rocks, siliciclastic deposits, syn-sedimentary faults, platform margin, travertine, hydrogeology.

Program Summary

As displayed in Figure 1, the trip begins on Day 1 on the Quaternary deposits of the Tiber Valley, where siliciclastic fluvial-deltaic deposits and travertines representative of the Tyrrhenian Apennine margin occur. On Day 2, the visited outcrops show the Upper Cretaceous to Miocene Latium-Abruzzi carbonate platform succession and the relationships between the inherited Tethys passive margin and the Olevano-Antrdoco thrust. On Day 3, remnants of the long-lasting Gran Sasso base-of-slope system between the Latium-Abruzzi platform to the south and the Marche-Abruzzi basin to the north is preserved. In this frame, the current hydrogeological setting and its evolution is also presented. On Days 4 and 5, the stratigraphic relationships among the Maiella platform and its Tethyan passive margin structures, the stratigraphic architecture of the Cenozoic ramp, as well as the tectonic setting of the Lower Cretaceous-Upper Miocene carbonate succession are described.

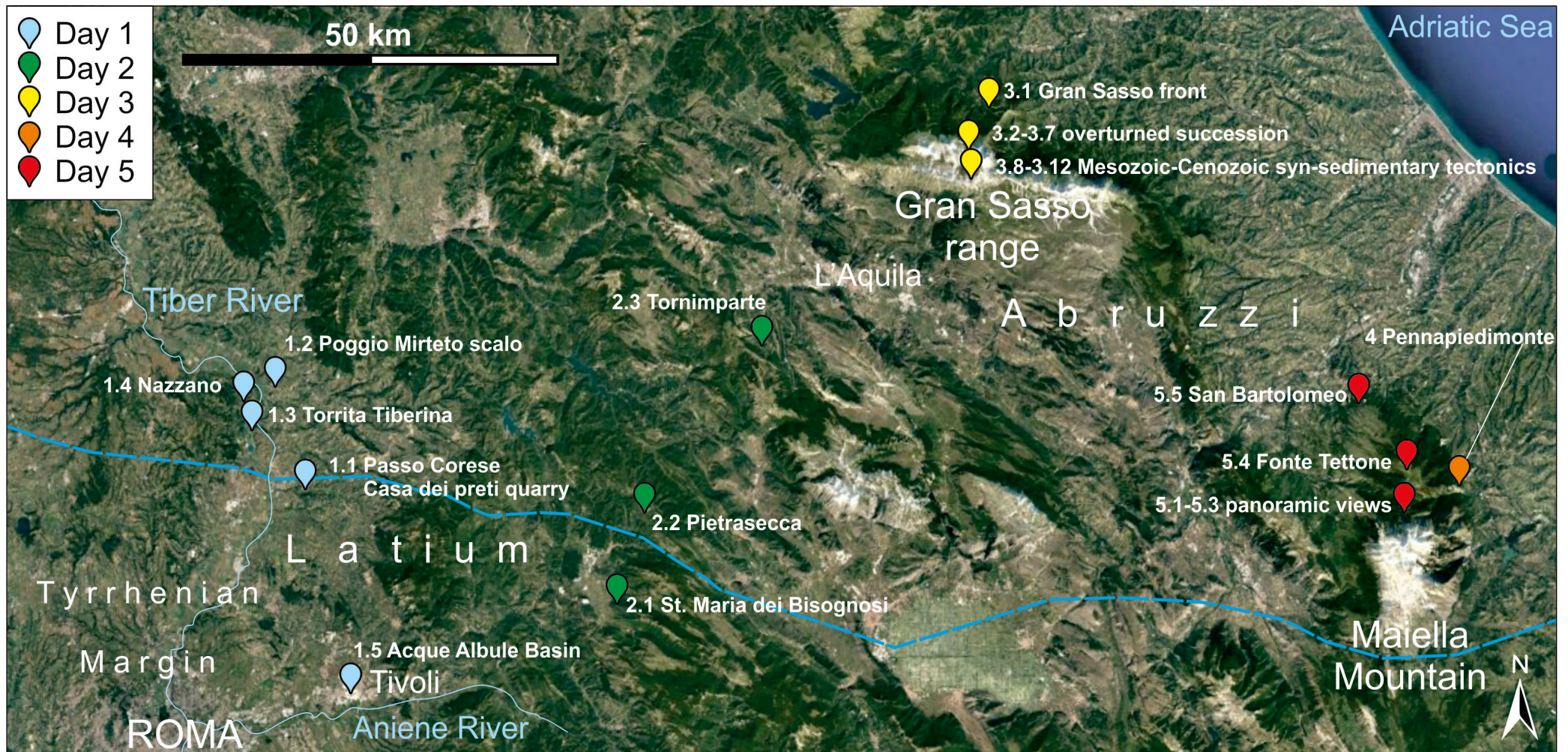


Fig. 1 - Google Earth view of the field trip itinerary with locations of the geological stops. The dashed blue line marks the CROP-11 trace (Billi et al., 2006).

Day 1 – Quaternary evolution of the Tyrrhenian Apennine margin

- 1.1. The Middle Pleistocene Tiber deposits at Passo Corese
- 1.2. The Early Pleistocene transgression at Poggio Mirteto Scalo
- 1.3. The progradational shallow water delta of Torrita Tiberina
- 1.4. The Calabrian nearshore and the Middle Tiber Valley palaeogeographic evolution at Nazzano

- 1.5. The Acque Albule Basin and the *Lapis Tiburtinus* travertine
- 1.6. The *Testina* travertine

Day 2 The Latium-Abruzzi carbonate platform: insights on the oceanographic events affecting the Tethyan margin

- 2.1. On the origin of the Palaeogene unconformity and Cretaceous platform facies at Santa Maria dei Bisognosi
- 2.2. The Miocene carbon isotope events at Pietrasecca
- 2.3. The Palaeogene succession and the Early Miocene Carbon Maximum at Tornimparte
- 2.4. The Tortonian phosphatic horizon of Tornimparte: hardground or conglomerate?

Day 3 – The Gran Sasso range: sedimentary succession, tectonics, and hydrogeology

- 3.1. A panoramic view on the Gran Sasso thrust
- 3.2. Approaching the overturned succession
- 3.3. The Middle Miocene inner to outer ramp deposits
- 3.4. The Early Miocene starving and siliceous production
- 3.5. The Oligocene distal ramp deposits
- 3.6. The waterfall on the “Fonte Gelata fm”
- 3.7. The Rio Arno geology and hydrogeology
- 3.8. The Corniola syn-sedimentary features
- 3.9. The polyphase tectonics of the Tre Selle Fault
- 3.10. Pizzo Cefalone: a view on the Cretaceous base-of-slope architecture
- 3.11. Campo Pericoli: a glimpse on the Upper Jurassic carbonates
- 3.12. The Campo Pericoli reduced and discontinuous succession

Day 4 – The Maiella Mountain Pennapiedimonte section

- 4.1. The Pennapiedimonte section: the Upper Cretaceous Maiella slope at the Eocene/Oligocene boundary

Day 5 – The Maiella Mountain Mesozoic and Cenozoic evolution

- 5.1. The Monte D’Ugni and Murelle panoramic view

- 5.2. The Monte Rotondo panoramic view
- 5.3. Monte Cavallo panoramic view on the platform-to-basin succession
- 5.4. Fonte Tettone section
- 5.5. The San Bartolomeo Valley section

Safety

Safety in the field is closely related to self-awareness. The excursion takes place up to 2200 m in altitude. Most of the outcrops are along road, trail, caves, and quarries, but some are along well-marked mountain paths that generally are well-maintained. Some outcrops are reached by driving along sinuous roads. We recommend: to wear walking mountain boots, to bring a sun protection, hats or headscarves, and sunglasses. Locally, rain showers and temperature drops can occur in any season. A waterproof coat/jacket and warm clothing are strongly recommended. Therefore, a rucksack is needed for daily use to carry your waterproofs, a spare T-shirt (and may be a fleece/sweater), a bottle of water, and small snacks. Mobile/cellular phone coverage is generally good, although in some place it can be poor to absent.

Useful phone numbers

General Emergency and Firefighters – Emergenze generiche e Pompieri. Tel: 112
Hospital San Giovanni Evangelista, Via A. Parrozzani, 3, Tivoli (Rome). Tel: +39 0774 3161
Hospital Giuseppe Mazzini, Piazza Italia, Teramo; +39 0861429292
Hospital Santissima Annunziata, Via dei Vestini 31, Chieti. +39 0871358539.
First aid station of Manoppello, Corso Santarelli 70, Manoppello (Pescara). +39 085859700.
Police – Pietracamela Carabinieri command station (on Day 3). +39 0861 955122
Police – Guardiagrele Carabinieri command station (on Day 4 and 5). +39 0871 801895
Helicopter rescue – Soccorso con elicottero. +39 800 258239

Overnight accommodation

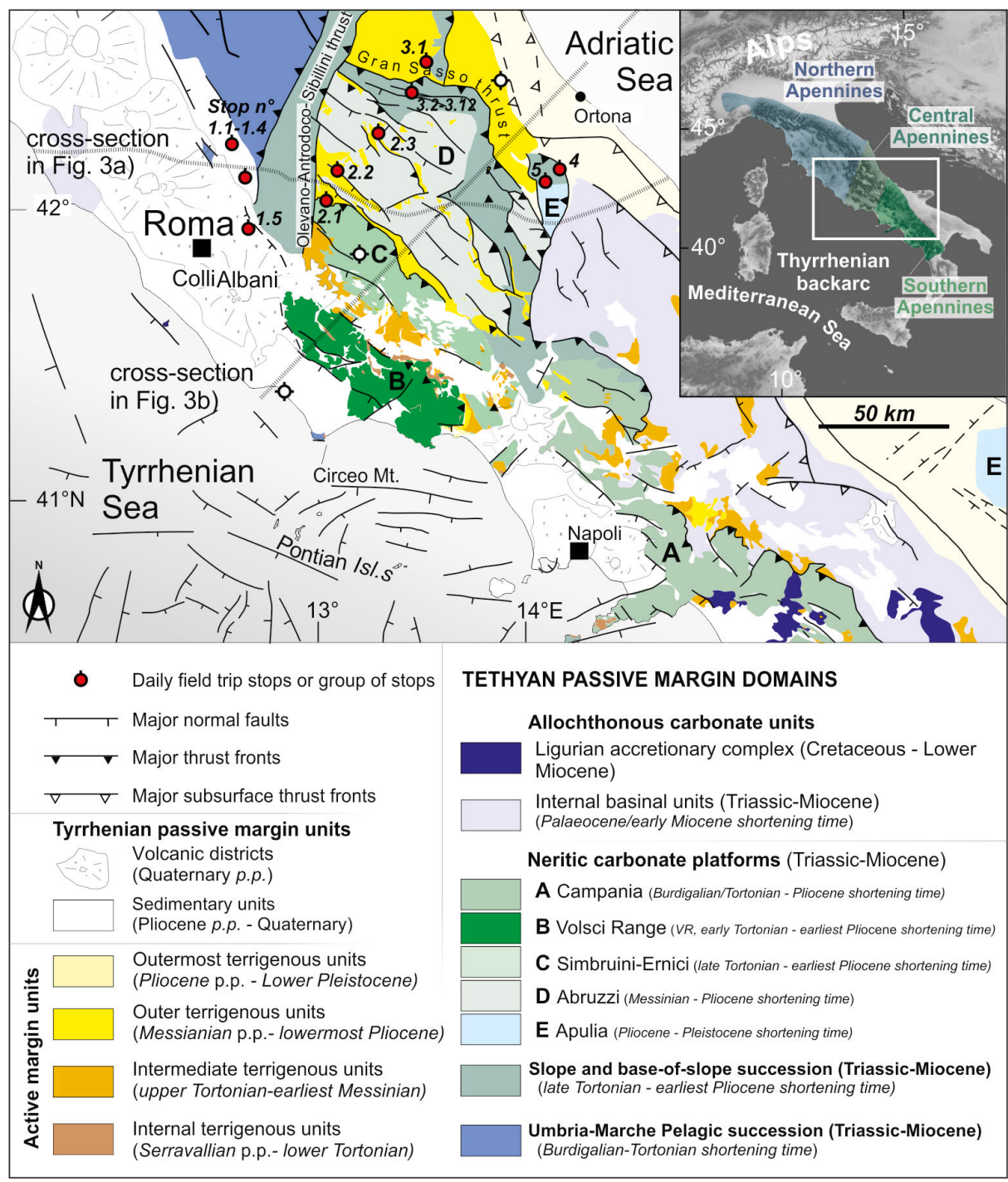
The hereby proposed stops are next to touristic facilities that include overnight accommodation. Touristic information: <https://www.visitlazio.com/>; <https://abruzzoturismo.it/>;
National parks: <http://www.gransassolagapark.it/>; <https://www.parcomajella.it/>

Excursion notes

The Apennines are part of a larger orogenic system shaping the Mediterranean region. They share similar evolution patterns with many of the Alpine-Himalayan fold-and-thrust belts (c.f.: [Cloetingh et al., 2004](#); [Carminati & Doglioni, 2012](#); [Reuter et al., 2013](#); [Brandano et al., 2016a](#); [Cardello et al., 2019](#); [Schmid et al., 2020](#)). In particular, the low- to non-metamorphic diagenetic status of the Central Apennines preserve the carbonate-dominated (Tethyan) and siliciclastic (Tyrrhenian) passive margin record (Figs. 1, 2). The regional stratigraphic architecture was influenced by the inherited Pangea continental break-up to oceanic spreading structures of the Alpine Tethys Ocean ([Bernoulli et al., 1979](#); [Channell et al., 1979](#); [Accordi et al., 1988](#); [Bernoulli, 2001](#); [Scrocca et al., 2007](#); [Vezzani et al., 2010](#); [Calamita et al., 2011](#); [Le Breton, 2017](#); [Tavani et al., 2021](#)). During the Late Triassic–Early Jurassic continental rift, the syn-sedimentary horst-and-graben structure influenced facies and thickness distribution of the carbonate deposits determining different tectonic-related stratigraphic settings ([Accordi et al., 1988](#)), whose architecture later influenced the orogenic structures. East of the Olevano-Antrodoco-Sibillini thrust (Fig. 2), persistent neritic carbonate platforms occur. Around them, base-of-slope to basinal domains are present (e.g., Gran Sasso: [Adamoli et al., 1978](#); [Cardello & Doglioni, 2015](#); Maiella: [Rusciadelli & Di Simone, 2007](#); [Brandano et al., 2016a](#)). During the Cretaceous, rimmed inner platforms were affected by areal shrinking as *Scaglia* pelagic basins developed ([Tavani et al., 2015](#); [Cipriani & Bottini, 2019](#); [Capotorti & Muraro, 2021](#); [Cardello et al., 2021](#); [Vitale & Ciarcia, 2021](#)).

During the Neogene, those tectono-stratigraphic passive margin units were accreted on top of the subducting Adria plate during the progressive E/NE-ward migration of frontal thrusts ([Boccaletti & Guazzone, 1974](#); [Malinverno & Ryan, 1986](#); [Bigi et al., 1992](#)) and the related forebulge to foredeep and wedge-top deposits (e.g., [Royden et al., 1987](#); [Carminati et al., 2007](#); [Vitale & Ciarcia, 2013](#); [Fabbi et al., 2014](#); [Cardello et al., 2021](#)). In Figures 2 and 3, they are grouped into four active margin units representative of different stages of wedge accretion (cf., [Accordi et al., 1988](#); [Curzi et al., 2020](#)).

From the Pliocene onward the fold-and-thrust belt underwent crustal stretching, which resulted in two Tyrrhenian margins related to the back-arc extension of the Apennine crust ([Sartori et al., 2004](#); [Acocella & Funicello, 2006](#); [Carminati et al., 2014](#); [Beaudoin et al., 2017](#)): the Sardo-Corsican and the Apennine margins. As shown from deep seismic lines (Fig. 3), the Apennines crust is subdivided in two domains: a compressional one in the Adriatic Sea and an extensional towards the Tyrrhenian Sea ([Malinverno & Ryan, 1986](#); [Patacca et al., 1990](#)). The extension affecting the Tyrrhenian margin reached the external Apennines during the Early



Pleistocene. In the axial part of the chain, the Neogene compressive structures were uplifted, while towards the Tyrrhenian Sea they were partly buried below Pliocene-Quaternary graben-like basins (Acocella & Funicello, 2006; Cosentino et al., 2010; Cardello et al., 2020; Marra et al., 2021). During the Quaternary, volcanism migrated to the southeast (Barberi et al., 1994). Also, the Tyrrhenian coastal plains locally host widespread travertine deposits (Capezzuoli et al., 2009, 2010; Brogi & Capezzuoli, 2014; Mancini et al., 2019), that are generally associated with hydrothermal activity and deep CO₂ degassing (Barnes et al., 1978; Chiodini et al., 2000; Mancini et al., 2019). This results at the surface in tectonically controlled thermal springs (Chiodini et al., 2004; Minissale, 2004; Frondini et al., 2008; Brogi & Capezzuoli, 2009; Brogi et al., 2012; Mancini et al., 2019; Barberio et al., 2021). Often in the Central Apennines,

Fig. 2 - Simplified Tectonic map of Central Italy (modified from Cardello et al., 2021), showing the active margin units and the Mesozoic passive margin units. The shortening time is in italic. The Latium-Abruzzi carbonate platform consists of B, C and D units. Dashed lines are the traces of the cross-sections presented in Figure 3.

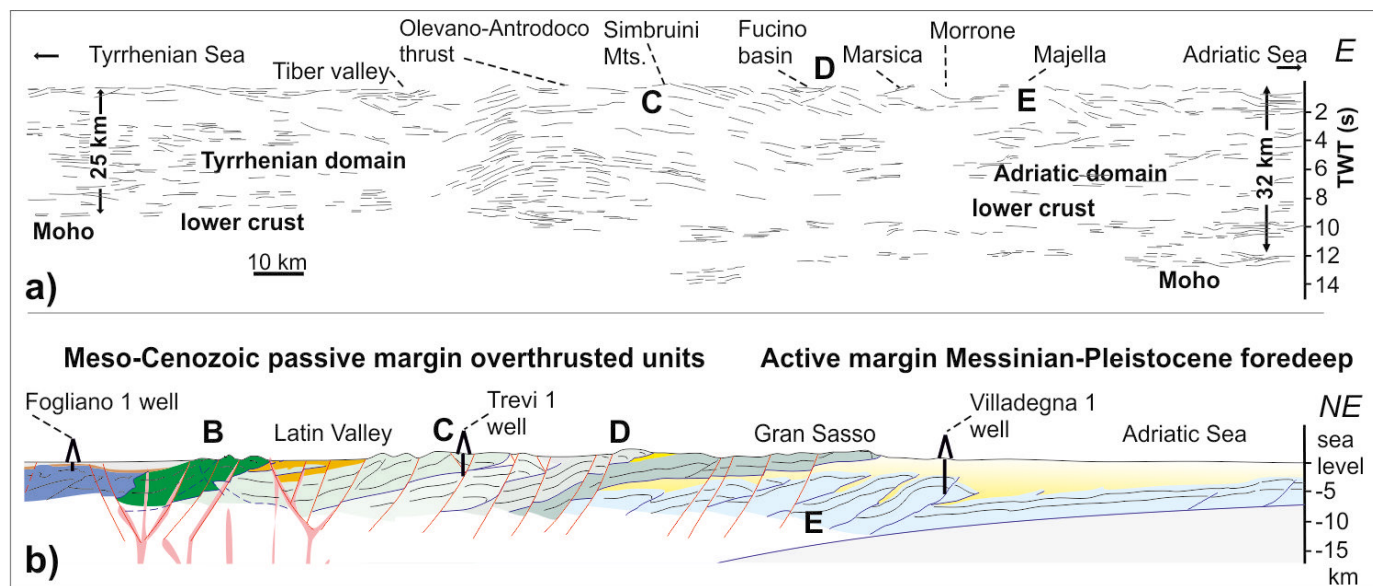


Fig. 3 - Crustal structure of Central Italy (modified from Cardello et al., 2021), showing the different structural domains. a) Line drawing of the E-trending CROP-11 seismic profile (redrawn after Billi et al., 2006). b) Depth interpretation of a NE-trending cross-section modified after Cardello et al. (2021). The traces of the cross-sections are presented in Figure 2.

faults are seismically active (e.g., Valoroso et al., 2013), or display neotectonics evidence (Galadini & Galli, 2000; Roberts & Michetti, 2004; Schlagenhauf et al., 2011; Alessandri et al., 2021). Locally, fluid overpressure and fluid uprising in fault zones have been affecting fault zones with cyclic veining (cf. Cardello & Mancktelow, 2015; Clemenzi et al., 2015) as also supported by hydrological and isotopic studies (e.g., Barberio et al., 2021; Gori & Barberio, 2021; Coppola et al., 2021).



Day 1 – Quaternary evolution of the Tyrrhenian Apennine margin

The first part of this day is dedicated to the Quaternary Tiber Valley deposits north of Rome; while the second part is on the travertine deposits of the Acque Albule Basin (Figs. 1, 2). This day shows the relationships among sedimentation, long-term (> 1 Myr) tectonics, volcanism, and the shorter-term climatic and eustatic controls on the Quaternary succession of the Tyrrhenian passive margin.

The Middle Valley of Tiber River (MVT) is a hilly area that extends for about 60 km along the NNW–SSE direction north of Rome (Fig. 4). Overall, the Tiber River is an axial drainage system with a single-channel meandering style that lies within the Paglia-Tevere Graben (Funicello & Parotto, 1978), a Neogene–Quaternary NNW–striking fault-bounded basin infilled with 1 km thick Plio-Quaternary marine and continental siliciclastic and volcanoclastic deposits (Martini & Sagri, 1993; De Rita et al., 1993; Barberi et al., 1994; Cavinato et al., 1994; Cavinato & De Celles, 1999). The valley is bordered to the east by the Amerini-Narnesi-Sabini carbonate ridge, and to the west by Quaternary volcanic edifices and the Mt.

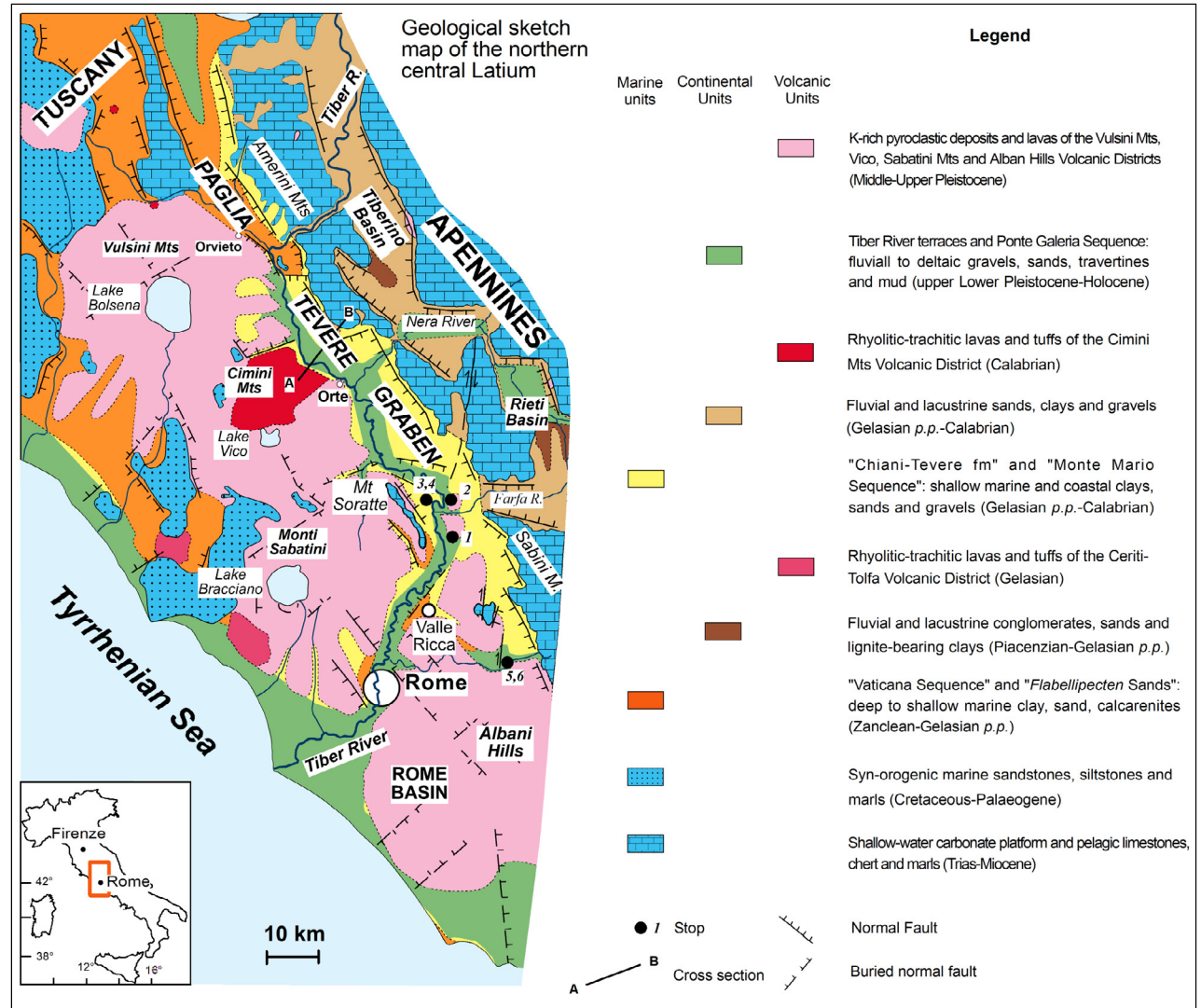


Fig. 4 - Geological sketch map (modified after Mancini et al., 2004) of the northern and central Latium showing the areal extent of the Pliocene and Quaternary marine, continental and volcanic deposits, all grouped into high rank stratigraphic units: depositional sequences and volcanic complexes. AB represents the location of a schematic cross section later presented in Figure 6.



Soratte horst (Fig. 4). This valley constitutes a complex graben (Buonasorte et al., 1987), whose depositional architecture is primarily controlled by extensional tectonics. Three 3rd order depositional sequences (*sensu* Vail et al., 1988) compose the basin fill that are also found in the Roman Basin (or Rome Basin in Fig. 4), which is partly laterally contiguous SW-ward to the Paglia-Tevere Graben. The sequences are interrupted by regional scale unconformities, slightly diachronous in the two basins (Fig. 5). As a whole, the sequences evolve from an open marine environment to a nearshore and fluvial-dominated environment. The chronological constraints are mainly provided by foraminifera biostratigraphy (benthic and plankton; Di Bella et al., 2002 and references therein), and subordinately by magnetostratigraphy (Sagnotti et al., 1994; Borzi et al., 1998), tephrochronology (Barberi et al., 1994), Sr isotope stratigraphy (Mancini et al., 2007). Here, we describe the succession from the bottom to the top (cf. Figs. 5, 6).

The Vaticana sequence crops out mostly in Rome (Milli, 1997; Milli et al., 2016) and spans from the late Zanclean to the early Gelasian (*G. punctulata*-*G. aemiliana* chronozones interval, from 4.0 to 2.2 Ma; Malatesta, 1974; Ambrosetti et al., 1987; Di Bella et al., 2002).

The second sequence spans from the late Gelasian to the Calabrian (*G. inflata*-*G. cariacensis* chronozones, from 2.1 to 1.3 Ma; Ambrosetti et al., 1987; Girotti & Mancini, 2003) and is composed by the two laterally continuous "Chiani-Tevere" and "Poggio Mirteto" formations (Mancini et al., 2004) that are over 300 m thick, and respectively representing the evolution from shallow marine, nearshore, to complex fluvial and delta plain settings.

The third sequence developed during the regional uplift that set about 1.4-1.3 Ma with an uplift rate ranging between 0.30 and 0.15 mm/yr, decreasing from NNE to SSW (Milli, 1997; Mancini & Cavinato, 2005; Mancini et al., 2007). Overall, the syn-uplift sedimentation is represented in the Paglia-Tevere Graben by a series of depositional fluvial terraces that are interlayered with tephra and lava flows (Fig. 6; Mancini & Cavinato, 2005). The recent alluvial plain developed in the last 20 ka.

Geological setting of the Acque Albule Basin

At the foothill of Tivoli (Figs. 1, 7), the Acque Albule locality occurs (Travertino di Bagni di Tivoli; TBTa, b, c, d; Servizio Geologico d'Italia, 2016). The homonymous basin is bordered by normal faults cross-cutting the inherited fold-and-thrust belt at the Cornicolani and Lucretili-Tiburtini mounts to the East and the Colli Albani volcano to the South. The basin is crossed by the Aniene River, a tributary of the Tiber River that runs to the W (Figs. 1, 2). The Acque Albule Basin (Fig. 7a, b) is famous for the *Lapis Tiburtinus* travertine, a material

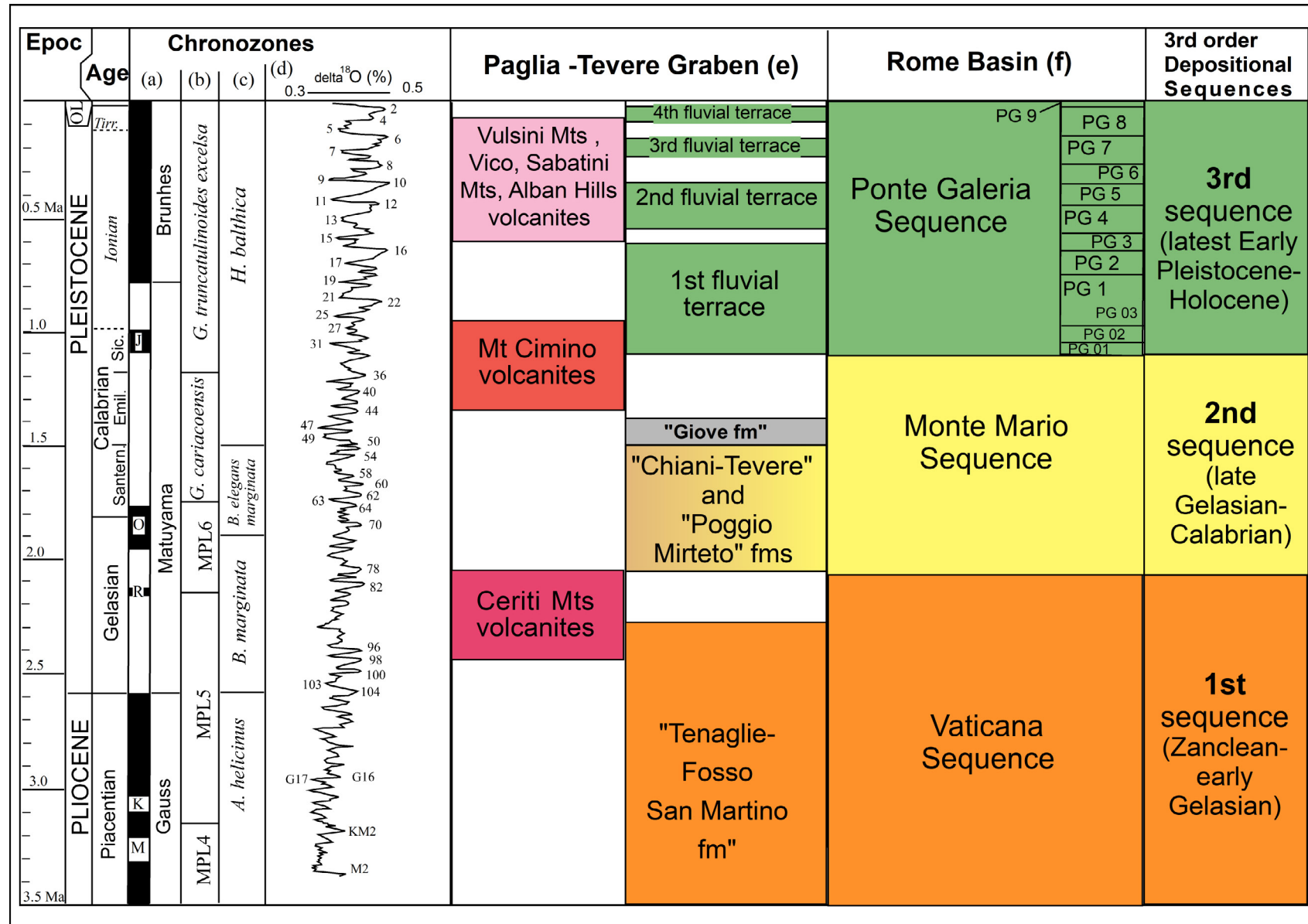


Fig. 5 - Litho-chronostratigraphic scheme of the Paglia-Tevere Graben and Rome Basin (Cavinato et al., 2004; modified). The two adjoining basins show a common history of infill, with three III order depositional sequences from the deep marine to continental environment. References: (a) Cande & Kent (1992); (b) Cita (1975); (c) Colalongo & Sartoni (1979); d) Shackleton et al. (1990); e) Mancini et al. (2004); f) Milli et al. (2016).

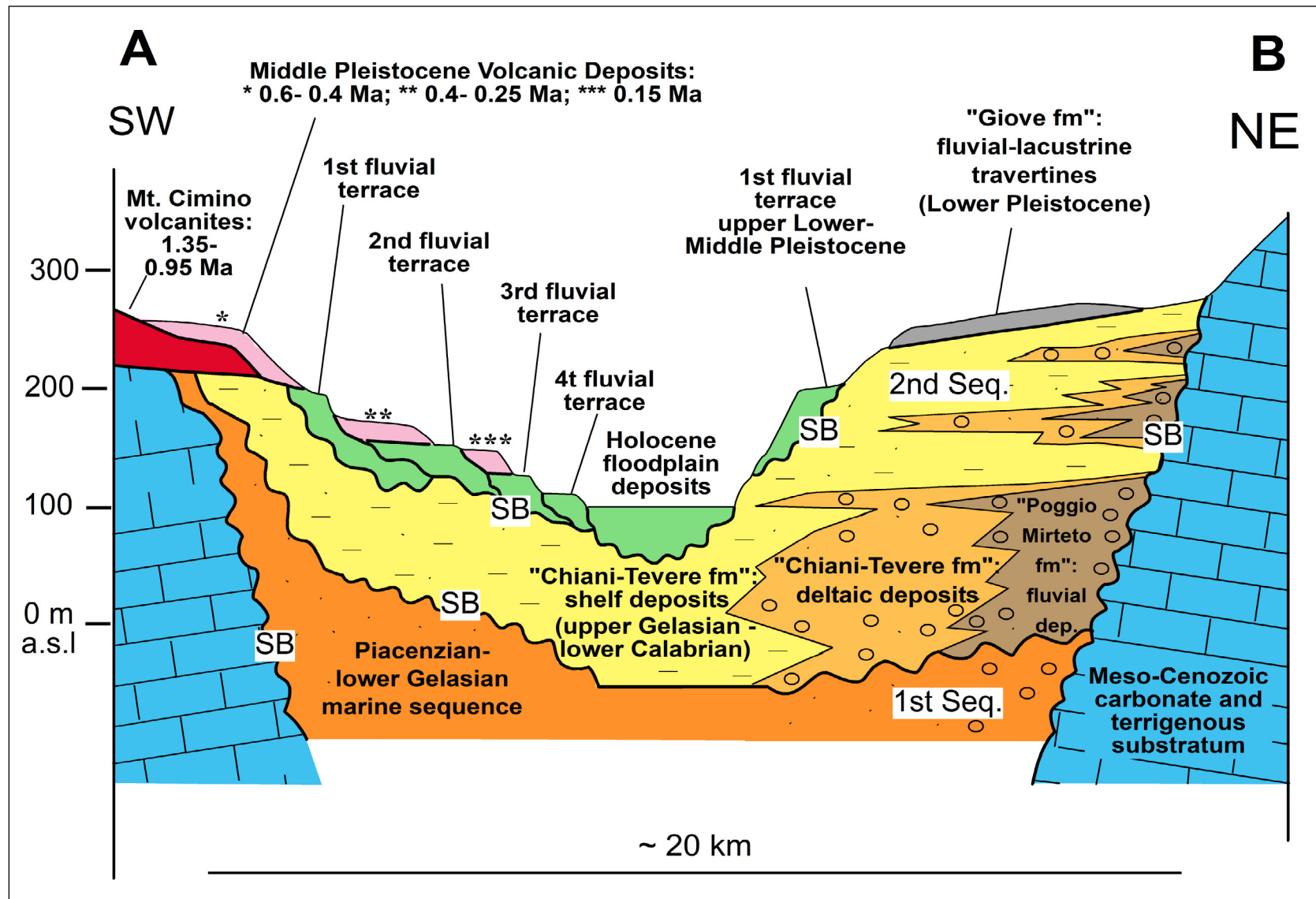


Fig. 6 - Schematic cross section showing the stratigraphic architecture of the Paglia-Tevere Graben (location in Fig. 4; partly modified after Mancini et al., 2007). SB = sequence boundary. From the oldest to the youngest, the terraces correspond to: "Civita Castellana unit" (first terrace: upper Lower-Middle Pleistocene *p.p.*, 1.2-0.6 Ma); "Graffignano unit" (second terrace: Middle Pleistocene, 0.55-0.4 Ma; Marine Isotope Stages MIS 14-11); "Rio Fratta unit" (third terrace: Middle Pleistocene, 200-150 ka; MIS 7-6); "Sipicciano unit" (fourth terrace: Upper Pleistocene; 100-20 ka).

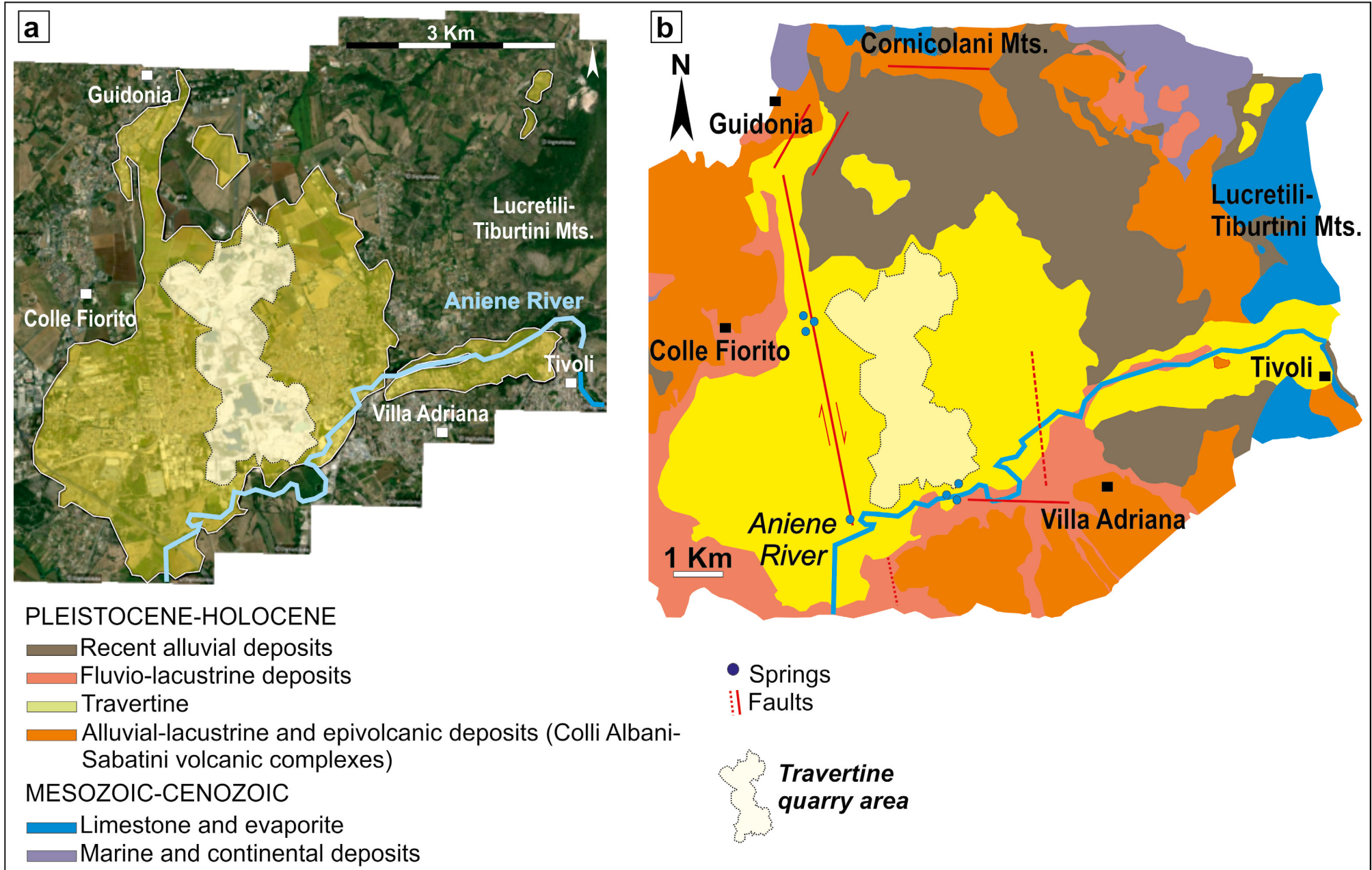


Fig. 7 - a) The quarried area in the Acque Albule Basin (modified from Google Earth, digital globe 2018). b) Geological map of the Acque Albule Basin (modified from Mancini et al., 2021).



largely used as ornamental stone by Roman architects since the I century BC. During the Late Pleistocene (115–30 ka; [Faccenna et al., 2008](#)), this deposit developed with a maximum thickness of ca. 90 m on the top of a Pleistocene siliciclastic succession ([De Filippis et al., 2013a, b](#)). A poorly lithoid travertine, known as *Testina* (TBTc; [Servizio Geologico d'Italia, 2016](#)), represents the uppermost and last carbonate depositional episode (29 ± 4 ka, [Faccenna et al., 2008](#); [Scalera et al., 2021](#)). The main N-striking fault coincides with the two main thermal springs of highly mineralised waters that reach ~23 °C. Their composition has H₂S, Fe, and other elements, and has a natural discharge volume of ca. 3000 l/s. The *Lapis Tiburtinus* travertines show carbon and oxygen isotope data mainly related to spring waters heated during transit in a high heat-flow area, enriched by CO₂ derived mainly from decarbonisation of Meso-Cenozoic limestones in the substratum, but also from a deeper source ([Minissale et al., 2002](#); [Mancini et al., 2019, 2021](#)).

The Lapis Tiburtinus travertine

The travertine lithofacies associations of [Erthal et al. \(2017\)](#) and [Della Porta et al. \(2017\)](#) have been here combined to simplify lateral and vertical heterogeneities ([Mancini et al., 2019a, 2021](#)). Shrub lithofacies association is a predominant facies association (Fig. 8a) characterised by clotted peloidal dendrite boundstone organised in tabular bodies, showing high lateral continuity (> 100 m) and a thickness of 40 m ([Chafetz & Folk, 1984](#); [Chafetz et al., 1991](#); [Guo & Riding, 1998](#); [Rainey & Jones, 2009](#)). The laminated deposit is a laminated micrite boundstone, that also forms tabular and lenticular bodies with a thickness up to 40 m (Fig. 8b).

The crystalline crust lithofacies association is a 10 m thick cementstone with lenticular convex upward geometries (Fig. 8c). The non-laminated deposit lithofacies association has mudstone to packstone texture with gastropods, mould of plants (up to 1 cm long), ostracods, charophytes stems. Beds are up to 5 m thick. The reworked deposit lithofacies have dark lenticular bodies with erosional surfaces at the base and are 1.5 m thick (Fig. 8e). Moderately sorted packstone to rudstone/floatstone with well-rounded to sub-angular intraclasts and extraclasts are common and have palaeocurrent clast-imbrication. The coated reed and phytoclast lithofacies association is ubiquitous and has a maximum thickness of 2 m (Fig. 8f). It occurs as boundstone with cylindrical moulds of plant stems. Intraclast deposit has laterally discontinuous beds (2 m thick) of floatstone/wackestone, packstone, and rarely rudstone with reworked angular intraclasts (Fig. 8g).

Travertine lithofacies are alternating with terrigenous and volcanic deposits ([Mancini et al., 2021](#)). Palaeosoils are mainly made of clay to coarser brown-orange clastic deposits (Fig. 8h) that sometimes fill karst cavities. Claystone and marlstone deposits have variable thickness and lateral extension (Fig. 8i) and are also composed



Fig. 8 - The different lithofacies regarding travertine, terrigenous and volcanic deposits of the Acque Albule Basin are indicated by arrows. a) Shrub lithofacies. b) Laminated deposit. c) Crystalline crust. d) Non-laminated deposit. e) Reworked deposit. f) Coated reed and phytoclast. g) Intraclast deposit. h) Palaeosoils (yellow arrow). i) Claystone and marlstone deposits. j) Sand, sandstone, and conglomerate (black arrow). k) Volcanoclastic deposits.

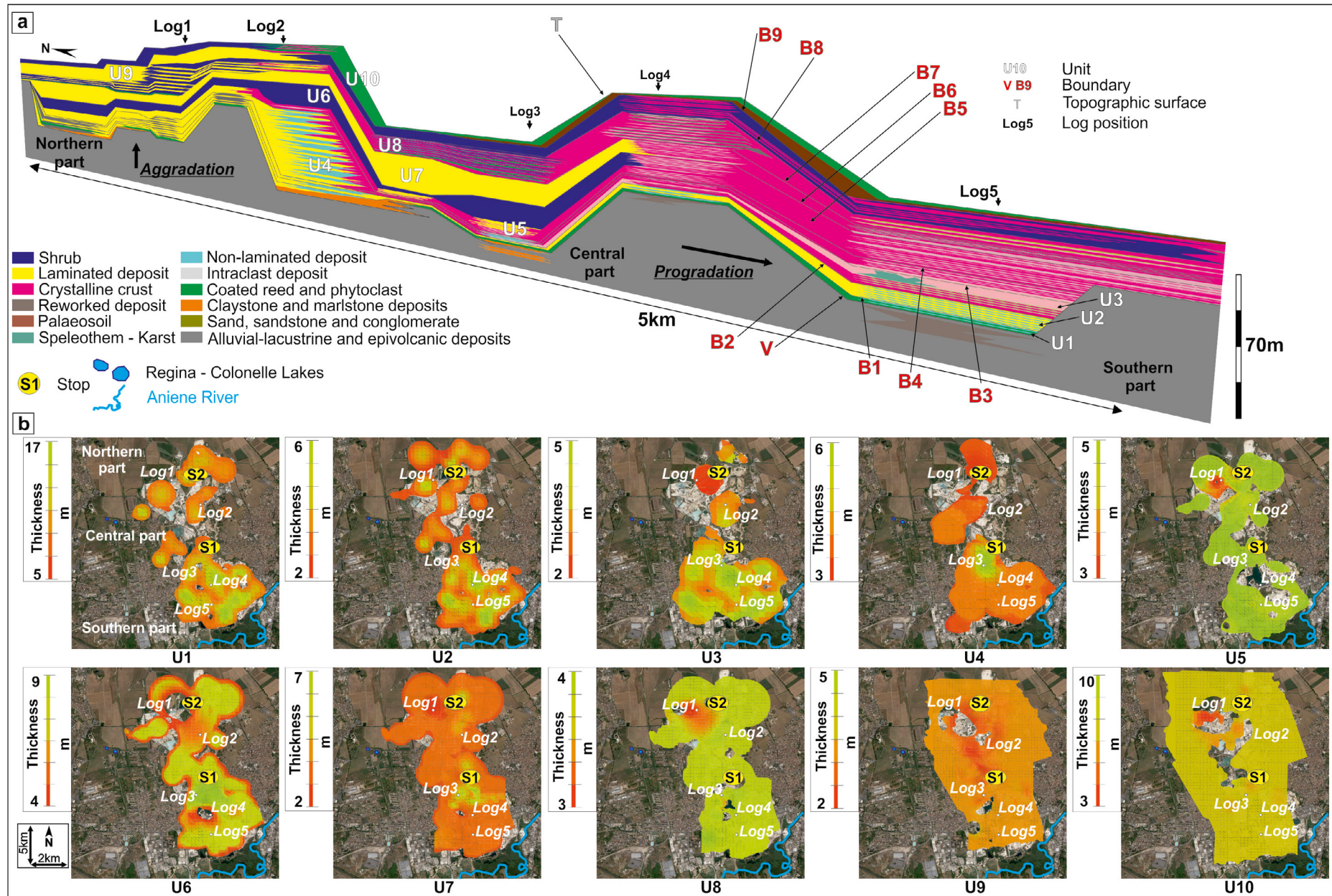


Fig. 9 - a) 2D model showing the relationships and the geometries of the different depositional units. b) the isopach model shown in Fig. 9a highlights the variation in thickness and the position of the stratigraphic logs (modified from Mancini et al., 2021).



of fine-grained silt, sand, and dark brown to yellow clay. Polymictic cross-bedded well-sorted conglomerates have extraclasts from the Apennines and a fine sandy matrix (Fig. 8j). The volcanoclastic deposits display different colours from brown, to black, grey or red (Fig. 8k) and have a maximum thickness of 5 m. They have been related to the Colli Albani and Sabatini volcanoes ([Della Porta et al., 2017](#)).

Surfaces, palaeoenvironments, and depositional model

In its 1.1 km³ volume, the *Lapis Tiburtinus* travertine displays several, superposed unconformity surfaces, related to non-deposition and erosion. These surfaces are associated with intraclast/reworked lithofacies or thin layers of brown claystone and marlstone. Surfaces reconstruction allows to identify the geometries of the depositional units mainly related to 1-2 km² sub-basin with subaqueous conditions and vertical thickness variations (Fig. 9).

Based on the lithofacies associations, four depositional environments were reconstructed (Fig. 10):

- 1) Subaqueous: shallow lakes, waterlogged flats, and pools with rare slopes envisaged from the alternation of lithofacies associations related to shrub, laminated deposit with aggradational trend.
- 2) Palustrine: swamps evolving into shallow lakes characterised by the association of non-laminated and laminated deposits, coated reed, and phytoclast lithofacies, alternating with intraclast deposits and palaeosoils. Phytoclasts and charophytes suggest the presence of cooled thermal water or/and mixed freshwater.
- 3) Travertine channels: high hydrodynamism is testified by reworked travertine with well-rounded clasts, whose imbrication and traction structures are the result of the Aniene River dynamics.
- 4) Slopes: crystalline crusts with laminated deposits and occasionally coated reed and phytoclast lithofacies are representative of high-energy setting with very thin sheets of water flowing over a planar, low-angle slope surface (7-10°) and rapid CO₂ degassing ([Guo & Riding, 1998](#); [Della Porta et al., 2017](#); [Mancini et al., 2019](#)).

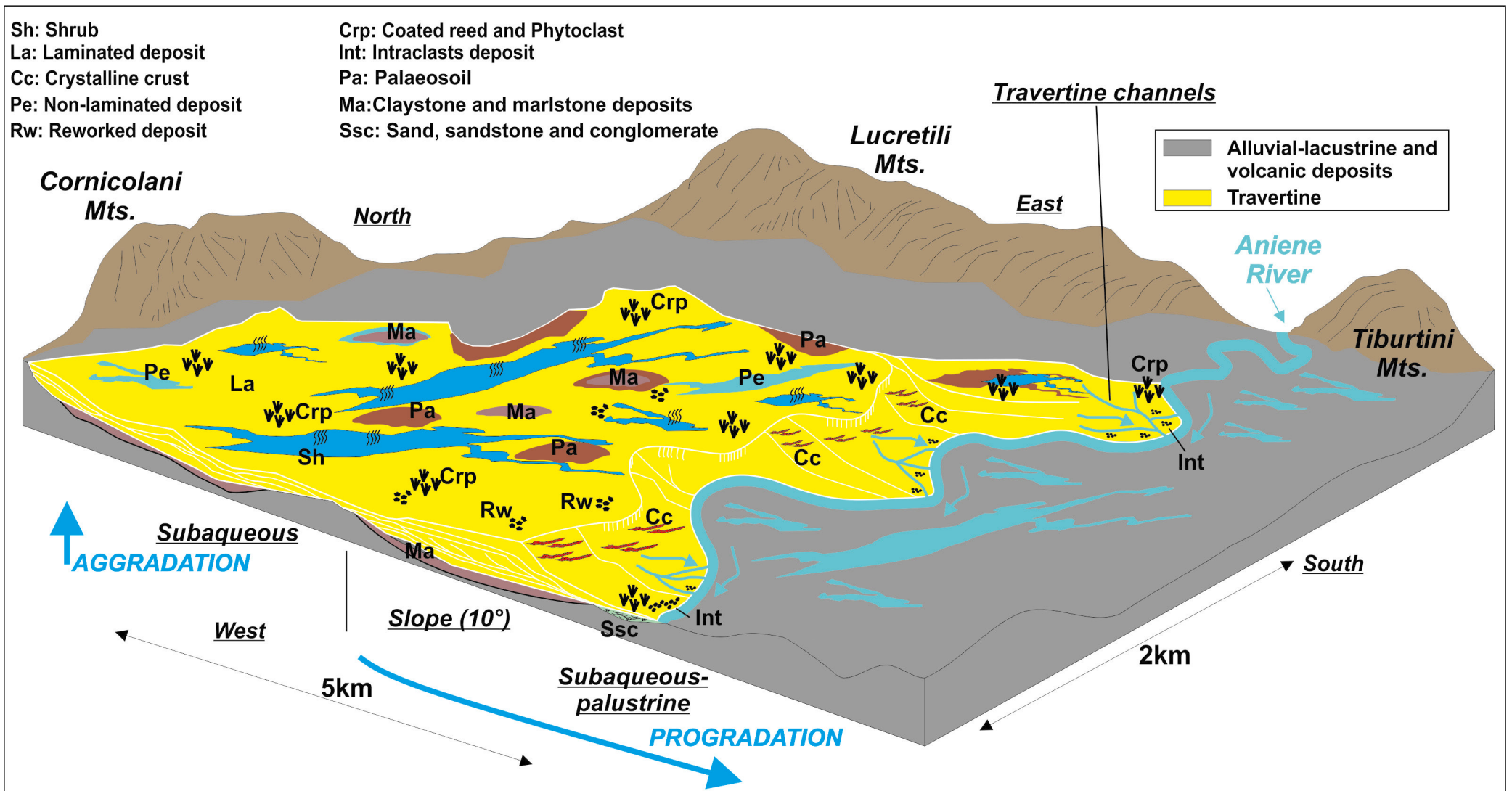


Fig. 10 - Depositional model of the Acque Albule Basin (modified after Mancini et al., 2021).



Stop 1.1. The Middle Pleistocene Tiber deposits at Passo Corese (42°10'29"N; 12°38'26"E)

The first stop (Figs. 4, 11) is in the abandoned "Casa dei Preti" quarry with cliffs. Excavation fronts are NW- and NE-oriented (Fig. 12a), thus allowing a 3D vision of the fluvial lithofacies distribution.

As shown in Figure 11, two lithostratigraphic units are exposed: at the base the fluvial "Graffignano unit" (up to 20 m thick); at the top the "*Tufi stratificati varicolori di Sacrofano* Auct."

From the base (Fig. 12), the "Graffignano unit" is composed of: a) massive calcareous floodplain sands with interbedded palaeosoils and lenses of channel gravels (ribbon structure); b) a 6-10 m thick interval of amalgamated gravels, cross-bedded and planar horizontal bedded (Gt and Gh lithofacies in Miall, 1996); c) a 3-5 m thick interval of planar bedded floodplain silty sand interbedded in hydromorphic soil horizons and pebbly ribbons; d) 4-5 m thick layered freshwater tufa, with pisoids and root traces.

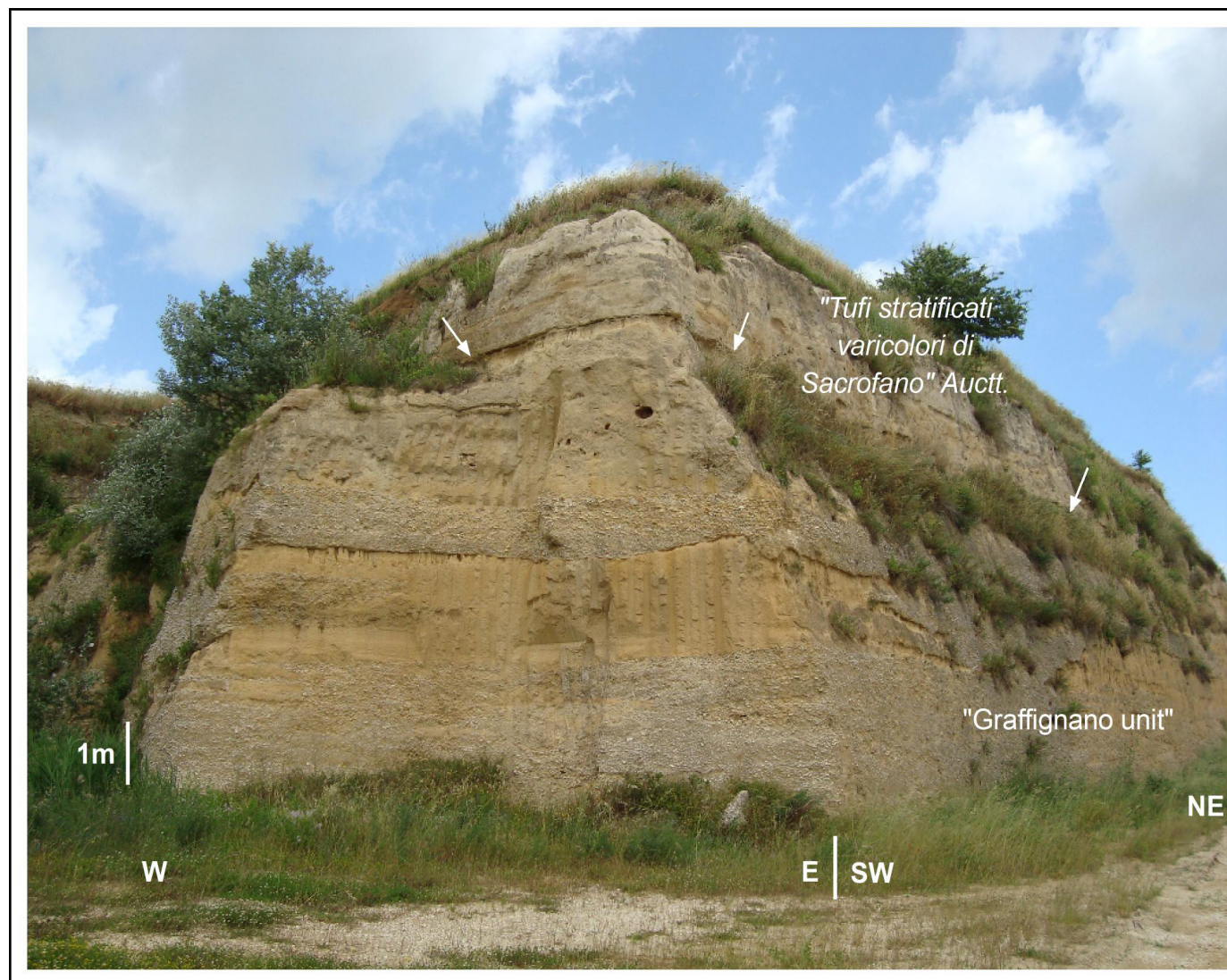
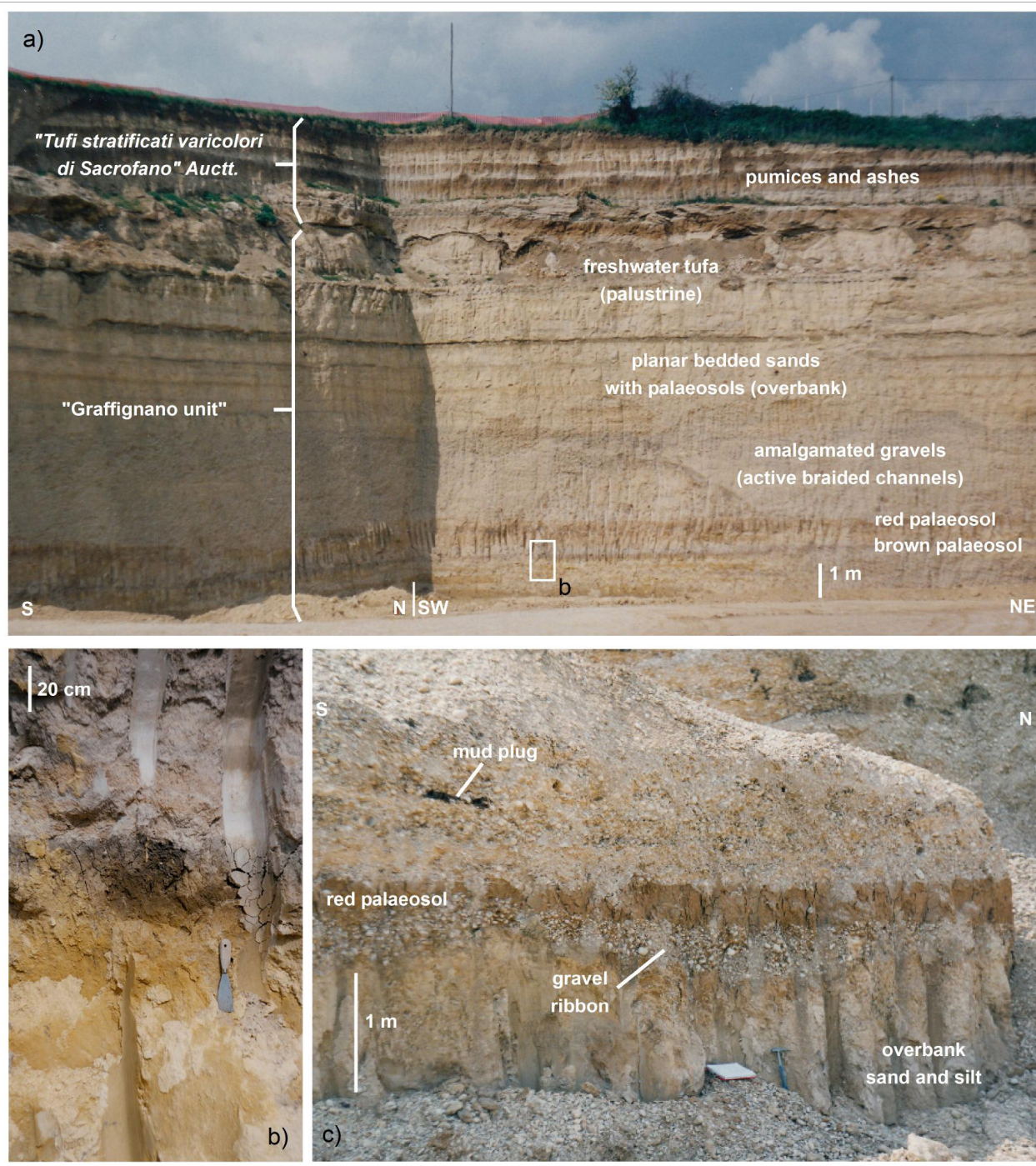


Fig. 11 - "Casa dei Preti" quarry. Middle Pleistocene gravelly and sandy fluvial deposits of the "Graffignano unit" overlain by freshwater tufa and tuffs ("*Tufi stratificati varicolori di Sacrofano*" Auctt., ~ 500 kyr old; Sottili et al., 2004). White arrows mark the lithostratigraphic limit.



Gravel pebbles are mostly derived from the Apennines while the sandy matrix, that is carbonate-rich, also contains quartz, feldspar, and volcanic ferro-magnesian minerals. Mud clasts derive from the nearby Plio-Pleistocene marine successions. The stacking pattern of gravels is the expression of the complex amalgamation of active channel bedforms and bar-forms in a braided river environment (Miall, 1996). The overlaying silty sands are referred to a dominance of overbank fines isolating small active pebbly channels (ribbons). Hydromorphic palaeosoils suggest conditions of partial waterlogging in the alluvial plain; the palustrine tufa on top indicate the abandonment of the active channels and a permanent supply of CaCO₃-enriched water from nearby springs. The facies organisation shows a

Fig. 12 - a) 3D view of the depositional architecture of the "Graffignano unit" (II terrace of the Tiber) with the fining upward stacking of facies, from active channel gravels to overbank sands and palustrine freshwater tufa; note the laterally continuous palaeosols. b) Grey-brown, organic rich palaeosol (Inceptisol; Retallack, 2001), with well-distinguished horizons. c) Red-orange oxidised palaeosol (Entisol), interbedded between gravels and sands.



clear fining-upward trend. During the Middle-Late Pleistocene, this portion of the valley was more inland with respect to the coeval coast, thus out of the glacio-eustatic influence (Mancini & Cavinato, 2005). This suggests that terrace degradation and aggradation were exerted mostly by the cyclic glacial-interglacial alternance under ongoing tectonic uplift (Fig. 13), which modulated stream power and sediment load (Blum & Törnqvist, 2000).

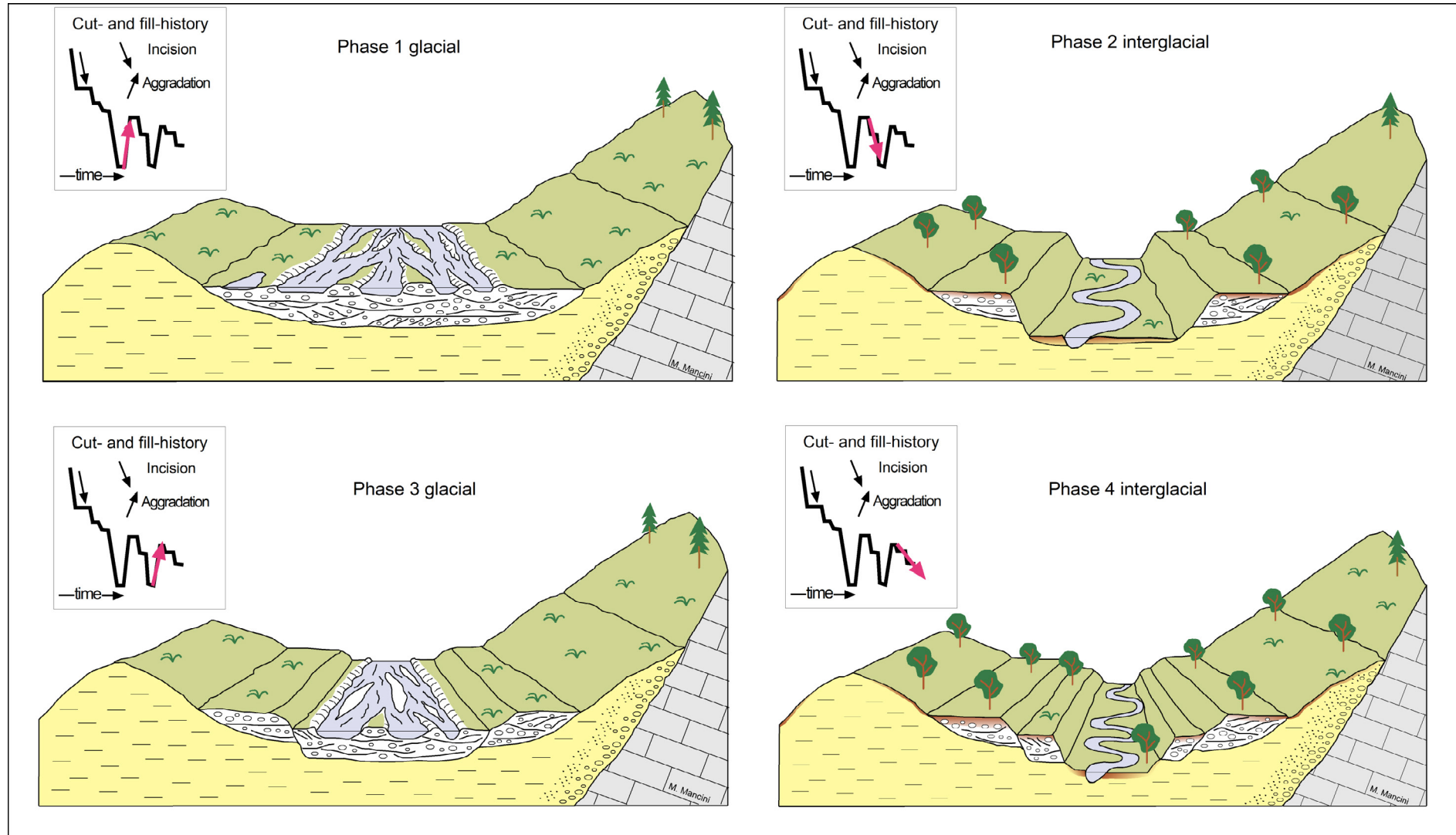


Fig. 13 - Cycles of climate-related syn-uplift terraces aggradation and degradation. Not to scale.



Stop 1.2. The Early Pleistocene transgression at Poggio Mirteto Scalo (42°14'23"N; 12°38'05"E)

The Poggio Mirteto section (Fig. 14) exposes the Gelasian-Calabrian transition between the "Poggio Mirteto fm" in the lower portion, and the "Chiani-Tevere fm" on the top. The base consists of 8 m of cross-bedded fluvial gravels with lenses of beige silty sands and pedogenised blue clays with *Helicidae* and root traces, referred to a fluvial-delta plain environment (Fig. 15a). The gravels produced by braided-river channels (Fig. 15b) are stacked in typical multilateral-multistorey pattern; the finer sediments are referred to the overbank sub-environment of the alluvial-inner delta plain. Then, a 3-4 m thick tabular body of horizontally bedded blue-grey clays (lagoon pelite in Fig. 15b) crops out, with lignite horizons and sandy fossiliferous lenses. Clays are referred to the basin lagoon environment and are organised into massive beds, up to 30 cm thick (Fig. 15c), or with planar lamination (Fig. 15d). These lagoon clays and sands contain alternated shell-beds of freshwater (*Melanospis nodosa*) and brackish water molluscs (*Cerastoderma glaucum*, *Anadara* sp., *Potamides tricinctus*), while ichnofossils are represented by sand-infilled traces (*Callianassa* isp., *Ophiomorpha* isp.) and diffuse tiering in the underlain clays (Fig. 15c). The lagoon deposits are then overlain by 5 metres of cross-bedded fluvial-delta plain gravels and sands (Figs. 15a and 15b).

In the upper portion of the section the fluvial-lagoon deposits are truncated by a horizontal net surface, above which a hard, well-cemented calcarenite level, 2-3 m thick, occurs (Figs. 15a, 15b, and 16a) with basal pebbles and widespread fragments of mollusc shells, echinoids, bryozoans, foraminifers (*Elphidium* sp., *Ammonia* sp.) and red algae. On the calcarenite level, grey-blue massive silt, and clay with intercalated dm-thick cross-laminated sandy beds with hummocky cross-stratification crop out. These deposits belong to an open marine



Fig. 14 - Panoramic view of the Poggio Mirteto Scalo section from south-west.

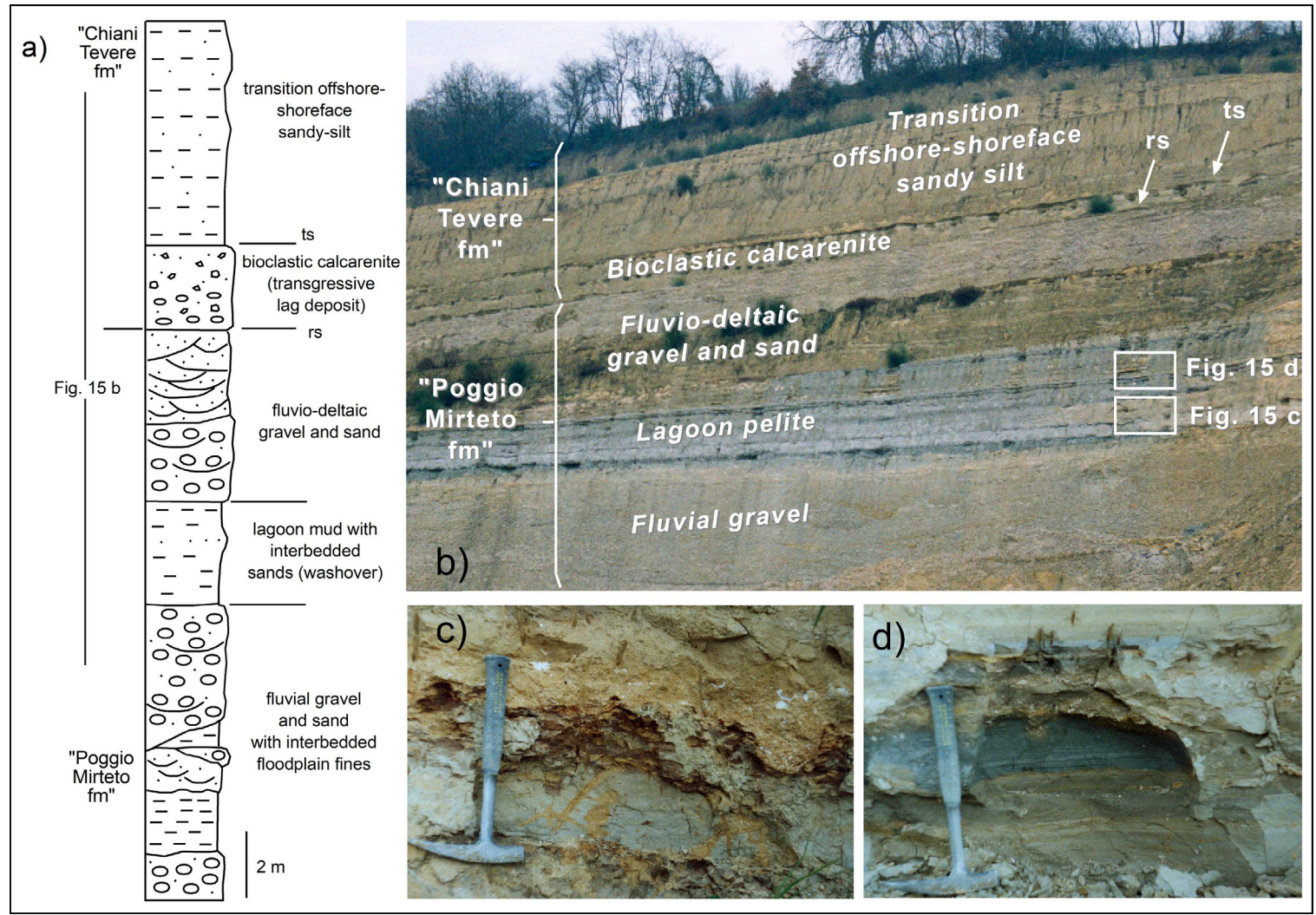


Fig. 15 - a) Poggio Mirteto Scalo stratigraphic log: rs = ravinement surface; ts = transgressive surface. b) Vertical stack of the fluvial, lagoon and open marine facies in the section. c-d) Details of the lagoon deposits: c) grey-blue massive clay, intensely bioturbated by crustaceans' burrows (*Callianassa* isp., *Ophiomorpha* isp.), and overlain by yellow coarse-sized sands with erosional base and a reworked association of brackish-marine molluscs (*Cerastoderma glaucum*, *Potamides tricinctus*); the sands are interpreted as wash-over sediments transported from the shore to the inner lagoon, probably by after storm events. d) Planar, thinly laminated blue-grey clay (undisturbed inner lagoon pelite). The hammer is 35 cm long.



environment (transition offshore-shoreface; Fig. 15a and 15b) and contain a rich malacofauna with *Pelecypora brocchii* (Fig. 16) and *Panopaea glycimeris* in life position.

In summary, the Poggio Mirteto Scalo section shows a fining/deepening upward trend of facies from the river-delta plain to the lagoon and the open marine environment. The calcarenite level and the overlaying fine sediments with *P. brocchii* are commonly found in several other sections of this portion of the basin (Fig. 16) and are interpreted as transgressive deposits on the deltaic bodies. The basal surface of the calcarenite is sharp and erosional and is interpreted as a Ravinement Surface (RS) likely incised by the waves action on the underlying fluvial-coastal deposits during a rapid phase of shore retreat. The upper boundary of the calcarenite, below the marine, is a transgression (marine flooding) surface.

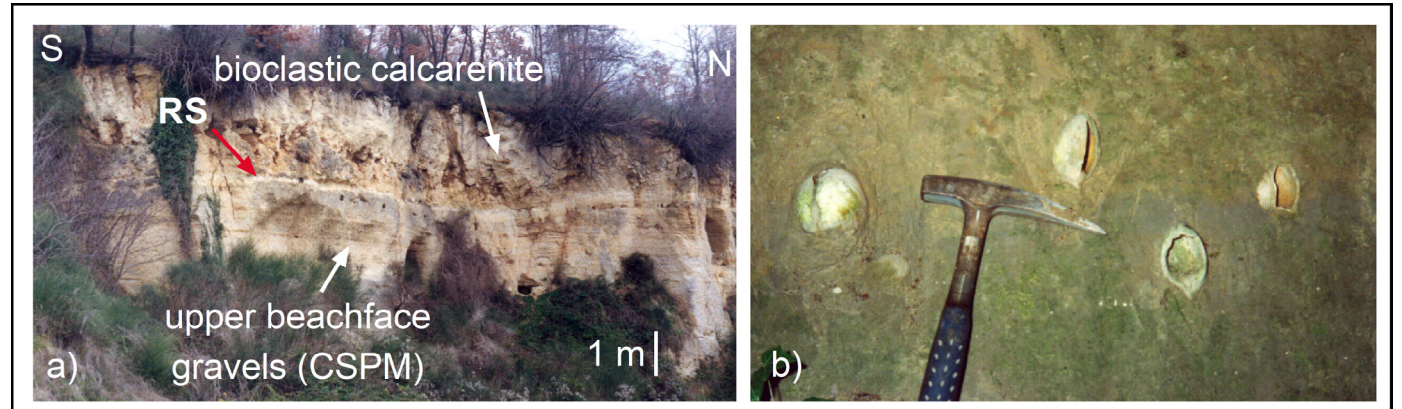


Fig. 16 - a) Bioturbated and weathered bioclastic calcarenite (transgressive lag, 2.5 m high) overlaying planar bedded, upper beachface gravels of the "Civitella San Paolo member" (first prograding wedge of the "Chiani Tevere fm", Mancini et al., 2004, CNH in Sheet 345; Servizio Geologico d'Italia, 2019). The calcarenitic basal surface is slightly erosional and is interpreted as a ravinement surface (RS). b) Grey massive sandy clays of offshore environment with *Pelecypora brocchii* in life position (credits Dr M. Borzi, 1991). The hammer is 35 cm long. These clays overlay the transgressive lag deposits throughout the entire basin.

Continental to brackish water association: ostracods to molluscs

The lithofacies variability observed in the paralic palaeo-environments of MVT is also well expressed in the rich and diversified fossil assemblages preserved in the sediments. Ostracods, foraminifers, and molluscs dominate such associations. The most representative ostracod and mollusc species are shown in figures 17 and 18 respectively. Generally, Pleistocene fluvial deposits often contain marine specimens reworked from Pliocene clays in their catchments, the latter forms being characterised by more opaque, white shells. The most common species is *Cyprideis torosa*, a euryhaline temporary and permanent water

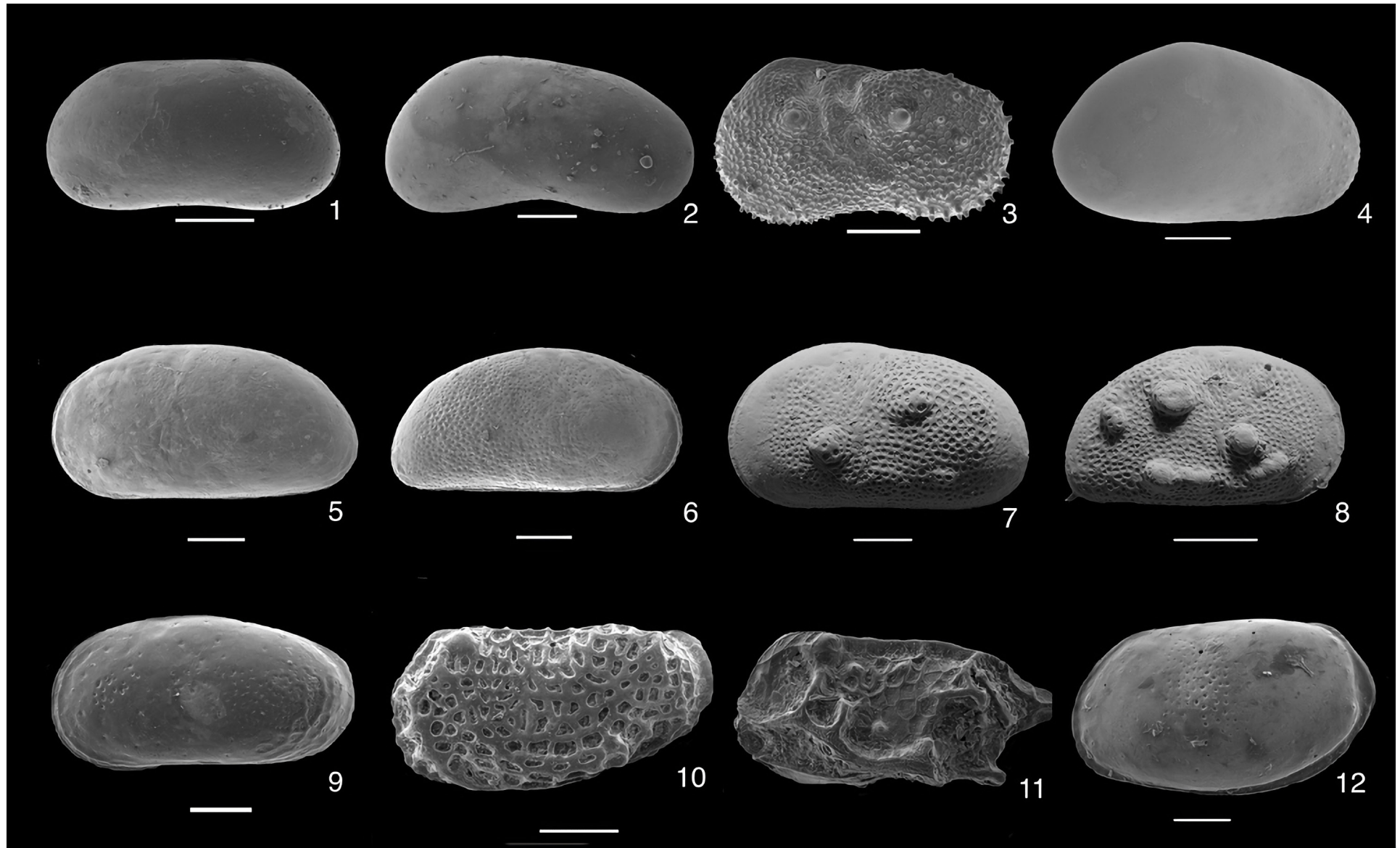


Fig. 17 - SEM pictures of the most represented ostracod species in selected sites along the Middle Valley of the Tiber River. Freshwater assemblage: 1) *Candona candida*; 2) *Candona neglecta*; 3) *Ilyocypris monstrifica*; 4) *Heterocypris salina*. Euryhaline assemblage: 5) *Cyprideis torosa*, smooth form; 6) *Cyprideis torosa*, smooth form; 7) *Cyprideis torosa*, noded form; 8) *Cyprideis torosa*, noded form. Shallow marine assemblage: 9) *Leptocythere ramosa*; 10) *Loxoconcha littoralis*; 11) *Semicytherura dispar*; 12) *Palmoconcha turbida*. Scale bars = 0.1mm



dweller (Fig. 17; 5-8). The shell surface can be characterised by nodding, an ecophenotypical morphology related to salinity variations: smooth shells occur in typically euryhaline waters whereas noded shells characterise environments with salinities around 8 per mill. In samples, where *C. torosa* is dominant, the accompanying fauna could be very indicative. In euryhaline environments (i.e., coastal lagoons or deltas), *C. torosa* could be accompanied by the shallow marine *Leptocythere ramosa*, *Loxoconcha littoralis*, *Semicytherura dispar*, *Palmoconcha turbida* (Fig. 17; 9-12). At Nazzano, in the sandy terms also ostracods, *Pecten* spp. and *Balanus* spp. are common. The benthic foraminifers are characterised by the association *Ammonia beccarii-Lobatula lobatula* typical of an infralittoral environment (Di Bella et al., 2002). The lagoonal facies are characterised by *C. torosa* as a monotypic assemblage. When the *C. torosa* occurs in its noded form, often *Heterocypris salina* (Fig. 17; 4) is the accompanying species indicating a salinity range of 5-8 per mill. The foraminifers are dominated by *Ammonia tepida* and *Haynesina germanica* (Di Bella et al., 2002). The macrofauna is abundant and consists of *Cerastoderma glaucum*, *Potamides* spp., *Melanoides curvicosta*, and sometimes *Melanopsis nodosa* (Fig. 18; c-f). In more typically freshwater environments, the ostracods *Candona neglecta*, *C. candida* and *Ilyocypris monstifica* occur (Fig. 17; 1-3), while foraminifers disappear, and molluscs are represented mainly by *Bithynia opercula* and by the typical late Villafranchian assemblage with *Theodoxus (N.) groyanus* and *Melanopsis nodosa* (Fig. 18; a-b; see also Esu & Girotti, 2020).

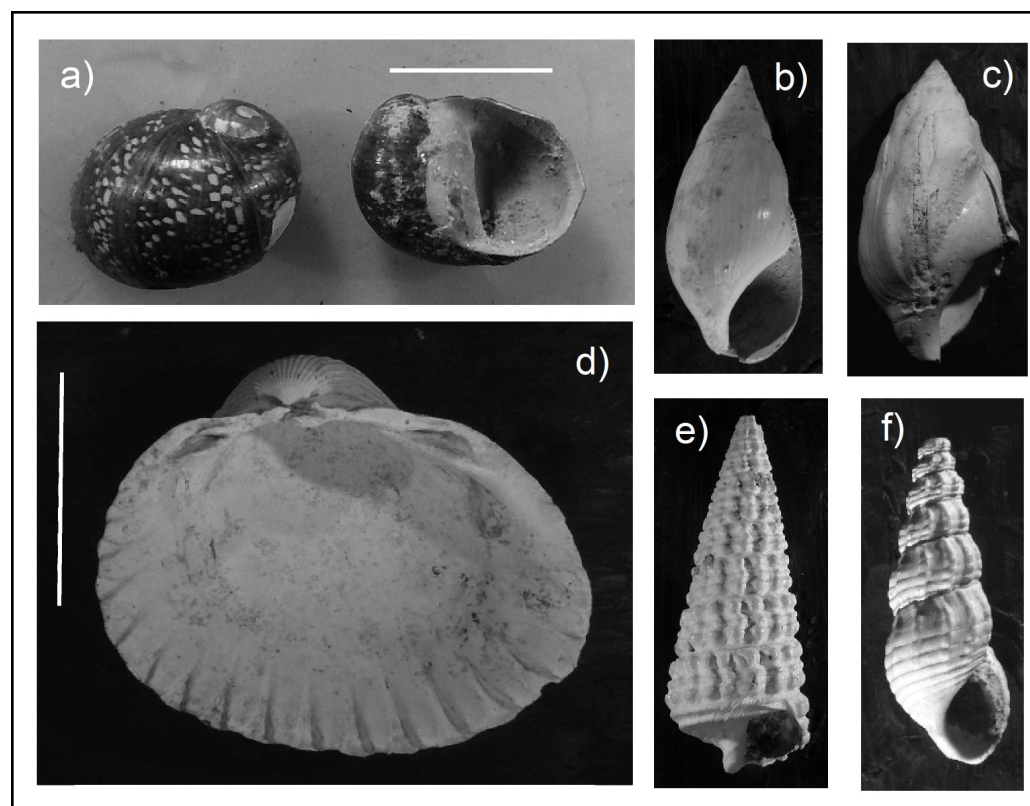


Fig. 18 - Optical microscope pictures of the most represented mollusc species in selected sites along the Middle Valley of the Tiber River. Freshwater assemblage: a) *Theodoxus (Neritaea) groyanus* (scale bar: 0.5 cm); b) *Melanopsis nodosa*, typical freshwater form (1 cm long); c) *Melanopsis nodosa*, typical brackishwater form (1 cm long); d) *Cerastoderma glaucum* (scale bar: 1 cm); e) *Potamides tricinctus* (2 cm long); f) *Melanoides curvicosta* (1 cm long).



Stop 1.3. The progradational shallow water delta of Torrita Tiberina (42°14'05"N; 12°36'42"E)

This stop is in the Nazzano Tevere-Farfa Regional Nature Reserve, on the western Tiber bank and it consists of steep incised cliffs (Fig. 19), preserving a succession with:

- a) blue-grey, massive, sandy clays and silts that are up to 20 m thick, rich in marine molluscs (*Pelecypora brocchii*, *Pecten* spp.) correlated to the uppermost marine deposits of Stop 1.2;
- b) cross-bedded gravels and sands > 40 m thick of the "Torrita Tiberina member" (TTM, Mancini et al., 2004; CNH₁, Servizio Geologico d'Italia, 2019);
- c) grey silty sand (some 10 m thick) on the top, containing infralittoral marine molluscs: *Callista chione*, *Nassarius mutabilis*, *Amyclina semistriata*.

The TTM gravels and sands define a WSW-prograding coarse-grained river delta of the shallow-water/shelf type (Reading & Collinson, 1996), embedded into shelf clays and sands at the base and top. This succession is interpreted as a delta front that shows a coarsening upward trend of facies: from sandy pebbles with lenses of cross-stratified sands, in the lower portion, to cross-stratified gravels above. The cross-

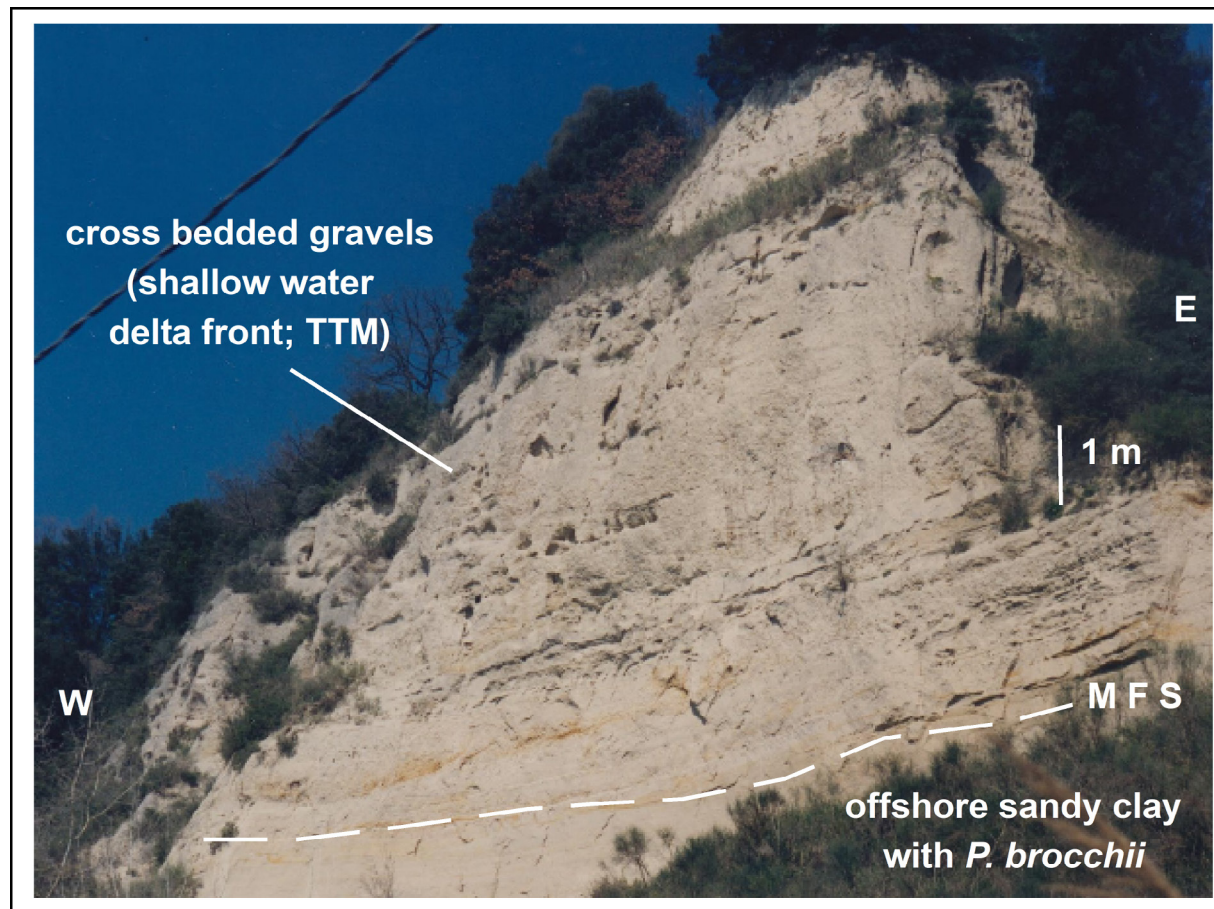
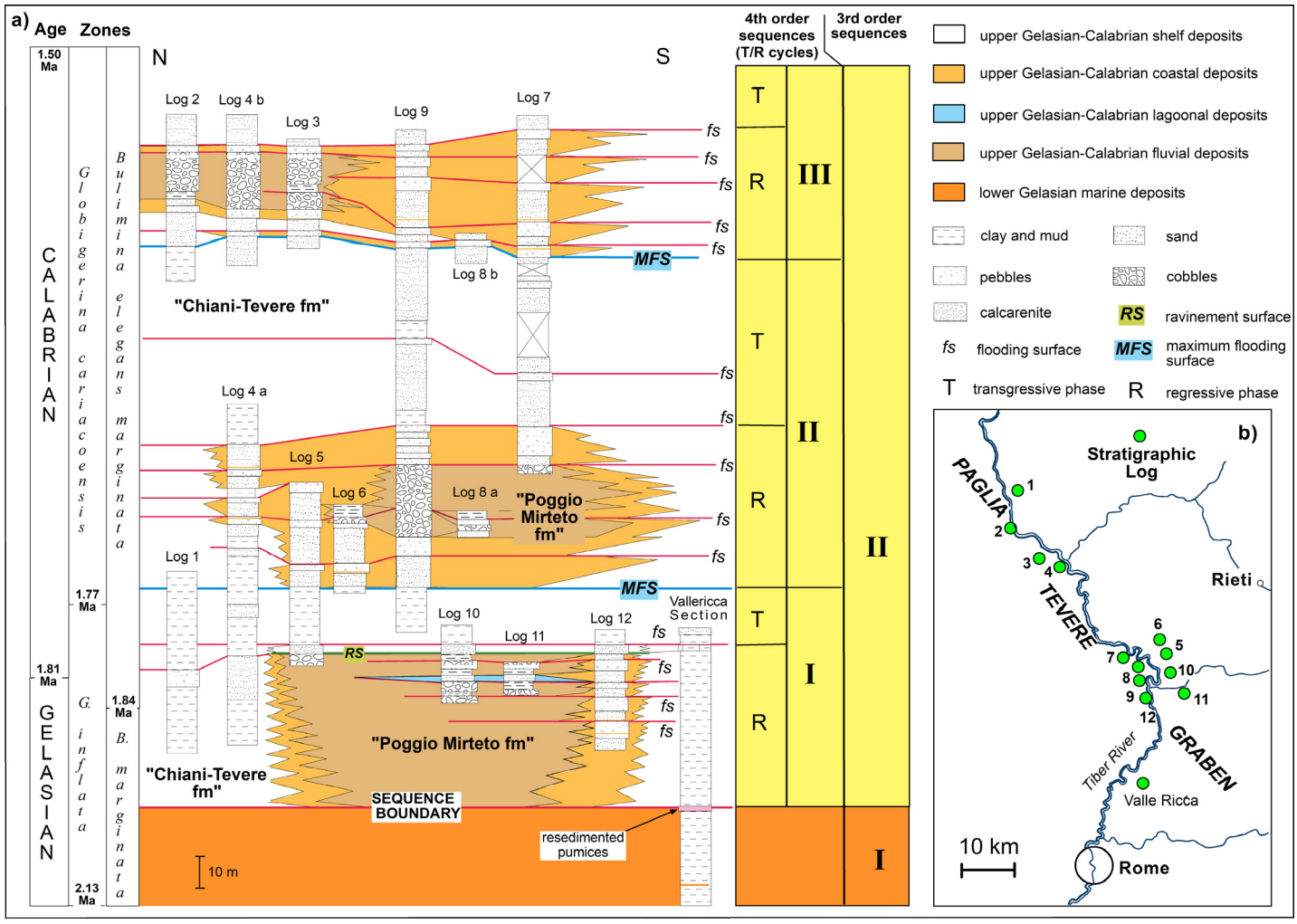


Fig. 19 - Shelf clays of the "Chiani-Tevere fm" with *Pelecypora brocchii* overlain by the westward-directed (to the left) progradational delta-front gravels and sands of the "Torrita Tiberina member" (TTM; Calabrian; CNH *sensu* Servizio Geologico d'Italia, 2019). The "Torrita Tiberina member" represents the second prograding clastic wedge within the "Chiani-Tevere fm" and is referred to a coarse-grained shallow-water river. MFS is a maximum flooding surface of an IV order cycle within the "Chiani-Tevere fm" (III order, composite, depositional sequence); this is placed at the base of the progradational regressive TTM. The outcrop corresponds to the lower portion of Log 9 in Figure 20.



bedding indicates prevailing WSW-directed palaeo-flows. The basal surface above the clays is sharp and slightly undulate and marks the transition from transgressive shelf clays to overlying regressive gravelly-sandy delta, typical of a depositional regression. The topmost grey silty sands above the deltaic body are again transgressive onto the gravels. The Torrita Tiberina section is directly correlated with the Poggio Mirteto Scalo section (logs 9 and 10 in Fig. 20) through the common occurrence of the *Pelecypora brocchii* bearing shelf clay and silt. The presence of the same marker beds in various sections, such as

Fig. 20 - a) Correlation panel among selected stratigraphic and sedimentological logs, in along-strike view. In the left columns, there are reported the geochronological and biostratigraphic (plankton and benthic foraminifers) units. In the centre, the three main progradational clastic wedges are shown, in pale and dark brown, found within the "Chiani-Tevere" and corresponding to the "Civitella San Paolo" fms (CNH in Servizio Geologico d'Italia, 2019), "Torrita Tiberina" and "Vasanello" members (Mancini et al., 2004), in chronological ascending order. In the right columns, there are reported the III and IV order depositional sequences; the IV order d.s. are defined by R-T regressive-transgressive cycles, with the R regressive half-cycles corresponding to the clastic wedges. Maximum flooding surfaces are referred to the high frequency cyclicity; RS is a ravinement surface. Log 10 is the Poggio Mirteto Scalo section, while Log 9 is the composite Torrita Tiberina-Nazzano section (modified after Girotti & Mancini, 2003; Cavinato et al., 2004). b) Location map of the stratigraphic logs.



the bioclastic calcarenite level or the *Pelecypora brocchii* clay and silt seen in the stops, coupled with available bio-, magneto- and tephra-stratigraphic data allow to correlate sections of the “Chiani-Tevere” and “Poggio Mirteto” formations (Fig. 20). This lets us reconstruct the whole stratigraphic architecture of the upper Gelasian-lower Calabrian 3rd order depositional sequence of MVT (Fig. 20; see also Fig. 5), interpreted as a composite sequence (*sensu* Mitchum & Van Vagoner, 1991), and to recognise 4th order depositional sequences within it.

Stop 1.4. The Calabrian nearshore and the Middle Tiber Valley palaeogeographic evolution at Nazzano (42°14'07"N; 12°36'04"E)

The panoramic view shows the late Quaternary fluvial terraces, the Plio-Pleistocene deposits, and the carbonate substratum (Fig. 21). The MVT sequences sedimentological studies have led to the palaeogeographic reconstructions shown in Figs. 22 and 23. In the Pliocene-Early Pleistocene, up to ~1.4 Ma, the MVT Paglia-Tevere Graben was actively subsiding, because of the transtensive tectonics related to the opening of the back-arc Tyrrhenian Basin. The basin developed at the western front of the Apennines and hosted a dominant marine sedimentation. The neighbouring intermountain Tiberino and Rieti basins were also subject to the tectonic extension but were not interested by marine transgression as in Pliocene times the Apennines were already emerged (Mancini & Cavinato, 2005). The major changes in the coastline position were related to the cyclic progradation and retrogradation of the fluvio-deltaic systems. Flowing with transverse drainage with respect to the main morpho-structural axis, the rivers provided sediment supply to the slowly subsiding Paglia-Tevere Graben.



Fig. 21 - Panoramic view on the Tiber valley from Nazzano to the south. In the foreground, the plain crossed by the river and bounded by the Quaternary terraces, in the Nazzano Tevere-Farfa Regional Nature Reserve; in the background, the Lucretili and Cornicolani Mts.

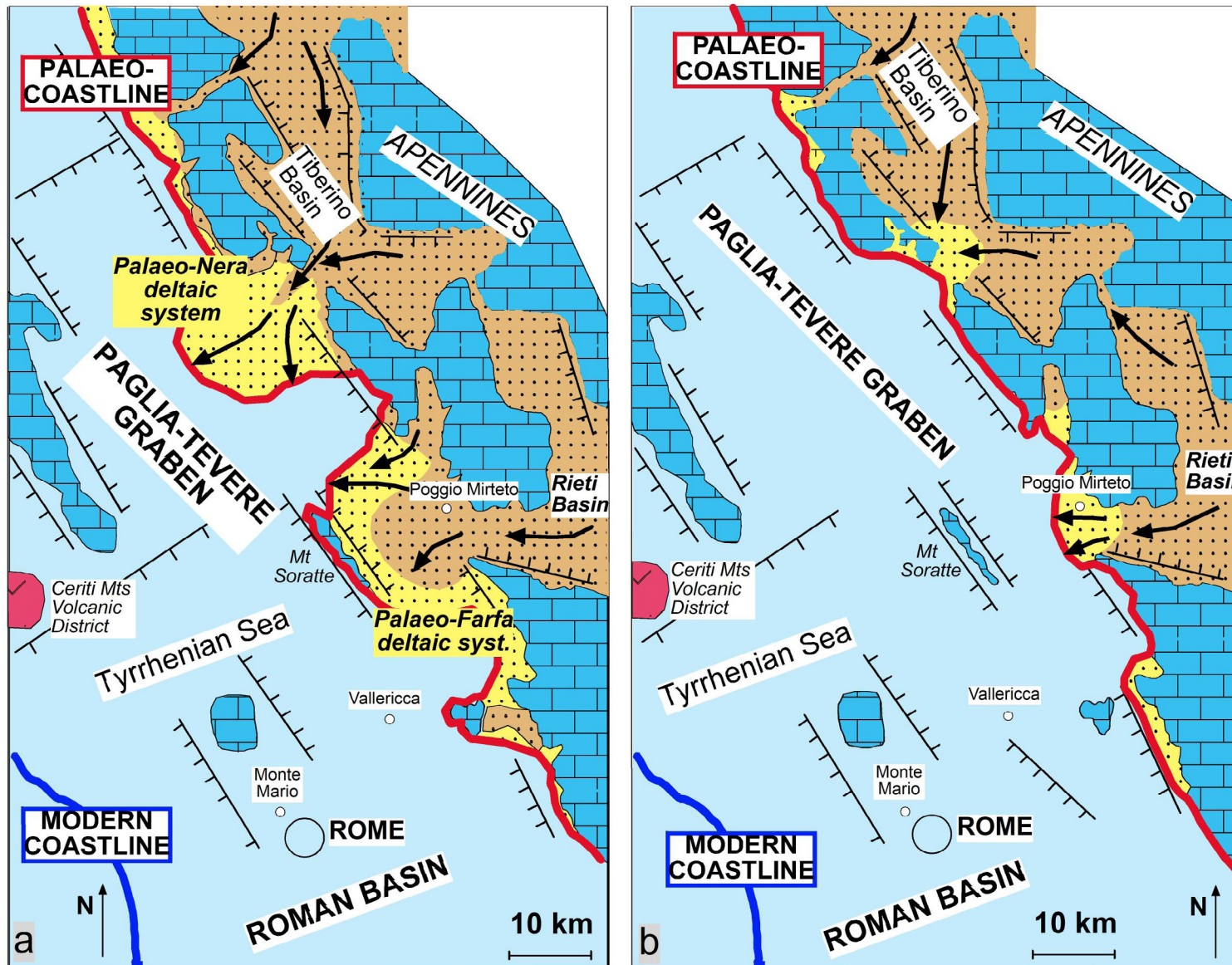


Fig. 22 - Palaeogeography of the Middle Tiber Valley basin during the Gelasian-Calabrian p.p. (2.1-1.4 Ma) subsidence. a) The WSW-directed progradation of fluvio-deltaic systems (in yellow) in the marine basin fed by the inner alluvial systems (in brown), during a depositional-regressive phase of the 4th order cycles. b) Transgressive phase of the 4th order cycles with landward NE-directed retreat of the coast (red line) (modified after Mancini et al., 2004).

The sedimentary response of the periodic coastline migration is recorded in the 4th order, regressive-transgressive R-T cycles, at the eastern margin of the graben.

Major palaeogeographic changes occurred at about 1.4 Ma when a renewed tectonic uplift in the Central Apennines reached the western margin of the chain and the Paglia-Tevere Graben (Fig. 23). The area began to emerge, and the river system reorganised into a new network of drainage. The ancient rivers connected into the newly formed Tiber River system. In this period, the Tiber delta rapidly shifted downward to the present position. Local deviations of the main river course were due to the activation of minor tectonic structures, such as north of Mt. Soratte, or



to the growing of volcanic complexes (e.g., Sabatini Mts.). The sedimentary response of this uplift-dominated phase is featured by the fluvial terraced sequences that are strongly controlled by the global Quaternary climate changes and by the regional effects of volcanism on topography, which is also traced by the reconstructed phyletic evolution of fluvial fishes (Bellucci et al., 2021).

Stop 1.5. The Acque Albule Basin and the Lapis Tiburtinus travertine (41°57'35.56"N; 12°44'24.42"E)

The Pacifici 1 quarry walls display the internal geometry of the upper portion of the Acque Albule Basin in its eastern and central sectors. In the north, laminated deposits represent the major lithofacies, while in the southern part, crystalline crust lithofacies are associated with a laminated deposit (Fig. 24). In the eastern part of the quarry, the walls show well-developed karstic features. Geometry and facies association recall a slope paleoenvironment with an inclination of 7-10° towards the south and to the Aniene paleo-river evidencing a direct relation between this river and the

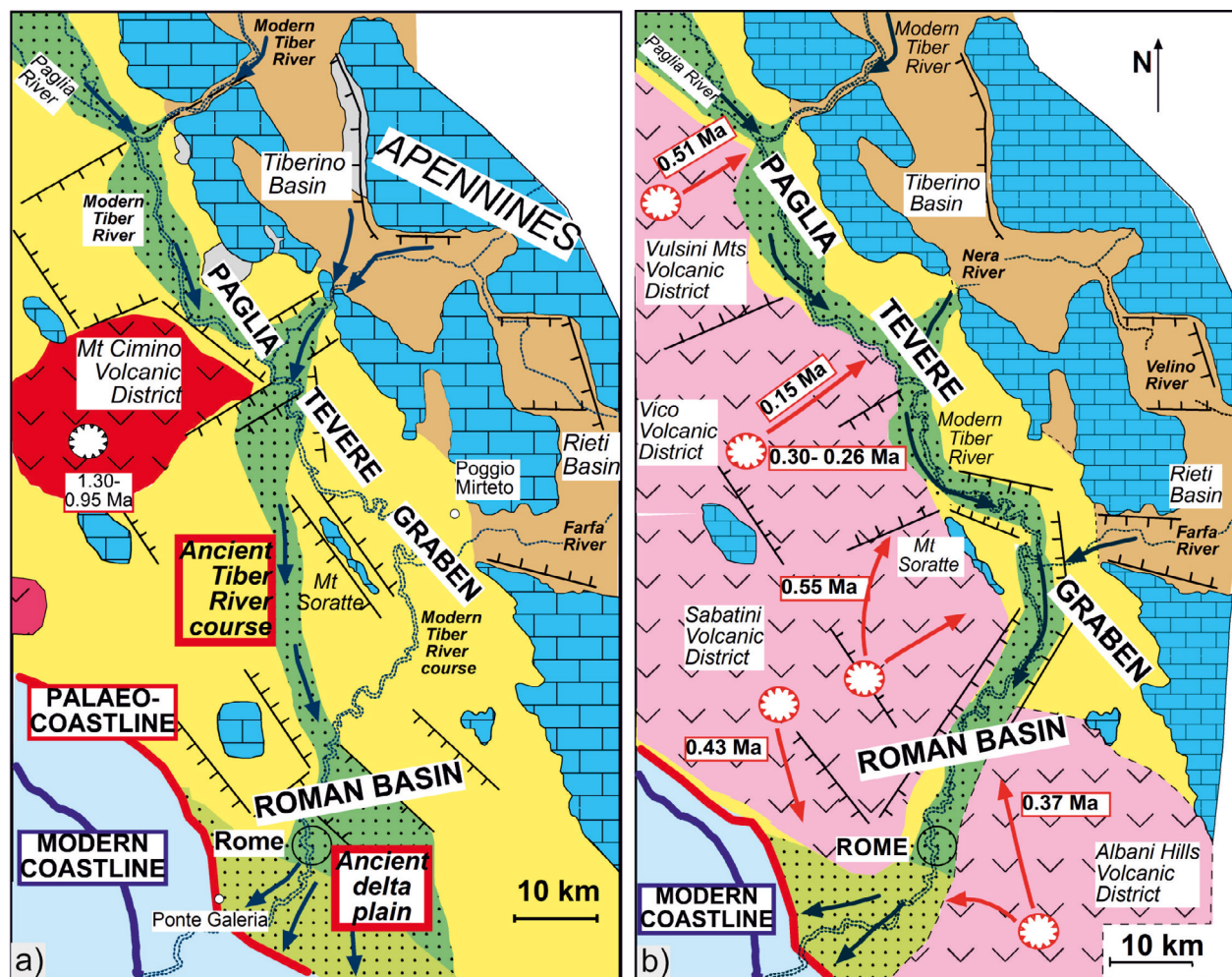


Fig. 23 - Palaeogeography of the Middle Tiber Valley Basin during the uplift dominated phase (latest Early Pleistocene-Late Pleistocene, from 1.3 to 0.1 Ma). To the left, regional uplift of the marine sequences (in yellow) is recorded at the west Apennines foothill and in the newly formed Tiber fluvial system (in green with axial drainage). The rapid seaward shift of the ancient coastline, the juvenile Tiber River flowing west of the Mt. Soratte, and the onset of the Cimino Mts. Volcanic activity (in red). To the right, volcanic activity of the Vulsini Mts., Vico, Sabatini Mts. and Albani Hills Volcanic Districts (in pink) and their impact on the Tiber fluvial. The main pyroclastic flows are dated and reported with red arrows system (redrawn and modified after Mancini et al., 2004).

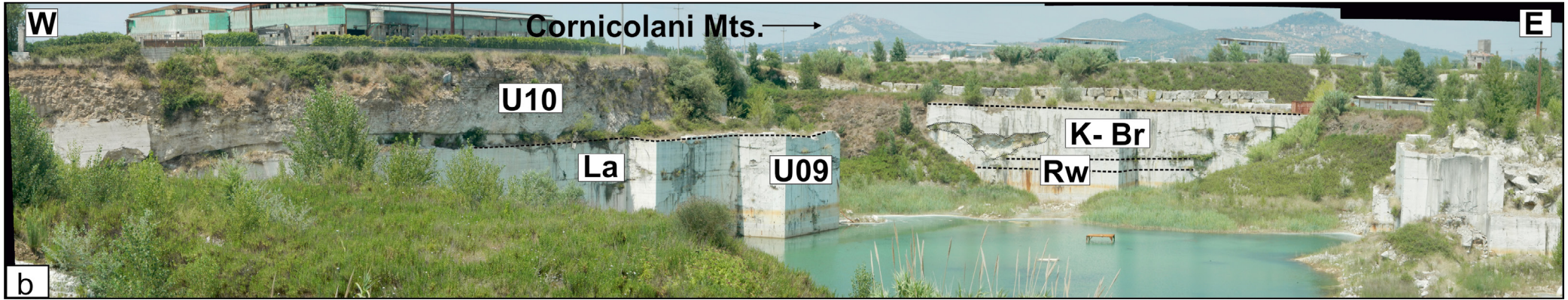
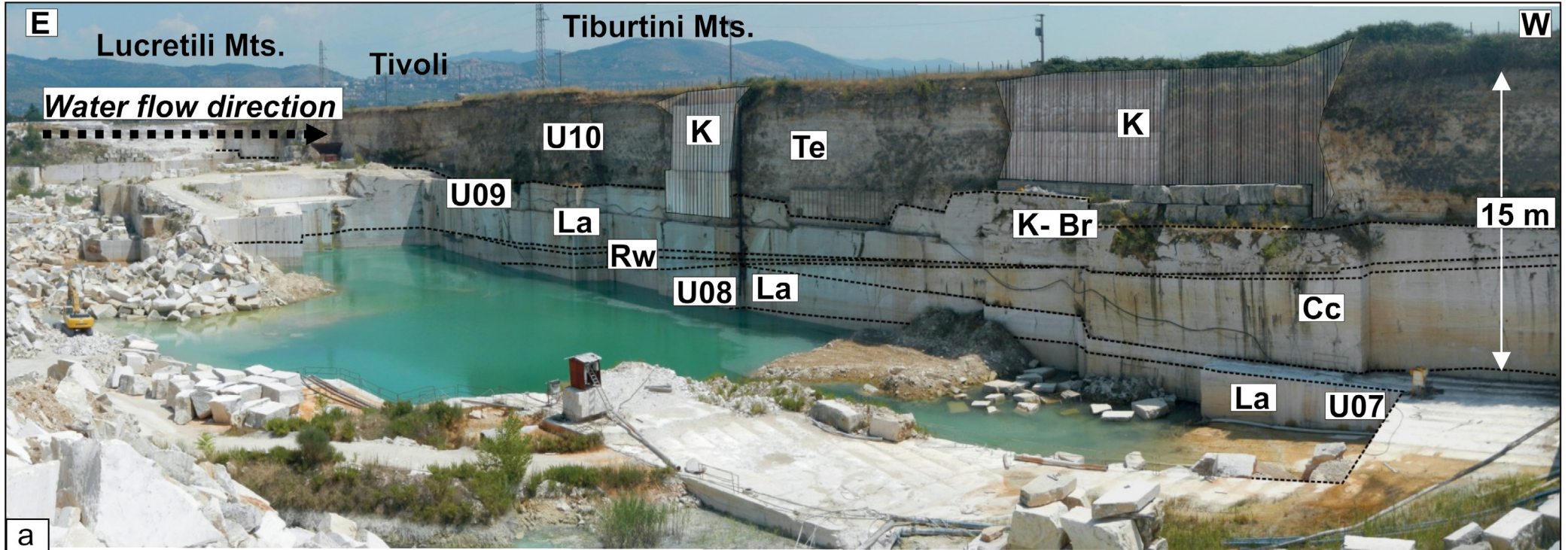


Fig. 24 - a) The southern walls of Pacifici 1 quarry and its stratigraphic relationships. La: laminated deposit; Rw: intraclast deposit; Cc: crystalline crust; K - Br: karstic features and breccia; Te: *Testina*; U07-08-09-10: depositional units (for more details see Mancini et al., 2021). b) More stratigraphic relationships between the different units. La: laminated deposit; (for more details see Mancini et al., 2021).



evolution of the *Lapis Tiburtinus* travertine geobodies.

Fluvial to fluvio-palustrine-lacustrine deposits, interfingering with the Albani and Sabatini volcanic units characterise the Ponte Galeria Sequence (PGS: PG1-PG9; Milli et al., 2016). The stratigraphic organisation of the PGS sequence is similar to the succession described below the V surface. The deposition of travertine started at 115 ± 12 ka, continuing till 29 ± 4 ka (Faccenna et al., 2008), and the PG9 can be considered coeval with the *Lapis Tiburtinus* and the V basal surface. Furthermore, the V surface can be correlated with the eustatic sea-level fall of MIS 6, while the end of travertine deposition corresponds with other eustatic fall (MIS 2) also related to the Last Glacial Maximum (Faccenna et al., 2008; Clark et al., 2009) (Fig. 25).

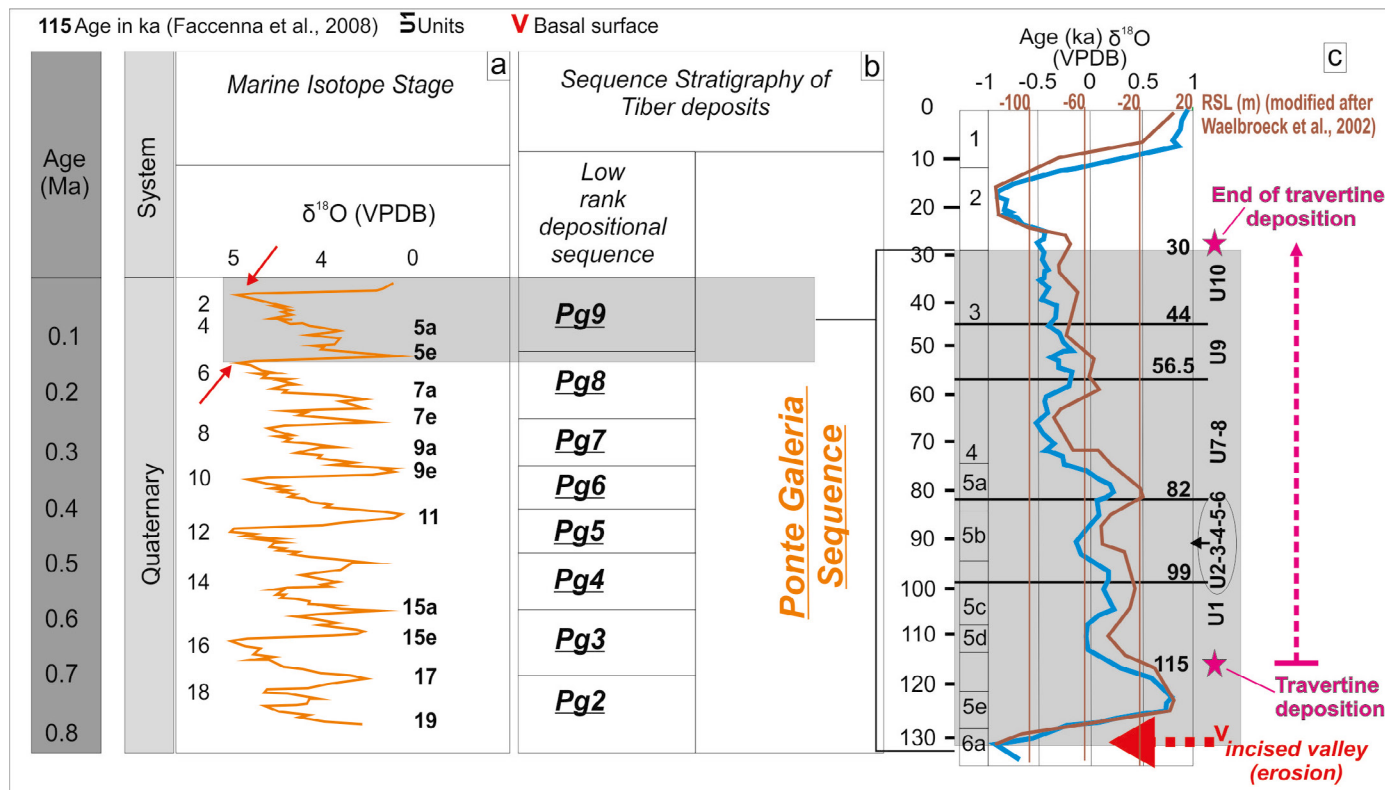


Fig. 25 - Marine isotope stages and glacio-eustasy compared with the stratigraphy of the Tiber River deposits (Roman Basin). The radiometric ages obtained by Faccenna et al. (2008) and the temporal distribution of the stratigraphic units and the relative sea level fluctuations are reported. a) Marine Isotope Stage curve modified after Cohen & Gibbard (2011); b) sequence stratigraphy of Tiber deposits modified after Milli et al. (2016). The PG9 time interval is coeval with the deposition of the *Lapis Tiburtinus* travertine in the Acque Albule Basin (modified from Mancini et al., 2021). c) Age (ka) $\delta^{18}O$ curve modified after Shackleton (1969).

Stop 1.6. The Testina travertine (41°58'29.83"N; 12°44'12.37"E)

This stop is located within one of the northern quarries. The predominant lithofacies is a laminated deposit intercalated with shrub lithofacies layers separated by erosional surfaces formed in a subaqueous environment.

<https://doi.org/10.3301/GFT.2022.05>



In the upper part of the quarry walls, poorly cemented deposits occur related to the locally called *Testina* travertine (Scalera et al., 2021) (Fig. 26). Inside, all the lithofacies that we observed in the lower travertine succession are recognisable, but thinner and less lithoid (Fig. 26). The contact between the travertines and the *Testina* is marked by clay layers (Fig. 26a). This unit is tabular and increases in thickness in the central part of the basin. Above this unit, a well-developed palaeosoil occurs (Fig. 26c). As supported by the presence of typical gastropods (*Lymnaea stagnalis*), the input of freshwater is higher than the environment where travertine develops (Fig. 26e). The depositional units gently dip towards the East and are crossed by N-, WSW- and WNW-striking fractures. The two latter bear FeO (marcasite and limonite) and mineralisation with mm – cm gypsum crystals. Possibly, this evidence is related to fluids rich in H₂S that rose up from these fractures. Also, the current distribution of active thermal springs, sinkholes, and other karstic features is tectonically controlled and related to regional N-S striking seismically active faults (Gasparini et al., 2002; Faccenna et al., 2008; Billi et al., 2016). Evidence of faults offsetting the travertines occurs in the northern part of the Acque Albule Basin (Faccenna et al., 2008; De Filippis et al., 2013a; Anzalone et al., 2017). In the central and the southern part instead, clear evidence of faults is absent and the travertine units (U1-U10 *sensu* Mancini et al., 2021) show high lateral continuity (more than 400 m) only locally affected by fractures (De Filippis et al., 2013a).

In the northern part of the basin, the travertine succession (units U8, U9, and U10) is NE-tilted of about 25° (Fig. 27) and is overlain by a clastic succession with lenticular concave-upward geometry. Faccenna et al. (2008) suggested that such tilting was related to fault activity. Differently, Billi et al. (2016) interpreted this tilt as due to local subsidence. In this view, water table and palaeoclimate fluctuations influence the travertine lithofacies association thickness and distribution, that in places are affected by alternating deposition and erosion, associated with palaeoclimatic cycles, controlling the oscillations of the groundwater level (Faccenna et al., 2008; De Filippis et al., 2013b; Mancini et al., 2021). In this regard, the Acque Albule Basin can be considered as a flat and low elongated incised valley system, fluvially eroded by the Aniene River, controlled by the interaction between tectonics, volcanism, and eustatic fluctuations. Such fluctuations influence the travertine formation over a short period (100 kyr), while tectonic probably was effective on longer periods (500 kyr).



Fig. 26 - Different sketches of the facies that compose *Testina* travertine deposits. a) Clay deposit between the travertine succession and the *Testina* deposits. b) Reed and phytoclasts lithofacies. c) Palaeosoils at the top of *Testina* deposits overlying a black claystone layer. d) Intraclast lithofacies. e) *Lymnea stagnalis*. f) Laminated deposit lithofacies. g) Shrub lithofacies (modified after Scalera et al., 2021).

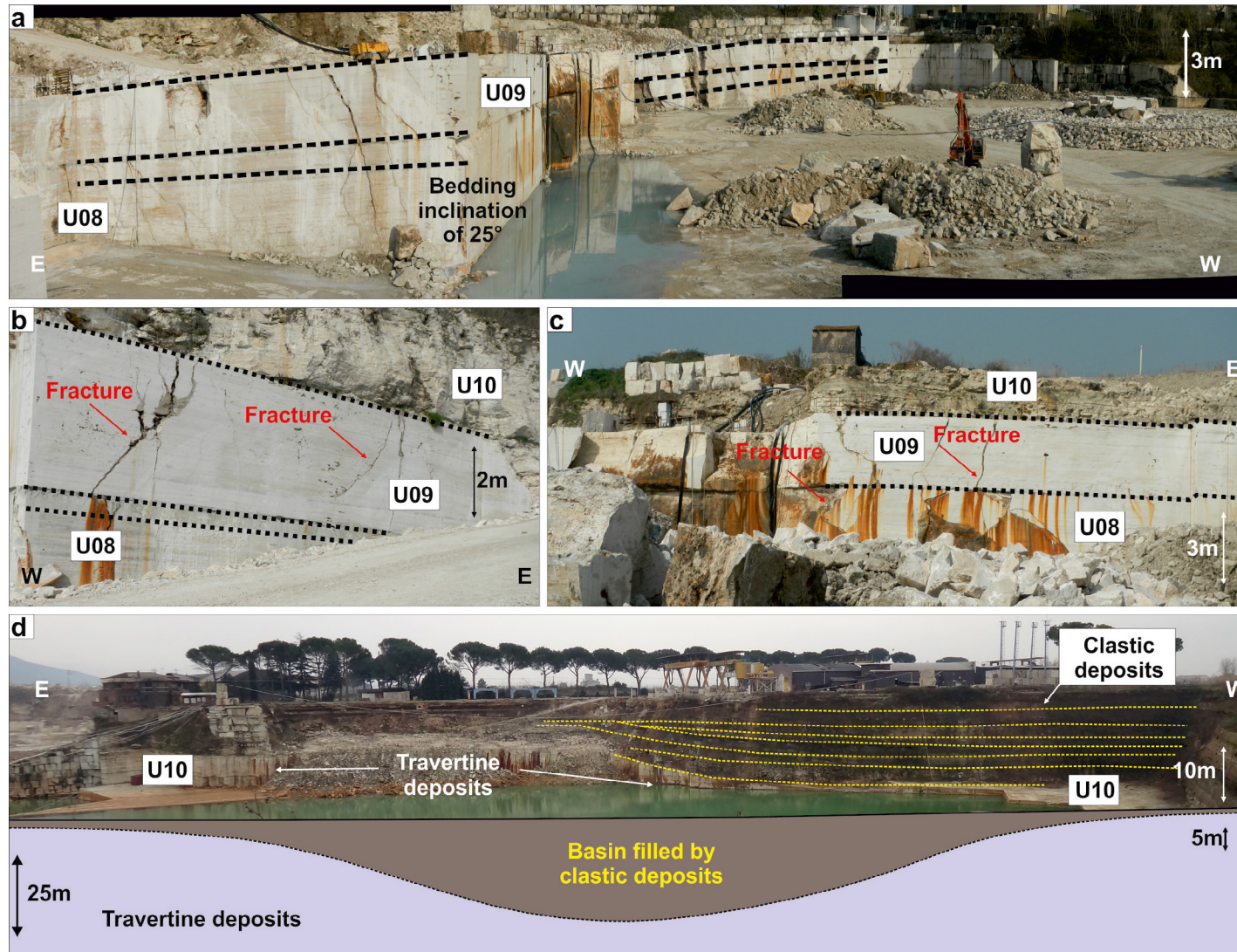


Fig. 27 - a-c) The Travertine deposits in the northern part of the Acque Albule Basin are affected by tilting of the travertine deposits of 25° toward the NE. d) In the northern part of the basin, on top of the travertine succession, mixed carbonate-siliciclastic deposits occur. The thickness of the succession increases to the east. The concave-upward to lenticular geometry of the mixed carbonate-siliciclastic deposits on top of travertine succession is possibly tied to the evolution of a sub-kilometre size basin, whose U08-09-10 are depositional units modified from Mancini et al. (2021).



Day 2 The Latium-Abruzzi carbonate platform: insights on the oceanographic events affecting the Tethyan margin

The Day-2 trip (Figs. 1, 2) is focused on the Tethyan passive margin dynamics preserved in the Latium-Abruzzi Carbonate Platform succession.

The Latium-Abruzzi Carbonate Platform represents a sector of the western passive margin of Adria that consists of Mesozoic to Cenozoic neritic carbonates. During the Mesozoic, it was a flat-topped platform organised in peritidal cycles in the Jurassic and Lower Cretaceous and dominated by rudists in the Upper Cretaceous (Parotto & Pratulon, 1975; Accordi & Carbone, 1988). During the Palaeogene, a long-lasting hiatus characterises the platform top (Accordi et al., 1967; Brandano, 2017), while Palaeocene-Oligocene discontinuous deposits occur on the platform margins and within inherited topographic depressions (Tomassetti et al., 2016; Tomassetti & Benedetti, 2020). In the Early Miocene, an homoclinal carbonate ramp developed, represented by the “*calcari a briozei e litotamni*” (“bryozoan and lithotamnion limestone” – CBZ) formation (Burdigalian-Tortonian, Civitelli & Brandano, 2005). The CBZ ramp drowns in the Tortonian. This drowning is marked by a phosphatic hardground (Cipollari & Cosentino, 1995), which is overlain by the hemipelagic “*unità argilloso-marnosa*” (“clayey marly unit” – UAM, cf. *Orbulina* Marl). Lastly, between the Tortonian and the Messinian, the turbiditic siliciclastic sedimentation attests the onset of the Apennine foredeep development (Carminati et al., 2007; Vezzani et al., 2010).

Stop 2.1. On the origin of the Palaeogene unconformity and Cretaceous platform facies at Santa Maria dei Bisognosi (42°02'29.0"N; 13°05'40.8"E)

The Palaeogene unconformity

This outcrop shows the Palaeogene hiatus that characterises the Latium-Abruzzi carbonate succession (Fig. 28). Between the Cretaceous carbonate platform and the Burdigalian carbonate ramp a paraconformity marked by a stylolite occurs, recognisable by a change in the skeletal composition. The discontinuity is planar, without cavities, open fractures, or neptunian dykes, and lacks subaerial exposure signs (i.e., palaeokarst, palaeosoils, root horizons, conglomerates, or breccias, Fig. 28). Cretaceous beds may bear boring traces (*Gastrochaenolites* isp. and *Entobia* isp.). This Palaeogene hiatus has long been interpreted as due to prolonged subaerial exposure, even if no evidence of such exposure has ever been documented in the Latium-Abruzzi carbonate platform. Conversely, coeval



Fig. 28 - The paraconformity that marks the K/Pg boundary (yellow dotted line) in the Latium-Abruzzi carbonate platform, where the Cretaceous beds (K) and the overlying Miocene beds (M) are geometrically parallel. The red line marks a fault.

and adjacent Apulia and Lessini carbonate platforms show a broadly developed palaeokarst system formed between Eocene and Early Miocene. Furthermore, the fact that this surface is perfectly flat, bioeroded, and paraconformable rules out the hypothesis that the Miocene marine transgression deeply eroded the karstified Cretaceous substrate. Brandano (2017) proposed a marine origin for this unconformity. From late Palaeocene to Early Miocene, the Latium-Abruzzi carbonate platform was a shaved isolated platform (*sensu* James et al., 1994), exposed to wave action in the middle of the proto-Mediterranean area. Bioclastic sediments accumulated during transgressive and sea level highstand phases, whereas in the falling and lowstand stages sediment was eroded as the seafloor came into the zone of wave abrasion.

Then, the eroded sediment was shed into the basin forming coarse bioclastic intercalations in the hemipelagic "Scaglia" formations. Finally, in the early Burdigalian, the Mediterranean evolved into a semi-closed sea due to the progressive closure of the Indo-Pacific connection and the consequent reduction of the wave-base depth, typical of an enclosed sea, increased the accommodation space, allowing sediments to accumulate and form the complete ramp facies belt that evolved during the Miocene as the Latium-Abruzzi ramp.



The Cretaceous platform facies

In the Santa Maria dei Bisognosi area the Upper Cretaceous portion of the Latium-Abruzzi succession is represented by ~500 m-thick limestones and dolomitised limestones (Coniacian to Campanian in age) characterised by dm- to m-thick beds and organised in peritidal cycles (Cestari et al., 1992; Fabbi et al., 2020). In the upper part, rudist-rudstones to floatstones in a packstone to grainstone matrix, characterised by a sharp base, normal gradation, and occasional hummocky cross-stratification are common and represent high-energy deposits. The Coniacian–Campanian rudist-dominated limestones of the Southern Apennines were interpreted as deposited in an open-shelf setting dominated by bioclastic sedimentation of mainly molluscs and foraminifers, with subordinate green algae, red algae, ostracods, and echinoids (Carannante et al., 1995, 1999, 2000; Ruberti et al., 2006). Storm- and wave-induced currents-controlled sediment distribution on the seafloor. Brandano & Loche (2014) evidenced how high lateral facies heterogeneity characterised the Coniacian Latium-Abruzzi carbonate platform, with the same depositional cycle showing different expressions within a few hundred of metres. Some of the vertical facies transitions observed in the outcrops may be ascribed to autocyclic processes. In fact, the passage from intertidal to fully subtidal environments occurs in only few hundred of metres as a facies mosaic. As evidenced by Wright & Burgess (2005), there is a continuum of carbonate factories and facies related to many environmental and depositional processes.

Stop 2.2. The Miocene carbon isotope events at Pietrasecca I (42°08'00.85"N; 13°07'21.16"E) and Pietrasecca II (42°08'08.41"N; 13°08'05.78"E)

The Pietrasecca composite section comprises the CBZ and the UAM formations. Here, the CBZ consists of three lithofacies, representative of an aphotic outer ramp (Brandano et al., 2010). Age constraints are referred to Brandano et al. (2017). The first lithofacies (Burdigalian), 25-m thick, is a packstone with small benthic foraminifera and echinoid fragments. The second lithofacies (upper Burdigalian-Langhian) is 44 m-thick and consists of a floatstone to packstone with bryozoans and minor echinoid fragments. The third lithofacies (Langhian-lower Tortonian) is a 31 m-thick packstone with planktonic foraminifera and echinoids (Brandano et al., 2010, 2017). The CBZ fm ends with a phosphatic hardground surface that marks the drowning of the platform and the onset of the hemipelagic UAM sedimentation (Cipollari & Cosentino, 1995; Brandano et al., 2010). The hardground surface has been constrained between 11.02 (top of the CBZ Fm) and 9.7 Ma (base of the UAM), thus lower Tortonian.



The C-isotope record of the Pietrasecca section shows a long-term positive excursion between upper Burdigalian and lower Serravallian, correlated with the global Monterey Carbon Isotope Excursion (Brandano et al., 2017; Fig. 29). The maximum positive excursion (+ 2.48‰ $\delta^{13}\text{C}$) was recorded at the base of the bryozoan-dominated unit (Brandano et al., 2017). The spread of bryozoans is due to the increased nutrient availability related to the Monterey Event and enhanced by regional factors such as i) the closure of the Indian Gateway that weakened Mediterranean water circulation and favoured upwelling; ii) higher continental-derived runoff due to the migration of the Apennine accretionary wedge (Brandano & Corda, 2002); and iii) subduction-related, western Mediterranean, volcanism that sustained high nutrients and CO_2 levels in surface waters (Brandano et al., 2010, 2017). This abundant aphotic carbonate production led to the development of very low-

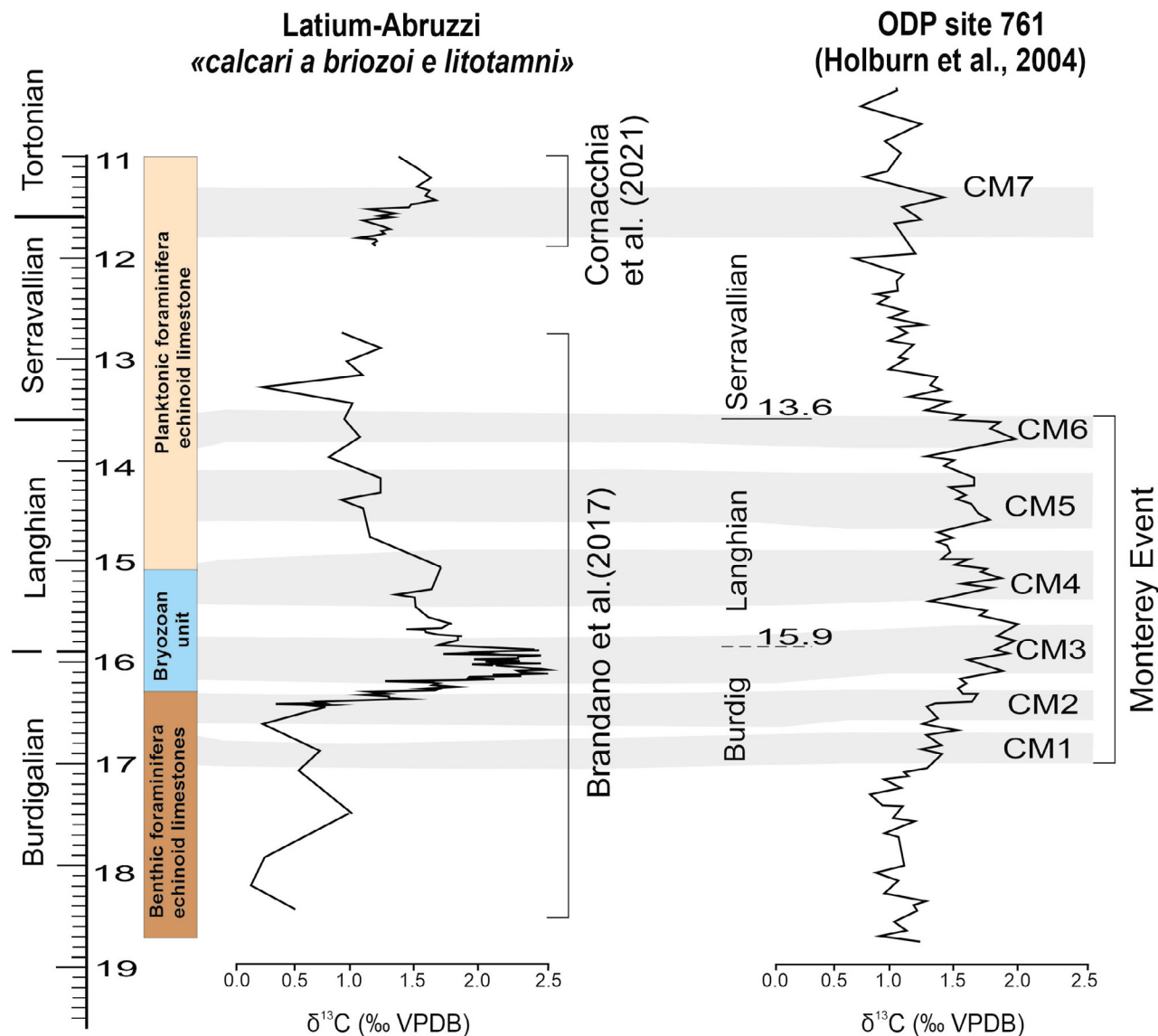


Fig. 29 - Comparison of the carbon isotope curves of the Pietrasecca section, calibrated according to sedimentation rates of Brandano et al. (2017), and the Miocene portion of the ODP core 761 (southern margin of Australia, Holbourn et al., 2004). Modified and redrawn after Brandano et al. (2017) and Cornacchia et al. (2021).



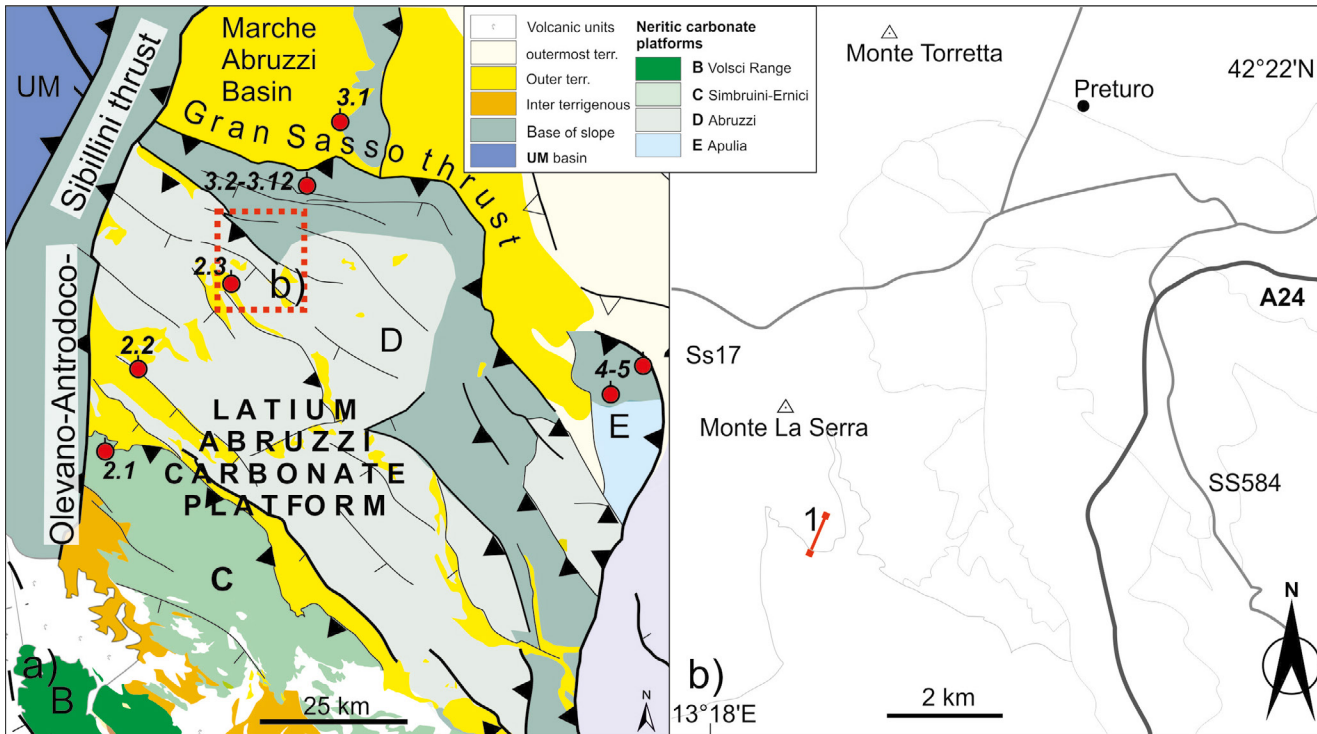
angle ramps in the inherited Apennine Tethyan margin during Middle Miocene (Brandano et al., 2017). Lastly, one last positive carbon isotope shift was recorded in the lower Tortonian (11.4 Ma – Cornacchia et al., 2021) and correlated with the global Carbon Maximum 7 (CM7 – Holbourn et al., 2004). The CM7 testifies for higher nutrient availability of surface waters linked to the strengthening of global ocean circulation consequent to the Late Miocene cooling (Holbourn et al., 2013). These circulation changes and increased nutrient availability favoured the upwelling and, thus, the formation of the phosphatic hardground that marks the drowning of the CBZ (Brandano et al., 2020a; Cornacchia et al., 2021).

Stop 2.3. The Palaeogene succession and the Early Miocene Carbon Maximum (42°18'16.64"N, 13°15'16.44"E)

At Monte La Serra, the Palaeocene to upper Eocene carbonate sediments characterise the slope sedimentation record of the Latium–Abruzzi carbonate platform (Fig. 30), while its inner zones are defined by a Palaeogene long-lasting hiatus. The preserved Palaeogene deposits occur in several small depressions upon the Cretaceous substrate (Zalaffi, 1963; Devoto, 1964; Tomassetti et al., 2016; Tomassetti & Benedetti, 2020) and along the margin of the Cretaceous platform. These deposits are known in the literature as the “*Calcarenita a macroforamiferi*” (“larger benthic foraminifers calcarenite” – CFR) and the “*Unità spongolitica*” (“spongolitic unit” - SPT) formations (“*membro di Guadagnolo*”; “Guadagnolo member” – SPT₁, Chattian to Serravalian), and both outcropping in the Monte La Serra section. The CFR is characterised by reworked material coming from the Latium–Abruzzi ramp and represents deposition onto its margins and slopes (Fig. 30). This material consists of bioclastic grainstone to wackestone and bioclastic packstones, rich in larger and small benthic foraminifera, and coralline algal nodules and debris (Tomassetti & Benedetti 2020). The base of the Monte La Serra section consists of 1 m thick Palaeocene (Thanetian) pelagic sediments rich in planktonic foraminifera. The boundary with the overlying Eocene sediments is marked by a 0.2 m bed rich in glauconite. The top of the section is highlighted by a conglomerate bearing clast of pelagites with glauconite, that marks the passage to the Oligo-Miocene portion of the section (SPT₁; Tomassetti & Benedetti, 2020).

Age constraints

Tomassetti & Benedetti (2020) ascribed the base of the Monte La Serra section to the late Palaeocene due to the occurrence of *Morozovella velascoensis* and *Planorotalites pseudomenardi*. A bioclastic grainstone

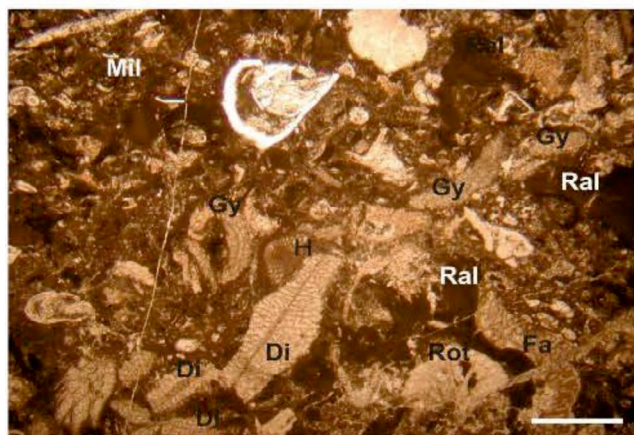


rich in *Discocyclus* sp. identifies the Palaeocene–Eocene boundary. The occurrence of ortho-phragmines assemblages associated with the *Fabiania cassis*, *Halkyardia minima*, *Chapmanina gassinensis*, *Silvestriella tetraedra*, and *Heterostegina* sp. point out to the middle to late Eocene age (base of the SBZ18 of Serra-Kiel et al., 2016).

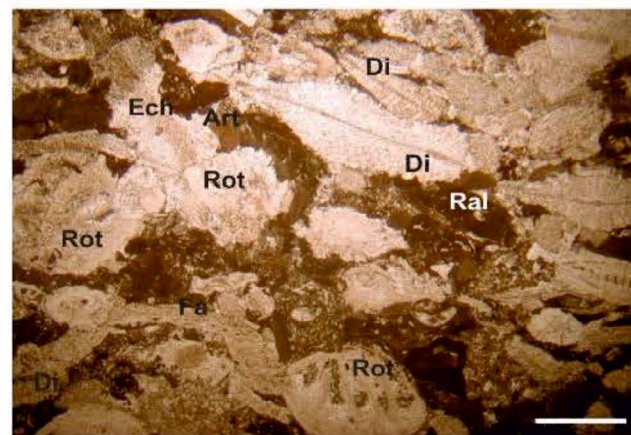
Facies association and carbonate factories during the Palaeocene–Eocene interval

In the Palaeogene portion of the section, two facies associations are recognisable: a grain-supported facies (FA1) and a mud-supported one (FA2, Fig. 31). FA1 consists of grainstone-to-grainstone/packstone facies with

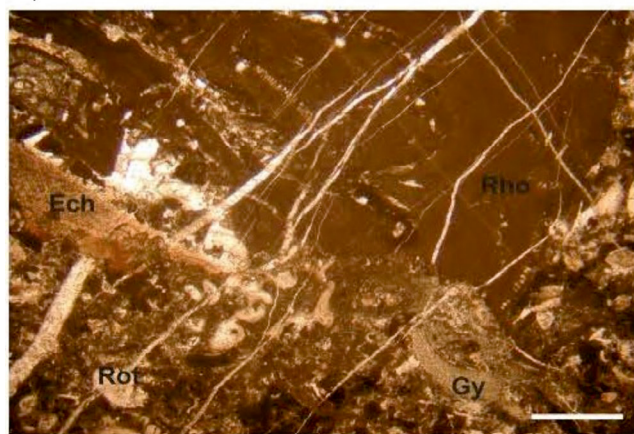
Fig. 30 - a) Schematic geological map of the Latium–Abruzzi carbonate platform with the main carbonate platforms and pelagic domains (from Fig. 2). b) Location of the Monte La Serra section (after Tomassetti & Benedetti, 2020); c) Stratigraphic architecture of the Latium–Abruzzi carbonate platform and transition to the Umbria–Sabina Basin (after Brandano et al., 2015).



a)



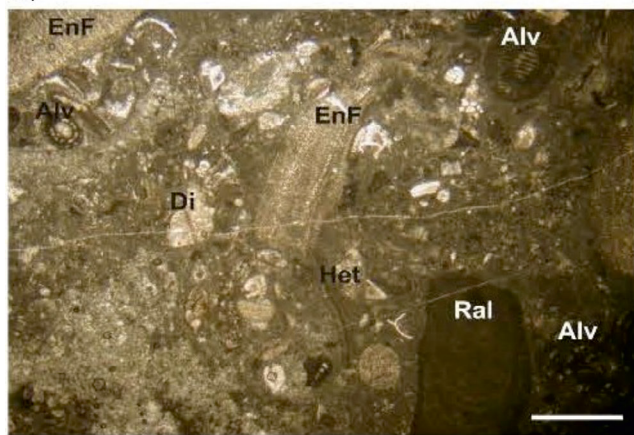
b)



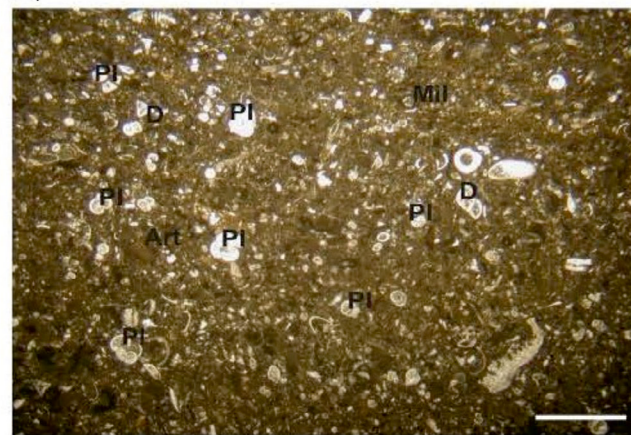
c)



d)



e)



f)

Fig. 31 - Photomicrographs of the two main facies recognised in the investigated outcrops. A-C) FA1 packstone-to-grainstone facies. A-B) Bioclastic packstone-to-grainstone with autochthonous relatively deep-water components such as orthoherminid, red algal fragments, and nodules, and shallow-water components including large rotaliids, miliolids, and encrusting foraminifera constituting the allochthonous bioclasts; C) Rhodolith floatstone with a bioclastic packstone matrix made up of autochthonous shallow-water components such as encrusting foraminifera and small rotaliids. D-F) FA2-Mudstone-to-wackestone facies; D) Wackestone with coral fragments, miliolids, and small rotaliids reworked with orthoherminid in a fine packstone matrix; E) Mud-to-wackestone with shallow-water allochthonous porcelaneous and encrusting foraminifera. F) Autochthonous deep-water planktic mud to-wackestone with some allochthonous shallow-water components as miliolids and articulated red algal fragments. Scale bar is 500 µm. Mil = miliolid; Ral = red algal nodule; Gy = *Gypsina* sp.; H = *Halkyardia* sp.; Di = *Discocyclina* sp.; Rot = rotaliid; Fa = *Fabiania*; Ech = echinoid; Art = articulated red algae; Ast = *Asterocyclina* sp.; Cor = coral; Rho = rhodolith; EnF = encrusting foraminifera; Alv = alveolinid; Pl = planktonic foraminifera; D = discorbid; Spi = *Spiroclypeus* sp. (modified from Tomassetti & Benedetti, 2020).



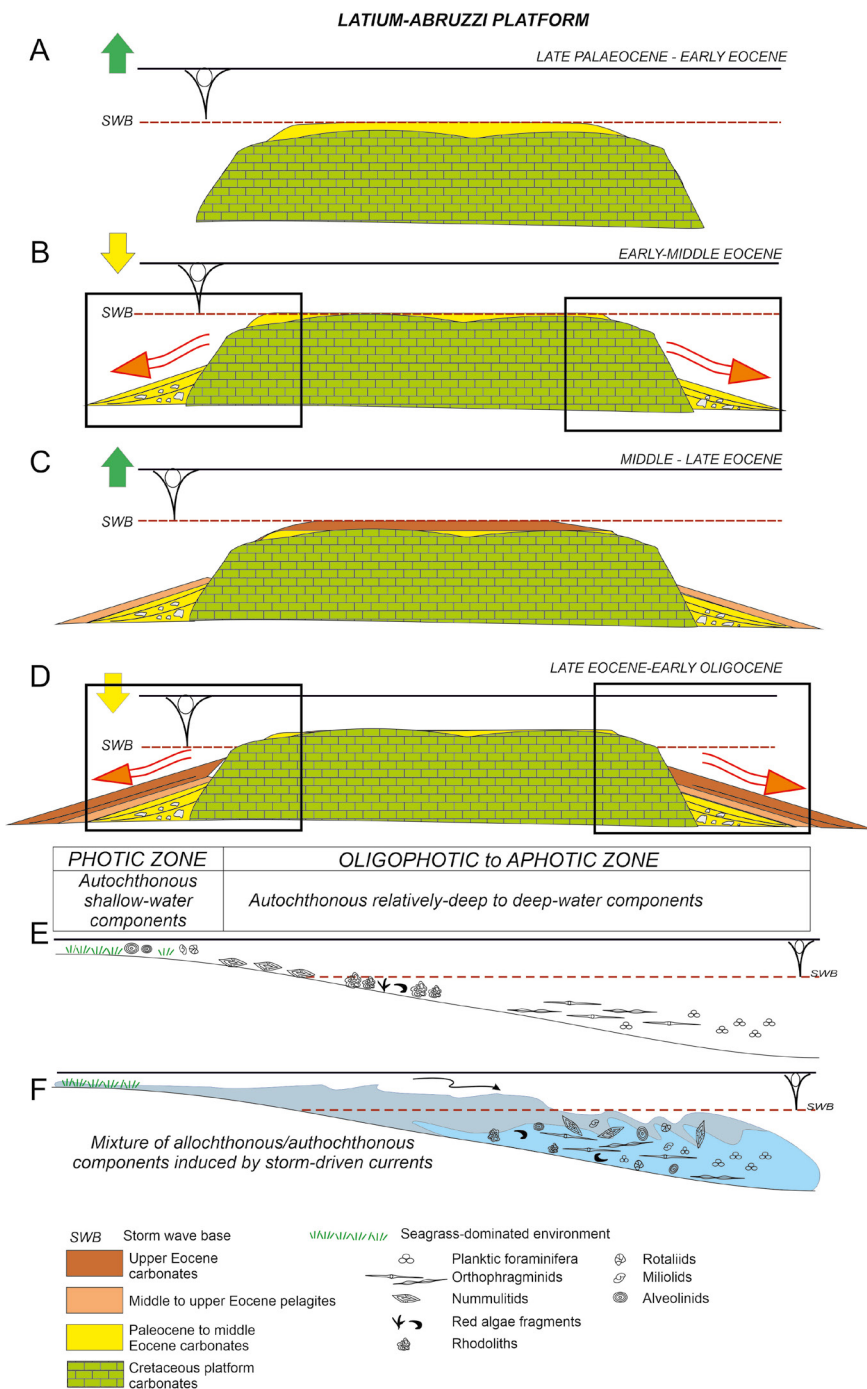
larger benthic foraminifers (LBF), small benthic foraminifers (SBF) and coralline algae. FA2 is a mudstone-to-wackestone facies with LBF, SBF, planktonic foraminifera, coralline algal crusts, and corals. Both FA1 and FA2 facies are characterised by autochthonous and allochthonous skeletal components. In FA1, the autochthonous component (mainly orthophragmines and nummulitids) is up to 58% and allochthonous is up to 42%. In the FA2, the autochthonous percentage is up to 39% and the allochthonous is up to 61% (mainly porcelaneous and encrusting foraminifera, corals) and is dispersed in a mudstone-to-wackestone matrix.

The compositional analysis of the facies, within a palaeoecological context, reveals three different sediment factories that supplied this allochthonous/autochthonous material: a euphotic shallow factory mainly characterised by seagrass biotic assemblages (porcelaneous and encrusting forams); a meso-oligophotic factory mainly composed of orthophragmines, nummulitids, and red algae, and an aphotic factory with planktonic foraminifera, molluscs, and echinoid fragments. The main carbonate factories feeding these mixed deposits are the euphotic and oligophotic factories. The euphotic factory represents the allochthonous part transported from the inner sector of the platform and resedimented on the slope, where it is mixed with the autochthonous counterpart represented by the oligophotic factory.

The Monte La Serra section shows a picture of what ruled the sediment deposition along the slope of the Latium–Abruzzi carbonate platform during the Palaeocene–Eocene interval. During lowstands, storm-driven currents, and occasionally internal waves impinging upon the slope, remobilised, resuspended, and reworked sediments on the carbonate platform, which evolved as a shaved platform. The remobilised material was transferred from the inner platform onto the slope, generating a mixture of detrital shallow- and deep-water biotic assemblages and depositing as autochthonous/allochthonous facies (Fig. 32) (see [Tomassetti & Benedetti, 2020](#) for further details).

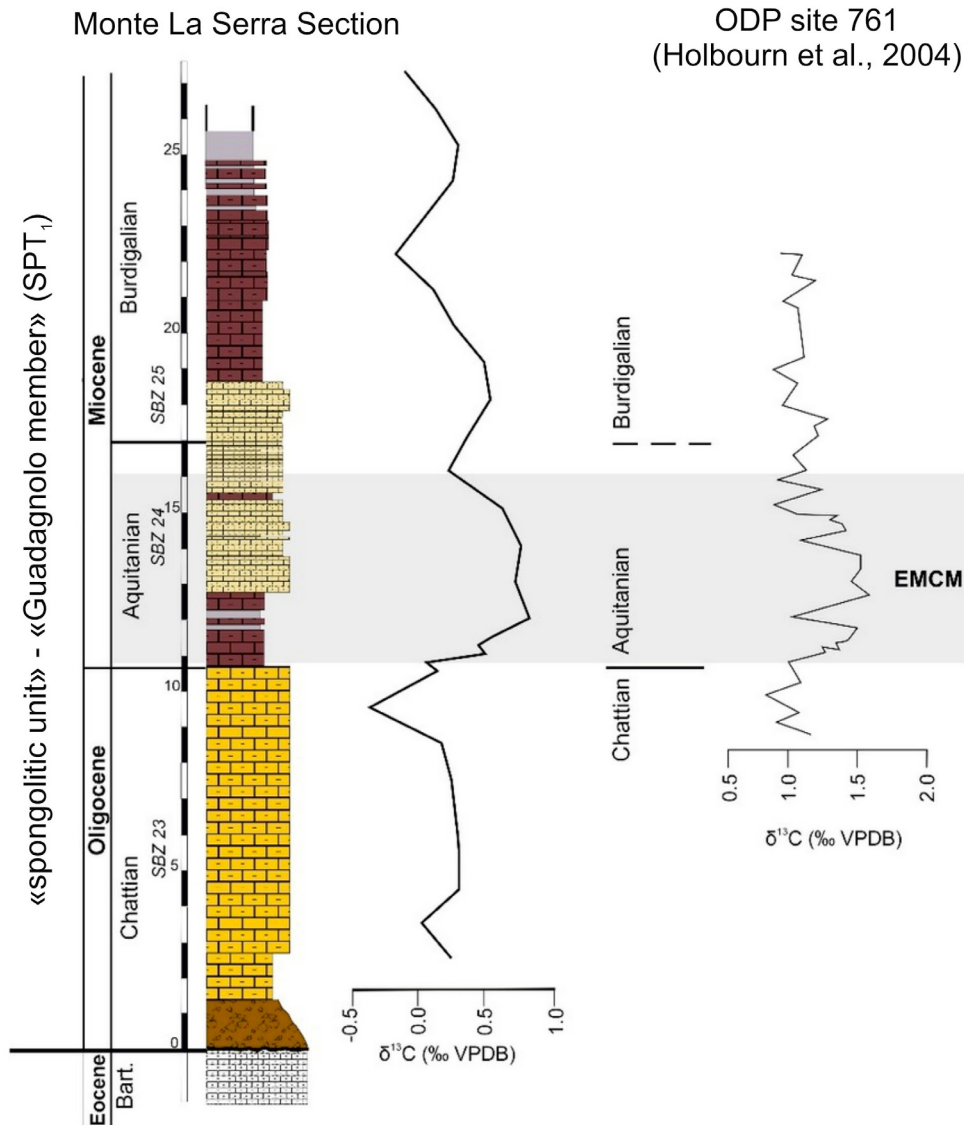
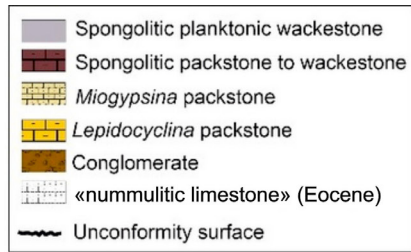
The Monte La Serra section - The Early Miocene Carbon Maximum and the "spongolitic unit"

The Monte La Serra section comprises also the upper Oligocene-Lower Miocene portion of the "Guadagnolo member" (SPT₁) of the "spongolitic unit", identified by oligophotic middle ramp deposits with LBF, and an aphotic outer ramp facies dominated by siliceous sponge spicules (Figs. 33, 34 – [Brandano et al., 2015](#)). Here, the Oligocene-Miocene boundary is marked by a facies change between grainstones with *Lepidocyclina* and spongolitic marls, as well as by a positive C isotope shift (Fig. 34 – [Brandano et al., 2015](#)). At the beginning of the Aquitanian, a rapid expansion of the Antarctica Polar Ice Cap took place, testified by a global positive oxygen isotope shift (Mi-1 Event, [Miller et al., 1991](#)). Contemporary, a positive $\delta^{13}\text{C}$ isotope shift occurs in the global pelagic record (Early Miocene Carbon Maximum, EMCM, [Zachos et al., 2001](#)), attesting an increased primary



productivity of surface waters, linked to a perturbation in the atmosphere-ocean CO₂ budget (Lear et al., 2004) and increased runoff due to the glaciation (John et al., 2003). The δ¹³C isotope curve of the Monte La Serra section perfectly records the EMCM and the consequent demise of photic carbonate producers (such as LBF). Furthermore, in the area, this carbon cycle perturbation is enhanced by western Mediterranean volcanism, whose influence is also attested by siliceous sponges, which thrived due to the higher SiO₂ availability in Mediterranean waters (Brandano & Corda, 2002; Brandano et al., 2015).

Fig. 32 - Schematic reconstruction of slope evolution of the Latium–Abruzzi carbonate platform from late Palaeocene to late Eocene–early Oligocene (modified after Brandano, 2017). A-D) From the late Palaeocene to the early Oligocene, the Latium–Abruzzi carbonate platform was a shaved isolated platform exposed to wave action in which sedimentation took place during sea-level transgressive and highstand phases (A, C); in the following falling-stage lowstand phases (B, D), the platform is within the zone of wave abrasion with consequent sediment erosion and generation of the mixed allochthonous/autochthonous sediment. This mixture of displaced and partially reworked sediments was produced by the action of storm-driven currents that acted on the carbonate platform remobilising, resuspending, and reworking sediment towards the slope and toe-of-slope with consequent accumulation of autochthonous and allochthonous deposits (E, F) (modified from Tomassetti & Benedetti, 2020).



Stop 2.4. The Tortonian phosphatic horizon of Tornimparte: hardground or conglomerate? (42°17'01.22"N, 13°17'02.00"E)

This stop focuses on the contact between the “Guadagnolo member”, represented by a bryozoan-rich unit, and the “marly clayey unit”. In the Apennines, the drowning of the Miocene carbonate ramp is evidenced by a phosphatic hardground (Zalaffi, 1963; Carannante, 1982; Brandano et al., 2009), overlain by the marly clays. In this outcrop, in contrast to the rest of the Latium-Abruzzi domain, the phosphatic deposits occur as a series of condensed and allochthonous phosphate-rich beds (Fig. 35 - Brandano et al., 2020a). The first phosphatic interval (level A), occurring 5 m below the top, is a 10 cm-thick horizon with phosphatised and glauconitic lithoclasts up to 1 cm in size. The second phosphatic bed (level B), which lies at the top of the unit, is a grain-supported conglomerate 10 to 15 cm thick, within a grey to brownish packstone to wackestone matrix. The pebbles, 1 mm to 5 cm in size, are intensely phosphatised and bioeroded. On top of the conglomerate, a 1–2 cm thick phosphatised hardground occurs, consisting of phosphate pebbles, phosphatised and non-phosphatised solitary corals, pectinids, oysters, gastropods, brachiopods, palatal and shark teeth. The last

Fig. 33 - Monte La Serra stratigraphic section plotted against stratigraphic depth, and correlation between the local carbon isotope curve across the Oligocene-Miocene boundary and the ODP core 761 record (southern margin of Australia - Holbourn et al., 2004). Modified and redrawn after Brandano et al. (2015).

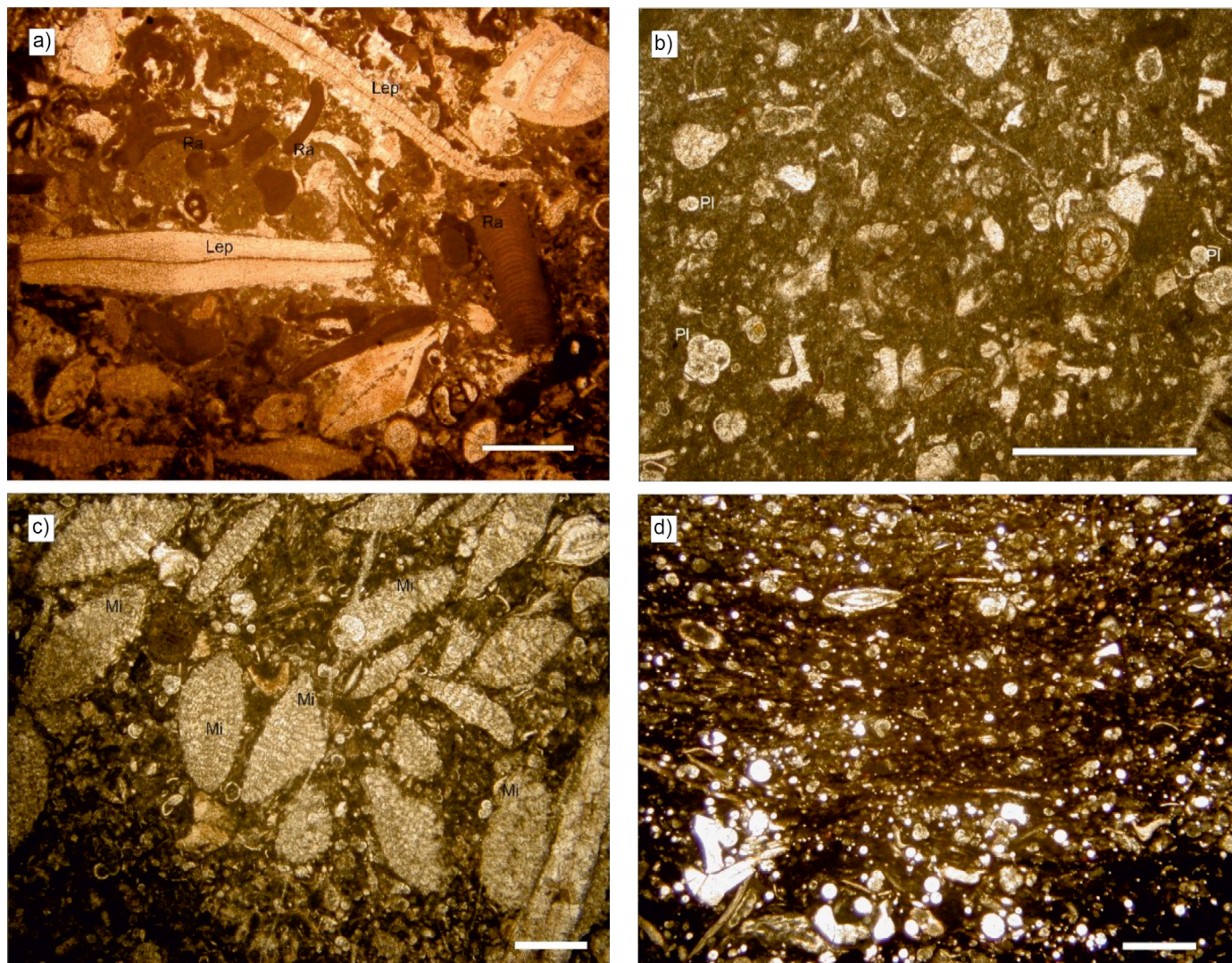
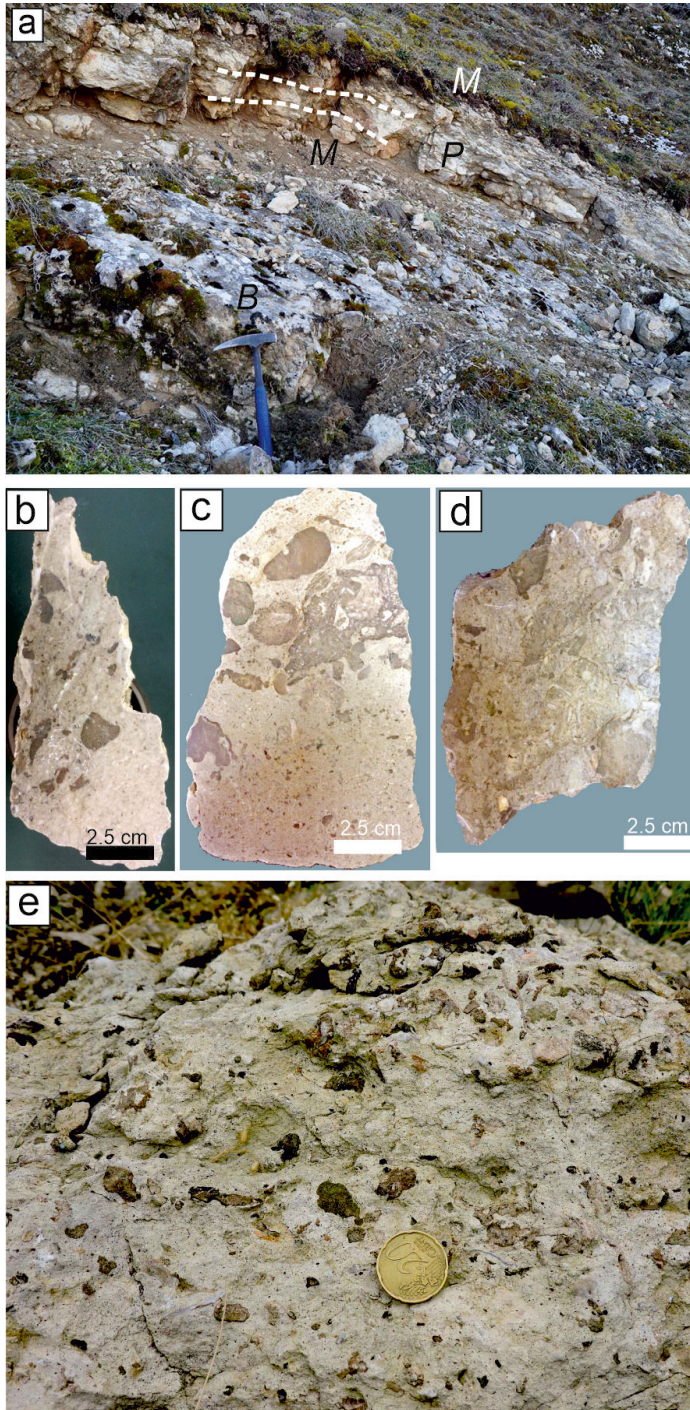


Fig. 34 - Microfacies of the Oligocene-Lower Miocene portion of the "Spogolitic unit" ("Guadagnolo member" SPT₁), cropping out at Monte La Serra section. a) *Lepidocyclina*-bearing packstone to floatstone within a bioclastic packstone matrix; b) Fine bioclastic packstone with planktonic foraminifera; c) *Miogypsina* packstone; d) sponge spicule-rich packstone to wackestone (middle member of the SPT₁). Modified after Brandano et al. (2015). Lep= *Lepidocyclina*; Mi= *Miogypsina*; Pl= Planktonic foraminifera; Ra= Red Algae. Scale bar = 1 mm.

phosphatic interval (level C) is 40 cm thick occurring 15 cm above the boundary between the SPT₁ and the UAM. The base lies on an erosive and irregular contact, and it consists of planktonic marly limestones with abundant phosphate grains, lithoclasts, and nodules and it is covered by a thin phosphate crust up to 5 cm thick (Fig. 35). Electron microprobe analyses, carried out on pebbles of the second and third phosphatic intervals and on the planktonic wackestone of the UAM (see Brandano et al., 2020a for details), show that the green clay phases occurring within the pebbles fall within the compositional field of glauconite. The overall composition of phosphate concretions are comparable to that of carbonate-fluorapatite (CFA, Brandano et al. 2020a). The presence of the planktonic foraminifera biostratigraphic markers *Globorotalia menardii* and *Neogloboquadrina acostaensis* is indicative of early Tortonian age (Iaccarino et al., 2007).



The Central Apennines sedimentary succession documents the transition from the Lower to Middle Miocene Latium-Abruzzi ramp to the Upper Miocene foredeep basin, and it hosts a unique history of phosphogenesis, erosion, and reworking produced by the interaction of coastal upwelling and internal waves (Fig. 36). Phosphate precipitation took place in the sediment accumulated in the outer ramp under the influence of coastal upwelling. Here, phosphatic hardgrounds are the product of the early diagenetic precipitation of carbonate fluorapatite in sub-oxic, organic-rich sediments. Similar phosphatic deposits occur in different Miocene sedimentary successions of the Mediterranean area (Föllmi et al., 2008, 2015). The key aspect that triggered the erosive processes affecting the phosphate deposits is the density-stratified seawater in coastal areas. The latter is characterised by a permanent pycnocline along which perturbations often propagate as internal waves (Pomar et al., 2012). The phosphorite beds of this study accumulated due to the gravity flow triggered by the turbulence at the breaking of the internal waves on the seafloor. The Miocene phosphogenesis phases match the main carbon cycle perturbations. The investigated phosphorite deposits accumulated in early Tortonian during the carbon perturbation known as CM7 (Brandano et al 2020a; Cornacchia et al., 2021).

Fig. 35 - Outcrop appearance and slabbed samples of the Tornimparte phosphatic hardground. a) phosphatic levels characterise the upper portion of the Miocene calcarenites (b) and the first meter of the overlying UAM (M). In the marls the phosphatic interval (P) consists of three distinct layers with thickness ranging in between 5 and 15 cm; b-d) three phosphatic intervals constituting the hardground, the first interval (b) occurs in the upper part of the "Guadagnolo member" (SPT₁) calcarenites with eroded phosphatised lithoclasts dispersed in a free-matrix made of bryozoan floatstone; the second interval (c) phosphatic lithoclasts are dispersed in a phosphatised bioclastic matrix associated with corals and gastropods and separated by irregular surfaces; in the third interval (d) the phosphatic pebbles are dispersed in a marly planktonic wackestone matrix associated with phosphatised fossils and shark tooth (e).

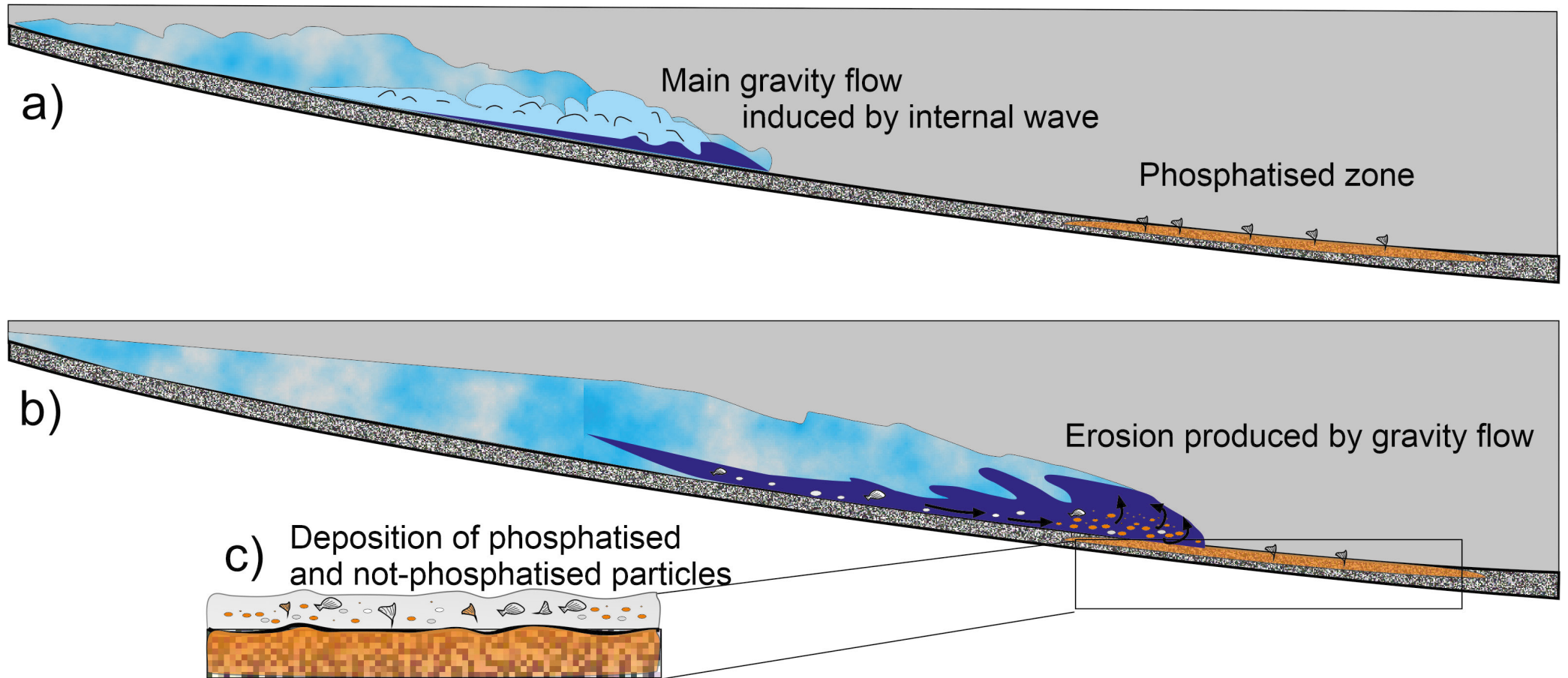


Fig. 36 - Schematic diagram showing the mechanism that rules the origin of the hardground. a) Break of the internal waves produces a backwash return flow that may be turbulent (modified from Pomar et al., 2012); b) the turbulence produced by internal waves at the breaker may easily carry the low-bulk density bioclasts and may create a sediment gravity flow that impacted on the phosphatisation zone where phosphatic crusts and laminae were developed; c) the resulting phosphatic deposits include phosphatised and not-phosphatised particles that were reworked and eroded from the hardground.



Day 3 – The Gran Sasso range: sedimentary succession, tectonics, and hydrogeology

The trip across the Gran Sasso range offers a multidisciplinary approach to the study of the Mesozoic to Miocene sedimentary succession with some hydrogeology hints. The outcrops are on a hiking path that provides a glimpse on the long-lasting sedimentary response to the tectonic-induced palaeogeographic changes (i.e., syn-rift extension, post-break-up extension, foreland extension, orogenic compression). The current Gran Sasso front morphology is a thrust salient with the highest morphologic and structural elevation in the Apennines (Corno Grande; 2914 m a.s.l.; Fig. 37) and has a NE-vergence (Vezzani et al., 2010).

After the lithostratigraphic review of Cardello (2008), later improved by Cardello & Doglioni (2015), a combination of traditional (e.g., Passeri et al., 2008) and newer names are hereby reported in Figure 38. Besides the use of formally defined units for the Jurassic, the Cretaceous, and the Palaeogene, we have adopted names and subdivisions of van Konijnenburg et al. (1998, 1999).

By summarising, the sedimentary and tectonic aspects, six major stages of the Gran Sasso tectonic and sedimentary evolution can be recognised: (1) Late Triassic–Early Jurassic rifting determined the shape of the ‘Umbrian palaeo-highs’, which persisted into the Early Cretaceous (e.g., Corno Grande). (2) Late Cretaceous–early Palaeogene westward tilt of the post-break-up Upper Jurassic to lower Palaeogene formations to the west of the Corno Grande

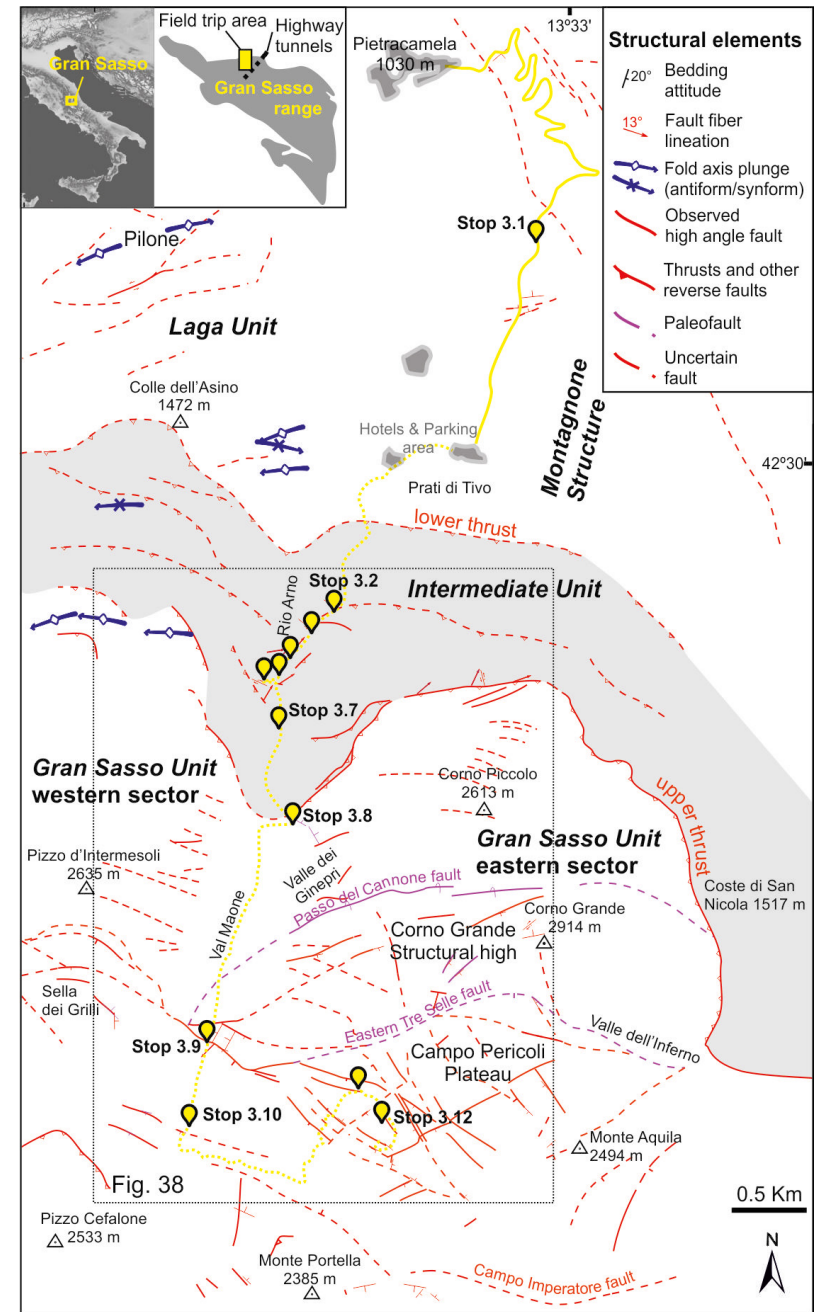


Fig. 37 - Schematic tectonic setting of the Gran Sasso range and stratigraphy modified from Cardello & Doglioni (2015). The continuous yellow line indicates the road while the yellow dotted line highlights the mountain path of this fieldtrip.

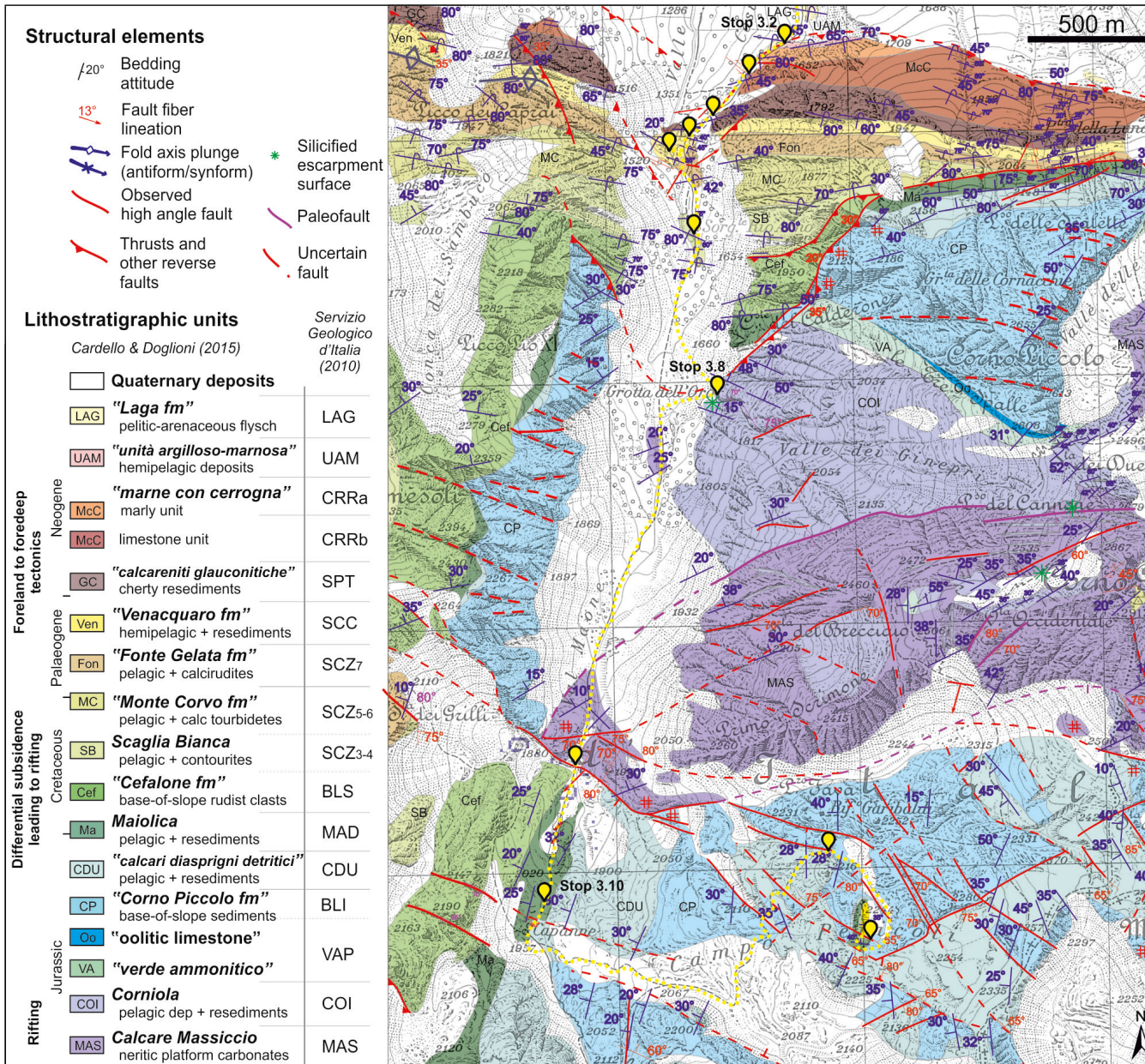


Fig. 38 - Geological map modified from Cardello (2008) with stops 3.2 in yellow symbols from 3.2 to 3.12. A stratigraphic comparison chart is presented along with the lithostratigraphic units.

structural high possibly due to renewed extensional tectonics during the Cretaceous. (3) Oligocene and Middle Miocene syn-sedimentary extension initiated a new generation of faults and possibly the partial reactivation of older fault segments (e.g., Tre Selle Fault). (4) Messinian NNE-directed forward thrusting of the calcareous units onto the siliciclastic deposits forms an asymmetric growth anticline whose geometry is affected by the inherited structure. During convergence (cf. structures in Lucca et al., 2019), the Gran Sasso range already experienced uplift and erosion (Rusciadelli et al., 2005). (5) Earliest Pliocene tilt towards the foreland and back-thrusting, which involved the western edge of the Gran Sasso–Laga front. (6) Post-shortening extension (Quaternary to present day), which has locally intercepted pre-existing syn-sedimentary faults that had been previously passively transported within the thrust sheets. The NE–SW extension is expressed by orthogonal normal faults or WNW-striking right-lateral transtensional faults (i.e., Tre Selle Fault; cf. Demurtas et al., 2016).

<https://doi.org/10.3301/GFT.2022.05>



Hydrogeological framework and evolution

The Gran Sasso hydrostructure is a single basal regional aquifer of about 700 km² (Fig. 39), defined by high water quality and quantity. Its high permeability is locally enhanced or reduced by different faults, and by the highly effective infiltration that feeds important springs at the boundaries of the hydrostructure. The Gran Sasso internal circulation is influenced by the distribution of facies and faults with different transmissivity properties, that drive the underground flow directivity. Permeability limits are constituted by the stratigraphic regional aquitards; e.g., the “*formazione della Laga*” (“Laga fm”) represents the regional aquiclude with no flow limit. The hydrogeological basin is well-defined at the thrust front, while towards the southwest the limits are loose due to the presence of normal faults that connect with the hydrostructures of Sirente and Morrone mounts (Fig. 39) and give rise to groundwater seepages (Petitta & Tallini, 2002). The Gran Sasso aquifer feeds springs that are divided into six groups based on groundwater flow and hydrochemical characteristics (Barbieri et al., 2005). Before becoming a National Park in 1991, the area encountered severe water nappe deployment due to the construction of the highway tunnel and physics laboratory (Monjoie, 1980; Catalano et al., 1986) and probably also as a result of

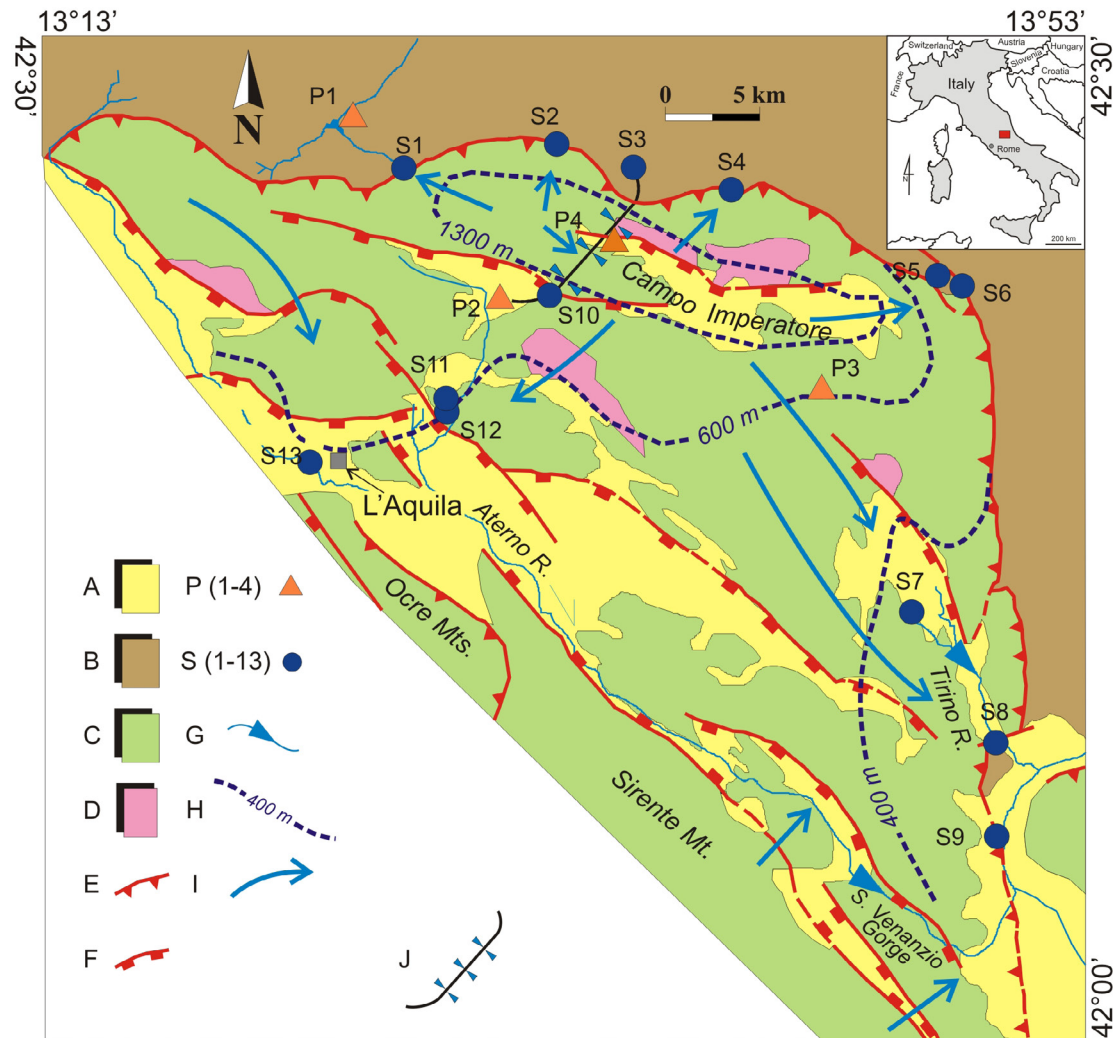


Fig. 39 - Gran Sasso hydrogeological setting. A: aquitard (continental detrital units of intramontane basins, Quaternary); B: aquiclude (terrigenous turbidites, Mio-Pliocene); C: aquifer (calcareous successions of platform, Meso-Cenozoic); D: low permeability substratum (dolostone, Upper Triassic); E: thrust; F: extensional fault; P(1-4) climatic gauges, S(1-13) main springs; G: streambed spring; H: presumed water; I: regional groundwater flow path; J: highway tunnel drainage (from Lorenzi et al., 2022).

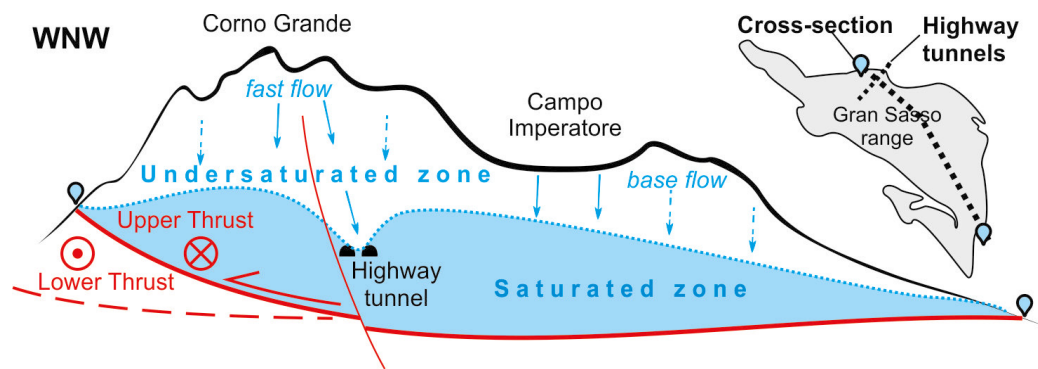


Fig. 40 - Schematic hydro-tectonic scheme (not to scale) of the Gran Sasso aquifer flowpath, modified from Tallini et al. (2013). On the right, the cross-section location, and the trace of the draining highway tunnels.

climate change. In the years 1996–2000, spring discharge has risen slightly, indicating that the aquifer groundwater, also due to drainage by the tunnels, has reached a new steady state (Petitta & Tallini, 2002). The recharge of the groundwater resources is about 700–800 mm/yr (Boni et al, 1986) and it is mainly driven by karst features, and infiltrating groundwater moves vertically, in the unsaturated zone (Fig. 40). Infiltration values are influenced by preferential recharge, fed by high-rainfall and snow rates. The combination of intense rainfall with endorheic morphology gives rise to concentrated infiltration, where an important role is played by the fractures, the vegetable cover, and

by the soil properties. Moreover, the groundwater velocity and the discharge inside the karst conduits/main fractures depend on the fault width and on the lithology. The Gran Sasso range is further subdivided in several sub-basins. As supported by tracer test performed during the highway tunnel excavation, each sub-basins feeds one main spring, as on the northern side (i.e., Rio Arno), or a group of them, as on the southern side.

Stop 3.1. A panoramic view on the Gran Sasso thrust front (42°30'49.26"N; 13°33'54.32"E)

This stop consists of a view of the external Apennines front, which juxtaposes and folds the passive margin-derived Meso-Cenozoic carbonates over the active margin siliciclastic succession (Fig. 41). There, the anticline is asymmetric, it verges towards the north. While the eastern part of the front is represented by an upper thrust that ramps up into the Triassic-Jurassic neritic succession of the Corno Grande, towards the west (e.g., Monte Corvo), the Cretaceous to Neogene rocks are overturned. These characteristics are typical of a fault-propagation-fold that laterally varies its geometry as it cuts across the inherited base-of-slope structure. Further unlike the geometric rule of this kind of structure, which normally dips towards the hinterland, the inner flank of the anticline is tilted toward the north. These deposits are overall tilted towards the foreland, suggesting the occurrence of a later, deep-seated, SSW-verging back-thrust, i.e., a triangle zone, active during (and after) deposition of the "Laga Fm". The thinning and pinching-out of this unit north of Monte Corvo indicates the late Messinian age of the fold (Milli et al., 2007).

<https://doi.org/10.3301/GFT.2022.05>

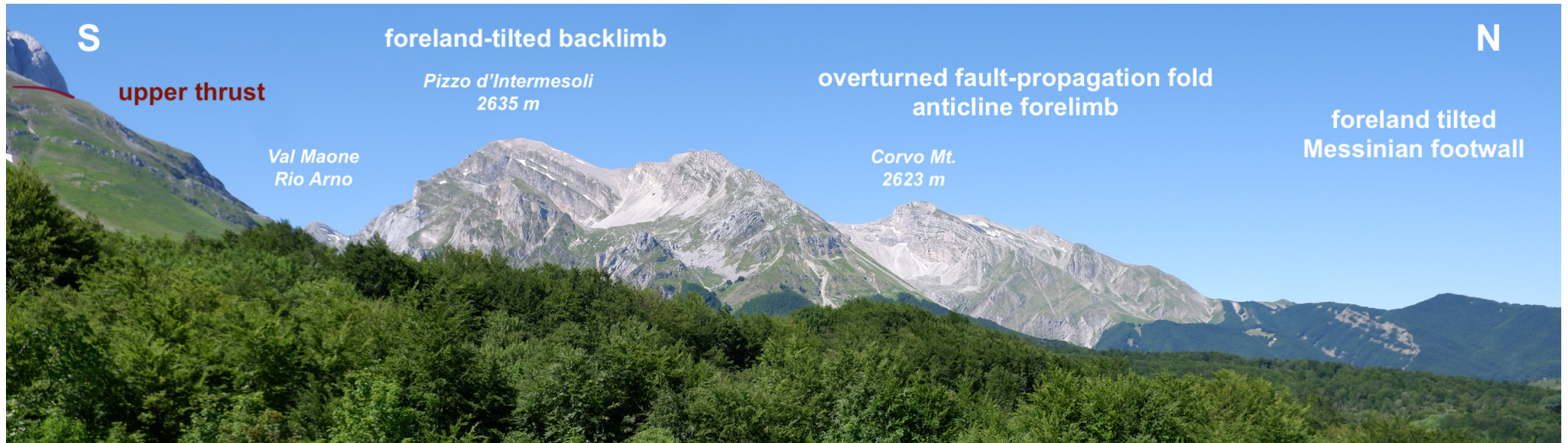


Fig. 41 - Panoramic view of the frontal anticline-syncline system north of Pizzo d'Intermesoli and Monte Corvo.

Stop 3.2. Approaching the overturned succession (42°29'22.61"N; 13°32'53.72"E)

The overturned succession begins with the contact between the "Laga fm", which marks the onset of the Alpine-derived siliciclastics and the UAM (Tortonian *p.p.*-early Messinian *p.p.*, Fig. 38), seen also on the previous day, that consists of 10 to 15 m bioturbated hemipelagic silty marls rich in planktonic foraminifer *Orbulina* sp. These layers are overturned. Further, they are affected by top-north S/C structures and by pressure solution seams that are locally overprinted by thin calcitic striated C-surfaces. This shows progressive deformation that first involves large-scale folding with overturned beds and later involves small-scale thrust-related shear structures. On the way to Stop 3.3, looking to the west a large-scale overturned and folded Cretaceous-Miocene succession occurs.

Stop 3.3. The Middle Miocene inner to outer ramp deposits (42°29'17.55"N; 13°32'44.41"E)

Heading to this stop, you will go across the two lithozones of the "Marne con cerrognà" ("cerrognà marl" (CRR) - Lower to Middle Miocene): a lower one dominated by rare calcirudites and calcarenites and an upper one

dominated by bioturbated marls with pectinids and planktonic foraminifera. As shown on the map (Fig. 38), the thickness of the unit generally increases WNW-ward. Syn-sedimentary normal faults appear to locally control both thickness and facies distribution of the Middle Miocene deposits. Along the lower frontal thrust, a thinner succession of 240 m of well-bedded, fine-grained calcarenites of the "cerroigna marl" is juxtaposed with a much thicker (at least 700 m) coeval succession of amalgamated strata of calcirudites and calcarenites of the Montagnone structure to the north (Fig. 37), which was shown already by Bigi et al. (2011). According to the proposed reconstructions, the difference in facies and formational thickness suggests an originally north-dipping Miocene normal fault that dissected the foreland basin by means of normal faults. In this interpretation, this syn-sedimentary structure once in the foredeep stage was rotated and overturned, and then probably reactivated or obliterated during late Messinian–Early Pliocene compression.

Stop 3.4. The Early Miocene starving and siliceous production (42°29'12.70"N; 13°32'39.23"E)

At this stop, the base of the overturned Miocene succession ("glaucopitic calcarenite" - Cardello & Doglioni, 2015) crops out with calcarenites with chert and glauconite (Fig. 42), suggesting that during the Early Miocene, the glauconitic and biogenic silica was high. These levels were more recently included in the "spongolitic unit" (Servizio Geologico d'Italia, 2010). Overall, the thickness (~70 m) and the facies of the "glaucopitic calcarenite" is relatively uniform also suggesting rather quiet tectonic conditions during the Early Miocene. As observed on erratic blocks along the path, the internal structure is



Fig. 42 - Example of cross-laminated silicified glauconitic calcarenite from a fallen block in the next to the Rio Arno outcrops.



characterised by cross-laminated silicified fabric, while the calcareous portions are defined by glauconite-bearing strata, representative of low-rate carbonate production in the platform (cf. [Adamoli, 1992](#)).

Stop 3.5. The Oligocene distal ramp deposits (42°29'7.84"N; 13°32'32.78"E)

According to [van Konijnenburg et al. \(1999\)](#), the "Venacquaro fm" is of late Rupelian–Chattian age, while for the [Servizio Geologico d'Italia \(2010\)](#) Scaglia Cinerea is Lutetian *p.p.* – Chattian. This informal unit is composed of greenish or rarely reddish pelagic marly limestones with interbedded redeposited calcarenites dominated by the displaced tests of *Lepidocyclina* sp. For a recent review on the Oligocene to the earliest Miocene, refer to [Schiavinotto & Benedetti \(2021\)](#). Moving southward, the lower boundary of the overturned "Venacquaro fm" consists of a paraconformity marked by seasonal water springs. As evident near the waterfall, the overturned strata tend to be horizontal and crossed by low- and high-angle faults. Asymmetric folds and top-north S/C structures can be observed along the path.

Stop 3.6. The Waterfall on the "Fonte Gelata fm" (42°29'6.47"N; 13°32'33.15"E)

Here you can observe a waterfall on the "Fonte Gelata fm" ([van Konijnenburg et al., 1999](#); cf. with the Paleogene "*membro micritico-calcarenitico con selce rossa*"; calcarenitic-micritic member with red chert – SCZ, of the "*scaglia detritica*" fm - SCZ; [Servizio Geologico d'Italia, 2010](#)), which consists of channelised coarse lithoclastic breccias and beds of graded bioclastic packstone, both bearing platform-derived clasts. These beds are interlayered with pink pelagic limestones. Overturned graded beds with cherty reddish nodules can be observed near the country-road bend.

Stop 3.7. The Rio Arno geology and hydrogeology (42°28'57.20"N; 13°32'34.22"E)

After having crossed a slope debris cover in the wood, the Upper Cretaceous–Cenozoic succession occurs folded around the upper thrust. This consists of a blind-thrust ramp geometry that accommodates a few hundred metres up to zero displacement at the fault tip. West of Rio Arno, in the basinal deposits, the thrust ramps up into the higher stratigraphic levels (Fig. 43) of the Pizzo d'Intermesoli area. Because the ramp of the thrust cuts obliquely across the inherited palaeogeographic setting, on the eastern side of the valley, the thrusts

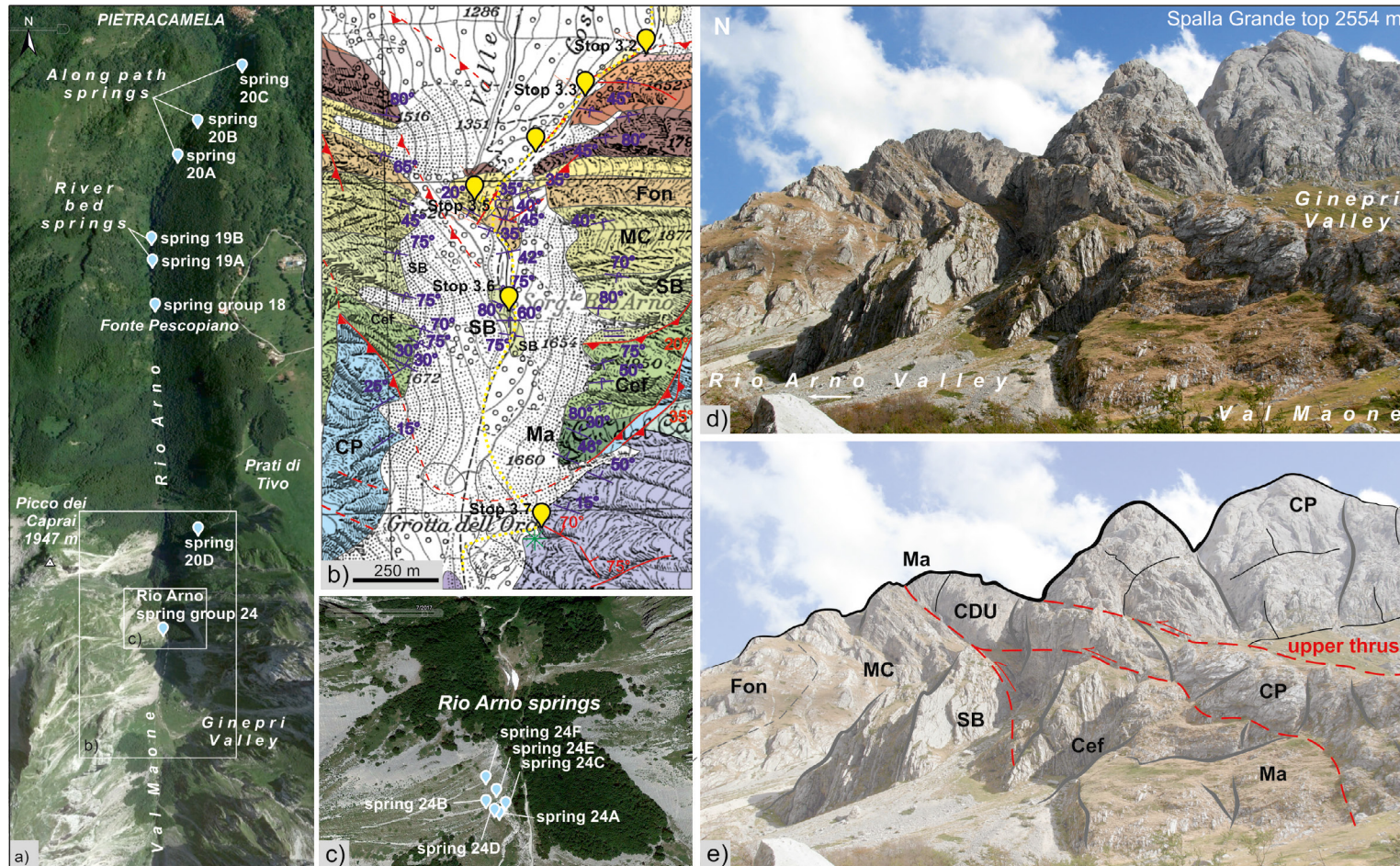


Fig. 43 - a) Rio Arno spring group distribution along the Val Maone: group 24 (tapped spring); group 18 (Pescopiano); group 19 (streambed springs), group 20 (lowest springs) (modified from Di Sabatino et al., 2005). b) Geological map of the Rio Arno (details in Figure 38). d-e) The Late Miocene upper thrust structure on the eastern side of the Rio Arno. The fault zone forms an aquitard for the present-day groundwater paths that infiltrate the upper unit. CP: "Corno Piccolo fm", Middle - Upper Jurassic base-of-slope deposits; CDD: "calcari diasprigni detritici", Upper Jurassic crinoid-bearing cherty calciturbidites; Ma: Maiolica, uppermost Jurassic - Lower Cretaceous pelagic limestone; Cef: "Cefalone fm", Upper Cretaceous base-of-slope; SB: Scaglia Bianca, Upper Cretaceous *p.p.* pelagic and contouritic deposits. MC: "Monte Corvo fm", Upper Cretaceous *p.p.* - Palaeocene *p.p.* pelagic and calciturbidites; Fon: "Fonte Gelata fm", Palaeocene *p.p.* - Eocene pelagic deposits and calcirudites.



juxtapose the inherited Corno Grande structural high that involves the more competent Jurassic limestones on the overturned Rio Arno basinal succession. From the latest Cenomanian to the early Campanian-middle Maastrichtian, the base-of-slope areas between the inherited Jurassic paleo-highs were dominated by the pelagic deposits of the “scaglia” formations (“Scaglia Bianca” and “Monte Corvo” formations; roughly corresponding to the SCZ₃₋₄ and SCZ₅₋₆ members respectively in Servizio Geologico d’Italia, 2010) with only minor turbiditic calcarenite intercalations in the lowermost part of the formation. Slumped intervals, low-angle unconformities, and biostratigraphic hiatuses indicate local slope instabilities and winnowing activity of contour currents. Lateral and down-slope transport of fine sediment is also suggested by the large variation in formational thickness across the Gran Sasso within the uppermost Cenomanian–lower Campanian interval (55–160 m – van Konijnenburg et al., 1999).

The Rio Arno stream and springs

Among the northern side springs of the Gran Sasso aquifer, the Rio Arno spring group is characterised by the contact between the carbonate aquifer and the low-permeability deposits outcropping along the main thrust; at the same time, recent fluvio-glacial deposits locally act as aquitard and/or drainage level, only partially hindering the seepage along the valley.

Rio Arno spring group includes the highest springs partially tapped (about 30-50 l/s) for drinking purposes, but the main streambed springs are located downstream, close to the waterfall. The spring discharge is additionally tapped for hydropower and continuously measured. Recent additional monitoring is related to the H2020 KARMA project (2019-22). The total discharge is variable with years, ranging from 0.13 to 0.36 m³/s in the last twenty years, with an average of 0.21 m³/s. Warning lowering of the discharge has been recorded in 2020, corresponding to the minimum historical discharge. The monthly regime shows the highest values in summer, due to the snowmelt effect, while the lowest discharges are expected in winter. The different springs in the group (Fig. 43) includes the highest ones, partially tapped for drinking purposes (group 24), the Pescopiano spring (group 18), located on the right slope and forming a small swamp, and the lowest streambed springs (group 19), with additional minor springs in the waterfall/hydropower diversion area (group 20). The hydrogeological basin feeding the spring group is smaller than the hydrographic basin, despite the expected geological limits. In fact, the highway tunnel drainages have probably modified the natural recharge area of Rio Arno springs, intercepting at lower elevation the groundwater flow. In detail, due to the water table depletion, the left tunnel of the highway is receiving most of the infiltration groundwater of the Rio Arno-Val Maone hydrographic basin,



which in the past probably fed the Rio Arno springs. Consequently, the present-day hydrogeological basin of these springs is smaller than in the past.

Stop 3.8. The Corniola syn-sedimentary features (42°28'37.77"N; 13°32'39.26"E)

Along the N-trending shoulder of the Corno Grande high, pelagic and mass-flow deposits of Corniola onlap its escarpments. At this stop (Fig. 44), the syn-rift Corniola is characterised by coarse to fine-grained resedimented dolostones as thick as 400 metres, a thickness typical of structural lows near the base of the palaeo-escarpment. NW-directed downthrown blocks are a few metres spaced. On top, the succession continuous with cherty well-bedded doloarenites with finer grain-sized layers and slumps. As shown by the presence of calcarenites and locally megabreccias composed of resedimented neritic material in the lower part of the section, structural lows were filled with carbonate re-sediments from the adjacent Latium-Abruzzi carbonate platform. Contrary, the structural highs were submarine reliefs bounded by faults and related escarpments that were onlapped also by pelagic and occasionally by turbiditic basinal sediments.

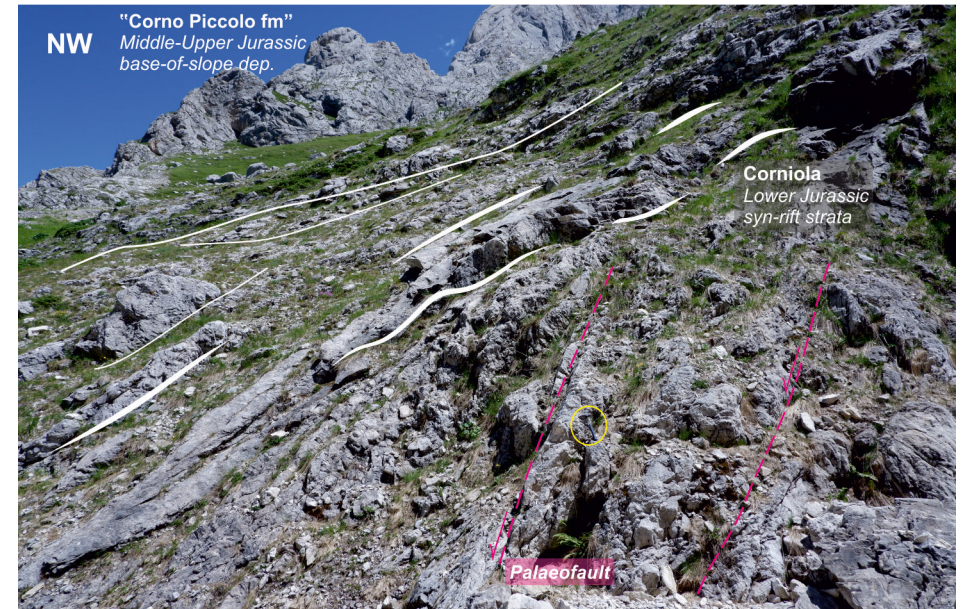


Fig. 44 - Inherited Early Jurassic syn-rift setting of normal faults (purple) and onlapping strata (white) of doloarenites and dolorudites with rare chert. The yellow dashed line circles the hammer.

Stop 3.9. The polyphase tectonics of the Tre Selle Fault (42°27'46.84"N; 13°32'16.08"E)

After a walk up the Val Maone, the path crosses the Tre Selle Fault, which consists of two segments (Fig. 37), an eastern segment preserving the Early Mesozoic palaeogeographic relationship between the Corno Grande high and the Campo Pericoli plateau; a western segment that shows a more complex polyphase history. On this outcrop, which is at the junction of these segments, (W)NW-striking normal faults seem to dissect the pre-existing E(NE)-striking Jurassic faults bounding the Corno Grande paleo high (Figs. 38, 45). Further, due to



stratigraphic thickening of the “Fonte Gelata” and “Venacquaro” fms in the southwest hanging wall block, that is also richer in resediments with respect to the footwall block to the northeast, Eocene-Oligocene and Middle Miocene extensional tectonics were also proposed (Cardello & Doglioni, 2015). In this frame, the Meso-Cenozoic faults were transported during the Late Miocene convergence within the thrust sheets. Finally, as shown in Figure 46, also moraines of the Late Glacial Maximum are dissected by the Tre Selle Fault, testifying for Holocene tectonics spanning to the 1349 CE earthquake (Galli et al., 2021).

Stop 3.10. Pizzo Cefalone: a view on the Cretaceous base-of-slope architecture (42°27'28.34"N; 13°32'9.36"E)

The type locality of the “Cefalone fm” (middle Albian–upper Cenomanian) can be observed on the eastern slope of Pizzo Cefalone peak (Fig. 47). This lithostratigraphic unit, locally defined by van Konijnenburg et al. (1999), records an episode of platform-

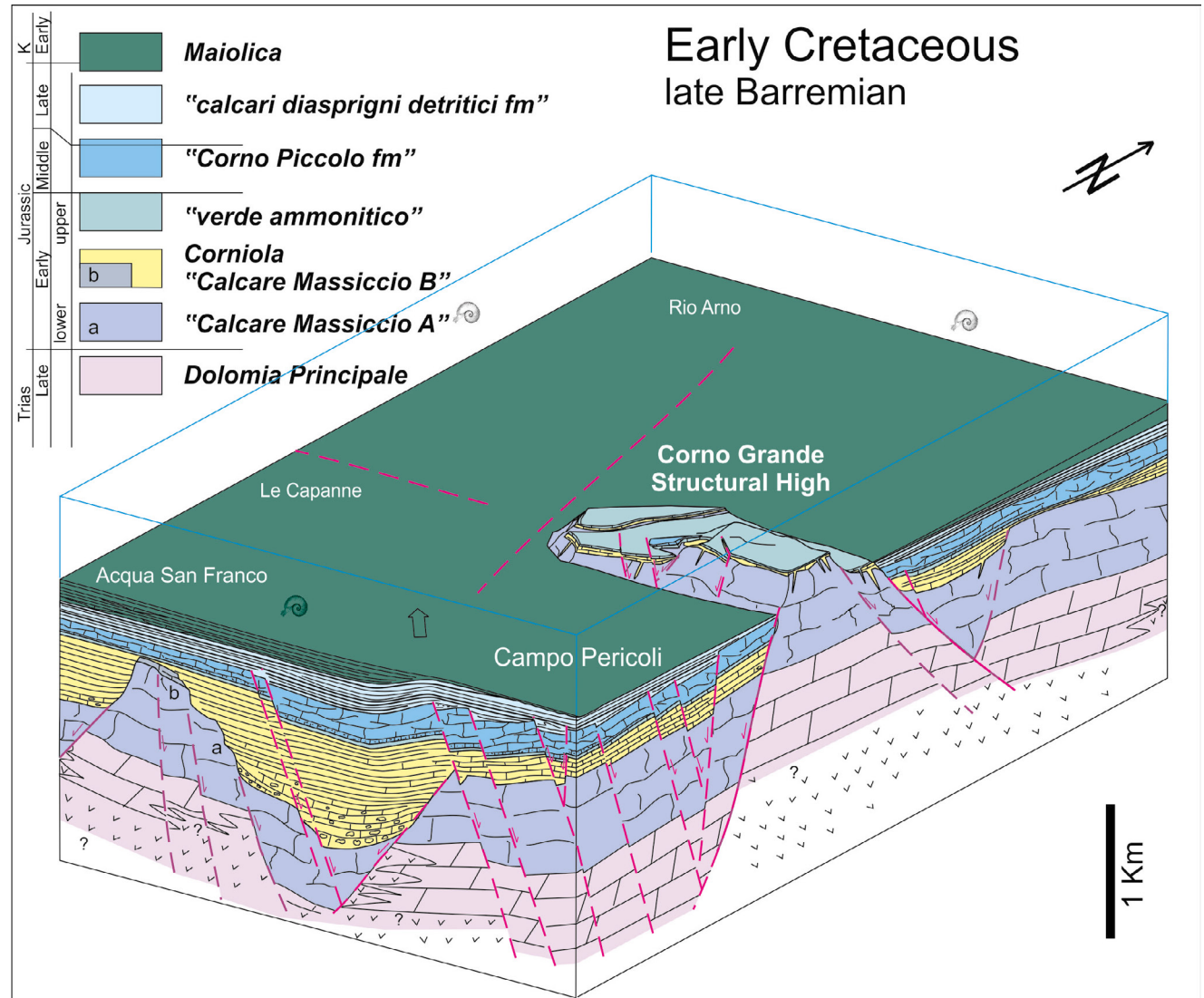


Fig. 45 - Tectono-sedimentary context during the Early Cretaceous when pelagic and redeposited limestones overlie the drowned remaining portions of the former platform: only the Corno Grande structural high and some minor plateaus with reduced sedimentation (Campo Pericoli) persist as submarine topographic highs. “Calcare Massiccio A” and “Calcare Massiccio B” are *sensu* Centamore et al. (1971). The syn-sedimentary tilt toward the west is marked by the change of thickness of the “Maiolica” pelagic layers. Figure modified from Cardello & Doglioni (2015).

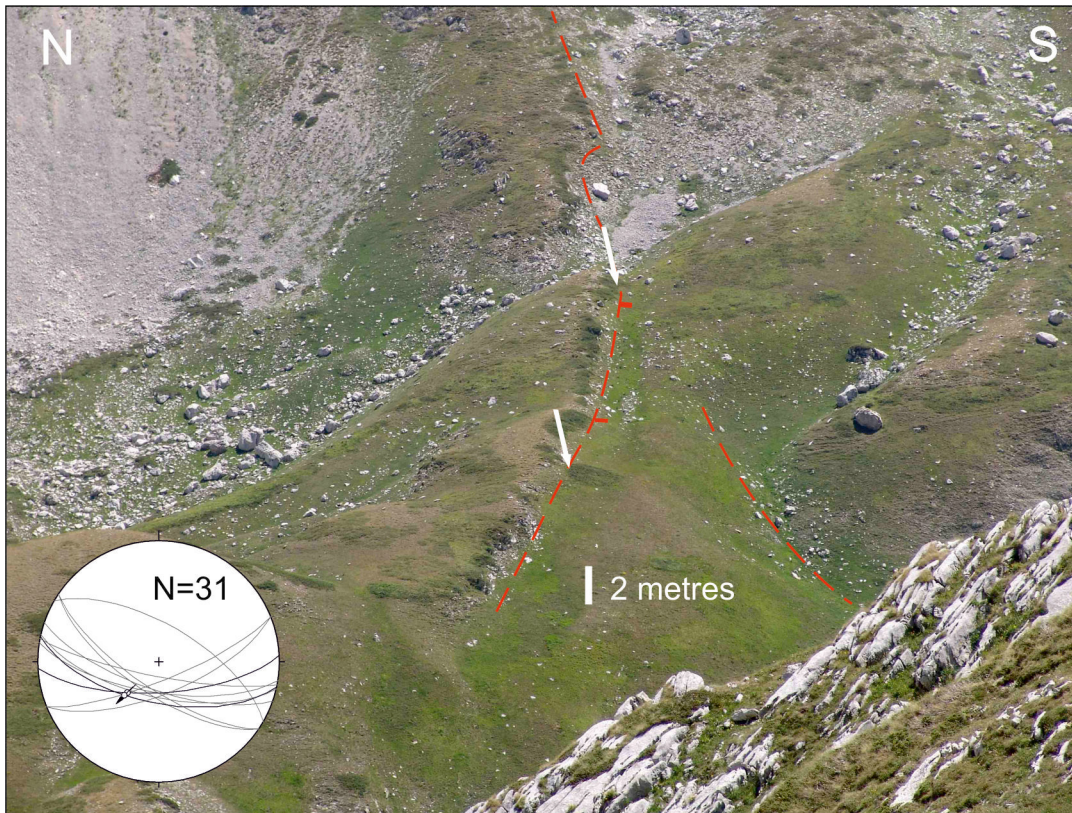


Fig. 46 - Normal-dextral transtensional active Tre Selle Fault outcropping between Val Maone and Campo Pericoli. A similar ribbon is present also in the adjacent valley to the west of Pizzo d'Intermesoli. The surface rupture can be more than 2 m high and indicates that the fault could have generated earthquakes with M_w 7.

margin collapse during mid-Cretaceous emersion of the platform. At the base of the peak, the basal olistostrome erodes the transitional terms between the Maiolica (upper Tithonian–lower Barremian) and “Cefalone” formations. The latter was also mapped as “*calcari bioclastici superiori*” (“upper bioclastic limestone” - BLS) by the Servizio Geologico d'Italia (2010) and is rich in calcirudites and calcarenites with rudist fragments.

Stop 3.11. Campo Pericoli: a glimpse on the Upper Jurassic carbonates (42°27'35.30"N; 13°32'54.92"E)

The western side of the Campo Pericoli area, the “Corno Piccolo fm” (cf. “*calcari bioclastici inferiori*” (BLI) – *sensu* Servizio Geologico d'Italia, 2010) shows a very variable thickness and carries large blocks of reefal limestones with corals and hydrozoans (*Ellipsactinia* sp.). Also, a wealth of other shallow-water organisms records the disintegration of the Upper Jurassic platform margin to the south. The local intercalation of pelagic limestones with *Saccocoma* sp. shows that the cyclic collapse of

the margin, whereas the higher thickness of the formation west and north of Corno Grande may be due to a combination of sediment by-pass and channeling effects induced by the submarine topography of the segmented margin. Below Pizzo d'Intermesoli, the upper surface of the “Corno Piccolo fm” shows a convex-upward geometry onto which the Upper Jurassic formations are onlapping (Figs. 38). The “*calcari diasprigni detritici*” (detrital cherty limestone” *sensu* Passeri et al., 2008; Calcari Diasprigni, CDU – Servizio Geologico d'Italia, 2010) is composed of turbiditic calcarenites with crinoid ossicles and bands of replacement chert,

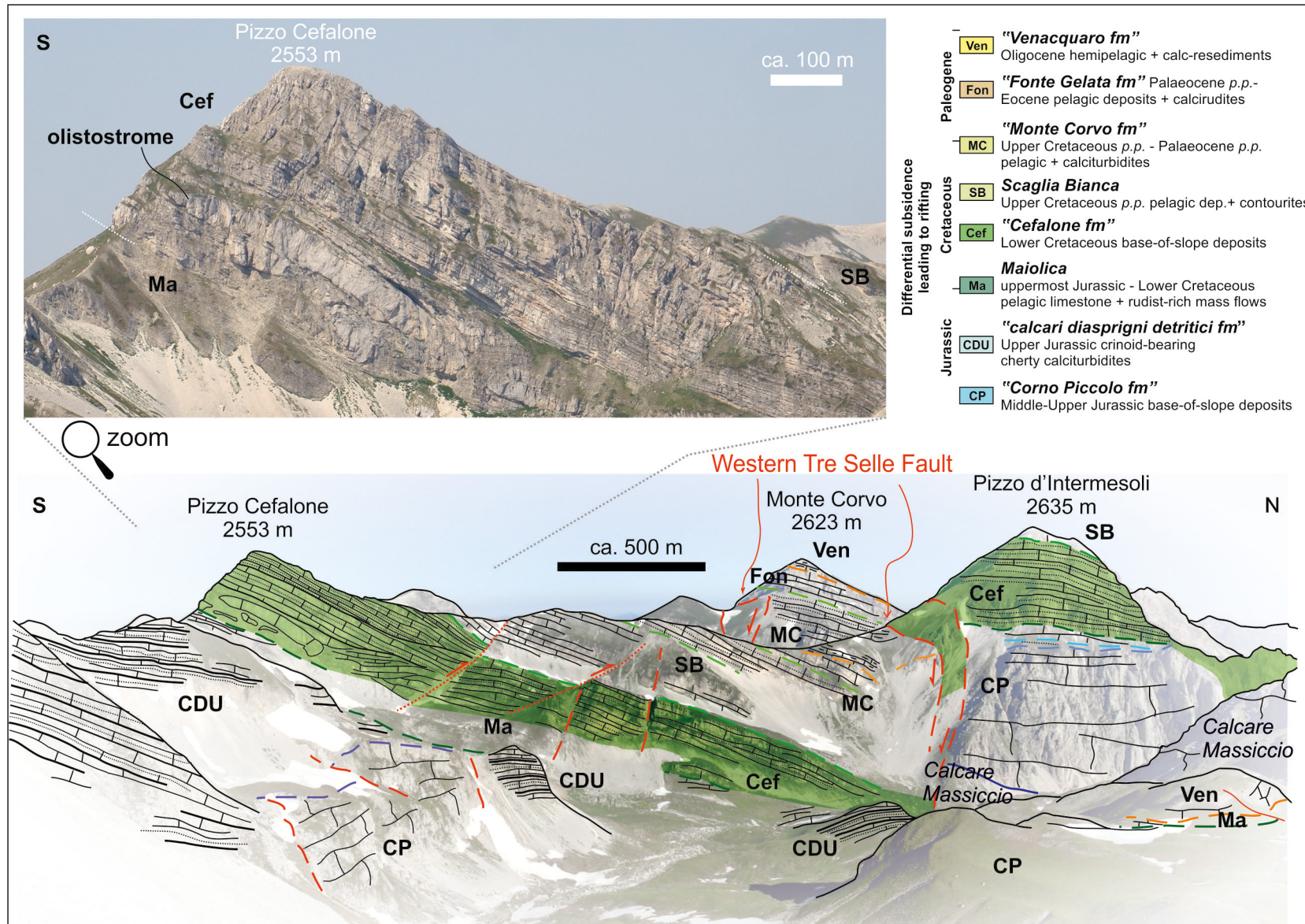


Fig. 47 - Panoramic view of Campo Pericoli, Pizzo Cefalone and Pizzo d'Intermesoli modified after Cardello & Doglioni (2015). The normal western Tre Selle Fault cuts across the Late Jurassic to early Cenozoic base-of-slope succession. The "Corno Piccolo fm" consists of coarse mass-flow breccias. Note large glides and slumps at the base of the "Cefalone fm" (green). Dotted brick pattern: breccias and calcarenites; brick pattern: pelagic limestones.



and lesser micritic slumped limestones. Variations of formational thicknesses are less pronounced up-section, suggesting that the submarine relief was, with the exception of the Corno Grande high, gradually buried by the sediments (Fig. 45). Up-section, the “*calcarei diasprigni detritici*” deposits pass into the Maiolica pelagic limestones.

Stop 3.12. The Campo Pericoli reduced and discontinuous succession (42°27'26.78"N; 13°33'8.06"E)

In the central part of Campo Pericoli (Figs. 48a-b), the Upper Jurassic to Palaeogene succession is much thinner than to the west and south and includes large stratigraphic gaps, showing that this block persisted high throughout the Cretaceous and the Palaeogene. The “*calcarei diasprigni detritici*” is overlain by about 5-15 metres of Maiolica formation (Fig. 48c), that reaches almost 200 m in thickness about 1 km more to the west. Furthermore, the overlying “Cefalone fm” is reduced to about 2 m of crudely bedded, white breccias and calcarenites. There is an angular unconformity between the Mesozoic strata, which dip gently westward, and the Oligocene “Venacquaro fm” breccias with *Lepidocyclina* sp. (Fig. 48d), dipping irregularly 30° to the north. This outcrop is fundamental for the palaeogeographic reconstruction of the post-breakup tectonics affecting the southern Tethyan passive margin during the Cretaceous.

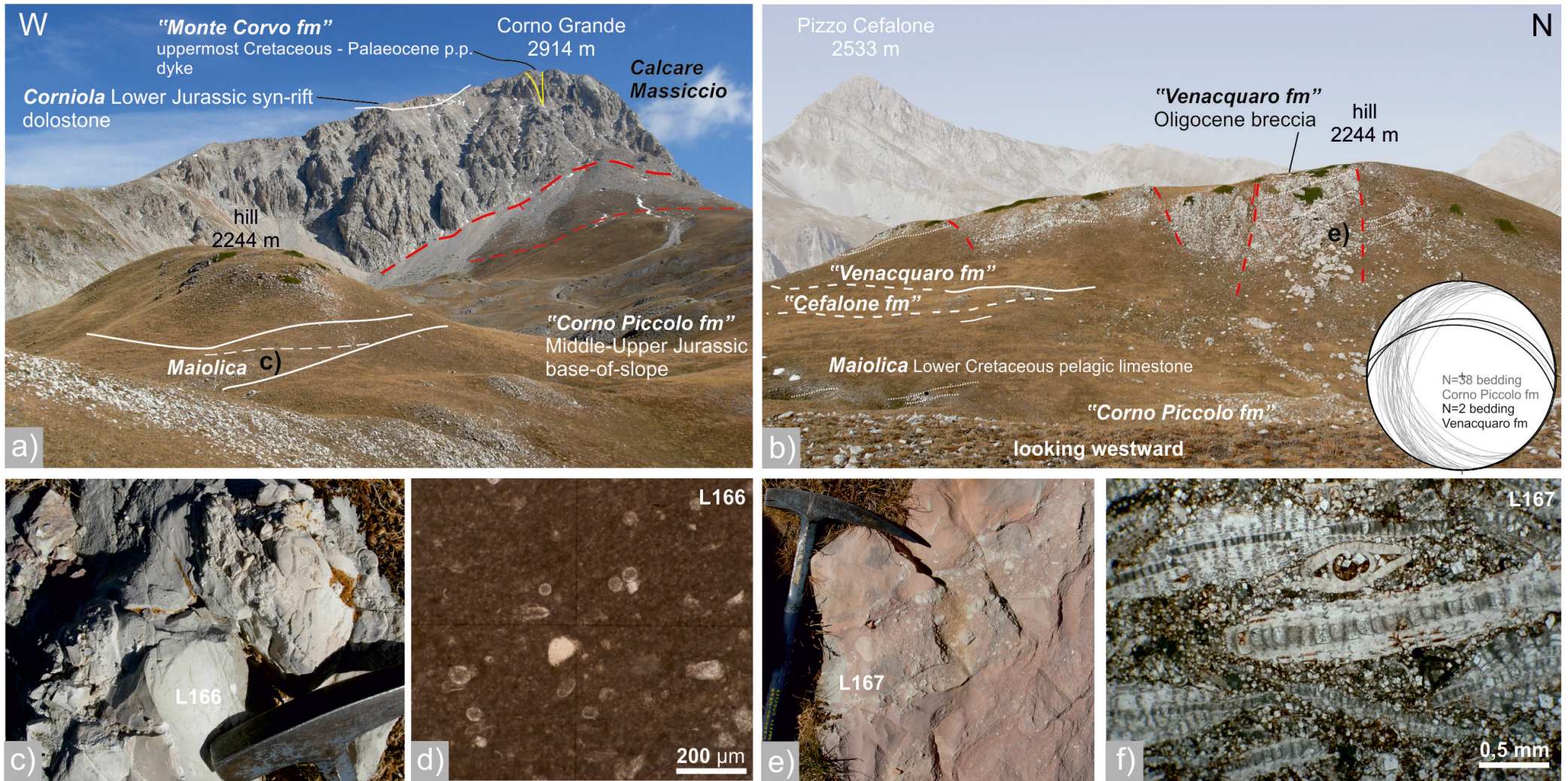


Fig. 48 - Campo Pericoli and Corno Grande geology: (a) lateral view of a very thin and discontinuous succession of Upper Jurassic to Oligocene deposits. The original stratigraphic relationships are weakly disturbed by high-angle faults. b) Frontal view. The Jurassic succession dips to the west (inset); only the younger "Maiolica" and "Venacquaro" formations dip toward the north. (c) Detail of Maiolica deposits (left) and its thin-section view of calpionellid-rich mudstone (right). d) Detail of "Venacquaro fm" sedimentary breccia (left) with sub-rounded clasts in a floatstone matrix rich in *Lepidocyclina* sp. and *Heterostegina* sp. (thin-section view, right).



Day 4 – The Maiella Mountain Pennapiedimonte section

During this day, the geometric relationships between platform and slope-to-basin successions will be analysed to reconstruct the platform margin architecture of the northern portion of the Apulia platform. Different geometries can be observed at the seismic scale along a natural section of Maiella Mountain. At Pennapiedimonte (Stop 4.1), about 90 Myr-long evolution is exposed along the road crosscutting a continuous several hundred metres thick section, which records the Upper Cretaceous to Miocene vertical transition from an escarpment-bounded platform margin to an accretionary prograding margin. In particular, the Eocene/Oligocene boundary is here described and discussed.

The geological-stratigraphic framework of the Maiella Mountain

The Maiella Mountain is one of the most spectacular structures of the external Central Apennines because it preserves the inherited Late Cretaceous-Palaeogene stratigraphic record and tectonics of the area (Fig. 49). The Maiella Mountain is an N- to NW-striking anticline with a culmination in the central sector (Monte Amaro, 2793 m a.s.l.; Fig. 50). The Mesozoic-Cenozoic carbonate succession was

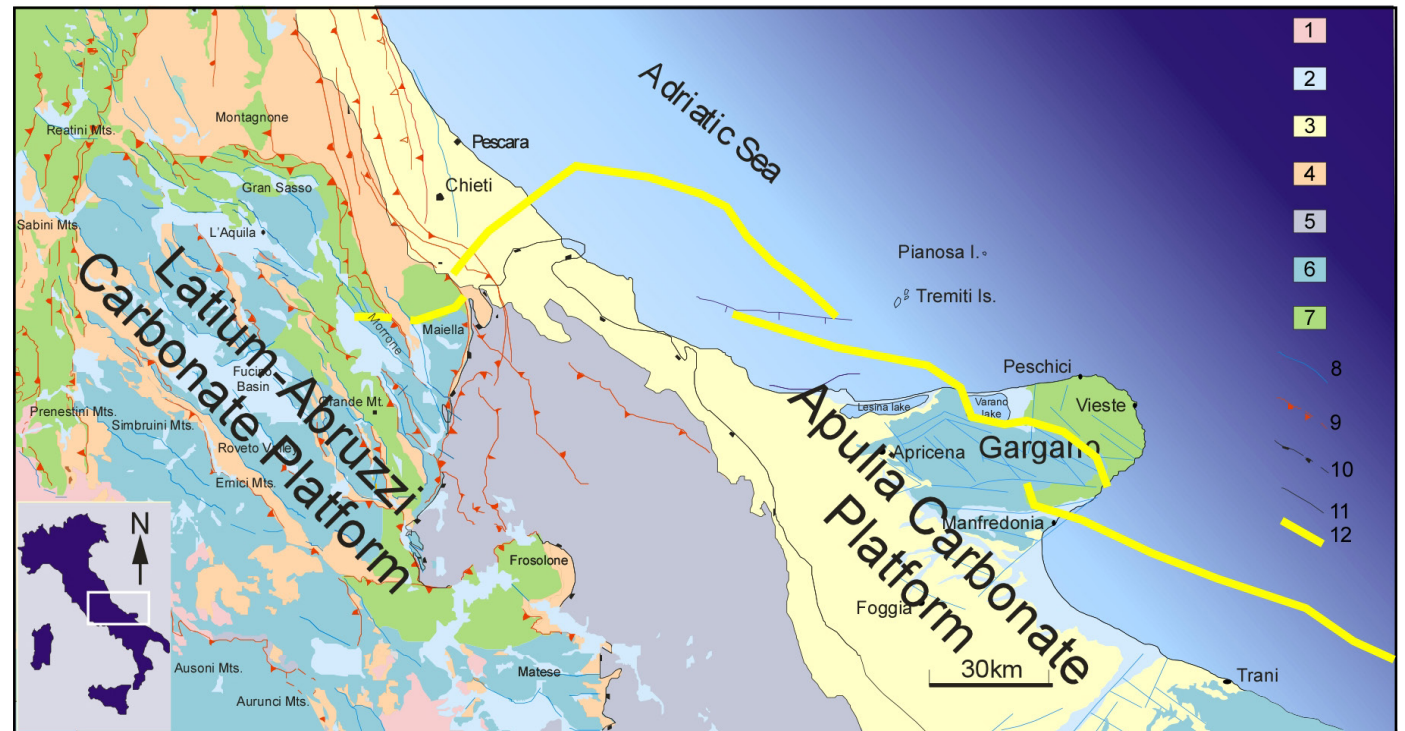


Fig. 49 - Geological map of the Central and Southern Apennines (modified from Morsilli et al., 2004). Key – 1: Quaternary volcanic rocks and volcanoclastic deposits; 2: Pleistocene continental deposits; 3: Middle Pliocene-Pleistocene marine deposits; 4: Miocene to Lower Pliocene foredeep deposits; 5: allochthonous Molise units (Cretaceous - Upper Miocene); 6: Carbonate platform succession (Triassic-Miocene); 7: Slope-to-basin carbonate deposits (Triassic-Miocene); 8: normal fault; 9: thrust fault; 10: basal thrust of the Allochthonous Molise Units; 11: main unconformity; 12 Apulia platform edge.

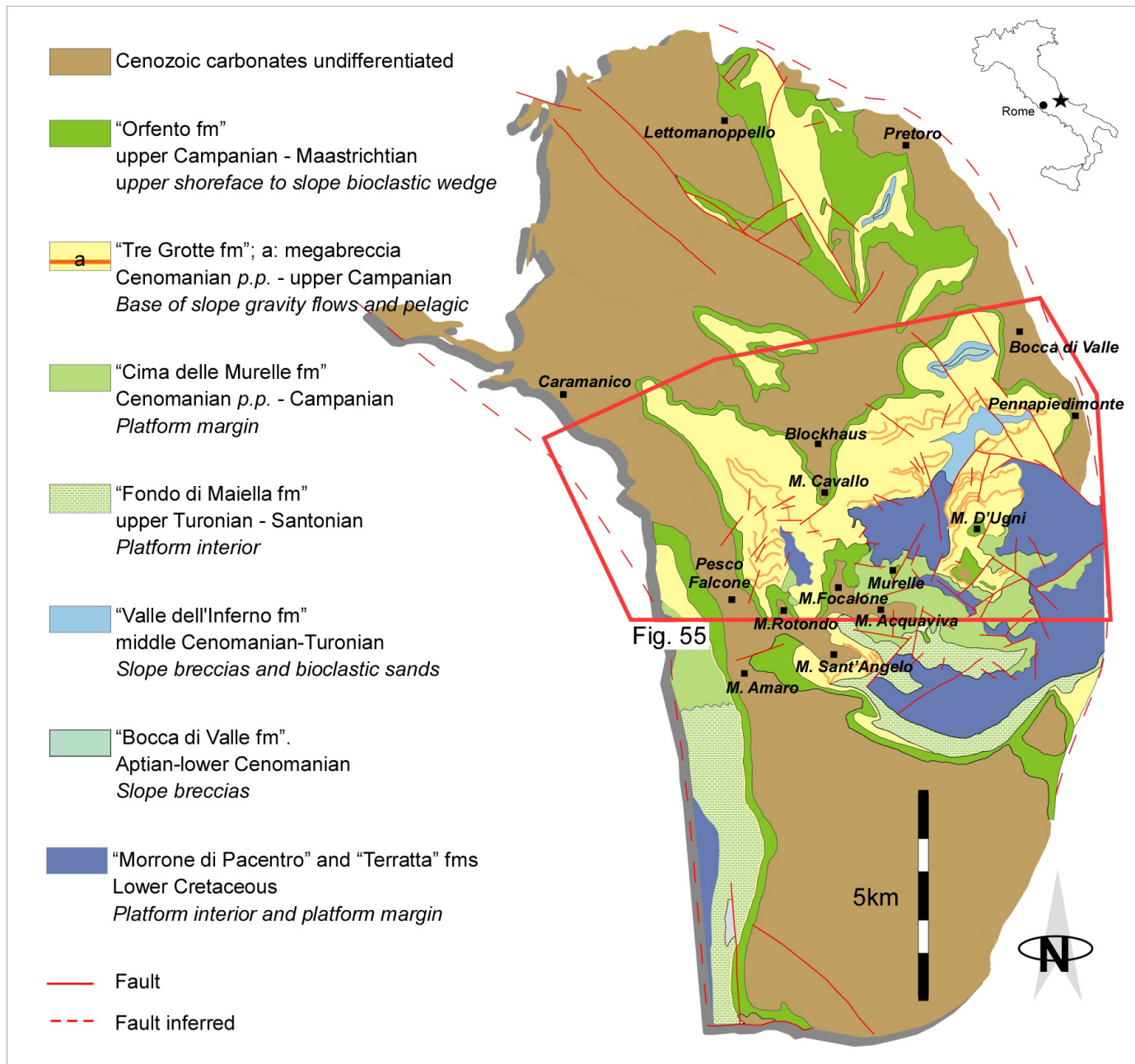
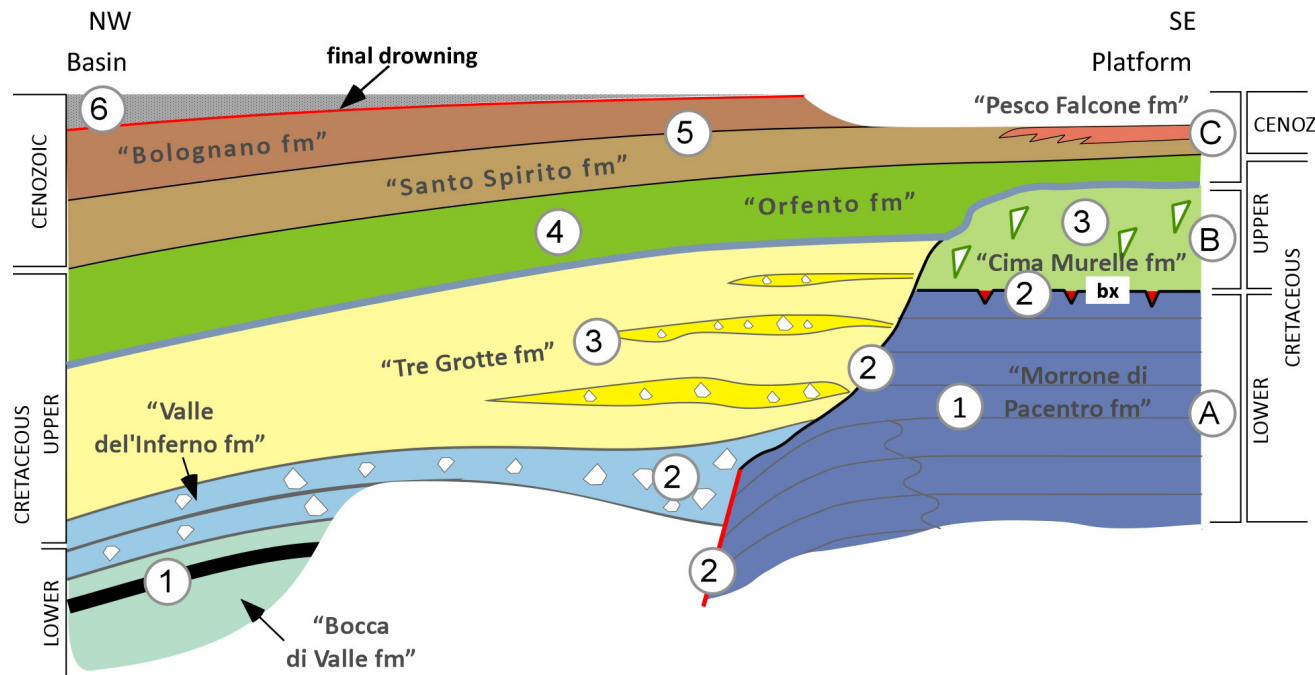


Fig. 50 - Geological scheme of the Maiella Mountain (modified from Morsilli et al., 2004).

involved into shortening during the Pliocene (e.g., Calamita et al., 1996 and references therein; Crescenti et al., 2004). Northward and eastward, gently eastward-tilted Upper Pliocene-Pleistocene deposits unconformably seal the thrust front up to the Lower Pliocene folded siliciclastic successions. The western flank of the Maiella anticline is truncated by a W-dipping normal fault, the Caramanico fault, extending for a length of about 30 km in an N-S to NW-SE direction, with a maximum downthrow of about 3 km (Donzelli, 1968). Its activity is thought to be Messinian to Pliocene (Scisciani et al., 2000) or Quaternary (Ghisetti & Vezzani, 2002). Southward, the Maiella anticline is confined by the Sangro-Volturno line, separating a structural depression, where the Molise allochthonous units crop out (Fig. 49). The Maiella sedimentary succession records the complete geodynamic evolution, from the late stages of the Alpine Tethyan passive margin (Early Cretaceous) to the plates convergence tectonics that precedes

The Tethyan and Tyrrhenian margin record of the Central Apennines: a guide with insights from stratigraphy, tectonics, and hydrogeology

G.L. Cardello - L. Tomassetti - I. Cornacchia - A. Mancini - M. Mancini - I. Mazzini - G. Rusciadelli - E. Capezzuoli - V. Lorenzi - M. Petitta - G.P. Cavinato - O. Girotti - M. Brandano



Platform architecture	Platform margin geometry	Slope depositional system
(A) aggradational	accretionary	slope apron?
(B) backstepping	erosional and by-pass	base-of-slope
(C) backstepping and progradational	accretionary/ramp	slope apron/middle to outer ramp

Platform evolution	
①	Early Cretaceous (Aptian-early Albian). Aggradational platform with an accretionary margin and slope, facing a relatively deep pelagic basin
②	Early- Late Cretaceous (late Albian - early Cenomanian). Platform exposure and formation of bauxitic soils. Main phase of margin collapse triggered by faults along the slope. The platform physiography changes from accretionary to erosional.
③	Late Cretaceous (middle Cenomanian - late Campanian). Shallow water sedimentation recovers on the platform top. The platform margin is dominated by rudists (high debris production). Platform margin growth enhances the collapse of discrete portions of the margin. The erosional slope is kept by gravity flows (by-pass). Sediments onlap the escarpment and gradually fill the basin.
④	Late Cretaceous (late Campanian - late Maastrichtian). Basin filling and blanketing of the morphological differences between the platform and the basin. End of the escarpment-bounded platform, beginning of the progradational platform system.
⑤	Palaeocene to Late Miocene . Development of carbonate ramps. Change of ecological associations from tropical to temperate. Erosional and non-depositional unconformities.
⑥	Messinian . The Messinian evaporitic crisis and the involvement in the foredeep system induce the demise of the shallow water carbonates.

the closure of the western Alpine Tethys (Late Cretaceous-Palaeogene), up to the final orogenic stages (Pliocene-Pleistocene) related to the opening of the Tyrrhenian Sea. The Cretaceous stratigraphic units represent different depositional environments (Fig. 50): Lower Cretaceous "formazione Morrone di Pacentro" ("Morrone di Pacentro fm" *sensu* Crescenti et al., 1969) and Upper Cretaceous "Fondo di Maiella fm" (*sensu* Sanders, 1994) platform interior, Lower Cretaceous "Formazione della Terratta" ("Terratta fm" *sensu* Crescenti et al., 1969) and Upper Cretaceous "Cima delle Murelle Fm" *sensu* Vecsei, 1991) platform margin, in the southern and central areas, Upper Cretaceous ("Tre Grotte fm" *sensu* Vecsei, 1991) slope and basin in the northern sectors. The uppermost Cretaceous interval is represented by a widespread bioclastic sand wedge recording platform margin-

Fig. 51 - Simplified stratigraphic architecture of the Cretaceous to Miocene Maiella Platform, illustrating the main platform architectures, geometries, and evolutionary stages (modified after Strata GeoResearch, 2019). Key - bx: bauxite.

to-slope environments. The Cretaceous evolution of the Maiella succession records the transition between an escarpment-bounded to an accretionary progradational platform margin. During the Cenozoic, depositional conditions were more homogeneous and dominated by carbonate ramps until the early Messinian. Starting from the late Messinian, concomitantly with the evaporitic event, the Maiella and the surrounding areas were progressively involved in the deformation associated to the migration of the thrust belt-foredeep-foreland system; the carbonate deposition stopped, and it was definitively replaced by siliciclastic sedimentation, which records the complete evolution from foredeep to shoreface deposition (Berti et al., 2021).

Stratigraphic framework of the Maiella Mountain

The Maiella Cretaceous lithostratigraphic framework mainly derives from the studies of Crescenti et al. (1969) and Catenacci (1974), that were successively implemented by Accordi et al. (1987), Accarie (1988), Vecsei, (1991), Eberli et al. (1993), Mutti et al. (1996), Sanders (1996), Rusciadelli & Vichi (1998), Stössel & Bernoulli (2000), Morsilli et al. (2000, 2002), Rusciadelli et al. (2003), Rusciadelli (2005), Patacca et al. (2021) (Fig. 52).

1) The "Morrone di Pacentro fm" (Lower Cretaceous) (Crescenti et al., 1969) represents the oldest platform interior succession exposed in Maiella Mountain and consists of mudstones/wackestones to bioclastic and/or oolitic and peloidal packstones, more rarely grainstones, and algal laminites, with frequent gastropods (nerineids), dasycladacean algae, benthic foraminifera and bivalves organised into 0.10 to a few metres thick peritidal cycles. At the top, above Urgonian-type lithofacies, the succession is capped by an unconformity corresponding to a

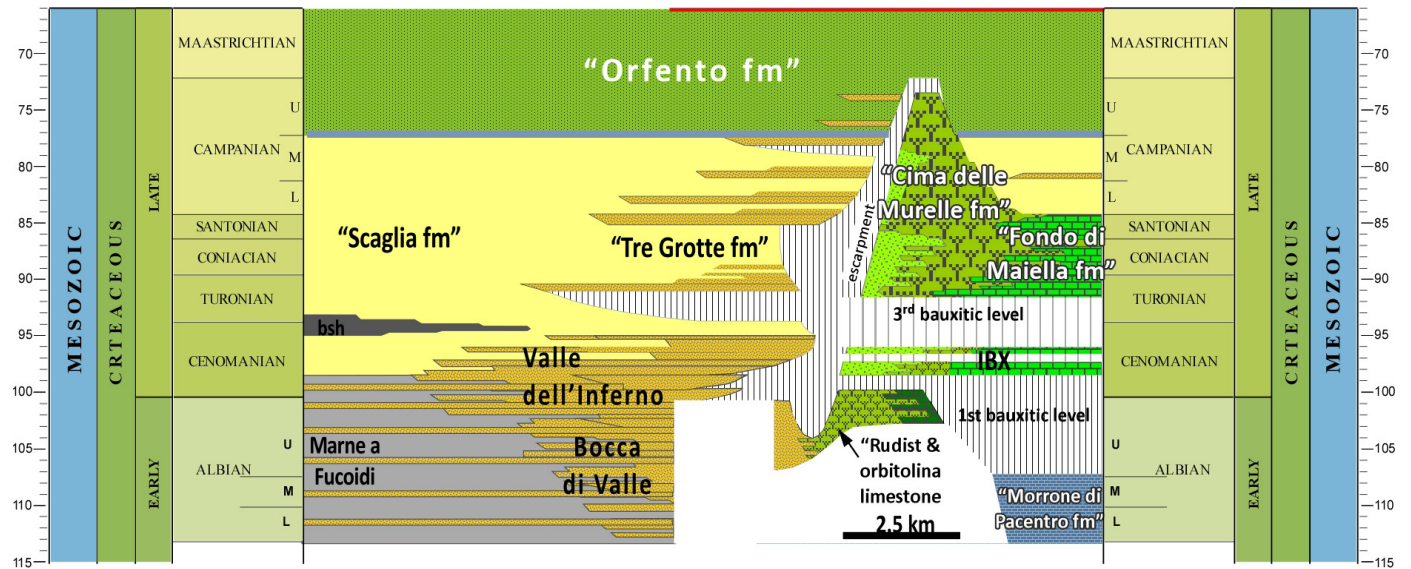


Fig. 52 - Chronostratigraphy and lithostratigraphic nomenclature of Cretaceous successions of the Maiella Mountain (modified after Morsilli et al., 2004). Key - bsh: black shale; IBX: "calcarei intrabauxitici".



major subaerial platform exposure event marked by karst features and a discontinuous bauxitic level. These lithofacies allow to refer this formation to an internal platform with transition to a sandy open margin.

2) The “Terratta fm” (Lower Cretaceous) represents the oldest platform margin succession exposed. It develops laterally to the upper interval of the “Morrone di Pacentro fm” and it consists of massive clinofolds composed of bioclastic grainstones, rudstones, and lithoclastic breccias, with microencrusters, large fragments of corals, and calcareous sponges, in both fragments and whole individuals, benthic foraminifera, and rudists.

3) An intra-bauxitic interval (upper Albian-lower Cenomanian) lies above the “Morrone di Pacentro fm”, on top of a discontinuous bauxite level, and corresponds to a unit bounded by unconformities, which records inner to outer platform margin successions (Rusciadelli & Ricci, 2008). A marked subaerial exposure, characterised by dissolution breccias and a dark brown marly level, intercalates in the lower part of the unit. The upper unconformity is evidenced by a thin reddish exposure level on which open shelf clinostratified bioclastic grainstone-rudstone downlap.

4) The “Fondo di Maiella fm” (Upper Cretaceous) represents the platform interior succession developed in the central and southern sectors of the Maiella anticline and consists of peritidal facies mud-dominated deposits with benthic foraminifera alternating with open shelf strata made of bioclastic grainstone, and floatstones with rudists and gastropods.

5) The “Cima delle Murelle fm” (upper Cenomanian *p.p.* – Campanian *p.p.*, Vecsei, 1991) lies on the intra bauxitic interval and represents the high energy platform margin facies, laterally developed to the “Fondo di Maiella fm”, on the platform edge inherited from the collapse of large portions of the Lower Cretaceous platform margin. It is composed of a whole range of textures, from mudstones to oolitic and bioclastic grainstones. Rudist biostromes (radiolitids and hippuritids) frequently occur at different stratigraphic intervals. These lithofacies are organised into a few metres thick cycles, frequently capped by subaerial exposure surfaces.

6) The “Bocca di Valle fm” (Albian *p.p.* – lower Cenomanian) corresponds to the Marne a Fucoidi fm of the basinal areas, developed in a base-of-slope setting. It is made up of thin micritic pelagic limestones alternating with medium to thick bioclastic packstones and grainstones and thick bodies of breccias with platform-derived clasts. Black shale levels intercalate in the lower part of the unit.

7) The “Valle dell’Inferno fm” (Cenomanian *p.p.*, Accarie, 1988; Vecsei, 1991) represents the first base-of-slope deposits that are seen to onlap the platform margin exposed on the Maiella Mtn. It is mainly composed



by metre scale beds, often amalgamated, made of bioclastic packstones and grainstones. Breccias and megabreccias bodies with platform-derived clasts characterise the lower part of this unit.

8) The “Tre Grotte fm” (Turonian – Campanian *p.p.*, [Vecsei, 1991](#)) represents a second base-of-slope unit lying on the “Valle dell’Inferno fm” and which extensively onlaps the Lower and Upper Cretaceous platform margin represented by a steep and deep palaeoescarpment. It consists of different lithofacies, such as thin to medium mudstones-wackestones with planktonic foraminifera, medium to thick bioclastic frequently graded packstones-grainstones, and lenticular, metre to ten metres thick breccias and megabreccias. This unit has been referred to a base-of-slope depositional system.

9) The “Orfento fm” (Campanian *p.p.* – Maastrichtian, [Crescenti et al., 1969](#)) is the unit that progressively drapes in the latest Cretaceous the topographic differences between the platform and the adjacent basin. It also marks the transition between the erosional bypass to accretionary platform margin geometry (Fig. 52). It is essentially composed by lenticular bodies and cross-bedded bioclastic grainstones and rudstones. The bioclastic fraction is represented by rudist fragments. Sedimentological features allow to refer this unit to a high-energy bioclastic sand apron with bioclastic shoals migrating toward a shallow basin ([Eberli et al., 1993, 2019](#); [Mutti et al., 1996](#)).

10) The “Santo Spirito fm” (Danian – Rupelian) identifies the Palaeogene carbonate ramp developed above the former Mesozoic platform to the basin system. Over the Mesozoic platform top, the succession is thin and discontinuous, while it is thicker and more continuous northward, over the platform margin and slope ([Vecsei et al., 1998](#)). Overall, the “Santo Spirito fm” consists of breccias with lithoclasts, biodetrital calcareous turbidites, and pelagic limestone deposited in an outer ramp to basin environment ([Vecsei et al., 1998](#); [Raffi et al., 2016](#); [Cornacchia et al., 2018](#)). Foraminifera grainstone shoal deposited on the top of the Mesozoic platform (“Alveolina Limestone” of [Bally, 1954](#)).

11) The “Bolognano fm” (upper Rupelian-lower Messinian) represents a homoclinal carbonate ramp. It can be divided into six different units, representative of six lithofacies associations ([Brandano et al., 2012, 2016a](#); [Tomassetti et al., 2021](#)) (Fig. 53).

The first unit, named “*Lepidocyclina calcarenites 1*” (cf. “*Lepidocyclina limestone*” in [Patacca et al., 2021](#); Rupelian *p.p.* – Chattian *p.p.*), mainly consists in coarse-grained, bioclastic, cross-bedded grainstones and packstones, dominated by LBF, which formed a wide dune field in the mesophotic middle ramp, under the action of northward-directed currents triggered by storms ([Brandano et al., 2012](#); [Tomassetti et al., 2021](#)). The second unit is the “cherty marly limestone” (cf. “Cerratina cherty limestone” of [Patacca et al., 2021](#); Chattian *p.p.* – Aquitanian *p.p.*,

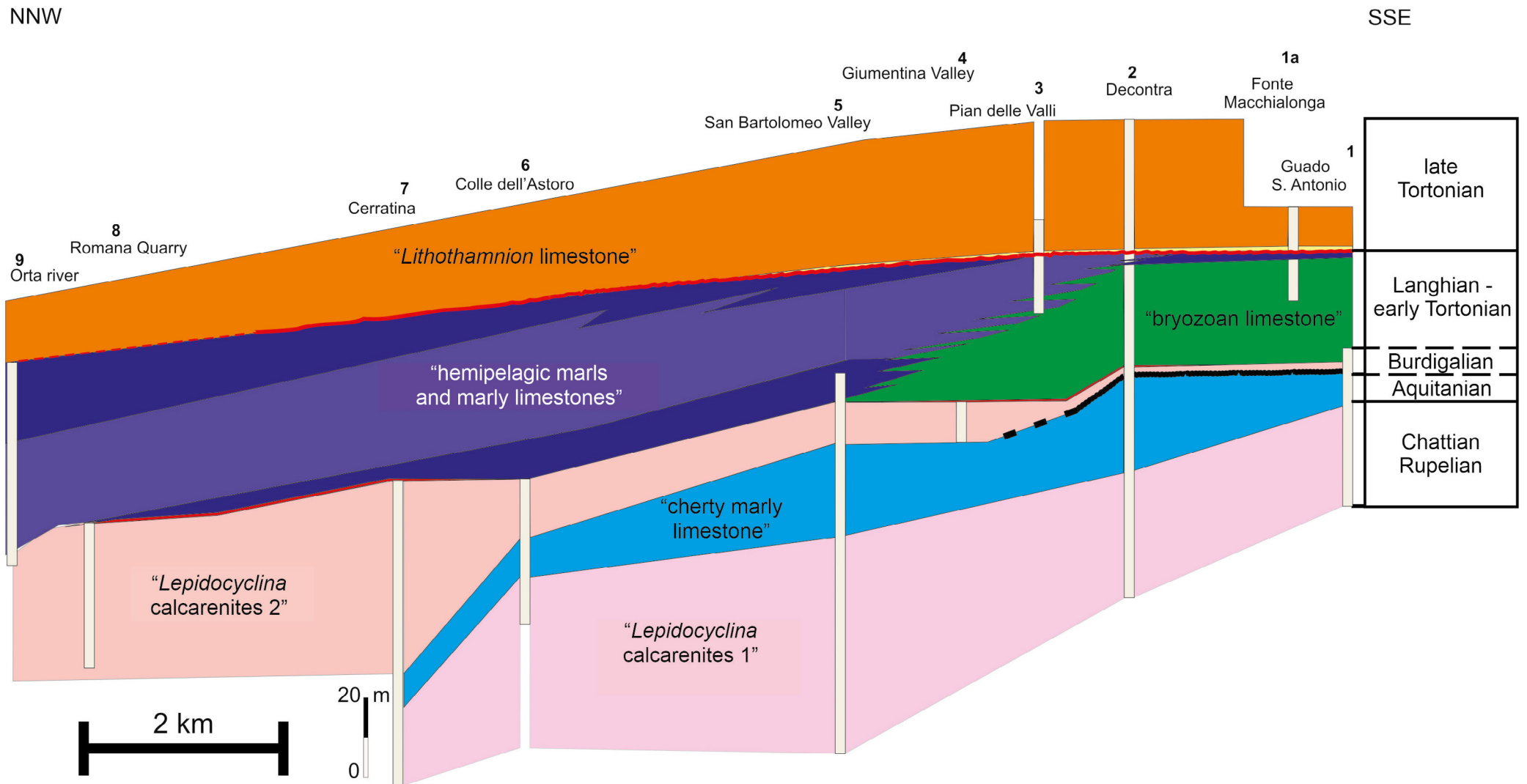


Fig. 53 - Schematic stratigraphic architecture of the "Bolognano fm" (modified from Brandano et al., 2016a).

Brandano et al., 2016a). It consists of fine bioclastic packstones and cherty packstones to wackestones dominated by SBF and planktonic foraminifera and deposited in an aphotic outer ramp environment. The third unit is the "*Lepidocyclina calcarenites 2*" (cf. "bryozoan limestone" *p.p.* of Patacca et al., 2021; upper Aquitanian-upper Burdigalian), which marks the re-establishment of the downslope migrating dune field



represented by the “*Lepidocyclina calcarenites 1*” (Brandano et al., 2012, 2016a; Tomassetti et al., 2021). The top of this unit is marked by a phosphatic hardground, identified over the entire ramp, above which, in the Orfento valley (Fig. 53) the “bryozoan limestone” crops out and passes laterally to the hemipelagic marls and marly limestones unit extended northward (Brandano et al., 2016a). The “bryozoan limestone” (cf. “bryozoan limestone” *p.p.* of Patacca et al., 2021; upper Burdigalian-Serravallian) consists of coarse cross-bedded packstones and grainstones dominated by bryozoans, identifying the sedimentation within the proximal outer ramp (Brandano et al., 2016a).

The hemipelagic marls and marly limestones (cf. “*Orbulina limestone*” *p.p.* of Patacca et al., 2021; upper Burdigalian-Serravallian) consists of fine bioclastic packstones to bioturbated wackestones with planktonic foraminifera (Brandano et al., 2016a) deposited in the distal outer ramp and transition to the basin.

The last unit of the “Bolognano fm” is the “*Lithothamnion limestone*” (cf. “Lithotamnium limestone” of Patacca et al., 2021; Tortonian-lower Messinian, Cornacchia et al., 2017). Overall, the main components are coralline red algae forming small rhodoliths, branches, and nodules, LBF, among which *Heterostegina* sp. and SBF. This unit identifies an inner ramp, characterised by seagrass meadows, that grades towards a proximal middle ramp dominated by the *maërl* facies (Brandano et al., 2016b). Towards the top of the unit, an increase of terrigenous input led to the deterioration of the trophic conditions, and the red algae are substituted by small benthic foraminifera such as buliminaceans or bolivinds adapted to live under low-oxygen conditions (Brandano et al., 2016b).

12) “*Turborotalita multiloba* marl” (lower Messinian, Patacca et al., 2013). They are planktonic-rich wackestones that identify hemipelagic sedimentation.

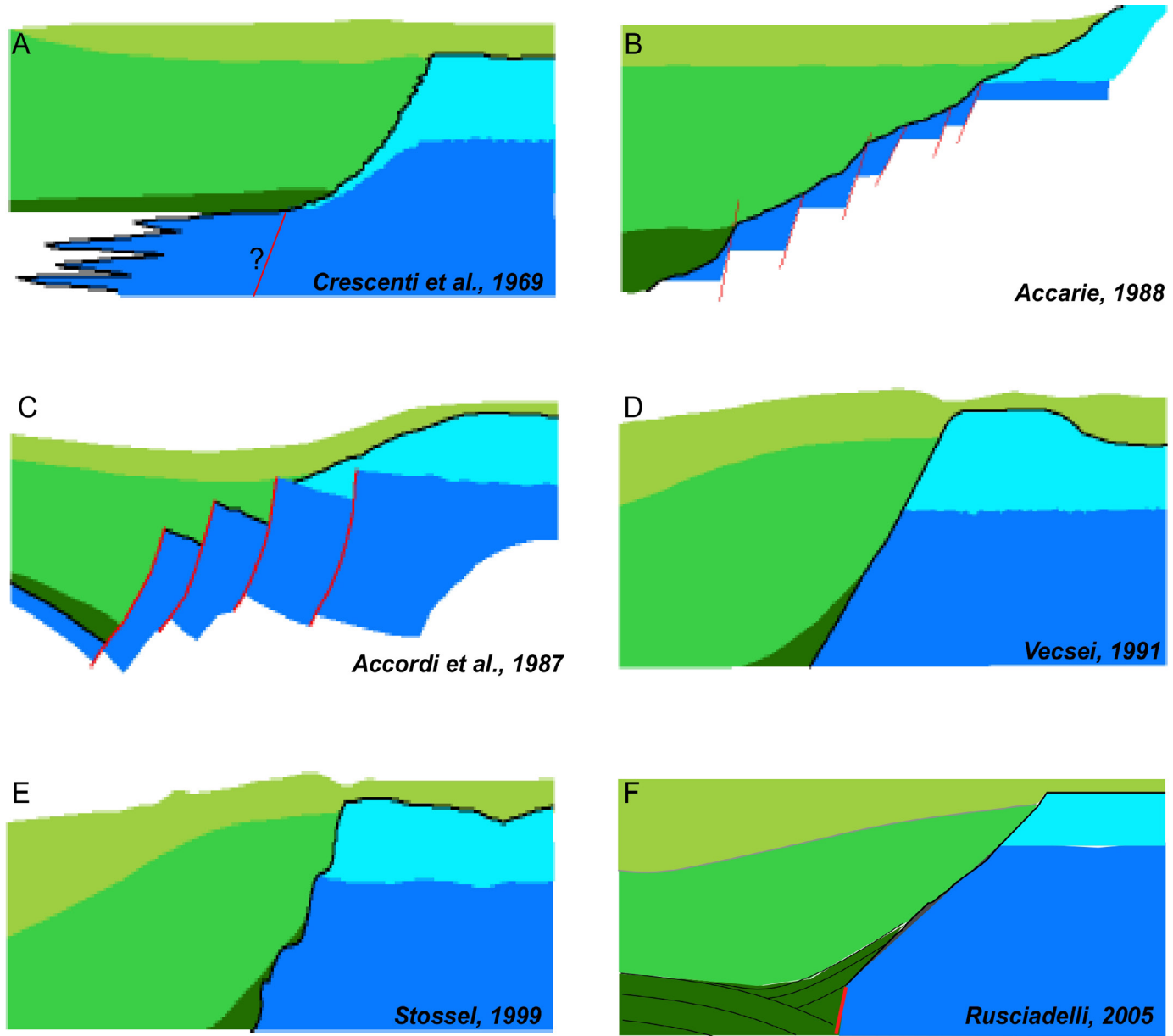
13) Gessoso-Solfifera (Messinian). It identifies the onset of the evaporitic deposition related to the Messinian Salinity Crisis (Crescenti et al., 1969).

The Maiella palaeoescarpment

The Maiella palaeoescarpment is one of the most intriguing features of the Central Apennines geology. It corresponds to a rather irregular surface, approximately E-W oriented and dipping northward with angles ranging between 20° and 40° (Crescenti et al., 1969; Accarie et al., 1989; Vecsei, 1991; Eberli et al., 1993; Morsilli et al., 2002; Rusciadelli, 2005). It truncates Lower and Upper Cretaceous platform facies (“Morrone di Pacentro” and “Cima delle Murelle” formations) along a 1000 m high surface on which Upper Cretaceous slope deposits onlap.

The Tethyan and Tyrrhenian margin record of the Central Apennines: a guide with insights from stratigraphy, tectonics, and hydrogeology

G.L. Cardello - L. Tomassetti - I. Cornacchia - A. Mancini - M. Mancini - I. Mazzini - G. Rusciadelli - E. Capezzuoli - V. Lorenzi - M. Petitta - G.P. Cavinato - O. Girotti - M. Brandano



From the first recognition of the palaeoescarpment (Crescenti et al., 1969), the interpretation of this palaeogeographic element has been referred both to sedimentary and structural models (Fig. 54). Structural models (Accordi et al., 1987; Accarie, 1988) apply the 1960s classical model of the faulted platform to basin transition, with the palaeoescarpment represented by a series of tilted blocks displaced by a fault system. A sedimentary model, based on the configurations of a modern platform to basin transitions (Bahamas model), is envisaged by the ETH group of Bernoulli (Vecsei, 1991; Stössel, 1999). This model considers the palaeoescarpment as the product of a long-lived evolution, started during the Tethyan rifting phase, with the dissection of the Lower Jurassic platform and the initial

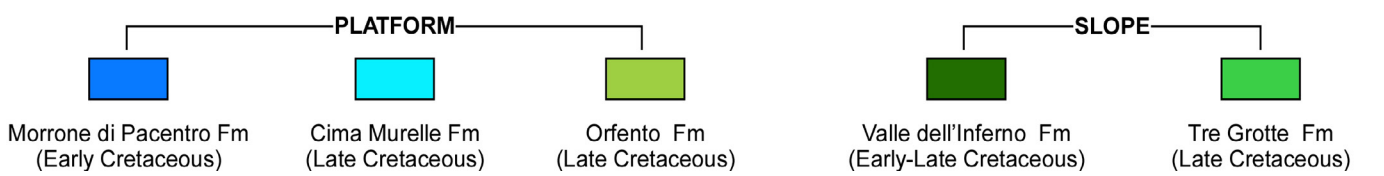


Fig. 54 - Comparison panel showing the different models proposed for the Maiella palaeoescarpment at the contact between the platform and slope-to-basin deposits.



separation between platform and basin sectors. According to this model, the palaeoescarpment represents a by-pass and erosive surface, separating basinal areas from an aggrading platform that kept up during the time. Only during the Late Cretaceous, the palaeoescarpment was sealed and the platform architecture changed from aggrading to prograding (Crescenti et al., 1969; Eberli et al., 1993). A more recent sedimentary model was proposed by Morsilli et al. (2002), who consider the palaeoescarpment as the remnant surface of a series of submarine landslides, formed during an imposing phase of platform margin collapses. Successively, through mechanical quantitative modeling, Rusciadelli et al. (2003) highlighted the fundamental role of earthquake swarms in the formation of the large-scale margin collapses. Syn-sedimentary faults along the slope facing the platform margin and post-dated by the Cenomanian base-of-slope deposits of the “Valle dell’Inferno fm” (Rusciadelli, 2005) provided evidence on the role of tectonics for the triggering of the platform margin collapse. This tectonic event is possibly related to the Cretaceous tectonic evidence recognised in the Gran Sasso and in the Volsci ranges (Cardello et al., 2021; Tavani et al., 2021) as well as elsewhere in the Central (Cipriani & Bottini, 2019) and Southern Apennines (Vitale & Ciarcia, 2021).

Stop 4.1. Pennapiedimonte section, the Upper Cretaceous to Miocene slope to distal ramp successions, and the Eocene/Oligocene transition (42°09’08.80’’N; 14°11’22.29’’E)

The Pennapiedimonte section is located on the eastern flank of the Maiella anticline, along the northern side of the Tre Grotte Valley (Fig. 55). Along this section the whole Cenomanian *p.p.* to Miocene slope-to-distal ramp succession is exposed (Fig. 56). The Cenozoic deposits are represented by the “Bolognano” (upper Rupelian-lower Messinian *p.p.*) and the “Santo Spirito” (Danian-lower Rupelian) formations. At the base, a few metres thick conglomerate separates the “Santo Spirito fm” from the underlying “Orfento fm”. This represents the last Cretaceous depositional unit that seals the morphologic differences between the platform and the basin, across the Maiella escarpment. It is characterised by about 200 m of bioclastic grainstones and rudstones, organised into staked convex bodies (submarine sand waves), some hundreds of metres long and a few tens of metres thick. Megabreccias deposits locally occur at a different stratigraphic level within the “Orfento fm”. Along the Pennapiedimonte section, the lower boundary of this unit corresponds to an erosive unconformity highlighted by the abrupt change from coarse bioclastic grainstones and rudstones to pelagic and fine-grained limestones of the underlying unit. Basinward, this boundary corresponds to correlative conformity and the depositional features change gradually from one unit to another.

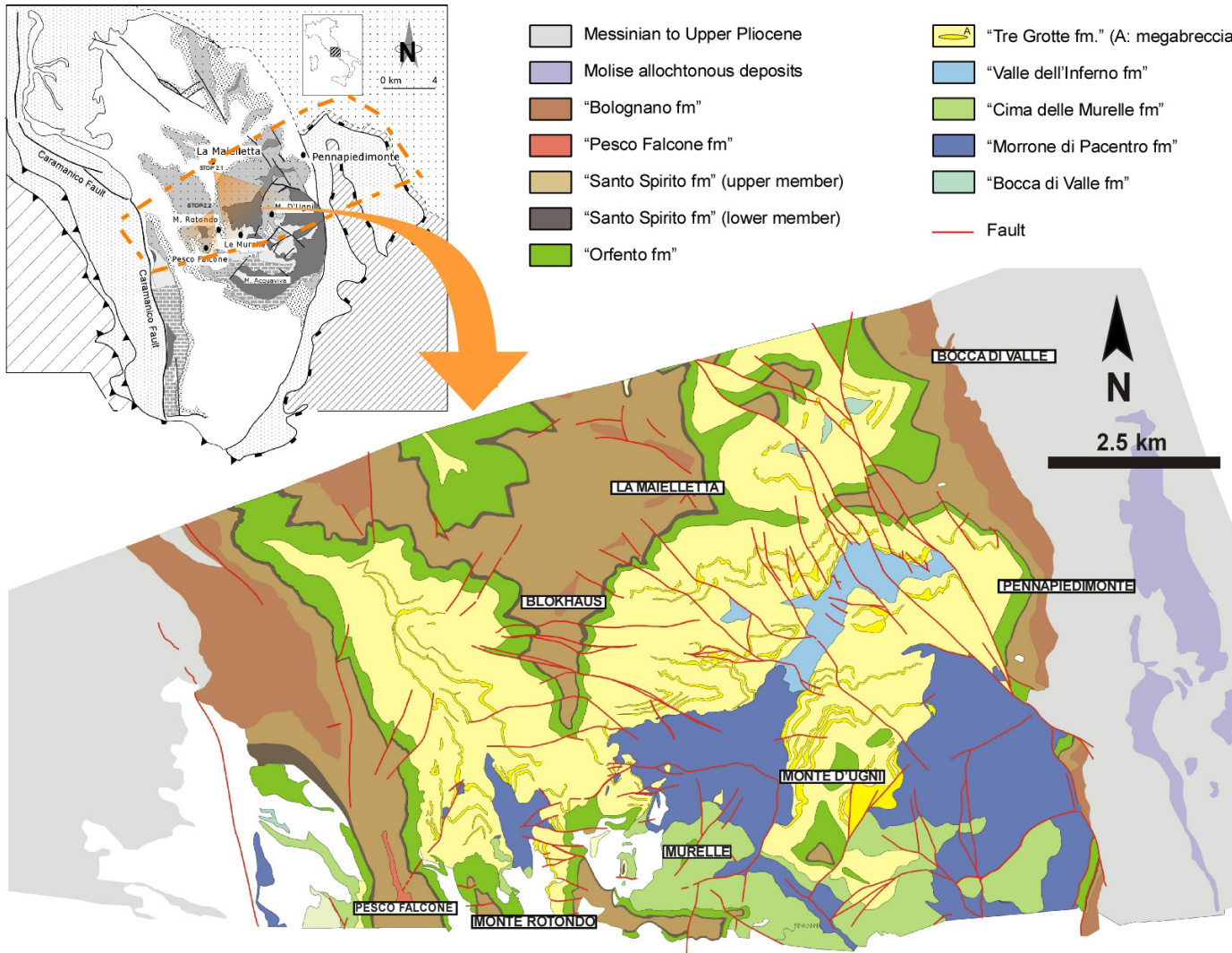
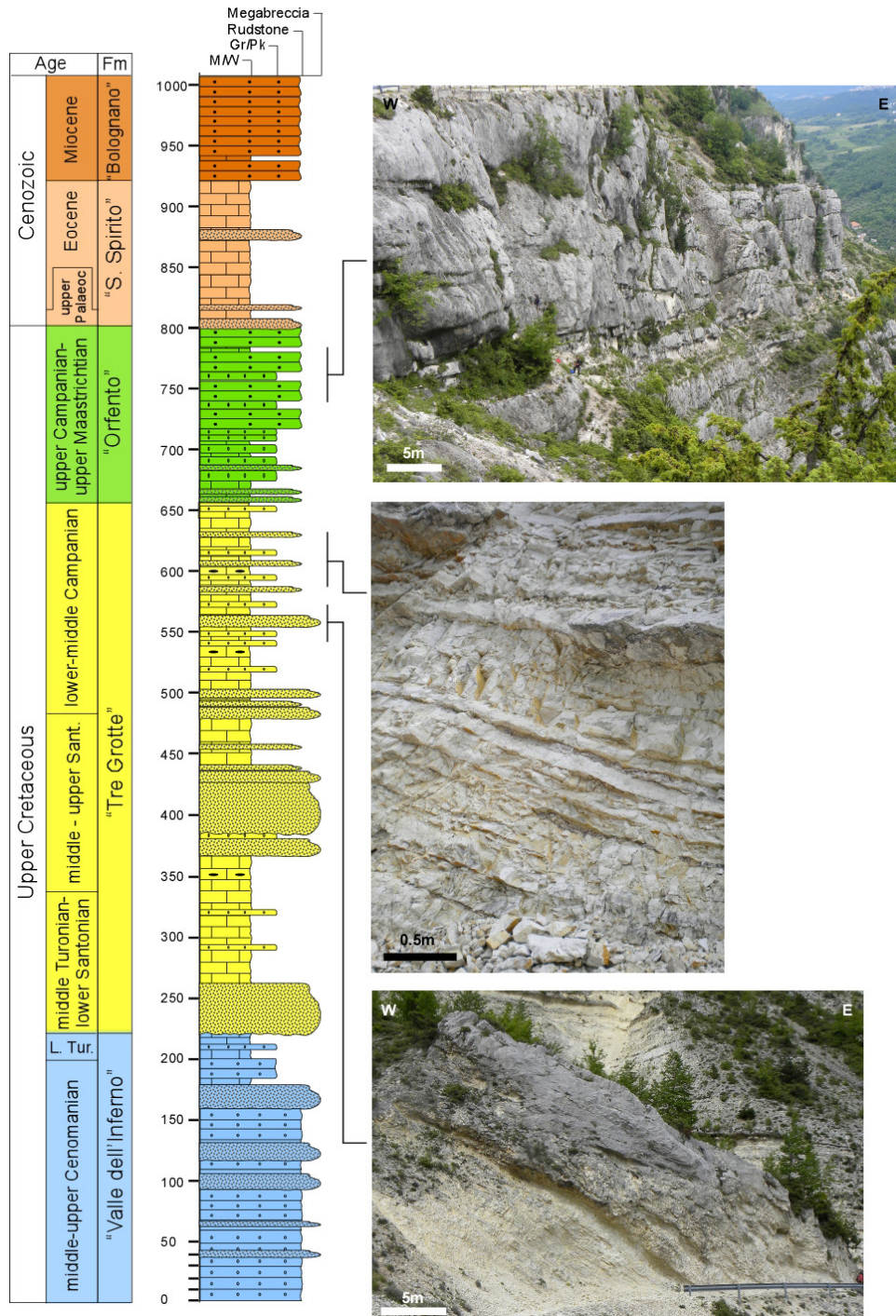


Fig. 55 - Geological map of the central sector of the Maiella Mountain (modified from Morsilli et al., 2002).

The underlying unit is the "Tre Grotte fm", defined by the alternation of a centimetre to decimetre thick coarse to fine bioclastic packstones, pelagic planktonic foraminifera-rich mudstones, and wackestones, pink and black chert levels. Metre- to few tens of metres-thick breccias and megabreccias bodies characterise the section along the whole thickness. In the Pennapiedimonte area, the "Tre Grotte fm" is 500 m thick, but it rapidly thins southward, along the palaeoescarpment. At the base of the unit (Fig. 57) a few metres to 20 m thick interval of fine-grained bioclastic packstones and pelagic mudstones, characterises the transition to the underlying "Valle dell'Inferno fm". This is the lowermost unit outcropping along the Pennapiedimonte section and is composed by bioclastic grainstones and packstones, with several breccias and megabreccias bodies. The maximum outcropping thickness is about 300 m.

At the Pennapiedimonte section, the "Santo Spirito fm" is 150 m-thick (Fig. 58). The first 53 m consist of locally bioturbated fine packstones with planktonic foraminifera and frequent chert nodules and lists, interrupted at the base by two beds of rudstones with LBF. Then, after a small landslide deposit that covers the section for



12 m, it continues with 14 m of breccias and bioclastic floatstones to rudstones separated by thin packstones layers. Above this coarse interval, 46 m of packstones with planktonic foraminifera crop out, characterised by extensive slumps whose thickness varies from 0.3 up to 10 m. The upper 25 m of the section consists of fine bioclastic packstones alternating with thin calcareous marls. Chert nodules increase before the contact with the overlying "Bologniano fm", at m 150 (Raffi et al., 2016). Calcareous nannofossil assemblages, recovered from marly interlayers or in the chalk preserved within the cherty nodules, allowed to ascribe this section to the Bartonian-Rupelian, with the slumped interval in correspondence to the Eocene-Oligocene boundary (Fig. 57). Slumps at the Eocene-Oligocene boundary were recognised in several other sections of the "Santo Spirito fm" (Raffi et al., 2016). Cornacchia et al. (2018) interpreted these slumps as the physical expression of the major greenhouse-icehouse transition that occurred at the Eocene-Oligocene boundary (Zachos et al., 2001; Coxall & Pearson, 2007) when an ~80 m sea-level fall (Miller et al., 2009; Houben et al., 2012) led to the deepening of the storm-weather wave-base. Furthermore, storms could have been more frequent and intense due to the onset of the icehouse climate, which triggered a global ocean reorganisation and the intensification of latitudinal thermal gradients and winds (Coxall & Pearson, 2007).

Fig. 56 - Schematic Pennapedimonte stratigraphic section with the main outcrop features of lithostratigraphic units.

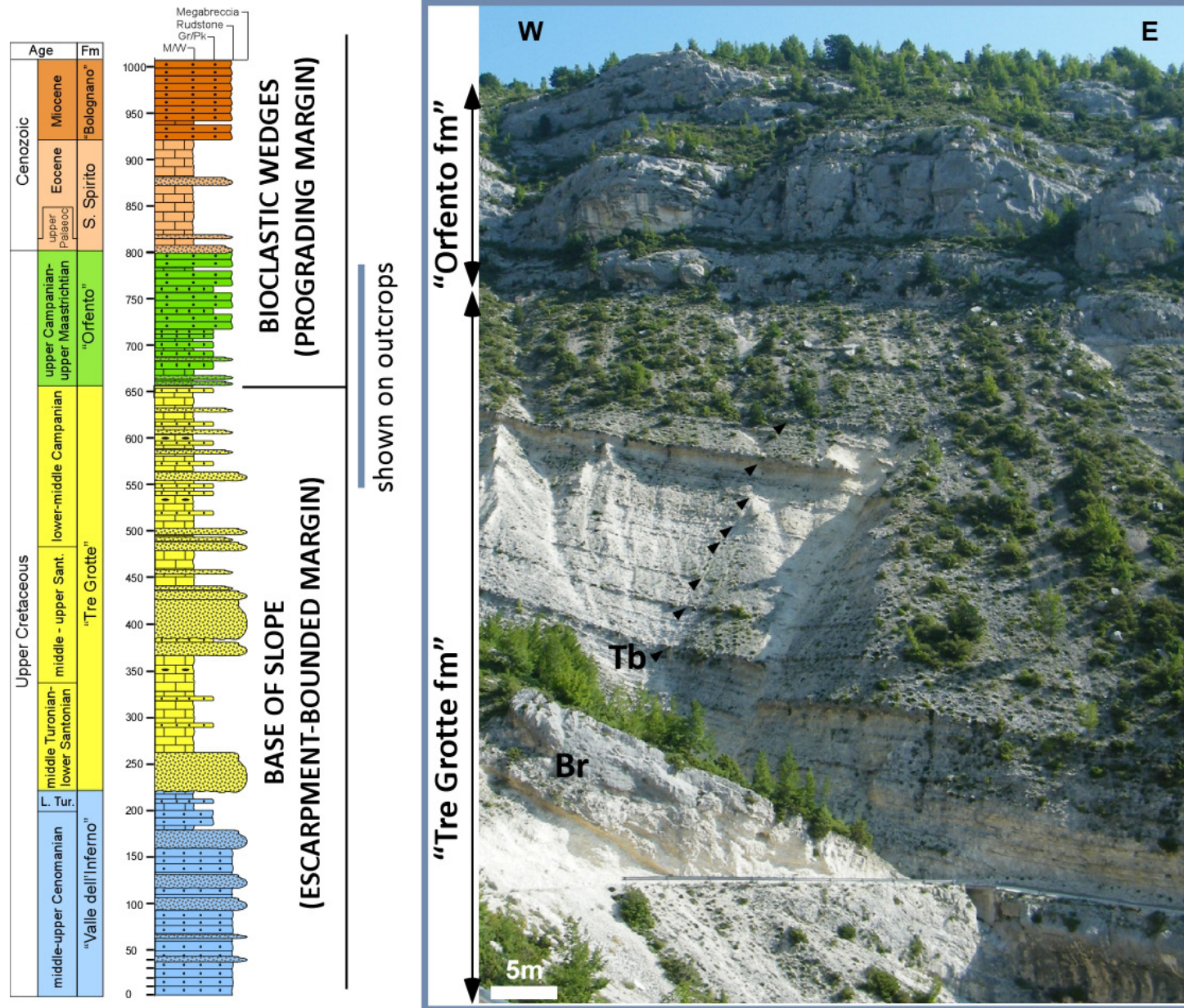


Fig. 57 - Pennapiedimonte section. The upper part of the "Tre Grotte fm" and the transition to the overlying "Orfento fm" is exposed. Note the thick megabreccia bed along the road. Key: Tb Turbidite; Br: Breccia.

The Tethyan and Tyrrhenian margin record of the Central Apennines: a guide with insights from stratigraphy, tectonics, and hydrogeology

G.L. Cardello - L. Tomassetti - I. Cornacchia - A. Mancini - M. Mancini - I. Mazzini - G. Rusciadelli - E. Capezzuoli - V. Lorenzi - M. Petitta - G.P. Cavinato - O. Girotti - M. Brandano

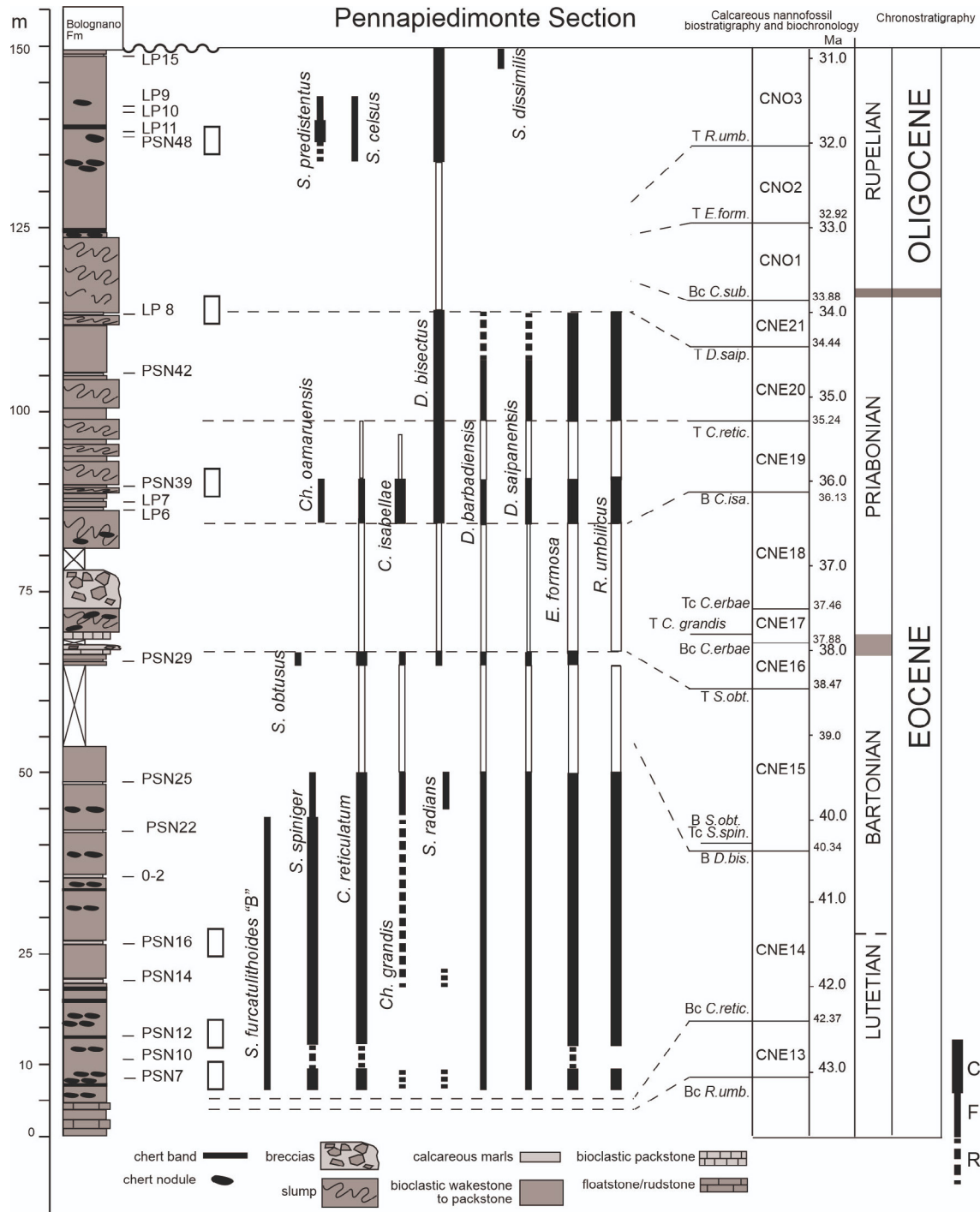


Fig. 58 - Pennapedimonte Eocene-Oligocene log plotted against stratigraphic depth and biostratigraphic constraints (modified from Raffi et al., 2016). Biozonation is referred to the Palaeogene Zonation of Agnini et al. (2014).

Day 5 – The Maiella Mountain Mesozoic and Cenozoic evolution

During the fifth day, the geometric relationships between platform and slope-to-basin successions will be analysed. The aim is to reconstruct the type of margin by characterizing the northern portion of the Tethyan Apulia platform margin. Along the natural section of the Maiella Mountain from Monte D'Ugni, different geometric settings are observable at the seismic scale (i.e., Monte Cavallo and Monte Rotondo; stops 5.1 to 5.5). Then, bioclastic intercalations within the "Santo Spirito fm" and the fabric arrangement of the bioclastic counterpart is hereby shown and discussed (stop 5.2). Finally, the stratigraphic architecture of the "Bolognano fm" carbonate ramp with the lateral and vertical relationships of its lithostratigraphic units is illustrated and discussed in the San Bartolomeo Valley (stop 5.3)

Successively, an overview of an exhumed part of a petroleum system that was active in the northern part of the Maiella Mountain is shown with beautiful exposure of bitumen shows and seepages (stop 5.4). Finally, a large dune field characterising one of the lithostratigraphic units constituting the "Bolognano fm", the "*Lepidocyclina* calcarenite 2", is shown and discussed at Piano delle Cappelle (stop 5.5).

Stop 5.1. The Monte D'Ugni and Cima delle Murelle panoramic view (42°09'31.49"N; 14°07'48.57"E)

We are in front of the platform to basin transition, in the central area of the Maiella Mountain, where an east-trending natural section across the valley crosscuts the anticline axis. Here, the depositional and geometric features of the northern portion of the Apulian platform margin will be illustrated through seismic scale outcrops (Fig. 59). The analysis of the stratigraphic features allows us to reconstruct the evolution of the Cretaceous escarpment-bounded platform that evolved into a carbonate ramp. This also allows to evaluate the control of large-scale collapses in the physiographic evolution of the platform margin and on the sedimentary succession architecture.

From this stop, looking southward, the Monte D'Ugni offers a panoramic view on the eastern Maiella platform margin (Fig. 60). From top to base, the sedimentary succession is represented by:

- "Orfento fm". Prograding deposits of the Upper Cretaceous bioclastic sand wedge;
- "Tre Grotte fm". Alternation of hemipelagic limestones, bio-calcarenites, and megabreccias bodies (see the cliffs between the trees) of the Upper Cretaceous slope;
- "Morrone di Pacentro fm". Lower Cretaceous inner platform succession;



- "Valle dell'Inferno fm". Alternation of biocalcarenites and megabreccia bodies of the Lower Cretaceous slope.

In this area, the Upper Cretaceous slope deposits of the "Tre Grotte fm" onlap the Lower Cretaceous inner platform succession of the "Morrone di Pacentro fm" through a low-angle surface (Fig. 60). In cross-section, this surface has an asymptotic profile decreasing downslope from a 60° to 20°-10°, within a distance of 2.5 km (Fig. 63). In a more distal position, the high angle contact (~45°) between Upper Cretaceous slope deposits and Lower Cretaceous platform deposits abruptly interrupts the platform northward extent. Along the Avella valley (Figs. 60, 61), the lower strata of the "Valle dell'Inferno fm" dip 30°-40° southward, whereas the upper strata dip 30° northward by onlapping the palaeoescarpment. These geometric relationships suggest the activity of a fault-related escarpment or of a fault system during the deposition of the "Valle dell'Inferno fm". This is also suggested by minor faults that are post-dated by the upper part of the late Albian-Cenomanian *p.p.* (about 100-93 Ma) "Valle dell'Inferno fm".

A 2 km-wide concave upward profile results from the E-trending cross sections in the Monte D'Ugni area (Fig. 62). Onlapping Upper Cretaceous slope deposits display maximal thickness in the centre of the indentation (500-600 m), thinning progressively up to few tens of metres laterally and upslope. The morphology filled by the

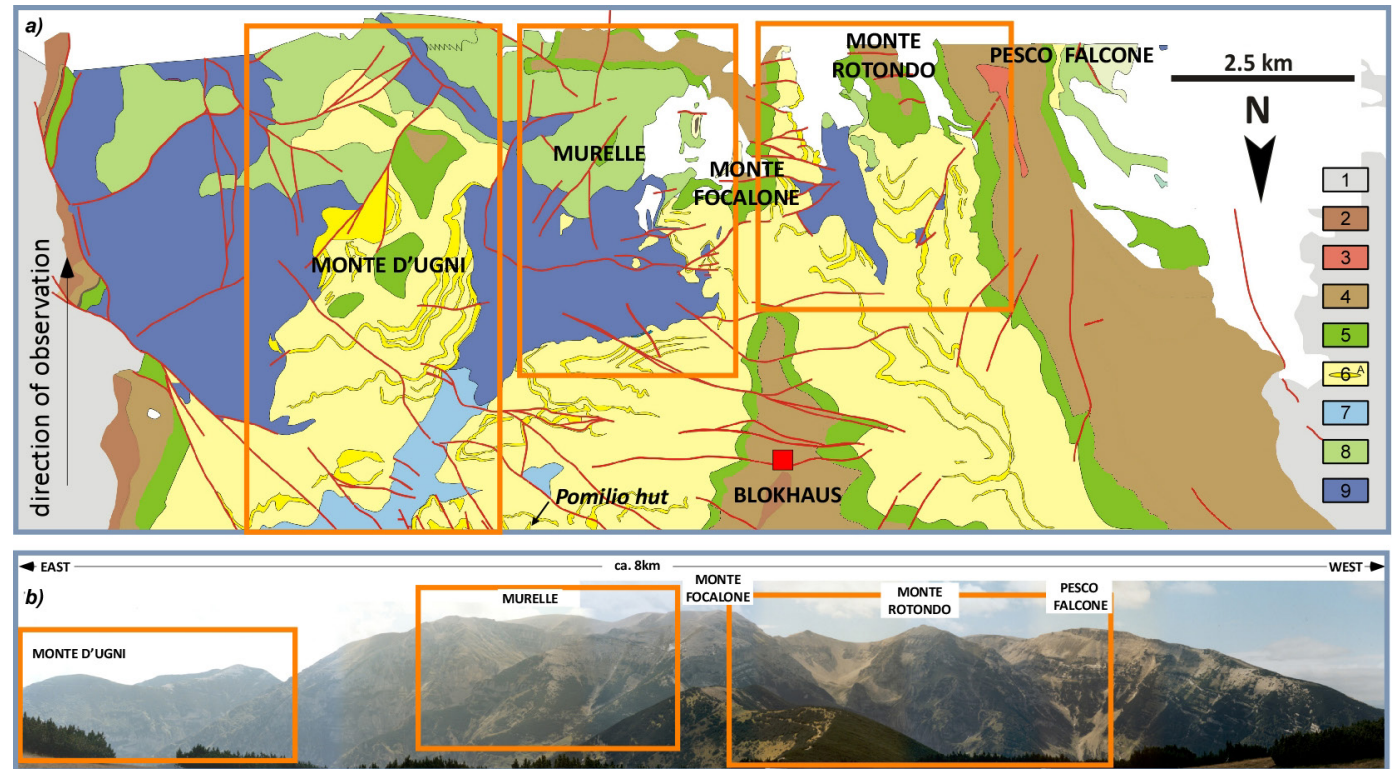


Fig. 59 - a) Simplified geological map of the central part of the Maiella Mountain. b) panoramic view of the central part of the Maiella Mountain. Key - 1: Messinian to Late Pliocene; 2: "Bolognano fm"; 3: "Pesco Falcone fm"; 4: "Santo Spirito fm"; 5: "Orfento fm"; 6: "Tre Grotte fm" (A: megabreccia); 7: "Valle dell'Inferno fm"; 8: "Cima delle Murelle fm"; 9: "Morrone di Pacentro fm".



Upper Cretaceous slope deposits appears as a large, scalloped area, incised on the underlying Lower Cretaceous platform succession. Moving westward, in the central sector of the platform margin (Fig. 59), the Murelle area records a different stratigraphic and geometric setting with respect to the Monte D'Ugni. Here, the Upper Cretaceous margin of the "Cima delle Murelle fm" lies unconformably above the Lower Cretaceous platform of the "Morrone di Pacentro fm". Upper Cretaceous slope deposits are represented by the "Tre Grotte fm", but with less frequent megabreccia events. Moreover, the palaeoescarpment is defined by a more regular and steeper profile, which remains generally constant with average angles of 30° (Figs. 63, 64). North of Cima delle Murelle, the palaeoescarpment is defined by the juxtaposition of Upper Cretaceous slope facies ("Tre Grotte fm") with angles of 10° to 25°, to the Lower Cretaceous proximal slope deposits ("Morrone di Pacentro fm"), represented by 30° dipping clinofolds. Upslope, the escarpment first truncates the Lower Cretaceous sub-horizontal platform margin deposits and then the Upper Cretaceous external platform (Fig. 64), possibly implying fault reactivation.

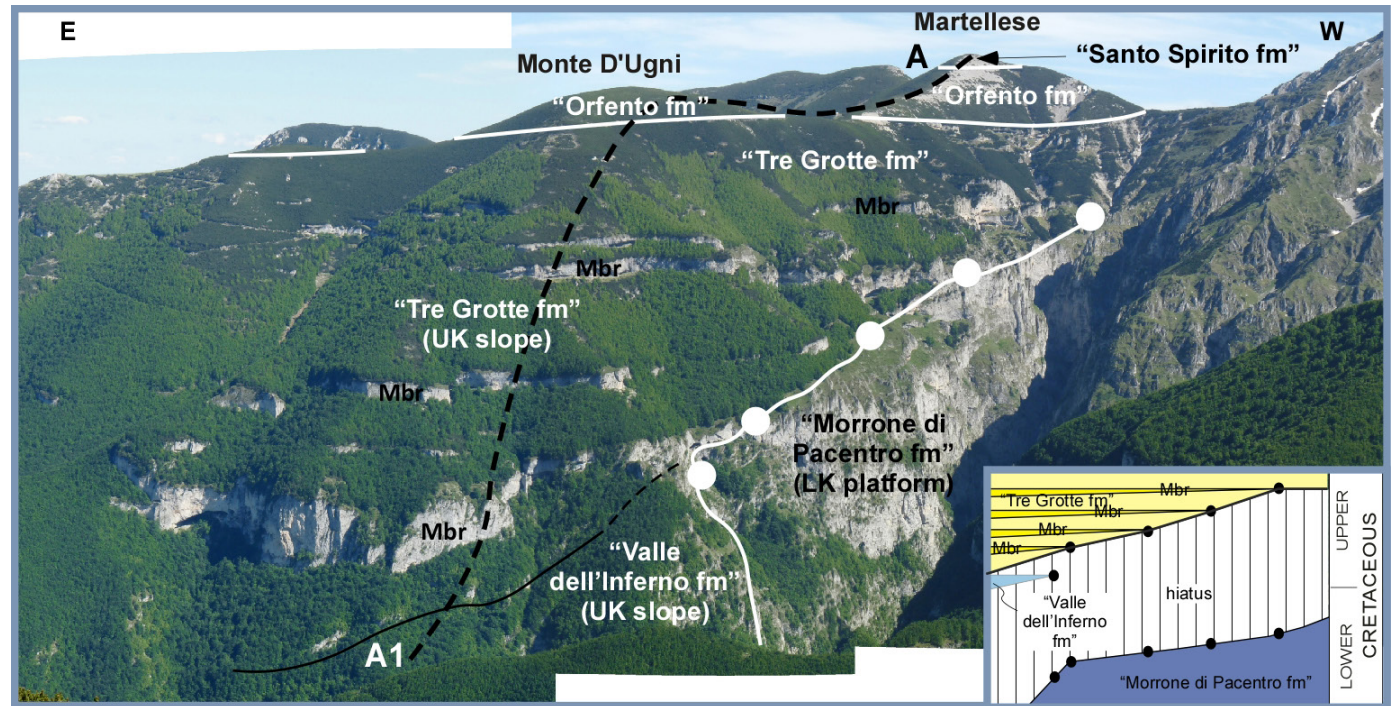


Fig. 60 - The abrupt contact between the Lower Cretaceous platform and the Upper Cretaceous slope-to-basin sediments in the Monte D'Ugni area. Cliffs in the wood are thick megabreccia bodies that onlap the Lower Cretaceous platform. Black dashed line indicates the trace of geological cross section of Figure 61. Bullets (white in the photograph, black in the scheme in the bottom right) indicate the onlap of sedimentary bodies ("Valle dell'Inferno fm" and megabreccias of the "Tre Grotte fm") along the escarpment. Key - Mbr: megabreccia; LK: Lower Cretaceous; UK: Upper Cretaceous.

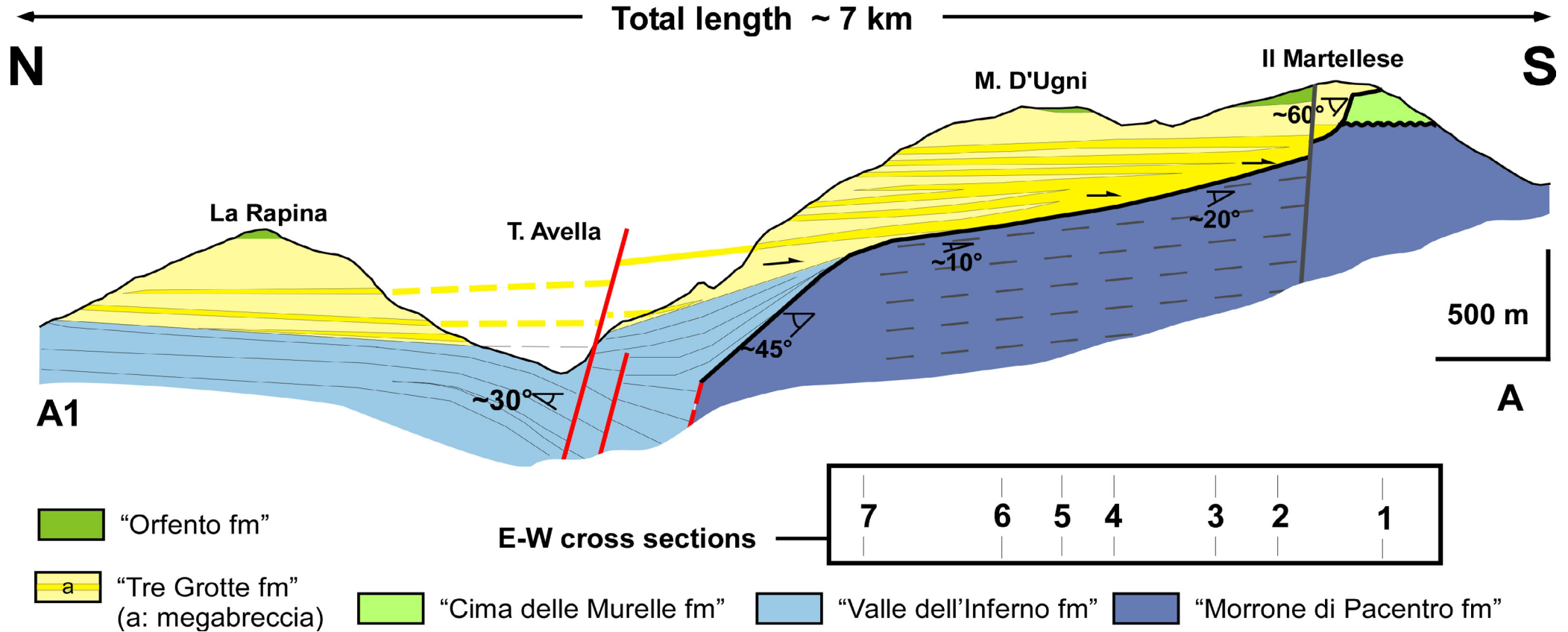


Fig. 61 - N-S cross section showing the escarpment geometry at Monte D’Ugni and the lithostratigraphic relationships between platform and slope formations. Note growth strata in the lower part of the “Valle dell’Inferno fm”.

Stop 5.2. The Monte Rotondo panoramic view (42°09’31.49’’N; 14°07’48.57’’E)

The Monte Rotondo area is the westernmost outcrop of the platform margin (Fig. 59), where depositional and geometric features recall those of the Monte D’Ugni and Murelle (Figs. 65, 66). Here, the Cenozoic succession is made up of an Eocene *p.p.* carbonate ramp (the upper white bar) and of an Oligocene *p.p.* corallgal reef (i.e., the uppermost cliff on top of Pesco Falcone). It seals the Cretaceous succession through an unconformity that records a long-term hiatus (Palaeocene to middle Eocene; Eberli et al., 1993). The Cretaceous succession is represented from top to base by the Lower to Late Cretaceous “Cima delle Murelle” and “Morrone di Pacentro” formations, which are

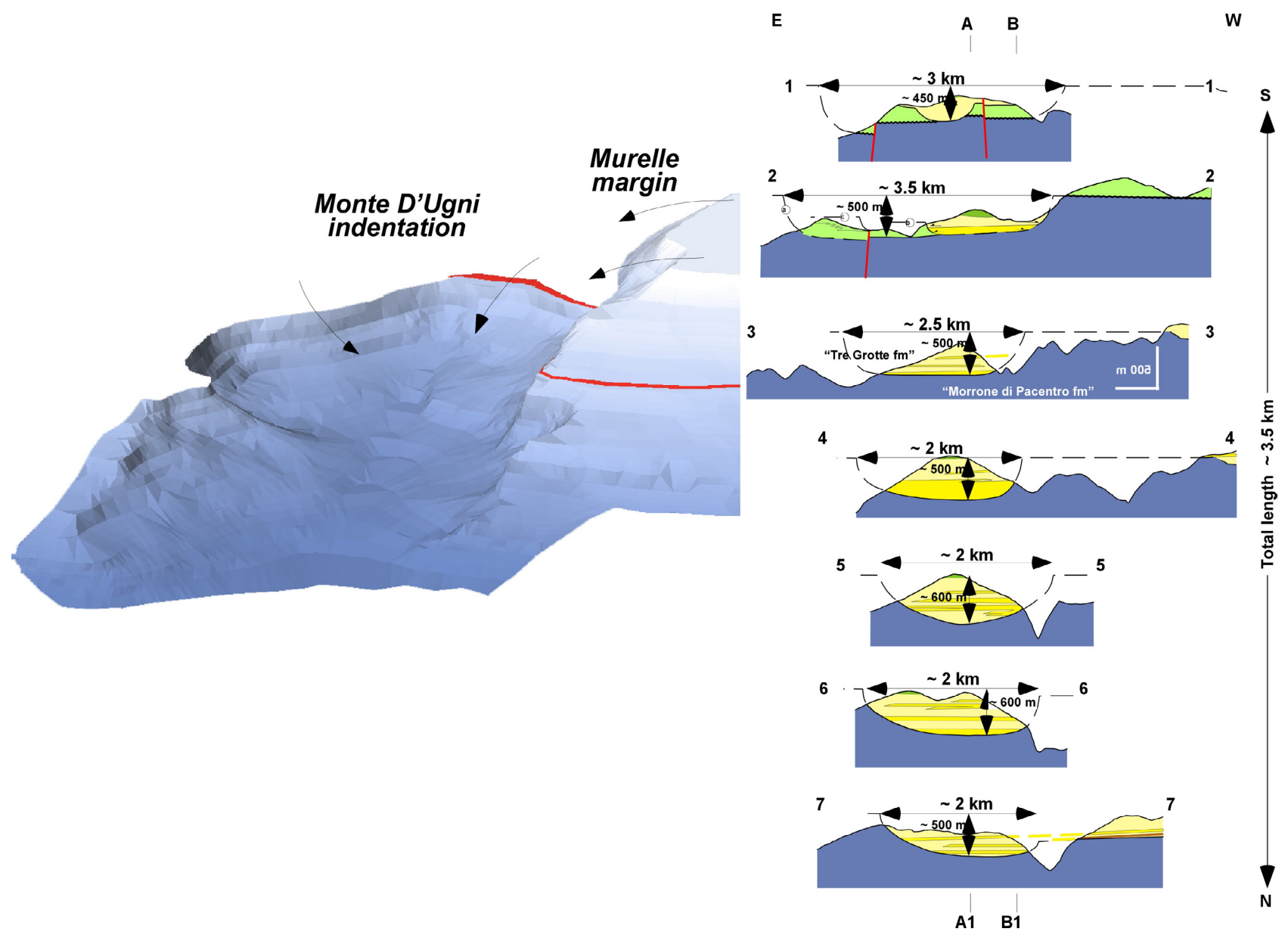


Fig. 62 - A 2 km-wide concave upward 3D profile resulted from the reconstruction of strata relationships between the "Tre Grotte fm" and the platform deposits of the "Morrone di Pacentro" and "Cima delle Murelle" fms. This morphology has been reconstructed through the cross sections (1 to 7) oriented E-W in the Monte D'Ugni area (position in Figure 67) (modified from Morsilli et al., 2002 and Rusciadelli, 2005).

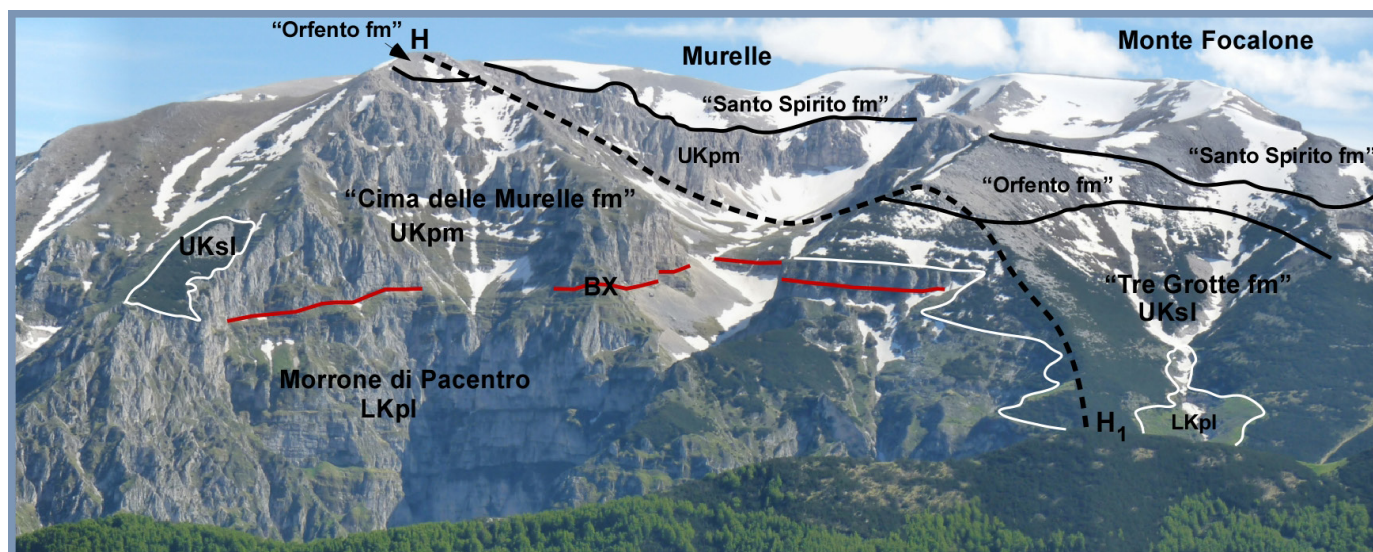


Fig. 63 - Panoramic view from north of the Cima delle Murelle-Monte Focalone area. The contact between slope and platform sediments is marked by the thick solid white dashed line. Black dashed line indicates the trace of geological cross section of Figure 64. Key - BX: Bauxitic level; LKpl: Lower Cretaceous platform interior; UKpm: Upper Cretaceous platform margin; UKsl: Upper Cretaceous slope.

onlapped by the Late Cretaceous "Tre Grotte" and "Orfento" formations. The contact between Upper Cretaceous slope facies ("Tre Grotte fm") and Lower Cretaceous platform deposits ("Morrone di Pacentro fm") is defined by a surface with angles of 25° to 35° (Fig. 66), similar to the Murelle area. Up-slope, the palaeoescarpment contact is between Upper Cretaceous slope deposits and Upper Cretaceous platform margin facies; the escarpment corresponds to a steeper surface with an average of 60° (Fig. 66), similarly to the Monte D'Ugni area. However, the lack of platform facies laterally to

the Monte Rotondo (Rava del Diavolo to the west and Rava della Sfischia to the east) (Fig. 65), and the absence of faults with a relevant downthrow, suggest a more complex morphology of the escarpment as regards other areas (Figs. 65, 66 and 67).

Stop 5.3. Monte Cavallo panoramic view of the platform-to-basin succession (42°07'45.78"N; 14°06'44.38"E)

From this belvedere, the northern margin of the Adria platform sticks into the landscape as it crops out along the east-trending natural section crossing the Maiella anticline. Here, we summarise the information of the previous stops to reconstruct the palaeomargin physiography and its evolution.

The Upper Cretaceous slope succession ("Tre Grotte fm") onlaps the Lower to Upper Cretaceous platform and margin facies with geometries that change from east to west. At Monte D'Ugni, where Upper Cretaceous margin

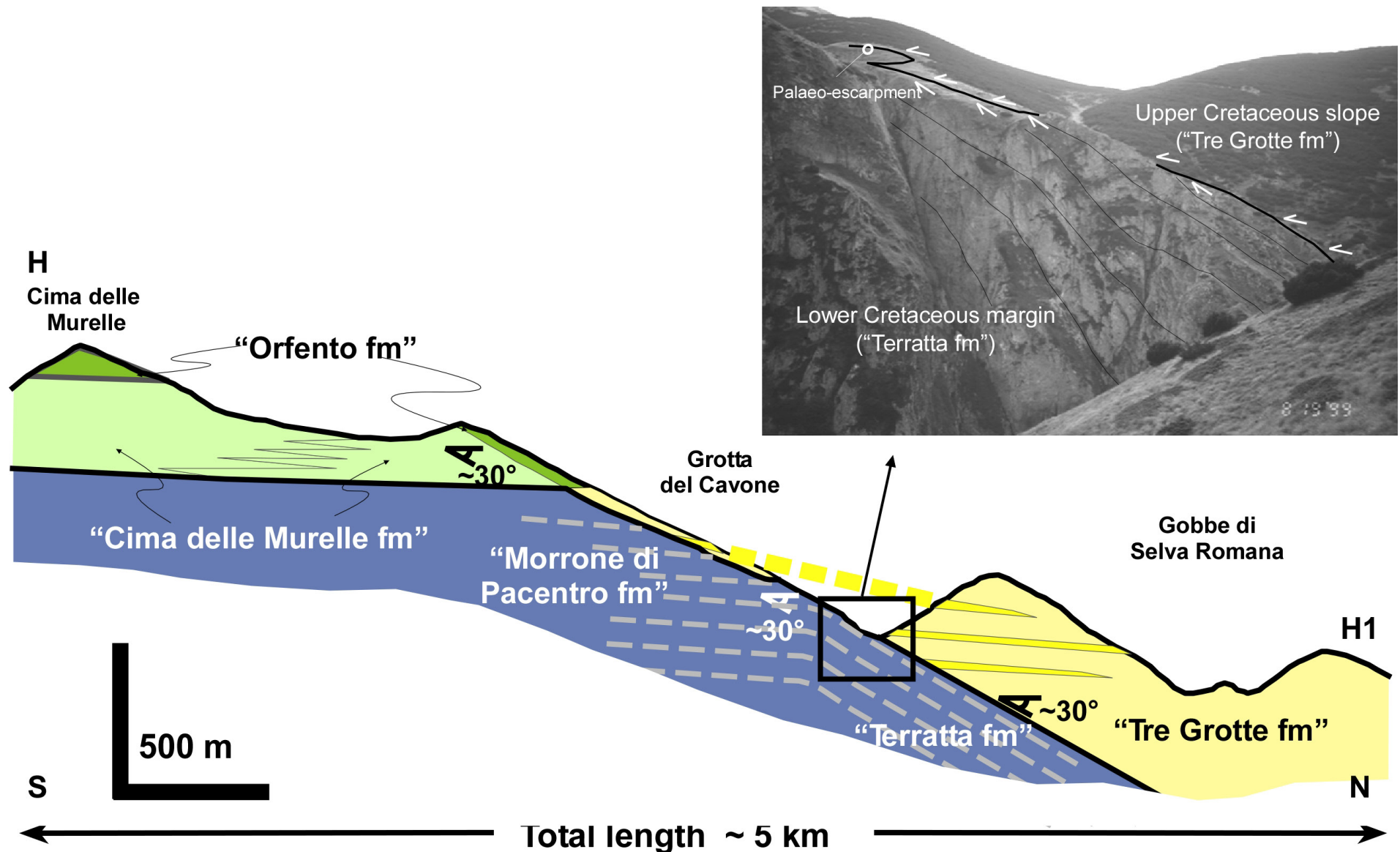


Fig. 64 - N-S cross section showing the escarpment geometry along the Cima delle Murelle transect and the relationships between platform and slope deposits (position of the cross section in Figure 63). In the photograph, there are clinoforms (around 30°) at the base of the Selva Romana Valley. Clinoforms are composed of alternating bio-intraclastic grainstones, rudstones and breccias related to the Lower Cretaceous platform margin ("Terratta fm").



deposits are lacking, the contact is a low-angle unconformity. At the Murelle (Fig. 67), the palaeoescarpment occurs with a regular and steep profile, with average angles of 30° between the Lower Cretaceous proximal slope to inner platform deposits and then overlying Upper Cretaceous slope and margin deposits. In the Monte Rotondo area instead, the Upper Cretaceous slope deposits onlap the Lower Cretaceous platform and the Upper Cretaceous margin through a surface with angles varying upward ranging from 25°-35° to 60°. To better evaluate the morphologic features and the evolution of the palaeoescarpment, a 3D model was reconstructed designed removing the Upper Cretaceous slope deposits and later by reconstructing the Upper Cretaceous margin morphology (Fig. 68).

The different geometric configurations of the palaeoescarpment observed throughout the Maiella anticline suggest the presence of a complex sinuous platform margin. This is similar also to what is observed elsewhere in other Upper Cretaceous margins such as in the Helvetics (cf. [Cardello & Mancktelow, 2014](#)). As shown in Figure 68, the margin is characterised by an alternation between deep indentations (Monte D'Ugni, Rava del Diavolo and Rava della

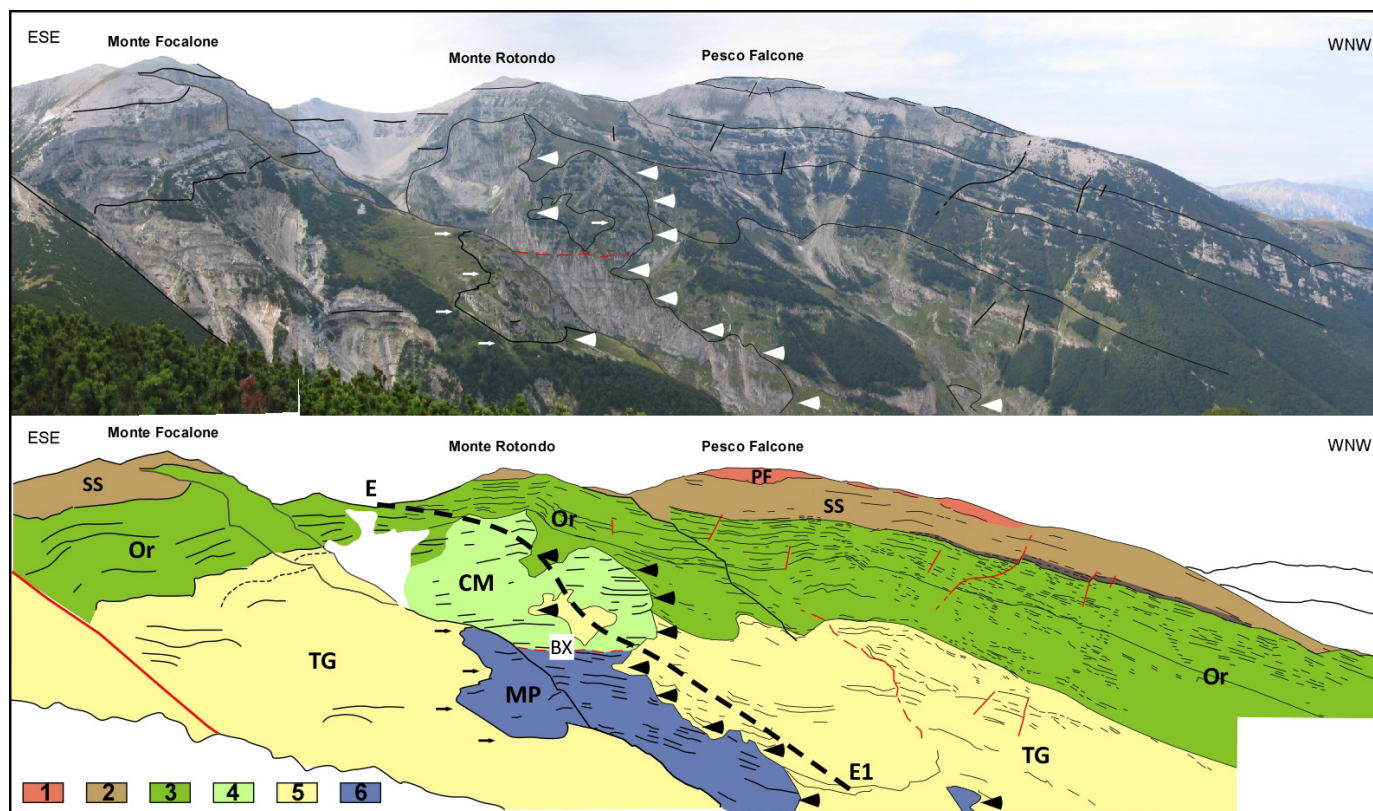


Fig. 65 - Seismic-scale escarpment geometry at Monte Rotondo and the stratigraphic relationships between platform and slope successions. Black dashed line indicates the trace of geological cross section of Figure 66 (modified from Rusciadelli & Di Simone, 2007). Key - 1: upper Eocene-lower Oligocene reef buildups ("Pesco Falcone fm" - PF); 2: Palaeocene-Eocene prograding ramp ("Santo Spirito fm" - SS); 3: Upper Cretaceous bioclastic sand wedge ("Orfento fm" - Or); 4: Upper Cretaceous rudist bearing platform margin ("Cima delle Murelle fm" - CM); 5: Upper Cretaceous slope ("Tre Grotte fm" - TG); 6: Lower Cretaceous inner platform ("Morrone di Pacentro fm" - MP); BX: bauxitic level.

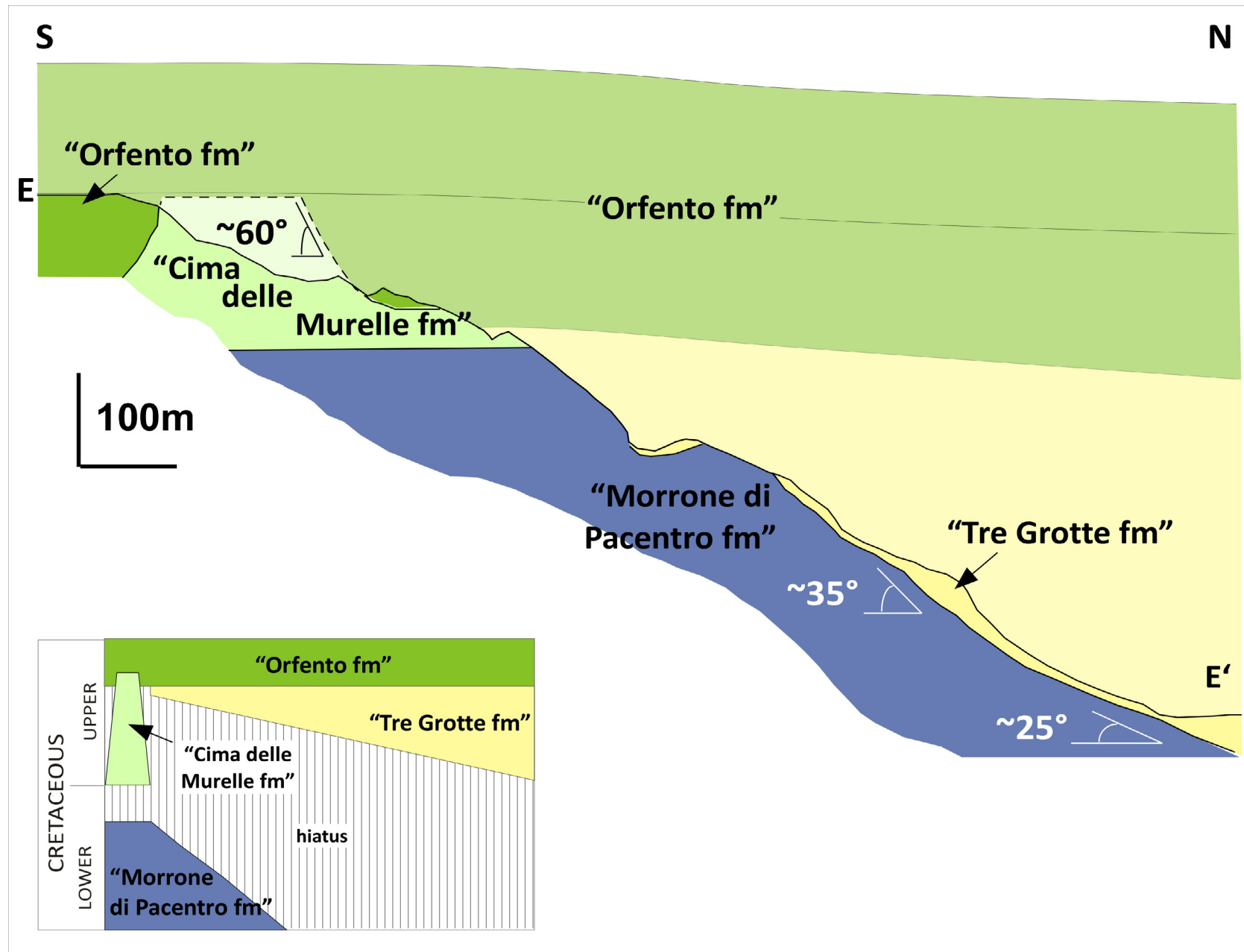
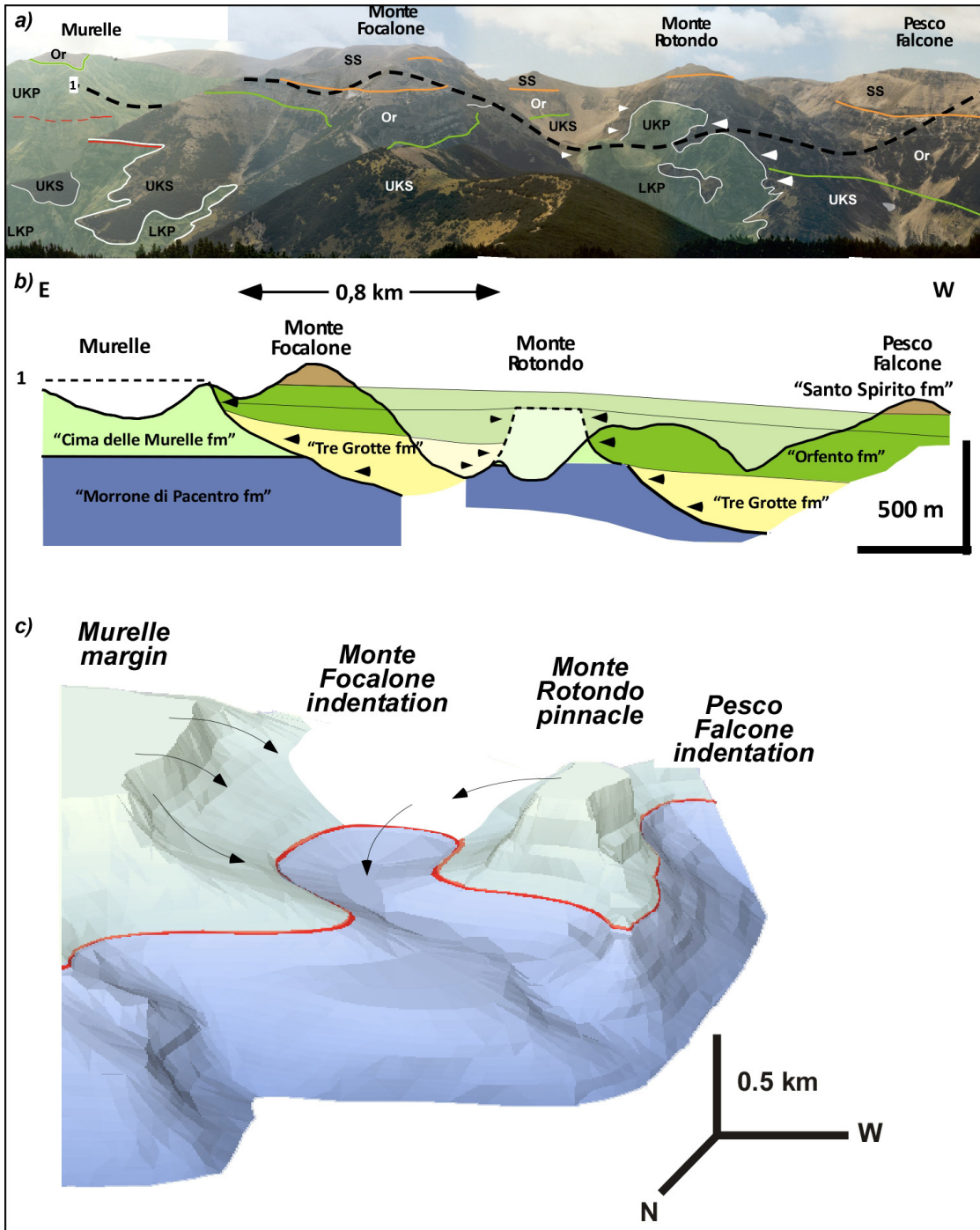


Fig. 66 - N-S cross section showing the escarpment geometry along Monte Rotondo area and the relationships between platform and slope deposits (position of the cross section in Figure 65).



Sfischia), and prominent ridges (e.g., Cima delle Murelle, Monte Rotondo, Pesco Falcone). The resultant morphology is a sort of a 10-km large groove-and-spur structure.

Indentations are similar in shape and size to those also observed in modern scalloped platform margins. On the Maiella Mountain, they are incised on Lower Cretaceous platform ("Morrone di Pacentro fm") and filled by Upper Cretaceous slope facies ("Tre Grotte fm"). Typical morphological features of landslides, such as crown, head scarp, flanks and slip plane, can be easily recognised in the Monte D'Ugni indentation (Fig. 68). In prominent ridge structures, the erosional processes are less pronounced, and the Lower Cretaceous platform is more preserved below the onlap.

Fig. 67 - Upper Cretaceous platform margin between Cima delle Murelle and Pesco Falcone. a) Photomosaic showing the distribution on outcrops of platform margin and base of slope successions. The white line indicates the contact and represents the palaeoescarpment. The green line indicates the base of the "Orfento fm". b) Geological cross section parallel to the platform margin showing the lateral distribution of lithostratigraphic units. c) 3D reconstruction of the platform margin morphology in the Late Cretaceous, filled by the slope deposits of the "Tre Grotte fm"; note the presence of two large-scale scallops located east and west of Monte Rotondo. Key - LKP: Lower Cretaceous platform interior; UKP: Upper Cretaceous platform margin; UKS: Upper Cretaceous slope; Or: "Orfento fm"; SS: "Santo Spirito fm".

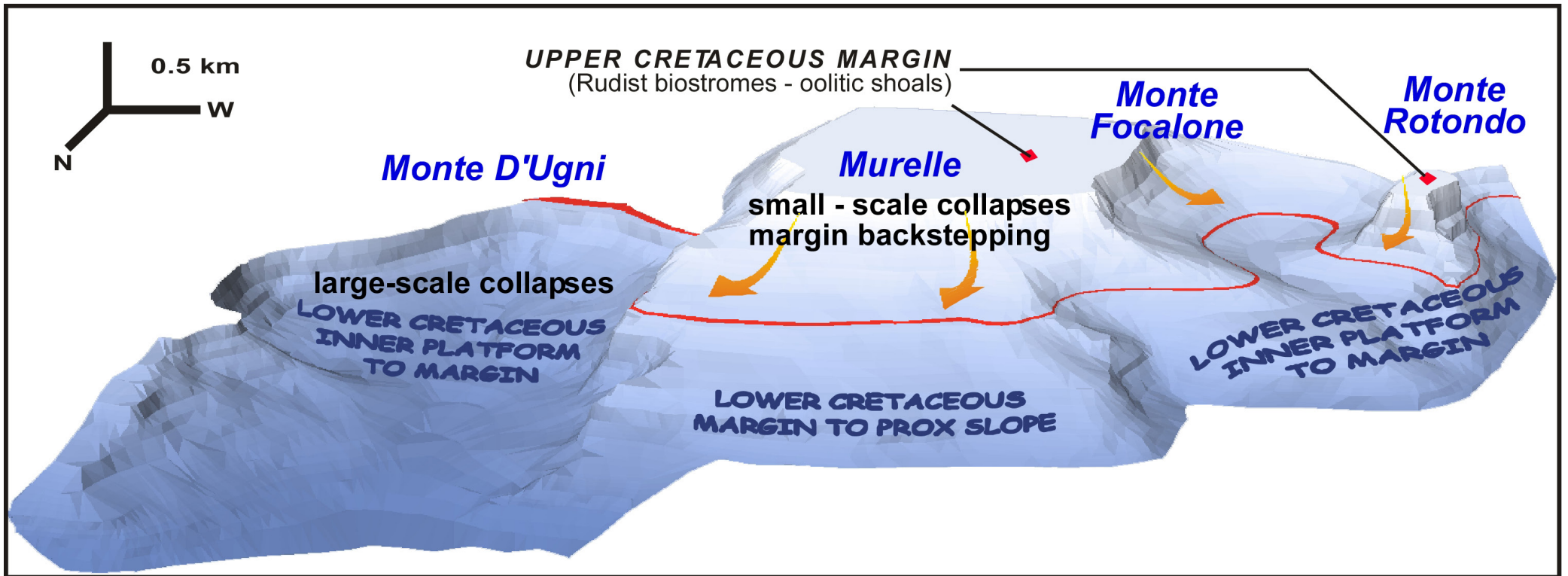


Fig. 68 - Extended 3D model of the Cretaceous Maiella palaeoescarpment. This three-dimensional view allows to easily identify a complex scalloped bank margin with scars of different shape and scale. Only in the Murelle area, the escarpment has a regular and planar profile. The red line marks the contact between the Lower and Upper Cretaceous platform facies.

The evolution of the palaeoescarpment

The 3D reconstruction points out two main features: the processes determining the complex platform margin configuration and the role of the inherited Lower Cretaceous morphology in the distribution of the Upper Cretaceous rudist-dominated margin. The complex margin morphology results in the sinuous alternation of large-scale indentations and prominent ridges, thus suggesting the presence of large-scale collapses of the platform margin (Morsilli et al., 2000, 2002; Rusciadelli et al., 2003; Rusciadelli 2005), possibly acting on the footwall of a major middle Albian-Cenomanian normal fault.

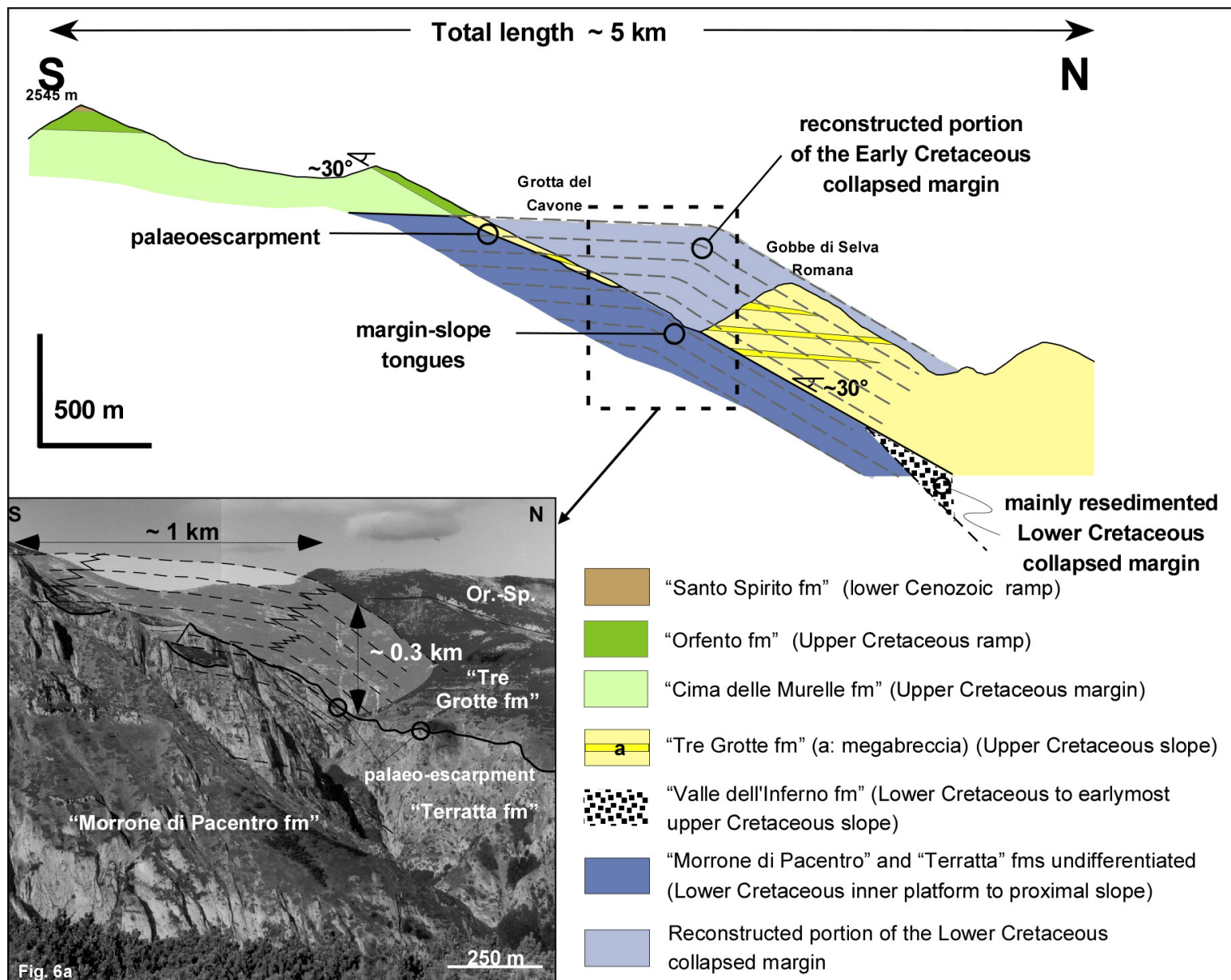
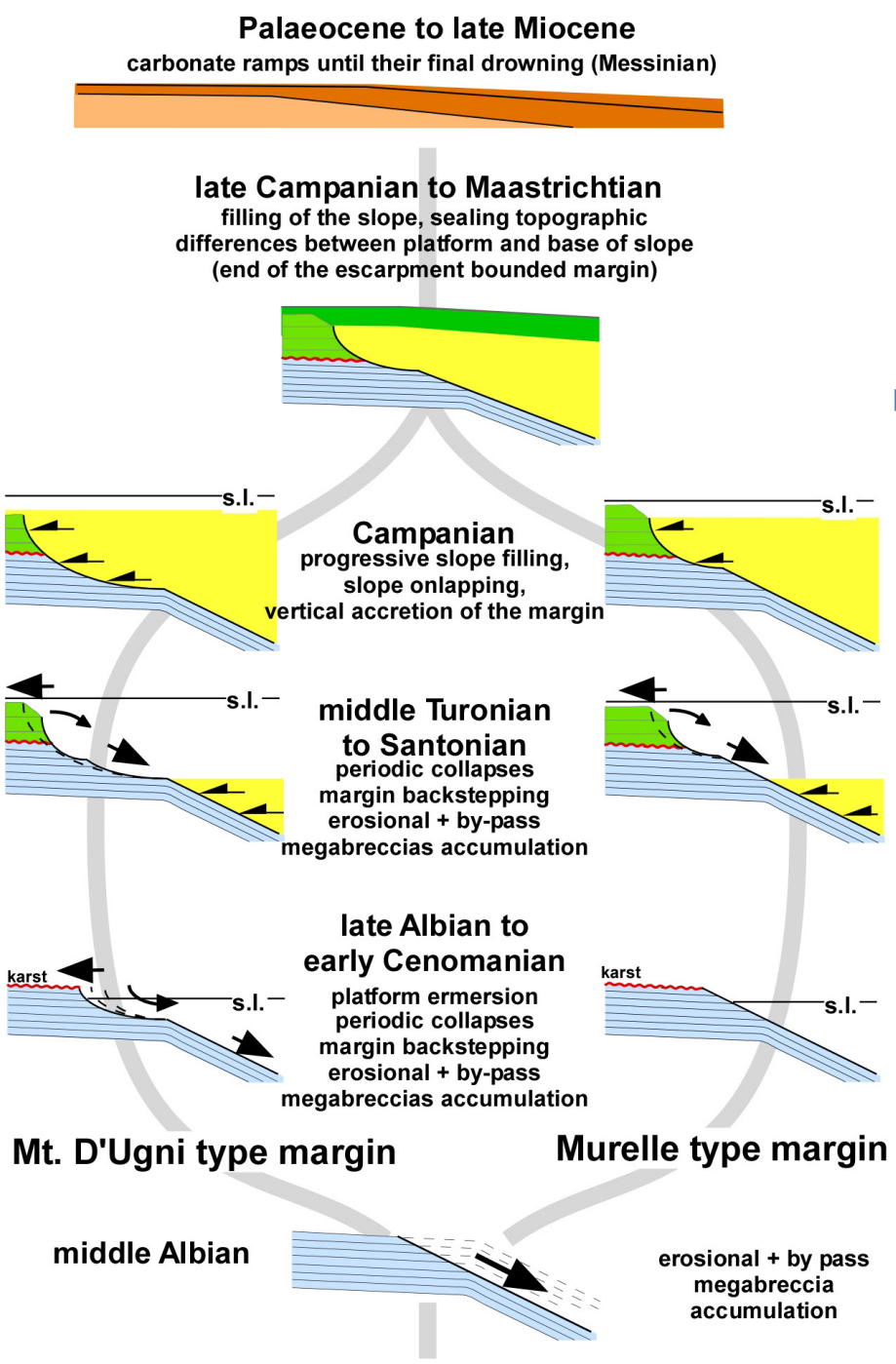


Fig. 69 - Reconstructed geometry of the pre-collapse depositional profile of the Maiella platform at the end of the Early Cretaceous. Following this reconstruction, the pre-collapse depositional profile corresponds to a depositional and essentially aggrading or weakly prograding platform with a slope inclined about 25-30°.

As supported by field evidence, the pre-collapse depositional profile of the platform-to-basin transition can be envisaged (Fig. 69) along prominent ridge structures, which preserve some of the original geometric and depositional features (Rusciadelli et al., 2003; Rusciadelli 2005). The reconstruction of the possible pre-collapse depositional profile of the Maiella platform margin at the end of the Early Cretaceous suggests that the platform edge extended 1 km further to the north, compared with the present position of the palaeoescarpment. The maximum thickness of the sediments eroded by the margin collapse is estimated at around 300 m (Rusciadelli et al., 2003). The presence of large and small-scale scalloped

<https://doi.org/10.3301/GFT.2022.05>



TRUE CARBONATE RAMPS

INCEPTION OF THE PROGRADING GEOMETRY
LOW ANGLE PROFILE ("ORFENTO fm")
END OF MARGIN COLLAPSES

SMALL-SCALE COLLAPSES (BRECCIAS OF THE "TRE GROTTIE fm")

EROSIONAL AND BY PASS PLATFORM MARGIN

LARGE-SCALE COLLAPSES SCALLOPPED MARGIN (BRECCIAS OF THE "BOCCA DI VALLE" & "VALLE DELL'INFERN"O fms)

ACCRETIONARY TO EROSIONAL PLATFORM MARGIN

structures and of breccia and megabreccia deposits, intercalated in the slope succession during two distinct time intervals, suggests that the current escarpment configuration was the result of two evolution stages, that were locally dominated by collapses on a pre-existing fault-escarpment of early to middle Albian age (Fig. 70). Soon thereafter, a first collapse occurred between the middle Albian and the early Cenomanian, as suggested by the age of megabreccias with platform-derived clasts outcropping northward within the "Bocca di Valle fm". This major collapse affected the platform margin along its whole length. Long after the

Fig. 70 - Interpretation of the origin and evolution of the Maiella palaeoescarpment during the Albian *p.p.* - Campanian *p.p.* time interval. For graphical simplicity, the interpretation focuses on the depositional processes, excluding faulting from the scheme but not as a driving morphotectonic processes. Faulting should have acted during the early stage of the palaeoescarpment evolution.



initial break-up tectonics, the Mesozoic platform experienced deep facies redistribution. This is to be related to the renewed tectonics that is associated with the escarpment evolution that changed to erosive and by-pass slope towards the basin. The inherited configuration was characterised by prominent ridges with an average 30° dipping stable slope, and by indentations with a less stable slope, affected by periodic different-scale collapses. These were responsible for the progressive backstepping of the platform edge. During this phase, large amounts of breccias, megabreccias, and bioclastic deposits were shed basin-ward over distances of 15 km as average from the platform edge and distributed over an area of 150 km² at least. Meanwhile or immediately after, a widespread emersion of the platform occurred by allowing the formation of bauxitic soils. The second stage started in the middle Cenomanian and was dominated by collapse events, that were accompanied by the general flooding of the platform sectors that were previously emerged. During this period, rudist biostromes and sand shoals newly colonised the platform margin, following the indented morphology of the platform edge, inherited by the previous large-scale collapse events. According to facies analysis and the study of the stratigraphic contacts, the presence of such a steep escarpment prevented the basin-ward progradational of the margin, which, instead, aggraded vertically on the platform edge. Large amounts of bioclastic material, which indicates high productivity rates of the margin, were shed basinward by-passing the slope. This configuration of the slope promoted small-scale collapses of margin portions during the Late Cretaceous, with the consequent progressive backstepping and reworking of the inherited platform edge. The products of these small-scale collapses correspond to the breccias and megabreccias deposits intercalated within the Upper Cretaceous slope succession. During this phase, the space in front of the platform margin was progressively filled and conditions along the slope changed from by-pass to depositional. Many triggering mechanisms have been invoked to explain margin collapses and the formation of steep escarpments and their related products such as megabreccias. The most widely accepted factors include: tectonically driven earthquakes, fault scarp formation, platform overstepping, thrust loading, undercutting bottom currents, differences in geotechnical behaviour of rocks, relative sea level changes, and bolide impacts (see discussion in [Spence & Tucker, 1997](#); [Bosellini, 1998](#); [Drzewiecki & Simo, 2002](#)). To better understand the mechanisms triggering margin collapses, quantitative modeling has been applied to the large-scale collapse of the Maiella Platform ([Rusciadelli et al., 2003](#)). The obtained results strengthen the hypothesis that the palaeoescarpment is produced by a series of large-scale collapses associated to earthquake swarms linked to the tectonic displacement along an East-striking and North-dipping normal fault located along the slope. Successively, direct stratigraphic data have carried new evidence for the presence of a fault system, whose activity was post-dated by Upper Cretaceous fault-reactivation ([Rusciadelli, 2005](#)).



Stop 5.4. Fonte Tettone section (42°10'14.47"N; 14°06'43.25"E)

Nearby the Fonte Tettone fountain a detail section of the Danian-Rupelian "Santo Spirito fm" crops out. This formation is thin and discontinuous over the former platform top, while it is more continuous northward, over the platform margin and slope, where it reaches 200 m of thickness. Here, bioclastic turbidites are well exposed along the road cut (Fig. 71). The main sedimentary body is represented by staked, thinning, and fining-upward beds of bioclastic rudstone to packstone, passing upward to thin beds of fine packstone to wackestone. This sedimentary body shows basal scours and represents the filling of a lensoidal and concave-plane wide channel. The bioclasts are mostly oriented parallel to bedding and are generally imbricated. The main skeletal components are represented by larger benthic foraminifers (*Nummulites millecaput*, *N. maximus*, *Discocyclina* spp.), echinoids, coralline algae, molluscs, and coral fragments. Rare lithoclasts are present.

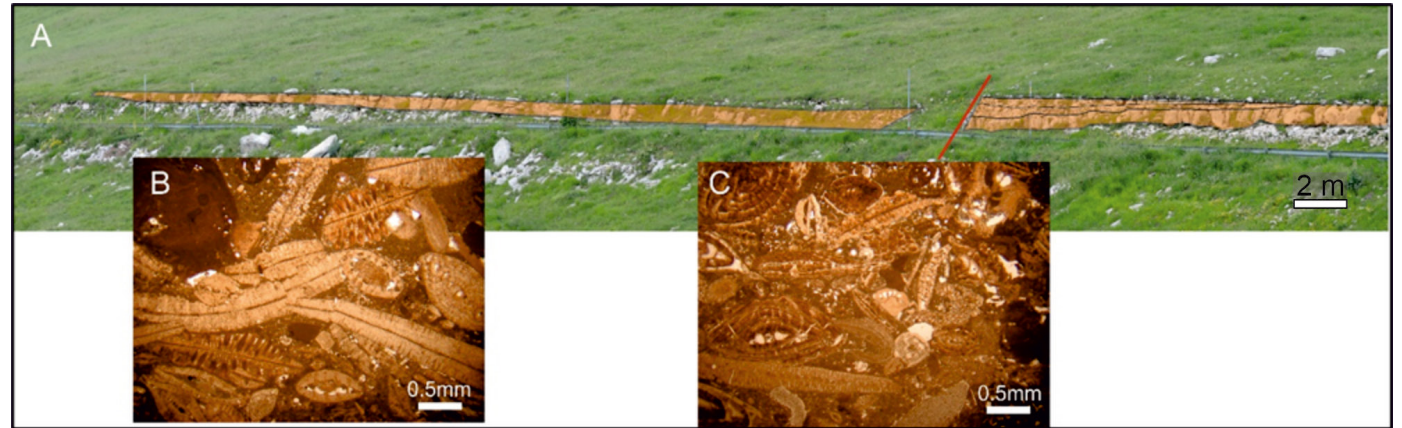


Fig. 71 - Bioclastic calciturbidite well exposes along the road cut in Fonte Tettone. The main sedimentary body is represented by staked, thinning, and fining upward beds of bioclastic rudstone to packstone, passing upward to thin beds of fine packstone to wackestone. The main skeletal components are represented by nummulitids (*Nummulites millecaput*, *N. maximus*, *Discocyclina* spp.), echinoids, coralline algae, molluscs, and coral fragments.

From a biostratigraphic view, foraminiferal assemblage is characterised by Lutetian to Bartonian foraminifers. However, the presence of *Pellatispira madaraszi* and *Heterostegina reticulata* implies a Priabonian age, suggesting long-lasting reworking. The compositional characters indicate that the bioclastic sediments were mainly derived from the middle and outer ramp environment, where currents were strong enough to gain high speed and evolve into turbidity currents flowing downslope through erosive-based gullies. However, although occasional or extraordinary storms could have been involved, this causes the paradox that no shallow-water skeletal components were involved.



Stop 5.5. The San Bartolomeo Valley Section (42°10'52.70"N; 14°02'05.61"E)

The panoramic view of the San Bartolomeo Valley from the Giumentina Valley represents one of the best places to see the stratigraphic architecture of the "Bolognano fm" (Fig. 72, Brandano et al., 2012; Brandano et al., 2016a). The riverbed in the valley lies within the "Santo Spirito fm". Above it, the "*Lepidocyclina* calcarenites 1" reach a thickness of 53 m (Brandano et al., 2016a). Above them, the "cherty marly limestones" crop out for 18 m and are then overlaid by the "*Lepidocyclina* calcarenites 2", 16-m thick in this section (Brandano et al., 2016a). At the top of this unit, a phosphatic hardground marks the drowning of the "*Lepidocyclina* calcarenites 2" and the onset of the hemipelagic marly limestones and calcareous marls sedimentation, which are in turn overlaid by the "*Lithothamnion* limestone" unit (Brandano et al., 2016a; 2016b). A clear positive $\delta^{13}\text{C}$ isotope shift is recorded in the San Bartolomeo section at the base of the Aquitanian (Fig. 72, Brandano et al., 2017), correlated with the Early Miocene Carbon Maximum (EMCM, Zachos et al., 2001). This shift coincides with the sharp facies change – from the "*Lepidocyclina* calcarenites 1" to the "cherty marly limestones" – linked to increased primary productivity of surface waters triggered by the global Mi-1 Event (Miller et al., 1991; Zachos et al., 2001; Lear et al., 2004). A wider positive $\delta^{13}\text{C}$ Carbon isotope excursion is recorded in the upper Burdigalian-Serravallian (Brandano et al., 2017) and correlated with the global Monterey Carbon Isotope Excursion (Holbourn et al., 2004, 2007). The onset of the Monterey Event coincides with the widest carbon isotope peak (+2‰ $\delta^{13}\text{C}$), recorded within the "*Lepidocyclina* calcarenites 2", characterised by abundant bryozoans (Fig. 72), which dominate the Langhian calcarenitic unit above the hardground surface in the Orfento Valley (Brandano et al., 2016a). Thus, as in the Latium-Abruzzi record, in the Maiella Mountain the enhanced nutrient availability of surface waters led to the spread of the filter feeders biota, such as bryozoans (Brandano et al., 2017).

Acknowledgments

The 'Gran Sasso and Monti della Laga' and the 'Maiella' National parks and the Nazzano Tevere-Farfa Regional Nature Reserve are sincerely thanked for the Research permits provided. We are also thankful to the quarry owners Alessandro, Francesco, Francesca, Aurelio, and Roberto of the Pacifici and Querciolaie-Rinascente quarries, who granted the possibility to access the quarries and for their logistic support. Funds from 'Fondi di Ateneo Sapienza 2020' of MB and from the Italian National Research council project 'Sistemi terrazzati e valli incise' (code CNR.DTA.AD003.316) of MM and IM are acknowledged. We thank the editors Andrea Zanchi, Stefano Tavani, Angelo Cipriani and Diego Pieruccioni and two anonymous reviewers for their comments that greatly contributed to refine the quality of this guide.

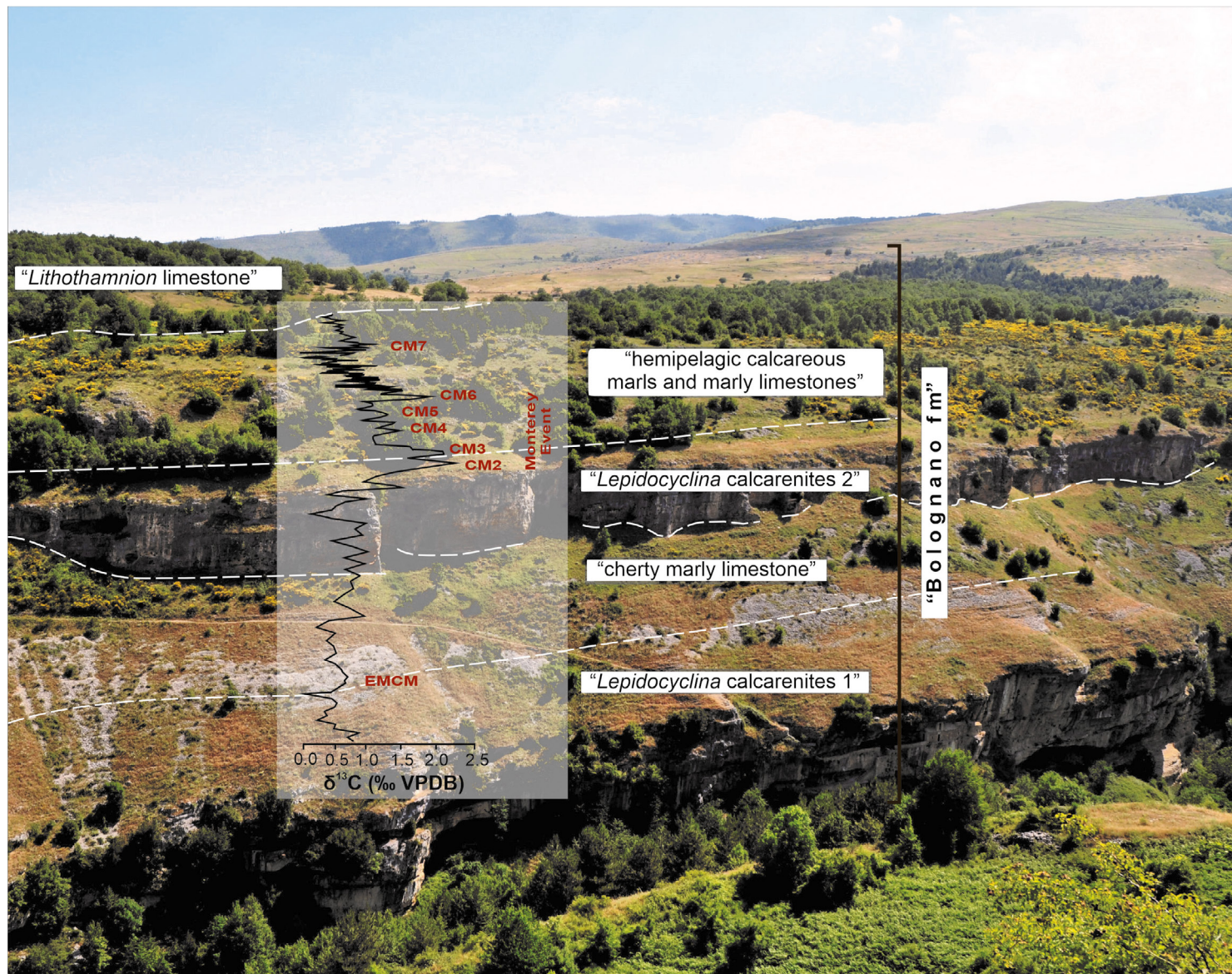


Fig. 72 - Panoramic view of the San Bartolomeo Valley (looking ENE) with photomapping of the outcropping units of the "Bolognano fm" and relative $\delta^{13}\text{C}$ Carbon isotope curve. Modified after Brandano et al. (2020b). Carbon isotope record of the EMCM and Monterey Event from Brandano et al. (2017), carbon isotope record of the CM7 from Cornacchia et al. (2021). EMCM = Early Miocene Carbon Maximum.

References

- Accordi G. & Carbone F. (1988) - Lithofacies map of Latium-Abruzzi and neighbouring areas. C.N.R., Quaderni de 'La Ricerca Scientifica', 114, Progetto Finalizzato "Geodinamica" Monografie Finali, v. 5.
- Accordi B., Devoto G., La Monica GB., Praturlon A., Sirna G. & Zalaffi M. (1967) - Il Neogene nell'Appennino laziale-abruzzese. Committee Mediterranean Neogene Stratigraphy, Proc. IV Session, Bologna. Giorn. Geol., 35, 235-268.
- Accordi G., Carbone F., Sirna G., Catalano G. & Reali S. (1987) - Sedimentary events and rudist assemblages of Maiella Mt. (Central Italy): paleobiogeographic implications. *Geologica Romana*, 26, 135-147.
- Accordi G., Carbone F., Civitelli G., Corda L., De Rita D., Esu D., Funicello R., Kotsakis T., Mariotti G. & Sposato A. (1988) - Note illustrative alla Carta delle litofacies del Lazio-Abruzzo e aree limitrofe. CNR, Progetto Finalizzato Geodinamica: Sottoprogetto 4. Quaderni della Ricerca Scientifica, 114(5).
- Accarie H. (1988) - Dynamique sedimentaire et structurale au passage plateforme/bassin. Les facies carbonates cretaces et tertiaires: Massif de la Maiella (Abruzzes, Italie). Ecole des Mines de Paris, Mémoire Science de la Terre, 5, 158.
- Acocella V. & Funicello R. (2006) - Transverse systems along the extensional Tyrrhenian margin of central Italy and their influence on volcanism. *Tectonics*, 25(2).
- Adamoli L. (1992) - Evidenze di tettonica d'inversione nell'area del Corno Grande-Corno Piccolo (Gran Sasso d'Italia). *Boll. Soc. Geol. It.*, 111, 53-66.
- Adamoli L., Bertini T., Chiocchini M., Deiana G., Mancinelli A., Pieruccini U. & Romano A. (1978) - Ricerche geologiche sul Mesozoico del Gran Sasso d'Italia (Abruzzo). II. Evoluzione tettonico-sedimentaria dal Trias superiore al Cretaceo inferiore dell'area compresa tra il Corno Grande e S. Stefano di Sessanio (F. 140 Teramo). *Studi Geol. Camerti*, 4, 7-18.
- Agnini C., Fornaciari E., Raffi I., Catanzariti R., Pälke H., Backman J. & Rio D. (2014) - Biozonation and biochronology of Paleogene calcareous nannofossils from low and middle latitudes. *Newsl. Stratigr.*, 47(2), 131-181.
- Alessandri L., Cardello G. L., Attema P.A.J., Baiocchi V., De Angelis F., Del Pizzo S., Di Ciaccio F., Fiorillo A., Gatta M., Monti F., Onori M., Rolfo M. F., Romboni M., Sottili G. & Troisi S. (2021) - Reconstructing the Late Pleistocene – Anthropocene interaction between the neotectonic and archaeological landscape evolution in the Apennines (La Sassa cave, Italy). *Quat. Sci. Rev.*, 265, <https://doi.org/10.1016/j.quascirev.2021.107067>.
- Ambrosetti P., Carboni M.G., Conti M.A., Esu D., Girotti O., La Monica G.B., Landini B. & Parisi G. (1987) - Il Pliocene ed il Pleistocene inferiore del Bacino del Fiume Tevere nell'Umbria meridionale. *Geogr. Fis. Dinam. Quat.*, 10, 10-33.
- Anzalone E., D'Argenio B. & Ferreri V. (2017) - Depositional trends of travertines in the type area of Tivoli (Italy). *Rend. Lincei Sci. Fis. Nat.*, 28(2), 341-361.
- Bally A.W. (1954) - Geologische Untersuchungen in den SE-Abruzzen. PhD thesis, Univ. Zürich, 291 pp.
- Bally A.W., Burbi C., Cooper C. & Ghelardoni R. (1986) - Balanced cross sections and seismic reflection profiles across the Central Apennines. *Mem. Soc. Geol. It.*, 35, 257-310.

- Barberi F., Buonasorte G., Cioni R., Fiordelisi A., Foresi L., Iaccarino S., Laurenzi M.A., Sbrana A., Vernia L. & Villa I.M. (1994) - Plio-Pleistocene geological evolution of the geothermal area of Tuscany and Latium. Mem. Descr. Carta Geol. d'It., 49, 77-134.
- Barberio M.D., Gori F., Barbieri M., Boschetti T., Caracausi A., Cardello G.L. & Petitta M. (2021) - Understanding the Origin and Mixing of Deep Fluids in Shallow Aquifers and Possible Implications for Crustal Deformation Studies: San Vittorino Plain, Central Apennines. Appl. Sci., 11(4), 1353.
- Barbieri M., Boschetti T., Petitta M. & Tallini M. (2005) - Stable isotope (^2H , ^{18}O and $^{87}\text{Sr}/^{86}\text{Sr}$) and hydrochemistry monitoring for groundwater hydrodynamics analysis in a karst aquifer (Gran Sasso, Central Italy). Appl. Geochem., 20(11), 2063-2081.
- Barnes I., Irwin W.P. & White D.E. (1978) - Global distribution of carbon dioxide discharges, and major zones of seismicity. Rep. U.S. Geological Survey, Water Resources Investigations. 39-78.
- Beaudoin A., Augier R., Jolivet L., Jourdon A., Raimbourg H., Scaillet S. & Cardello G. L. (2017) - Deformation behavior of continental crust during subduction and exhumation: Strain distribution over the Tenda massif (Alpine Corsica, France). Tectonophysics, 705, 12-32.
- Bellucci D., Novaga R., Freyhof J. (2021) - New data on the distribution of the Volturino spined loach *Cobitis zanandreae* (Teleostei: Cobitidae). J. Appl. Ichthyol., 37, 885-892.
- Bernoulli D. (2001) - Mesozoic-Tertiary carbonate platforms, slopes and basins of the external Apennines and Sicily. In: Vai G.B., Martini I.P. (eds) Anatomy of an Orogen: the Apennines and Adjacent Mediterranean Basins. Springer, Dordrecht. 307-325. https://doi.org/10.1007/978-94-015-9829-3_18.
- Bernoulli D., Kälin O. & Patacca E. (1979) - A sunken continental margin of the Mesozoic Tethys: the northern and central Apennines. In *Sédimentation jurassique W européen*, 197-210.
- Berti D., Bonomo R., Campo V., Chiarini E., Falcetti S., Graciotti R., Marino M., Pampaloni L., Papasodaro F., Ricci V., Rossi M., Silvestri S., Troccoli A. & Vita L. (2021) - Carta geologica dell'area pedemontana orientale della Majella in scala 1:25.000. ISPRA. <https://www.isprambiente.gov.it/it/attivita/suolo-e-territorio/cartografia/carta-geologica-dell-area-pedemontana-orientale-della-majella-in-scala-1-25.000>.
- Bigi S., Casero P. & Ciotoli G. (2011) - Seismic interpretation of the Laga basin; constraints on the structural setting and kinematics of the Central Apennines. J. Geol. Soc. London, 168(1), 179-190.
- Bigi G., Cosentino D., Parotto M., Sartori R. & Scandone P. (1992) - Structural Model of Italy, scale 1: 500 000, 6 sheets. CNR, Quaderni de La Ricerca Scientifica, 114(3).
- Billi A., De Filippis L., Poncia P. P., Sella P. & Faccenna C. (2016) - Hidden sinkholes and karst cavities in the travertine plateau of a highly-populated geothermal seismic territory (Tivoli, central Italy). Geomorphology, 255, 63-80.
- Billi A., Tiberti M.M., Cavinato G.P., Cosentino D., Di Luzio E., Keller J.V.A., Kluth C., Orlando L., Parotto M., Praturlon A., Romanelli M., Storti F. & Wardell N. (2006) - First results from the CROP-11 deep seismic profile, central Apennines, Italy: evidence of mid-crustal folding. J. Geol. Soc. London, 163(4), 583-586.
- Blum M.D. & Törnqvist T.E. (2000) - Fluvial responses to climate and sea-level change: a review and look forward. Sedimentology, 47, 2-48.

- Boccaletti M. & Guazzone G. (1974) - Remnant arcs and marginal basins in the Cainozoic development of the Mediterranean. *Nature*, 252(5478), 18-21.
- Boni C., Bono P. & Capelli G. (1986) - Schema idrogeologico dell'Italia centrale. *Mem. Soc. Geol. It.*, 35, 991-1012.
- Borzi M., Carboni M.G., Cilento G., Di Bella L., Florindo F., Girotti O., Piccardi E. & Sagnotti L. (1998) - Bio- and Magneto-stratigraphy in the Tiber Valley revised. *Quat. Int.*, 47/48, 65-72.
- Bosellini A. (1998) - Scalloped v s faulted carbonate platform margins and the origin of basinal megabreccias. *Mem. Soc. Geol. It.*, 53, 63-74
- Brandano M. (2017) - Unravelling the origin of a Paleogene unconformity in the Latium-Abruzzi carbonate succession: a shaved platform. *Palaeogeogr. Palaeoclimatol. Palaeoecol.*, 485, 687-696.
- Brandano M. & Corda L. (2002) - Nutrients, sea level and tectonics: constrains for the facies architecture of a Miocene carbonate ramp in central Italy. *Terra Nova*, 14(4), 257-262.
- Brandano M. & Loche M. (2014) - The Coniacian-Campanian Latium-Abruzzi carbonate platform, an example of a facies mosaic. *Facies*, 60(2), 489-500.
- Brandano M., Brilli M., Corda L. & Lustrino M. (2010) - Miocene C-isotope signature from the central Apennine successions (Italy): Monterey vs. regional controlling factors. *Terra Nova*, 22(2), 125-130
- Brandano M., Cornacchia I., Raffi I. & Tomassetti L. (2016a) - The Oligocene-Miocene stratigraphic evolution of the Majella carbonate platform (Central Apennines, Italy). *Sediment. Geol.*, 333, 1448 1-14.
- Brandano M., Cornacchia I., Raffi I., Tomassetti L. & Agostini S. (2017) - The Monterey Event within the Central Mediterranean area: The shallow-water record. *Sedimentology*, 64(1), 286-310.
- Brandano M., Lipparini L., Campagnoni V. & Tomassetti L. (2012) - Downslope-migrating large dunes in the Chattian carbonate ramp of the Majella Mountains (Central Apennines, Italy). *Sediment. Geol.*, 255, 29-41.
- Brandano M., Lustrino M., Cornacchia I. & Sprovieri M. (2015) - Global and regional factors responsible for the drowning of the Central Apennine Chattian carbonate platforms. *Geol. J.*, 50(5), 575-591.
- Brandano M., Mateu-Vicens G., Gianfagna A., Corda L., Billi A., Quaresima S. & Simonetti A. (2009) - Hardground development and drowning of a Miocene carbonate ramp (Latium-Abruzzi): from tectonic to paleoclimate. *J. Mediterr. Earth Sci.*, 1, 47-56.
- Brandano M., Tomassetti L., Sardella R. & Tinelli C. (2016b) - Progressive deterioration of trophic conditions in a carbonate ramp environment: the Lithothamnion Limestone, Majella Mountain (Tortonian-early Messinian, central Apennines, Italy). *Palaios*, 31(4), 125-140.
- Brandano M., Ronca S. & Di Bella L. (2020a) - Erosion of Tortonian phosphatic intervals in upwelling zones: The role of internal waves. *Palaeogeogr., Palaeoclimatol., Palaeoecol.*, 537, 109405.
- Brandano M., Tomassetti L., Cornacchia I., Trippetta F., Pomar L. & Petracchini L. (2020b) - The submarine dune field of the Bolognana Fm: depositional processes and the carbonate reservoir potential (Chattian to Burdigalian, Majella Carbonate Platform). *Geological Field Trips and Maps*, 12(2), 2-42.

- Brandano M., Tomassetti L., Sardella R. & Tinelli C. (2016b) - Progressive deterioration of trophic conditions in a carbonate ramp environment: the Lithothamnion Limestone, Majella Mountain (Tortonian–early Messinian, central Apennines, Italy). *Palaios*, 31(4), 125-140.
- Brogi A. & Capezzuoli E. (2009) - Travertine deposition and faulting: the fault-related travertine fissure-ridge at Terme S. Giovanni, Rapolano Terme (Italy). *Int. J. Earth Sci.*, 98, 931-947.
- Brogi A. & Capezzuoli E. (2014) - Earthquake impact on fissure-ridge type travertine deposition. *Geol. Mag.*, 151, 1135-1143.
- Brogi A., Capezzuoli E., Aque R., Branca M. & Voltaggio M. (2010) - Studying travertine for neotectonics investigations: Middle-Late Pleistocene syn-tectonic travertine deposition at Serre di Rapolano (Northern Apennines, Italy). *Geol. Rundsch.*, 99, 1383-1398.
- Brogi A., Capezzuoli E., Buracchi E. & Branca M. (2012) - Tectonic control on travertine and calcareous tufa deposition in a low-temperature geothermal system (Sarteano, Central Italy). *Geol. Soc. Lond. Mem.*, 169, 461-476.
- Buonasorte G., Fiordelisi A., Pandeli E., Rossi U. & Sollevanti F. (1987) - Stratigraphic correlations and structural setting of the pre-neoautochthonous sedimentary sequences of Northern Latium. *Per. Mineral.*, 56, 111-122.
- Calamita F., Coltorti M., Pierantoni P.P., Pizzi A., Scisciani V. & Turco E. (1996) - Relazioni tra le faglie quaternarie e la sismicità nella dorsale appenninica umbro-marchigiana: l'area di Colfiorito. *Studi Geol. Camerti*, XIV, 177-191.
- Calamita F., Satolli S., Scisciani V., Esestine P. & Pace P. (2011) - Contrasting styles of fault reactivation in curved orogenic belts: Examples from the Central Apennines (Italy). *GSA Bull.*, 123(5-6), 1097-1111.
- Cande S.C. & Kent D.V. (1992) - A new geomagnetic polarity time scale for the Late Cretaceous and Cenozoic. *J. Geophys. Res.*, 97, 13917-13951.
- Capezzuoli E., Gandin A. & Pedley H.M. (2009) - Travertines and calcareous tufa in Tuscany (Central Italy). In: 27th IAS meeting of sedimentology, Alghero, Italy. *Fieldtrip Guidebook*, 129, 158 pp.
- Capezzuoli E., Gandin A. & Sandrelli F. (2010) - Calcareous tufa as indicators of climatic variability: A case study from southern Tuscany (Italy) *Geol. Soc., London, Spec. Pub.*, 336(1), 263-281.
- Capotorti F. & Muraro C. (2021) - Post-rift extensional tectonics at the edge of a carbonate platform: insights from the Middle Jurassic-Early Cretaceous Monte Giano stratigraphic record (central Apennines, Italy). *Geologica Acta*, 19, 1-23.
- Carannante G. (1982) - Modello deposizionale e diagenetico di un livello fosfatico nel Miocene carbonatico dell'Appennino Campano. *Rend. Soc. Geol. It.*, 5, 15-20.
- Carannante G., Cherchi A. & Simone L. (1995) - Chlorozoan versus foramol lithofacies in Late Cretaceous rudist limestones. *Palaeogeogr. Palaeoclimatol. Palaeoecol.*, 119, 137-154.
- Carannante G., Graziano R., Pappone G., Ruberti D. & Simone L. (1999) - Depositional system and response to sea-level oscillation of the Senonian foramol-shelves. Examples from central Mediterranean areas. *Facies*, 40, 1-24.
- Carannante G., Ruberti D. & Sirna M. (2000) - Upper Cretaceous low energy ramp limestones from the Sorrento Peninsula (Southern Apennines, Italy): micro- and macrofossil associations and their significance in the depositional sequences. *Sediment Geol.*, 132, 89-124.

- Cardello G.L. (2008) – Struttura del fianco occidentale del Massiccio del Gran Sasso d'Italia. Master Thesis, Sapienza Università di Roma, 163 pp. <https://doi.org/10.13140/RG.2.1.4799.5607>.
- Cardello G.L. & Doglioni C. (2015) - From mesozoic rifting to Apennine orogeny: the gran Sasso range (Italy). *Gondwana Research*, 27(4), 1307-1334.
- Cardello G.L. & Mancktelow N.S. (2014) - Cretaceous syn-sedimentary faulting in the Wildhorn Nappe. *Swiss J. Geosci.*, 107(2-3), 223–250. <https://doi.org/10.1007/s00015-014-0166-8>.
- Cardello G.L. & Mancktelow N.S. (2015) - Veining and post-nappe transtensional faulting in the SW Helvetic Alps (Switzerland). *Swiss J. Geosci.*, 108(2), 379-400.
- Cardello G.L., Consorti L., Palladino D.M., Carminati E., Carlini M. & Doglioni C. (2020) - Tectonically controlled carbonate-seated maar-diatreme volcanoes: The case of the Volsci Volcanic Field, central Italy. *J. Geodyn.*, 139, 101763.
- Cardello G.L., Di Vincenzo G., Giorgetti G., Zwingmann H. & Mancktelow N. (2019) - Initiation and development of the Pennine Basal Thrust (Swiss Alps): a structural and geochronological study of an exhumed megathrust. *J. Struct. Geol.*, 126, 338-356.
- Cardello G.L., Vico G., Consorti L., Sabbatino M., Carminati E. & Doglioni C. (2021) - Constraining the Passive to Active Margin Tectonics of the Internal Central Apennines: Insights from Biostratigraphy, Structural, and Seismic Analysis. *Geosciences*, 11(4), 160.
- Carminati E. & Doglioni C. (2012) - Alps vs. Apennines: the paradigm of a tectonically asymmetric Earth. *Earth-Sci. Rev.*, 112(1-2), 67-96.
- Carminati E., Corda L., Mariotti G. & Brandano M. (2007) - Tectonic control on the architecture of a Miocene carbonate ramp in the central Apennines (Italy): insights from facies and backstripping analyses. *Sediment. Geol.*, 198, 233–253.
- Carminati E., Fabbi S. & Santantonio M. (2014) - Slab bending, syn-subduction normal faulting, and out-of-sequence thrusting in the Central Apennines. *Tectonics*, 33(4), 530-551.
- Catalano P.G., Cavinato G.P., Salvini F. & Tozzi M. (1986) - Analisi strutturale nei laboratori dell'INFN del Gran Sasso d'Italia. *Mem. Soc. Geol. It.*, 35(2), 647-655.
- Catenacci V. (1974) - Note illustrative della Carta Geologica d'Italia scala 1:100.000. Foglio 147 «Lanciano». Servizio Geologico d'Italia, 87 pp.
- Cavinato G.P. & De Celles P.G. (1999) - Extensional basins in the tectonically bimodal central Apennines fold-thrust belt, Italy: response to corner flow above a subducting slab in retrograde motion. *Geology*, 27, 955–958.
- Cavinato G.P., Cosentino D., De Rita D., Funiciello R. & Parotto M. (1994) - Tectono-sedimentary evolution of intrapenninic basins and correlation with the volcano-tectonic activity in Central Italy. *Mem. Descr. Carta Geol. d'It.*, 49, 63–76.
- Cavinato G.P., Mancini M., Milli S. & Moscatelli M. (2004) - Long term tectonic and short-term glacio-eustatic controls on Upper Pliocene to Quaternary shallow marine and fluvio-deltaic deposits in the lower and middle valley of the Tiber River. 32° International Geological Congress, Firenze 20-28 August 2004, Book of abstracts.
- Centamore E., Chiocchini M., Deiana G., Micarelli A. & Pieruccini V. (1971) - Contributo alla conoscenza del Giurassico dell'Appennino umbro-marchigiano. *Studi geol. Camerti*, 1, 1-89.

- Cestari R., Reali S. & Sirna M. (1992) - Biostratigraphical characteristics of the Turonian-?Maastrichtian p.p. (Upper Cretaceous) deposits in the Simbruini-Ernici Mts. (Central Apennines, Italy). *Geologica Romana*, 28, 359-372.
- Chafetz H.S. & Folk R.L. (1984) - Travertines; depositional morphology and the bacterially constructed constituents. *J. Sediment. Res.*, 54(1), 289-316.
- Chafetz H., Rush P.F. & Utech N.M. (1991) - Microenvironmental controls on mineralogy and habit of CaCO₃ precipitates: an example from an active travertine system. *Sedimentology*, 38(1), 107-126.
- Channell J.E.T., d'Argenio B. & Horvath F. (1979) - Adria, the African promontory, in Mesozoic Mediterranean palaeogeography. *Earth-Sci. Rev.*, 15(3), 213-292.
- Chiodini G., Allard P., Caliro S. & Parello F. (2000) - 18O exchange between steam and carbon dioxide in volcanic and hydrothermal gases: implications for the source of water. *Geochim. Cosmochim. Acta*, 64(14), 2479-2488.
- Chiodini G., Cardellini C., Amato A., Boschi E., Caliro S., Frondini F., Ventura G. (2004) - Carbon dioxide Earth degassing and seismogenesis in central and southern Italy. *Geophys. Res. Lett.*, 31(7), L07615.
- Cipollari P. & Cosentino D. (1995) - Miocene unconformities in the central Apennines: geodynamic significance and sedimentary basin evolution. *Tectonophysics*, 252, 375-389.
- Cipriani A. & Bottini C. (2019) - Early cretaceous tectonic rejuvenation of an Early Jurassic margin in the central Apennines: the "Mt. Cosce breccia". *Sediment. Geol.*, 387, 57-74.
- Cita M.B. (1975) - Studi sul Pliocene e sugli strati di passaggio dal Miocene al Pliocene. VII Planktonic biozonation of the Mediterranean Pliocene deep sea record. A revision. *Riv. It. Paleont. Strat.*, 81, 527-544.
- Civitelli G. & Brandano M. (2005) - Atlante delle litofacies e modello deposizionale dei Calcari a Briozoi e Litotamni nella Piattaforma carbonatica laziale-abruzzese. *Boll. Soc. Geol. It.*, 124(3), 611.
- Clark P.U., Dyke A.S., Shakun J.D., Carlson A.E., Clark J., Wohlfarth B., Mitrovica J.X., Hostetler S.W. & McCabe A.M. (2009) - The last glacial maximum. *Science*, 325(5941), 710-714.
- Clemenzi L., Storti F., Balsamo F., Molli G., Ellam R., Muchez P. & Swennen R. (2015). Fluid pressure cycles, variations in permeability, and weakening mechanisms along low-angle normal faults: The Tellaro detachment, Italy. *GSA Bulletin*, 127(11-12), 1689-1710.
- Cloetingh S.A.P.L., Burov E., Matenco L., Toussaint G., Bertotti G., Andriessen P. A. M., Wortel M.J.R. & Spakman W. (2004) - Thermo-mechanical controls on the mode of continental collision in the SE Carpathians (Romania). *Earth Planet. Sci. Lett.*, 218(1-2), 57-76.
- Cohen K.M., MacDonald K., Joordens J.C., Roebroeks W. & Gibbard P.L. (2012) - The earliest occupation of north-west Europe: a coastal perspective. *Quat. Int.*, 271, 70-83.
- Colalongo M.L. & Sartoni S. (1979) - Schema biostratigrafico per il Pliocene e il basso Pleistocene in Italia. Nuovi contributi alla realizzazione della Carta Neotettonica d'Italia, 251, 645-654.
- Coppola M., Correale A., Barberio M.D., Billi A., Cavallo A., Fondriest M., Nazzari M., Paonita A., Romano C., Stagno V., Viti C. & Vona A. (2021) - Meso-to nano-scale evidence of fluid-assisted co-seismic slip along the normal Mt. Morrone Fault, Italy: Implications for earthquake hydrogeochemical precursors. *Earth Planet. Sci. Lett.*, 568, 117010.

- Cornacchia I., Andersson P., Agostini S., Brandano M. & Di Bella L. (2017) - Strontium stratigraphy of the upper Miocene Lithothamnion Limestone in the Majella Mountain, central Italy, and its palaeoenvironmental implications. *Lethaia*, 50(4), 561-575.
- Cornacchia I., Brandano M., Raffi I., Tomassetti L. & Flores I. (2018) - The Eocene–Oligocene transition in the C-isotope record of the carbonate successions in the Central Mediterranean. *Glob. Planet. Change*, 167, 110-122.
- Cornacchia I., Munnecke A. & Brandano M. (2021) - The potential of carbonate ramps to record C-isotope shifts: insights from the upper Miocene of the Central Mediterranean area. *Lethaia*, 54(1), 73-89.
- Cosentino D., Cipollari P., Marsili P. & Scrocca D. (2010) - Geology of the central Apennines: a regional review. *J. Virtual Explor.*, 36(11), 1-37.
- Coxall H.K. & Pearson P.N. (2007) - The Eocene-Oligocene transition. Deep time perspectives on climate change: Marrying the signal from computer models and biological proxies. In: Williams M., Haywood A.M., Gregory F.J., Schmidt D.N. (Eds.), *The Micropalaeontol. Soc., Spec. Pub., Geol. Soc., London*, 351-387. <https://doi.org/10.1144/TMS002.16>.
- Crescenti U., Crostella A., Donzelli G. & Raffi G. (1969) - Stratigrafia della serie calcarea dal Lias al Miocene nella regione marchigiana abruzzese: Parte II. Litostratigrafia, biostratigrafia, paleogeografia. *Memorie della Società Geologica Italiana*, 9, 343–420.
- Crescenti U., Milia M.L., Rusciadelli G. (2004) - Stratigraphic and tectonic evolution of the Pliocene Abruzzi basin (Central Apennines, Italy). *Boll. Soc. Geol. It.*, 123(2), 163-173.
- Curzi M., Billi A., Carminati E., Rossetti F., Albert R., Aldega L., Cardello G.L., Conti A., Gerdes A., Smeraglia L., Van der Lelij R., Vignaroli G. & Viola G. (2020) - Disproving the presence of Paleozoic-Triassic metamorphic rocks on the Island of Zannone (central Italy): Implications for the Early Stages of the Tyrrhenian-Apennines Tectonic Evolution. *Tectonics*, 39(12), <https://doi.org/10.1029/2020TC006296>.
- De Filippis L., Anzalone E., Billi A., Faccenna C., Poncia P. & Sella P. (2013b) - The origin and growth of a recently-active fissure ridge travertine over a seismic fault, Tivoli, Italy. *Geomorphology*, 195, 13-26.
- De Filippis L., Faccenna C., Billi A., Anzalone E., Brilli M., Soligo M. & Tuccimei P. (2013a) - Plateau versus fissure ridge travertines from Quaternary geothermal springs of Italy and Turkey: Interactions and feedbacks between fluid discharge, paleoclimate, and tectonics. *Earth-Sci. Rev.*, 123, 35-52.
- Della Porta G., Capezzuoli E. & De Bernardo A. (2017) - Facies character and depositional architecture of hydrothermal travertine slope aprons (Pleistocene, Acquasanta Terme, Central Italy). *Mar. Pet. Geol.*, 87, 171-187.
- Demurtas M., Fondriest M., Balsamo F., Clemenzi L., Storti F., Bistacchi A. & Di Toro G. (2016) - Structure of a normal seismogenic fault zone in carbonates: the Vado di Corno Fault, Campo Imperatore, Central Apennines (Italy). *J. Struct. Geol.*, 90, 185-206.
- De Rita D., Di Filippo M. & Sposato A. (1993) - Carta Geologica del Complesso Vulcanico sabatino. In: *Sabatini Volcanic Complex, CNR Quaderni de La Ricerca Scientifica 114*, (Ed. M. Di Filippo), Progetto Finalizzato: Geodinamica, monografie finali, 11, Rome.
- Devoto G. (1964) - Zone ad Alveolinidae nel Cretaceo e Paleocene del Lazio ed Abruzzo centro-meridionale. *Geologica Romana*, 3, 405-414.
- Di Bella L., Carboni M.G. & Bergamin L. (2002) - Pliocene-Pleistocene foraminiferal assemblages of the middle and lower Tiber Valley: stratigraphy and paleoecology. *Geologica Romana*, 36, 129-145.

- Di Sabatino V., Manetta M., Sciannamblo D., Spizzico M. & Tallini M. (2005) - Il Radon come tracciante delle acque sorgive finalizzato alla vulnerabilità degli acquiferi carbonatici complessi: l'esempio del gruppo sorgivo del Rio Arno (Gran Sasso, Italia Centrale). *Giorn. Geol. Appl.*, 2, 413-419, <https://doi.org/10.1474/GGA.2005-02.0-61.0087>.
- Donzelli G. (1968) - Studio geologico della Majella: Pescara, Italy, Master Thesis Università Gabriele D'Annunzio, Dipartimento di Scienze della Terra, 49 pp.
- Drzewiecki P.A. & Simó J.A. (2002) - Depositional processes, triggering mechanisms and sediment composition of carbonate gravity flow deposits: examples from the Late Cretaceous of the south-central Pyrenees, Spain. *Sediment. Geol.*, 146(1-2), 155-189.
- Eberli G., Bernoulli D., Sanders D. & Vecsei A. (1993) - From aggradation to progradation: the Maiella platform, Abruzzi, Italy. In: Simo J.A.T., Scott R.W. and Masse J.P. (Eds.), *Cretaceous Carbonate Platforms*, AAPG Memoir, 56, 213-232.
- Eberli G.P., Bernoulli D., Vecsei A., Sekti R., Grasmueck M., Lüdmann, T., Anselmetti F., Mutti M. & Della Porta G. (2019) - A Cretaceous carbonate delta drift in the Montagna della Maiella, Italy. *Sedimentology*, 66(4), 1266-1301.
- Erthal M.M., Capezzuoli E., Mancini A., Claes H., Soete J. & Swennen R. (2017) - Shrub morpho-types as indicator for the water flow energy-Tivoli travertine case (Central Italy). *Sediment. Geol.*, 347, 79-99.
- Esu D. & Girotti O. (2020) - Cenozoic non-marine and brackish water gastropods from Italy. *Neritimorpha, Caenogastropoda, Heterobranchia systematic and chronostratigraphic revision*. Conchbooks, Harxheim (Germany), 221 pp.
- Fabbi S., Cestari R., Marino M., Pichezzi R. & Chiochini M. (2020) - Upper Cretaceous stratigraphy and rudist-bearing facies of the Simbruini Mts. (Central Apennines, Italy): new field data and a review. *J. Mediterr. Earth Sci.*, 12, 87-103.
- Fabbi S., Galluzzo F., Pichezzi R.M. & Santantonio M. (2014) - Carbonate intercalations in a terrigenous foredeep: Late Miocene examples from the Simbruini Mts. and the Salto Valley (Central Apennines - Italy). *It. J. Geosci.*, 133, 85-100.
- Faccenna C., Soligo M., Billi A., De Filippis L., Funiciello R., Rossetti C. & Tuccimei P. (2008) - Late Pleistocene depositional cycles of the Lapis Tiburtinus travertine (Tivoli, Central Italy): possible influence of climate and fault activity. *Glob. Planet. Change*, 63, 299-308.
- Föllmi K.B., Gertsch B., Renevey J.P., de Kaenel E. & Stille P. (2008) - Stratigraphy and sedimentology of phosphate-rich sediments in Malta and southeastern Sicily (latest Oligocene to early Late Miocene). *Sedimentology*, 55, 1029-1051.
- Föllmi K.B., Hofmann H., Chiaradia M., de Kaenel E., Frijia G. & Parente M. (2015) - Miocene phosphate-rich sediments in Salento (southern Italy). *Sediment. Geol.*, 327, 55-71.
- Fronzoni F., Caliro S., Cardellini C., Chiodini G., Morgantini N. & Parello F. (2008) - Carbon dioxide degassing from tuscany and northern latium (Italy). *Glob. Planet. Change*, 61, 89-102.
- Funiciello R. & Parotto M. (1978) - Il substrato sedimentario nell'area dei Colli Albani: considerazioni geodinamiche e paleogeografiche sul margine tirrenico dell'Appennino centrale. *Geologica Romana*, 17, 233-287.
- Galadini F. & Galli P. (2000) - Active tectonics in the central Apennines (Italy)-input data for seismic hazard assessment. *Natural Hazards*, 22(3), 225-268.

- Galli P., Galderisi A., Messina P. & Peronace E. (2021) - The Gran Sasso fault system: Paleoseismological constraints on the catastrophic 1349 earthquake in Central Italy. *Tectonophysics*, 229156.
- Gasparini C., Di Maro R., Pagliuca N.M., Pirro M. & Marchetti A. (2002) - Recent seismicity of the «Acque Albule» travertine basin. *Annals of Geophysics*, 45(3-4).
- Ghissetti F. & Vezzani L. (1991) - Thrust belt development in the central Apennines (Italy): Northward polarity of thrusting and out-of-sequence deformations in the Gran Sasso Chain. *Tectonics*, 10(5), 904-919.
- Ghissetti F. & Vezzani L. (2002) - Normal faulting, extension and uplift in the outer thrust belt of the Central Apennines (Italy): Role of the Caramanico fault: *Basin Res.*, 14, 225-236, <https://doi.org/10.1046/j.1365-2117.2002.00171.x>
- Girotti O. & Mancini M. (2003) - Plio-Pleistocene stratigraphy and relations between marine and non-marine successions in the Middle Valley of the Tiber River. *Il Quaternario (Italian Journal of Quatern. Sci.)*, 16 (1bis), 89-106.
- Gori F. & Barberio M.D. (2021) - Hydrogeochemical changes before and during the 2019 Benevento seismic swarm in central-southern Italy. *J. Hydrol.*, 127250.
- Guo L. & Riding R. (1998) - Hot-spring travertine facies and sequences, Late Pleistocene, Rapolano Terme, Italy. *Sedimentology*, 45(1), 163-180.
- Holbourn A., Kuhnt W., Clemens S., Prell W. & Andersen N. (2013) - Middle to late Miocene stepwise climate cooling: Evidence from a high-resolution deep water isotope curve spanning 8 million years. *Paleoceanography*, 28, 688-699.
- Holbourn A., Kuhnt W., Kochhann K.G., Andersen N. & Sebastian Meier K.J. (2015) - Global perturbation of the carbon cycle at the onset of the Miocene Climatic Optimum. *Geology*, 43(2), 123-126.
- Holbourn A., Kuhnt W., Schulz M., Flores J.A. & Andersen N. (2007) - Orbitally-paced climate evolution during the middle Miocene "Monterey" carbon-isotope excursion. *Earth Planet. Sci. Lett.*, 261, 534-550.
- Holbourn A., Kuhnt W., Simo J.T. & Li Q. (2004) - Middle Miocene isotope stratigraphy and paleoceanographic evolution of the northwest and southwest Australian margins (Wombat Plateau and Great Australian Bight). *Palaeogeogr., Palaeoclimatol., Palaeoecol.*, 208, 1-22.
- Houben A.J., van Mourik C.A., Montanari A., Coccioni R. & Brinkhuis H. (2012) - The Eocene–Oligocene transition: Changes in sea level, temperature or both? *Palaeogeogr., Palaeoclimatol., Palaeoecol.*, 335, 75-83.
- Iaccarino S.M., Premoli Silva I., Biolzi M., Foresi L.M., Lirer F., Turco E. & Petrizzo M.R. (2007) - Practical manual of neogene planktonic foraminifera. In: *International School on Planktonic Foraminifera, 6th Course*. University of Perugia, pp. 1-181 Perugia 19-23 February 2007.
- James N.P., Boreen T.D., Bone Y. & Feary D.A. (1994) - Holocene carbonate sedimentation on the west Eucla shelf, Great Australian Bight: a shaved shelf. *Sediment. Geol.*, 90, 161-177.
- John C. M., Mutti M. & Adatte T. (2003) - Mixed carbonate-siliciclastic record on the North African margin (Malta)—coupling of weathering processes and mid Miocene climate. *GSA Bulletin*, 115(2), 217-229.
- Lear C.H., Rosenthal Y., Coxall H.K. & Wilson P.A. (2004) - Late Eocene to early Miocene ice sheet dynamics and the global carbon cycle. *Paleoceanography*, 19(4).

- Le Breton E., Handy M. R., Molli G. & Ustaszewski K. (2017) - Post-20 Ma motion of the Adriatic Plate: New constraints from surrounding orogens and implications for crust-mantle decoupling. *Tectonics*, 36(12), 3135-3154.
- Lorenzi V., Sbarbati C., Banzato F., Lacchini A. & Petitta M. (2022) - Recharge assessment of the Gran Sasso aquifer (Central Italy): Time-variable infiltration and influence of snow cover extension. *J. Hydrol: Reg. Stud.*, 41, 101090.
- Lucca A., Storti F., Balsamo F., Clemenzi L., Fondriest M., Burgess R. & Di Toro G. (2019) - From submarine to subaerial out-of-sequence thrusting and gravity-driven extensional faulting: Gran Sasso Massif, Central Apennines, Italy. *Tectonics*, 38(12), 4155-4184.
- Malatesta A. (1974) - Malacofauna pliocenica umbra. *Mem. Descr. Carta Geol. d'It.*, 13, 1-468.
- Malinverno A. & Ryan W.B. (1986) - Extension in the Tyrrhenian Sea and shortening in the Apennines as results of arc migration driven by sinking of the lithosphere. *Tectonics*, 18, 108-118.
- Mancini A., Della Porta G., Swennen R. & Capezzuoli E. (2021) - 3D reconstruction of the Lapis Tiburtinus (Tivoli, Central Italy): glacio-eustasy variations affecting travertine deposition. *Basin Res.*, 00, 1-31.
- Mancini A., Frondini F., Capezzuoli E., Galvez Mejia E., Lezzi G., Matarazzi D., Brogi A. & Swennen R. (2019) - Evaluating the geogenic CO₂ flux from geothermal areas by analysing quaternary travertine masses. New data from western central Italy and review of previous CO₂ flux data. *Quat. Sci. Rev.*, 215, 132-143.
- Mancini M. & Cavinato G.P. (2005) - The Middle Valley of the Tiber River, central Italy: Plio-Pleistocene fluvial and coastal sedimentation, extensional tectonics and volcanism. In: Blum M., Marriot S., Leclair S. (Eds.), *Fluvial Sedimentology VII*, IAS Spec. Publ. 35, Blackwell Publishing, 373-396.
- Mancini M., D'Anastasio E., Barbieri M. & De Martini P.M. (2007) - Geomorphological, paleontological and 87Sr/86Sr isotope analyses of Early Pleistocene paleoshorelines to define the uplift of Central Apennines (Italy). *Quat. Res.*, 67, 487-501.
- Mancini M., Girotti O. & Cavinato G.P. (2004) - Il Pliocene e il Quaternario della Media Valle del Tevere (Appennino centrale). *Geologica Romana*, 37, 175-236.
- Marra F., Cardello G.L., Gaeta M., Jicha B.R., Montone P., Niespolo E.M., Nomade S., Palladino D.M., Pereira A., De Luca G., Florindo F., Frepoli A., Renne P.R. & Sottili G. (2021) - The Volsci Volcanic Field (central Italy): eruptive history, magma system and implications on continental subduction processes. *Int. J. Earth Sci.*, 110(2), 689-718.
- Martini I.P. & Sagri M. (1993) - Tectono-sedimentary characteristics of the late Miocene-Quaternary extensional basins of the Northern Apennine. *Earth-Sci. Rev.*, 34, 197-233.
- Miall A.D. (1996) - *The Geology of Fluvial Deposits: Sedimentary Facies, Basin Analysis and Petroleum Geology*. Springer-Verlag, Berlin, 582 pp.
- Miller K.G., Wright J.D. & Fairbanks R.G. (1991) - Unlocking the ice house: Oligocene-Miocene oxygen isotopes, eustasy, and margin erosion. *J. Geophys. Res. Solid Earth*, 96, 6829-6848.
- Miller K.G., Wright J.D., Katz M.E., Wade B.S., Browning J.V., Cramer B.S. & Rosenthal Y. (2009) - Climate threshold at the Eocene-Oligocene transition: Antarctic ice sheet influence on ocean circulation. In: Koeberl C., Montanari A. (Eds.), *The Late Eocene Earth: Hothouse, Icehouse, and Impacts*, 452, 169-178.

- Milli S. (1997) - Depositional setting and high-frequency sequence stratigraphy of the Middle–Upper Pleistocene to Holocene deposits of the Roman Basin. *Geologica Romana*, 33, 99-136.
- Milli S., Mancini M., Moscatelli M., Stigliano F., Marini M. & Cavinato G.P. (2016) - From river to shelf, anatomy of a high-frequency depositional sequence: The Late Pleistocene–Holocene Tiber Depositional Sequence. *Sedimentology*, 63, 1886-1928.
- Milli S., Moscatelli M., Stanzione O. & Falcini F. (2007) - Sedimentology and physical stratigraphy of the Messinian turbidites deposits of the Laga Basin (central Apennines, Italy). *Bollettino della Società Geologica Italiana*, 126, 37-48.
- Minissale A. (2004) - Origin, transport and discharge of CO₂ in central Italy. *Earth-Sci. Rev.*, 66, 89-141.
- Minissale A., Kerrick D.M., Magro G., Murrell M.T., Paladini M., Rihs S., Sturchio N.C., Tassi F. & Vaselli O. (2002) - Geochemistry of Quaternary travertines in the region north of Rome (Italy): structural, hydrologic and paleoclimatic implications. *Earth Planet. Sci. Lett.*, 203(2), 709-728.
- Mitchum R.M. & Van Wagoner (1991) - High-frequency sequences and their stacking patterns: sequence-stratigraphy evidence of high frequency eustatic cycles. *Sediment. Geol.*, 70, 131-160.
- Monjoie A. (1980) - Prévission et contrôle des caractéristiques Hydrogéologiques dans les tunnels du Gran Sasso (Apennin-Italie). *Livre Jubilaire, L. Calembert, Ed. Thone, Liège.* 209-229.
- Morsilli M., Rusciadelli G. & Bosellini A. (2002) - Large-scale gravity-driven structures: control on margin architecture and related deposits of a Cretaceous Carbonate Platform (Montagna della Maiella, Central Apennines, Italy). *Boll. Soc. Geol. It., Volume Speciale (1)*, 619-628.
- Morsilli M., Rusciadelli G. & Bosellini A. (2004) - The Apulia carbonate platform margin and slope, Late Jurassic to Eocene of the Maiella Mt. and Gargano Promontory: physical stratigraphy and architecture. *Field Trip P18, 32^o International Geological Congress, Firenze 2004.*
- Morsilli M., Rusciadelli G. & Bosellini A., (2000) - Gravity-driven processes: Control on margin architecture and slope evolution in a Cretaceous carbonate platform (Montagna della Maiella, Italy). *A.A.P.G. Bull. (Association Round Table abstract)*, 84, 1467.
- Mutti M., Bernoulli D., Eberli G.P. & Vecsei A. (1996) - Depositional geometries and facies associations in an Upper Cretaceous prograding carbonate platform margin (Orfento Supersequence, Maiella, Italy). *J. Sediment. Res.*, 66(4), 749-765.
- Parotto M. & Pratlurlon A. (1975) - Geological summary of the Central Apennines. In: Ogniben, L., Parotto, M., Pratlurlon, A. (Eds), *Structural Model of Italy: C.N.R., La Ricerca Scientifica*, 90, 257-311.
- Passeri L., Ciarapica G., Leonardis F., Reggiani L. & Venturi F. (2008) - The Jurassic succession in the Western part of the Gran Sasso Range (Central Apennines, Abruzzo, Italy). *Boll. Soc. Geol. It.*, 127, 141-149.
- Patacca E., Sartori R. & Scandone P. (1990) - Tyrrhenian Basin and Apenninic Arcs: kinematics relations since Late Tortonian times. *Mem. Soc. Geol. It.*, 45, 425-451.
- Patacca E., Scandone P. & Carnevale G. (2013) - The Miocene vertebrate-bearing deposits of Scontrone (Abruzzo, Central Italy): stratigraphic and paleoenvironmental analysis. *Geobios*, 46(1-2), 5-23.
- Patacca E., Scandone P. & Di Manna P. (2021) – Geological Map of the Majella Mountain. ISPRA-Servizio Geologico d’Italia.

- Petitta M. & Tallini M. (2002) - Idrodinamica sotterranea del massiccio del Gran Sasso (Abruzzo); muove indagini idrologiche, idrogeologiche e idrochimiche (1994-2001). *Boll. Soc. Geol. It.*, 121(3), 343-363.
- Pomar L., Morsilli M., Hallock P. & Bádenas B. (2012) - Internal waves, an under-explored source of turbulence events in the sedimentary record. *Earth-Sci. Rev.*, 111(1-2), 56-81.
- Raffi I., Ricci C., Garzarella A., Brandano M., Cornacchia I. & Tomassetti L. (2016) - Calcareous nannofossils as a dating tool in shallow marine environment: an example from an upper Paleogene carbonate platform succession in the Mediterranean. *Newsl. Stratigr.*, 49(3), 481-495.
- Rainey D.K. & Jones B. (2009) - Abiotic versus biotic controls on the development of the Fairmont Hot Springs carbonate deposit, British Columbia, Canada. *Sedimentology*, 56(6), 1832-1857.
- Reading H.G. & Collinson J.D. (1996) - Clastic coasts. In: Reading H.G. (Ed.), *Sedimentary Environments: Processes, Facies and Stratigraphy*, 3rd edition, Blackwell Science, 154-231.
- Retallack G.J. (2001) - *Soils of the Past. An Introduction to Paleopedology*. 2nd edition. Blackwell Science, 404 pp.
- Reuter M., Piller W.E. & Brandano M. (2013) - Fossil psammobiontic sponges and their foraminiferal residents, Central Apennines, Italy. *Palaios*, 28(9), 614-622.
- Roberts G.P. & Michetti A.M. (2004) - Spatial and temporal variations in growth rates along active normal fault systems: an example from The Lazio–Abruzzo Apennines, central Italy. *J. Struct. Geol.*, 26(2), 339-376.
- Royden L., Patacca E. & Scandone P. (1987) - Segmentation and configuration of subducted lithosphere in Italy: An important control on thrust-belt and foredeep-basin evolution. *Geology*, 15(8), 714-717.
- Ruberti D., Toscano F., Carannante G. & Simone L. (2006) - Rudist lithosomes related to current pathways in Upper Cretaceous temperate-type, inner shelves: a case study from the Cilento area, southern Italy. In: Pedley H.M., Carannante G. (Eds), *Cool-water carbonates: depositional systems and palaeoenvironmental controls*. *Geol. Soc. Spec. Publ.*, 255, 179-195.
- Rusciadelli G. (2005) - The Maiella Escarpment (Abulia platform, Italy): geology and modeling of an Upper Cretaceous scalloped erosional platform margin. *Boll. Soc. Geol. It.*, 124(3), 661-673.
- Rusciadelli G. & Di Simone S. (2007) - Differential compaction as a control on depositional architectures across the Maiella carbonate platform margin (central Apennines, Italy). *Sediment. Geol.*, 196(1-4), 133-155.
- Rusciadelli G. & Ricci C. (2008) - New geological constraints for the extension of the northern Apulia platform margin west of the Maiella Mt. (Central Apennines, Italy). *Boll. Soc. Geol. It.*, 127(3), 375-387.
- Rusciadelli G. & Vichi G. (1998) - Stratigrafia sequenziale, organizzazione e correlazione dei depositi di piattaforma e bacino del Cretacico superiore della Maiella, In "Atti del 79° Congresso Nazionale della SGI" (Palermo).
- Rusciadelli G., Sciarra N. & Mangifesta M. (2003) - 2D modelling of large-scale platform margin collapses along an ancient carbonate platform edge (Maiella Mt., Central Apennines, Italy): geological model and conceptual framework. *Palaeogeogr. Palaeoclimatol. Palaeoecol.*, 200(1-4), 245-262.
- Rusciadelli G., Viandante M.G., Calamita F. & Cook A.C. (2005) - Burial-exhumation history of the central Apennines (Italy), from the foreland to the chain building: thermochronological and geological data. *Terra Nova*, 17(6), 560-572.

- Sagnotti L., Faccenna C., Funiciello R. & Mattei M. (1994) - Magnetic fabric and structural setting of Plio-Pleistocene clayey units in an extensional regime: the Tyrrhenian margin of central Italy. *J. Struct. Geol.*, 16(9), 1243-1257.
- Sanders D.G.K. (1994) - Carbonate platform growth and erosion: the Cretaceous to Tertiary of Montagna della Maiella, Italy. PhD Thesis, ETH Zurich University.
- Sanders D.G.K. (1996) - Rudist biostromes on the margin of an isolated carbonate platform: the Upper Cretaceous of Montagna della Maiella, Italy. *Eclogae Geol. Helv.*, 89(2), 845-871.
- Sartori R., Torelli L., Zitellini N., Carrara G., Magaldi M. & Mussoni P. (2004) - Crustal features along a W-E Tyrrhenian transect from Sardinia to Campania margins (Central Mediterranean). *Tectonophysics*, 383(3-4), 171-192.
- Scalera F., Mancini A., Capezzuoli E., Claes H. & Swennen R. (2021) - The role of tectonic activity, topographic gradient and river flood events in the testina travertine (Acque Albule Basin, Tivoli, Central ITALY). *The Depositional Record*, 00, 1-26.
- Schiavinotto F. & Benedetti A. (2021). Nephrolepidina and unispiralled Miogypsinidae from the Oligo-Miocene toe-of-slope succession of Gran Sasso (L'Aquila, Central Apennines-Italy): biometric and evolutionary remarks. *Micropaleontology*, 67(5), 483-514.
- Schlagenhauf A., Manighetti I., Benedetti L., Gaudemer Y., Finkel R., Malavieille J. & Pou K. (2011) - Earthquake supercycles in Central Italy, inferred from 36Cl exposure dating. *Earth Planet. Sci. Lett.*, 307(3-4), 487-500.
- Schmid S. M., Fügenschuh B., Kounov A., Maženco L., Nievergelt P., Oberhänsli R., Pleuger J., Scheferc S., Schusterh R., Tomljenović B., Ustaszewski K. & Van Hinsbergen D. J. (2020) - Tectonic units of the Alpine collision zone between Eastern Alps and western Turkey. *Gondwana Research*, 78, 308-374.
- Scisciani V., Calamita F., Bigi S., De Girolamo C. & Paltrinieri W. (2000) - The influence of syn-orogenic normal faults on Pliocene thrust system development: the Maiella structure (Central Apennines, Italy). *Mem. Soc. Geol. It.*, 55, 193-204.
- Scrocca D., Carminati E., Doglioni C. & Marcantoni D. (2007) - Slab retreat and active shortening along the central-northern Apennines. In: Lacombe O., Roure F., Lavé J., Vergés J. (Eds.), *Thrust belts and foreland basins*. Springer, Berlin, Heidelberg, 471-487.
- Serra-Kiel J., Gallardo-Garcia A., Razin P., Robinet J., Roger J., Grelaud C., Leroy S. & Robin C. (2016) - Middle Eocene-Early Miocene larger foraminifera from Dhofar (Oman) and Socotra Island (Yemen). *Arab. J. Geosci.* 9(5), 344.
- Servizio Geologico d'Italia (2005) - Carta Geologica d'Italia alla scala 1:50.000, F. 359 L'Aquila. ISPRA, Roma. https://www.isprambiente.gov.it/Media/carg/359_LAQUILA/Foglio.html
- Servizio Geologico d'Italia (2010) - Carta Geologica d'Italia alla scala 1:50.000, F. 349 Gran Sasso d'Italia, ISPRA, Roma. http://www.isprambiente.gov.it/MEDIA/carg/349_GRANSASSO/Foglio.html.
- Servizio Geologico d'Italia (2016) - Carta Geologica d'Italia alla scala 1:50.000. F. 375 Tivoli, ISPRA, Roma. https://www.isprambiente.gov.it/Media/carg/375_TIVOLI/Foglio.html
- Servizio Geologico d'Italia (2019) - Carta Geologica d'Italia alla scala 1:50.000. F. 345 Viterbo, ISPRA, Roma. https://www.isprambiente.gov.it/Media/carg/345_VITERBO/Foglio.html

- Shackleton N.J. (1969) - The last interglacial in the marine and terrestrial record. *Proceedings of the Royal Society of London, B*, 174, 135-154.
- Shackleton N.J., Berger A. & Peltier W.R. (1990) - An alternative astronomical calibration of the Lower Pleistocene time scale based on ODP site 677. *Trans. R. Soc. Edinburgh Earth Sc.*, 81, 251-261.
- Sottili G., Palladino D.M. & Zanon V. (2004) - Plinian activity during the early eruptive history of the Sabatini Volcanic District, Central Italy. *J. Volcanol. Geotherm. Res.*, 135, 361-379.
- Spence G.H. & Tucker M.E. (1997) - Genesis of limestone megabreccias and their significance in carbonate sequence stratigraphic models: a review. *Sediment. Geol.*, 112(3-4), 163-193.
- Stössel I. (1999) - Rudists and carbonate platform evolution: the Late Cretaceous Maiella Carbonate Platform Margin, Abruzzi, Italy. *Mem. Inst. Geol. Univ. Padova*, 51, 333-413.
- Stössel I. & Bernoulli D. (2000) - Rudist lithosome development on the Maiella Carbonate Platform margin. *Geol. Soc. Lond. Mem.*, 178(1), 177-190.
- Strata GeoResearch (2019) - Carbonate analogues of Adriatic petroleum system elements. Field trip guidebook. Unpublished.
- Tallini M., Parisse B., Petitta M. & Spizzico M. (2013) - Long-term spatio-temporal hydrochemical and ²²²Rn tracing to investigate groundwater flow and water-rock interaction in the Gran Sasso (central Italy) carbonate aquifer. *Hydrogeology J.*, 21(7), 1447-1467.
- Tavani S., Granado P., Corradetti A., Camanni G., Vignaroli G., Manatschal G., Mazzoli S., Muñoz J.A. & Parente M. (2021) - Rift inheritance controls the switch from thin-to thick-skinned thrusting and basal décollement re-localization at the subduction-to-collision transition. *GSA Bulletin*, 133(9-10), 2157-2170.
- Tavani S., Vignaroli G. & Parente M. (2015) - Transverse versus longitudinal extension in the foredeep-peripheral bulge system: Role of Cretaceous structural inheritances during early Miocene extensional faulting in inner central Apennines belt. *Tectonics*, 34(7), 1412-1430.
- Tomassetti L. & Benedetti A. (2020) - To be allochthonous or autochthonous? The late Paleocene-late Eocene slope sedimentary succession of the Latium-Abruzzi carbonate platform (Central Apennines, Italy). *Facies*, 66(6), 1-23.
- Tomassetti L., Benedetti A. & Brandano M. (2016) - Middle Eocene seagrass facies from Apennine carbonate platforms (Italy). *Sediment. Geol.* 335, 136-149.
- Tomassetti L., Petracchini L., Brandano M., Mascaro G. & Scrocca D. (2021) - Stratigraphical and sedimentological relationships of the Bolognana Formation (Oligocene-Miocene, Majella Mountain, Central Apennines, Italy) revealed by geological mapping and 3D visualisations. *Geol. Carpath.*, 72(1), 3-16.
- Vail P.R., Audemard F., Bowman S.A., Eisner P.N. & Perez-Cruz C. (1988) - The Stratigraphic Signatures of Tectonics, Eustasy and Sedimentology — An Overview. In: Einsele G., Ricken W. and Seilacher A. (Eds), *Cycles and Events in Stratigraphy*, Springer-Verlag, Berlin, 617-659.
- Valoroso L., Chiaraluce L., Piccinini D., Di Stefano R., Schaff D. & Waldhauser F. (2013) - Radiography of a normal fault system by 64,000 high-precision earth-quake locations: the 2009 L'Aquila (central Italy) case study. *J. Geophys. Res.* 118, 1156-1176.
<https://doi.org/10.1002/jgrb.50130>

- van Konijnenburg J.H., Wernli R. & Bernoulli D. (1998) - Tentative biostratigraphy of Paleogene planktic foraminifera in thin-section, an example from the Gran Sasso d'Italia (Central Apennines, Italy). *Eclogae Geol. Helv.*, 91, 203-216.
- van Konijnenburg J.H., Bernoulli D. & Mutti M. (1999) - Stratigraphic Architecture of a Lower Cretaceous-Lower Tertiary Carbonate Base-of-Slope Succession: Gran Sasso d'Italia (Central Apennines, Italy). *SEPM Spec. Publ.*, 63, 291-315.
- Vecsei A. (1991) - Aggradation und progradation eines karbonatplattform-randes: kreide mis mittleres tertiar der Montagna della Maiella, Abruzzen. Ph.D. Thesis, Mitteilungen des Geologischen Institutes der Eidgenossischen Technischen Hochschule und der Universitat, 294.
- Vecsei A., Sanders D., Bernoulli D., Eberli G.P. & Pignatti J.S. (1998) - Sequence stratigraphy and evolution of the Maiella carbonate platform margin, Cretaceous to Miocene, Italy. In (Eds.) *The Mesozoic and Cenozoic Sequence Stratigraphy of European Basins*, *SEPM Spec. Publ.*, 60, 53-74.
- Vezzani L., Festa A. & Ghisetti F.C. (2010) - Geology and tectonic evolution of the Central-Southern Apennines, Italy. *GSA Special Publication*, 469, 1-58.
- Vitale S. & Ciarcia S. (2013) - Tectono-stratigraphic and kinematic evolution of the southern Apennines/Calabria–Peloritani Terrane system (Italy). *Tectonophysics*, 583, 164-182.
- Vitale S. & Ciarcia S. (2021). The dismembering of the Adria platforms following the Late Cretaceous-Eocene abortive rift: a review of the tectono-stratigraphic record in the southern Apennines. *Int. Geol. Rev.*, 1-24.
- Waelbroeck C., Labeyrie L., Michel E., Duplessy J.C., Mcmanus J.F., Lambeck K., Balbon E. & Labracherie M. (2002) - Sea-level and deep water temperature changes derived from benthic foraminifera isotopic records. *Quaternary science reviews*, 21(1-3), 295-305.
- Wright V.P. & Burgess P.M. (2005) - The carbonate factory continuum, facies mosaics and microfacies: an appraisal of some of the key concepts underpinning carbonate sedimentology. *Facies*, 51(1-4), 17-23.
- Zachos J., Pagani M., Sloan L., Thomas E. & Billups K. (2001) - Trends, rhythms, and aberrations in global climate 65 Ma to present. *Science*, 292(5517), 686-693.
- Zalaffi M. (1963) - Segnalazione di un livello con piccole coproliti fosfatiche e glauconite nel Miocene del Lazio meridionale. *Geologica Romana*, 2, 331-341.

*Manuscript received 17 January 2022; accepted 30 June 2022; published online 11 November 2022;
editorial responsibility and handling by S. Tavani.*